ISEA Power Electronics and Electrical Drives
RWTH AACHEN UNIVERSITY

Matthias Rogge

Electrification of Public Transport Bus Fleets with Battery Electric Buses

Development of a software toolchain for the changeover planning of entire bus fleets with consideration of technical and operational constraints

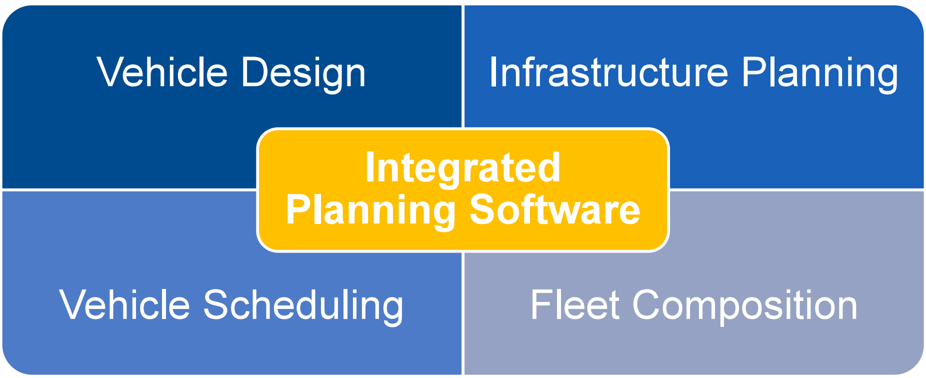

Aachener Beiträge des ISEA Band 148

Electrification of Public Transport Bus Fleets with Battery Electric Buses –

Development of a software toolchain for the changeover planning of entire bus fleets with consideration of technical and operational constraints

Von der Fakultät für Elektrotechnik und Informationstechnik
der Rheinisch-Westfälischen Technischen Hochschule Aachen
zur Erlangung des akademischen Grades eines Doktors der
Ingenieurwissenschaften genehmigte Dissertation

vorgelegt von

Diplom-Ingenieur
Matthias Rogge
aus Marl

Berichter:
Univ.-Prof. Dr. rer. nat. Dirk Uwe Sauer
Prof. Allan Larsen, Ph.D.

Tag der mündlichen Prüfung: 16. Juli 2020

Diese Dissertation ist auf den Internetseiten
der Universitätsbibliothek online verfügbar.

AACHENER BEITRÄGE DES ISEA
Vol. 148

Editor:
Univ.-Prof. Dr. ir. h. c. Rik W. De Doncker
Director of the Institute for Power Electronics and Electrical Drives (ISEA)
RWTH Aachen University

ISSN 1437-675X

Institute for Power Electronics and Electrical Drives (ISEA)
RWTH Aachen University
Jaegerstr. 17/19 • 52066 Aachen • Germany
Tel: +49 (0)241 80-96920
Fax: +49 (0)241 80-92203
post@isea.rwth-aachen.de

Vorwort (Preface)

Die vorliegende Dissertation entstand im Rahmen meiner Tätigkeit als wissenschaftlicher Mitarbeiter am Institut für Stromrichtertechnik und Elektrische Antriebe (ISEA) der Rheinisch-Westfälischen Technischen Hochschule (RWTH) Aachen. Mein besonderer Dank gilt zunächst meinem Doktorvater Professor Dirk Uwe Sauer, für die Möglichkeit zur Promotion und für das in mich gesetzte Vertrauen. Mein weiterer Dank gilt allen Kollegen und Wegbegleitern, ohne deren Unterstützung diese Arbeit nicht möglich gewesen wäre.

Ganz besonders bedanken möchte ich mich bei den Mitgliedern der Busgruppe. In unserem kleinen Team haben wir wegweisende Projekte umgesetzt, die den Elektrobusmarkt verändert haben. Besonders bedanken möchte ich mich bei Philipp Sinhuber und Werner Rohlfs, die mir die Möglichkeit gaben an innovativen Projekten mitzuarbeiten und mich für den ÖPNV begeisterten.

Ebenfalls bedanken möchte ich mich bei Climate-KIC für die Aufnahme in das europäische Doktorandenprogramm und die Finanzierung des Projekts LoCarUT. Der interdisziplinäre Austausch, die zahlreichen Workshops und die Möglichkeit des Forschungsaufenthalts waren eine echte Bereicherung.

Mein weiterer Dank geht an Allan Larsen und Evelien van der Hurk von der DTU in Lyngby für die erstklassige Betretung und die großartige Zeit während meines Forschungsaufenthalts in Dänemark. Sie haben es vollbracht, auch einem Elektroingenieur die Welt des Operations Research näherzubringen.

Ebenfalls großen Dank gebührt allen Kollegen von ebusplan. Insbesondere bedanken möchte ich mich bei Philipp Sinhuber und Max Sistig, mit denen ich über Jahre am Thema Elektrifizierungsplanung im ÖPNV arbeiten durfte und dies auch noch heute mit großer Freude tue. Unsere Diskussionsrunden waren eine echte Bereicherung für meine Arbeit.

Ganz besonders dankbar bin ich für den Rückhalt in meiner Familie. Vielen Dank an meine Eltern, die mir das Studium ermöglicht und mich von Anfang an unterstützt haben. Von tiefsten Herzen danke ich meiner Frau Constance, die mir in der gesamten Promotionszeit den Rücken freigehalten hat, verständnisvoll war und immer an mich geglaubt hat. Abschließend möchte ich mich bei meinem Sohn Carlo bedanken, der nochmal für einen extra Motivationsschub zur Vollendung dieser Arbeit gesorgt hat.

Aachen, Januar 2021
Matthias Rogge

Abstract

Electric buses are entering public transport bus fleets and introduce a new level of complexity in the strategic planning of public transport operators. Although numerous research activities focus on the field of electrification planning, there is thus far an absence of a comprehensive planning approach for the public transport domain covering all thematic areas, from technical design over operational planning to the assessment of lifecycle costs. The present thesis closes this gap by providing a software-based planning approach whose applicability has been proven through various case studies.

The novelty of this approach regards the high level of detail for all planning phases, which is enabled by the developed software toolchain utilizing state-of-the-art simulation and optimization methods as well as interfaces with existing planning software and third-party data. Efficient calculation methods facilitate analysis of large scenarios and a wide range of technical alternatives. The consequences of electrification with battery electric buses are elucidated for all stakeholders involved in the electrification process, such as operational planning and infrastructure departments. Furthermore, aggregated and normalized figures are provided to allow a neutral comparison of technical alternatives.

Kurzzusammenfassung

Elektrobusse drängen in die Busflotten des öffentlichen Personennahverkehrs und bringen eine neue Dimension der Komplexität in die strategische Planung der Betreiber. Obwohl sich zahlreiche Forschungsaktivitäten auf den Bereich der Elektrifizierungsplanung konzentrieren, gibt es für den öffentlichen Verkehr bisher keinen umfassenden Planungsansatz, der alle Themenbereiche von der technischen Planung über die Betriebsplanung bis zur Bestimmung der Lebenszykluskosten abdeckt. Die vorliegende Arbeit schließt diese Lücke durch die Bereitstellung eines softwarebasierten Planungsansatzes, dessen Anwendbarkeit in verschiedenen Fallstudien nachgewiesen wurde.

Neuheit des Planungsansatzes ist der hohe Detaillierungsgrad in allen Planungsphasen, der durch die entwickelte Software-Toolchain unter Einsatz modernster Simulations- und Optimierungsmethoden sowie durch Schnittstellen zu vorhandener Planungssoftware und externen Datenquellen ermöglicht wird. Effiziente Berechnungsmethoden erlauben die Analyse von großen Szenarien und einer Vielzahl von technischen Alternativen. Die Folgen einer Elektrifizierung mit batteriebetriebenen Elektrobussen werden für alle am Elektrifizierungsprozess beteiligten Akteure, wie zum Beispiel die Betriebsplanung und die Infrastrukturabteilung eines Verkehrsbetriebs, transparent gemacht. Darüber hinaus werden aggregierte und normalisierte Zahlen bereitgestellt, die einen neutralen Vergleich technischer Alternativen ermöglichen.

Table of Contents

1 Introduction

Electric buses are increasingly popular due to enforced emission regulations, air quality control and substantial funding schemes. More and more cities, regions and countries have committed to transforming bus sectors to zero emission, for example Paris, London, the Netherlands and Chile [1, 2]. The European Commission concretized the political aim by establishing zero-emission goals for public procurements in the revision of the Clean Vehicle Directive in June 2019 [3]. By two years after adopting the revision, member states must transpose the directive into national law and ensure that each public tender requests a certain percentage of clean and zero-emission vehicles. The targets vary by member state and sector, but highest are set for the bus sector with up to 65 % share of clean buses for public procurements in Germany planned for the time period from 2026 to 2030. Half must be zero-emission vehicles, either battery electric or fuel cell buses.

Almost any bus operator providing service in the public transport domain must therefore manage the electrification challenge. For bus fleets with various bus types of varying ages, a strategic plan is needed that defines the changeover and linked measures through infrastructure installation. The constraints of zero-emission vehicles impede effective manual planning regarding a larger number of vehicles. This thesis addresses this challenge by providing a software-based process for the strategic planning of entire-fleet electrification, where the focus is on battery electric buses (BEB) since they entail the most challenging constraints. The developed methodology can also be applied to the strategic planning of fuel cell bus fleets. The detailed problem definition is introduced in 1.1, which is followed by a description of the objective and solutions approach in 1.2.

1.1 Problem Definition

Public transport operators (PTO) have optimized the planning and operation of conventional bus fleets - in most cases diesel powered - over decades. With the support of planning software and optimization algorithms, they minimize vehicle demand and deadhead trips while maximizing service quality. In this process, conventional diesel buses were however relatively unconstrained, which is not the case for BEB whose planning and operation regards a paradigm shift and significant challenge for every PTO.

PTOs must choose among different BEB concepts available on the market, e.g., depot charging and opportunity charging which are concepts that significantly differ regarding infrastructure demand and operational constraints. Technology recommendations must therefore consider local situations and as well as operating schemes, structural boundary conditions, constraints regarding energy supply and constraints of the current market, such as the limited number of suppliers. Furthermore, choosing a BEB concept causes long-term consequences, as infrastructure installed today must be depreciated for several years and should therefore not become redundant by technical developments in the near future. Upward compatibility is required for a further rollout, which entails planning for the entire fleet during initial transformation steps.

The primary planning hurdles are related to vehicle scheduling and the dimensioning of technical components. Intensive interactions between these two optimization problems significantly increase their complexity, because the vehicle scheduling problem itself is NP-hard, when different vehicle types and depots are considered [4]. Figure 1-1 shows an illustration of the interaction.

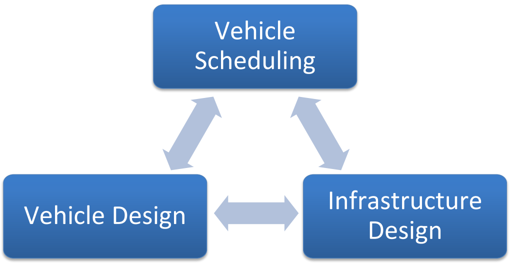

Figure 1-1: Major interactions within the design of BEB systems - Vehicle scheduling defines the operational scenario for vehicle and infrastructure design, but builds also on the technical constraints

Decisions on the technical level such as vehicle and infrastructure design are heavily influenced by the vehicle scheduling which defines the entire framework of a scenario by establishing the driving range of the buses as well as dwell durations at potential charging locations. On the other hand, vehicle scheduling is limited by technical constraints of BEB and charging infrastructure. The intense interaction of different planning and optimization tasks combined with the long-term perspective of strategic decisions define the core of this thesis.

Several consultancy companies and research institutions support PTOs in electrification planning. The typical approach is to retain existing vehicle scheduling and evaluate which bus run (set of trips assigned to one bus) can be electrified using current BEB technology [5]. Electrification of an entire fleet is however rarely possible due to constraints regarding battery capacity and charging power.

The limited scope of such studies is enlarged by considering anticipated future technological advancements, as illustrated in Figure 1-2 featuring a simplified example of depot-charging BEB. With an assumed increase in battery energy density for second-generation (Gen 2) buses, the range of BEB rises and additional bus runs become technically feasible. However even with Gen 2 depot-charging BEB, only 25 % of daily mileage is electrified and entire-fleet electrification is not achieved. The optimization potential of an adapted vehicle scheduling is not exploited. This highlights the necessity of integrating vehicle scheduling through a comprehensive planning approach.

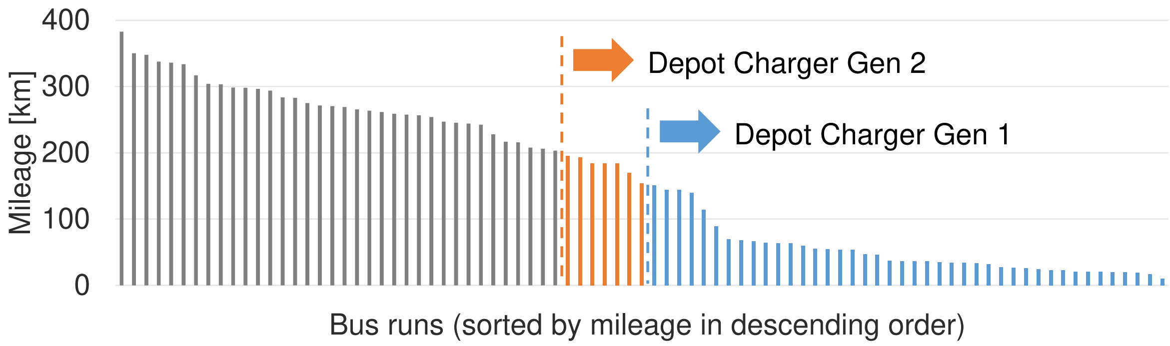

Figure 1-2: Bus run mileage of a small bus fleet indicating a large variety and intensive usage – highlighted columns indicate feasible bus runs for depot charging operation

Besides technical constraints, the varying economic consequences of individual BEB concepts increase planning complexity. The life cycle cost (LCC) calculation for conventional bus fleets builds on a profound experience regarding the durability of components [6]. However, in the case of BEB the LCC calculation faces high uncertainties. The aging of batteries relies on their actual operation which complicates general assumptions for battery lifetimes. Battery usage must therefore be considered during the planning process based on the desired operation.

Electrification initiatives are intended to improve the ecological footprint of public transport service, and therefore politicians and citizens desire an assessment of mitigation potential and a cost-benefit consideration for funding. Thus, emission calculation represents a further subject confronting PTOs. Assessing mitigation potential requires however more than a calculation for BEB. In order to calculate the improvements, the conventional bus fleet must be analyzed, which contributes a further dimension to the planning process.

In summary, comprehensive planning of fleet electrification must consider technical design and operational planning in a joint process. This highly constrained and complex task cannot be efficiently addressed using manual calculations. Existing planning approaches are limited by considering solely technical design or operation planning, as no comprehensive software tool for joint planning is available on the market.

1.2 Objective and Solution Approach

The main goal of this thesis is to provide planning guidance and required tools for the strategic planning of fleet transformation from conventional to battery electric operation. The approach must be able to model the current situation, assess technical feasibility, adjust or redo operational planning, calculate life cycle cost, assess mitigation potential and derive all results to reach a decision regarding a cost-efficient technology choice.

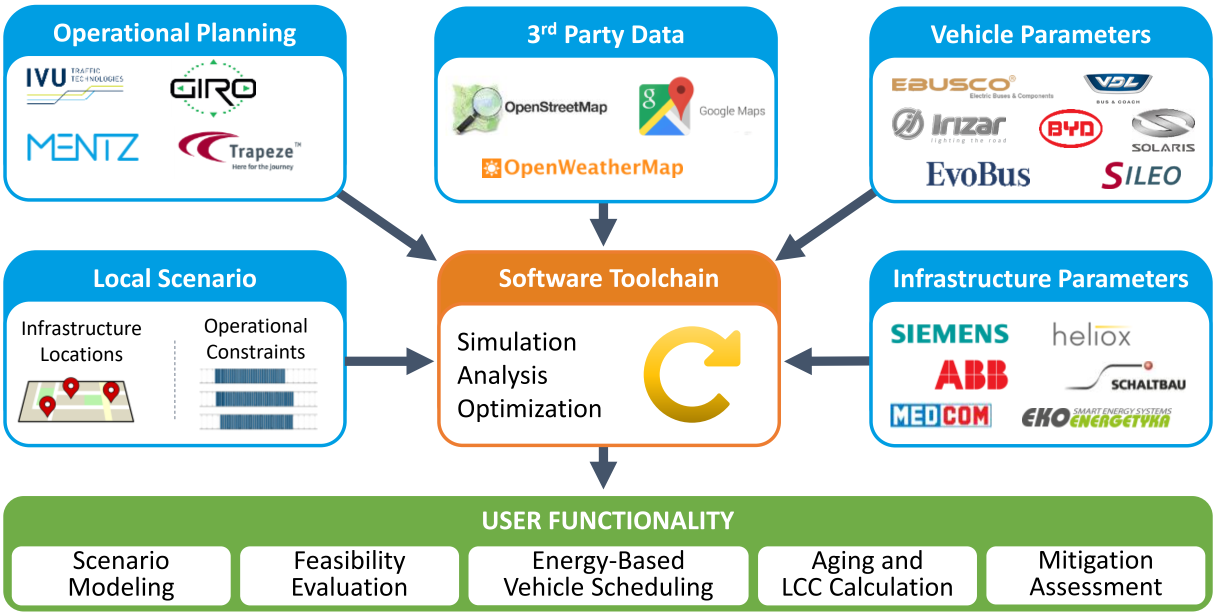

Figure 1-3: Overview of the software toolchain, input data and provided user functionality

The developed approach is based on a software toolchain covering the formulated demand. A general overview of the required input data and user functionality is shown in Figure 1-3, and detailed insight is provided in Section 1.

Input data describing current operational planning are imported from existing software solutions with minimal user effort. The data are afterwards enriched through automatized processing by specific information required for BEB modeling. The developed simulation can be applied to assess the technical feasibility of a BEB operation under various conditions. However, as described in the problem definition, this represents only one dimension of the problem. A further module enables the user to adjust or redo the vehicle scheduling of BEB according to technical constraints in the energy-based vehicle scheduling. By utilizing both methods, different BEB operating scenarios can be derived and further analyzed using the LCC calculation module. The computed LCC can be related to the mitigation potential of the corresponding BEB concept to provide all required information for the strategic fleet transformation decision. In the final changeover concept, the user is guided by recommendations based on the computed results and further methods for calculating costs and key performance indicators (KPI).

The developed software tool and planning process have been applied in various research and consultancy projects regarding PTOs in Europe. Bus fleets with up to 400 vehicles were analyzed in the Climate-KIC projects LoCarUT (Low Carbon Urban Transport) and MunEP (Municipal E-Bus Planner) at RWTH Aachen University [7]. Ongoing utilization and continuous development are ensured by the ebusplan GmbH, a consultancy spin-off of the ISEA of the RWTH Aachen University. The derived electrification strategies are currently realized in practice which proves the validity of the results.

2 Current State of Research

The emerging BEB market is supported by global extensive research activities. Beginning with the first public-funded prototype demonstrations until entire fleet operation, the rollout is often accompanied with scientific evaluations which enable an in-depth analysis and transfer of the results to other use cases [8–11]. An overview of the current BEB market and its development in the recent past is provided in 2.1, and afterwards planning processes for conventional bus operations in public transport companies are introduced in 2.2. Section 2.3 describes the current state of research in electrification planning and addresses the linked thematic areas such as life cycle cost calculation and mitigation assessment.

2.1 Battery Electric Bus Market

The external pressure and high demand of zero-emission public transport buses fertilize BEB market growth. The market overview in Section 2.1.1 highlights the dominant role of China where the highest number of BEB are in operation. The current status in Europe is discussed in 2.1.2 by presenting demonstrations in London and Eindhoven.

2.1.1 Market Overview

The majority of the global bus fleet is powered by diesel or compressed natural gas (CNG) [12]. However, the electric bus market has grown significantly in recent years. China represents the current hotspot where 99 % of the global BEB fleet (about 460,000 buses) is operated [2]. Electrification in China has been successfully stimulated by national as well as municipal funding. One well-known case regards the city of Shenzhen with about 16,000 BEB, a large share of which is delivered by the Shenzhen-based company BYD, one of the world's largest BEB manufacturers.

The current BEB market status and its development are illustrated in Figure 2-1. After beginning with redundant vehicles and prototype testing, the first dedicated bus routes were electrified as part of the ZeEUS project such as in Barcelona, Bonn and Münster [13]. The next level was achieved by the electrification of a subnetwork in Eindhoven where buses operated on several routes. A full electric bus network is the final goal and currently targeted in the Netherlands and Luxembourg.

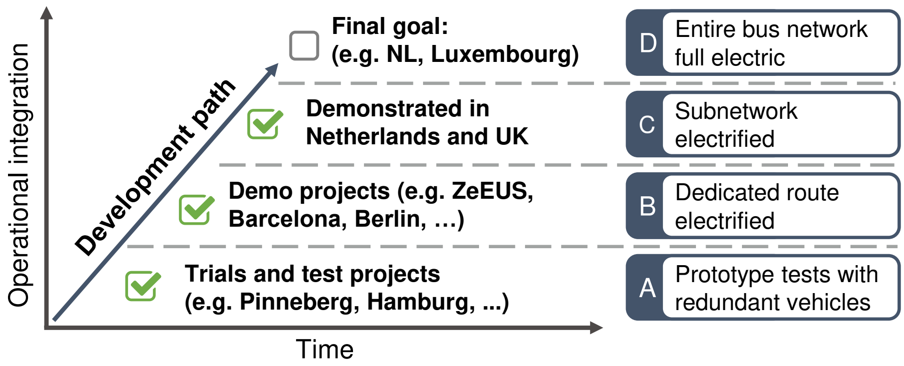

Figure 2-1: Development path of the BEB operation in Europe

The BEB market in Europe includes about 3,000 vehicles in 2019 [14]. The largest fleet is operated in the Schiphol area with about 100 BEB from the Dutch manufacturer VDL Bus & Coach. It is planned to increase the fleet size to 260 vehicles by 2021 [15]. In Germany, a total of 245 BEB are in operation as of mid-2019 [16], and according to the E-Bus-Radar of PwC this figure should be doubled in the second half of 2019 [16], which highlights the market uptake.

Table 2-1 lists current manufacturers active in the European market and their locations. The largest suppliers in terms of sold units regard Solaris, VDL and BYD / ADL. These manufacturers entered the market at an early stage, gained knowledge using initial prototypes and utilize this knowledge to achieve electrification of smaller fleets such as in Krakow (Solaris), Eindhoven (VDL) and London (ADL / BYD). The use cases of London and Eindhoven are discussed in the following section. The German manufacturers Evobus and MAN have not been involved in early BEB prototype phases, however Evobus has recently launched their BEB eCitaro.

Company	Country	Company	Country	Company	Country
ADL	UK	**Hybricon**	Sweden	**Skoda**	Czech Republic
Bluebus	France	**Irizar**	Spain	**Solaris**	Poland
BYD	China	**Linkker**	Finland	**SOR**	Czech Republic
Caetano	Portugal	**MAN**	Germany	**Temsa**	Turkey
Ebusco	Netherlands	**Optare**	UK	**Ursus**	Poland
Evobus	Germany	**Otokar**	Turkey	**Van Hool**	Belgium
Hess	Switzerland	**Rampini**	Italy	**VDL**	Netherlands
Heuliez	France	**Sileo**	Germany	**Volvo**	Sweden

Table 2-1: BEB manufacturers in Europe and their locations

2.1.2 Use Cases in Europe

The first subnetwork operations of a small BEB fleet were demonstrated in London (UK) and Eindhoven (NL). The case in London was initiated by Transport for London (TfL), which is the public transport authority responsible for the operation of 9,000 buses in the London area. In cooperation with the PTO Go-Ahead, the entire fleet of the bus depot Waterloo has been replaced by BEB from ADL/BYD. The manufacturers ADL and BYD cooperate to deliver BEB based on an ADL chassis with an electric drivetrain from BYD. Since 2016 a total of 51 standard buses have operated on routes 507/512 in regular service.

The BEB Enviro200EV and the electrified Waterloo depot are shown in Figure 2-2. The vehicle is equipped with a 324 kWh battery mounted in the rear of the vehicle and on the roof. Two onboard chargers in each vehicle enable charging up to 80 kW. The presence of an onboard charger allows a slim infrastructure setup in the depot. A modified wall box is installed at each parking position to which the BEB connect via cable. The usage of onboard chargers is not widespread today due to drawbacks caused by the number of chargers (minimum one per bus) and the fact that the charger increases the bus weight.

Figure 2-2: BEB Enviro200EV from the manufacturer BYD/ADL (left) and charging infrastructure at the Waterloo depot in central London (right)

In the Eindhoven use case, in December 2016 the PTO Hermes established an operation with 46 articulated BEB from VDL. The buses serve routes 400 to 407 in the city center and suburban areas. The particularity of this setup is that all routes have Eindhoven Station as a terminal stop, which is near the bus depot.

Although the vehicle is larger than in London where only standard buses are operated, the battery capacity is smaller. The Citea SLFA-181 electric has an installed battery capacity of 169 kWh, which limits the range to less than 80 km. This range limitation is managed by frequent fast charging at the depot, so that a daily mileage of 200 km to 300 km per bus is achieved. The short distance between the terminal stop and depot favors this mode of operation.

The charging in the depot is conducted via external DC-chargers and roof-mounted pantographs, as shown in Figure 2-3. A coupling hood is installed at each parking position outside and inside the building.

Figure 2-3: BEB Citea SLFA-181 from the manufacturer VDL and charging stations in the Hermes bus depot in Eindhoven (NL)

The two use cases reveal the varying BEB concepts throughout Europe. Whereas the London example utilizes high capacity batteries and a moderate charging power, has the operator in Eindhoven decided that smaller batteries and a high charging power is more appropriate for the local operation. This comparison points out that the selection of a BEB technology and a charging concept is determined by the local situation, which therefore needs to be addressed in an electrification planning.

2.2 Planning Processes in Transport Companies

The various options in designing and operating public transportation systems are determined in a sequential planning process which can be organized regarding the time horizon of decisions in strategic, tactical, operational and real-time problems [17]. The described processes are based on the characterization of Desaulniers and Hickman [17].

Strategic planning focuses on long-term decisions, such as concerning the network design where the overall goal is to meet the passenger travel demand, which is represented by an origin-destination matrix (O-D). The outcomes of this process regard a set of routes with corresponding service frequency. It is important to consider costs even during this early stage in order to create an economically viable solution. This is achieved via aggregating cost figures and budgets, which are included in the objective function as a minimization criterion or considered as a fixed budget in the constraints of the problem. A commonly considered approximation of the costs of a bus network concerns the resulting fleet size [18]. The network design problem is NP-hard [19]. Solutions can be derived from decomposition strategies [19, 20] or by simultaneously considering routes' design and service frequency settings [21]. A variety of metaheuristics have been applied to the problem including genetic algorithms, tabu search, local search or random search [22]. Cases with up to 1332 bus stops and 4076 arcs between them have been solved for example using genetic algorithms [23].

The basic elements of the transportation system are defined within the network design. Based on this, tactical planning addresses mid-term issues such as determining service schedules and adjusting frequencies. Adjustments could be caused by variations in passenger demand or smaller changes in route design. A major task of tactical planning regards timetabling, in which the desired frequency is converted to service trips with defined start and end times. Decisions are executed based on the route structure, duration of service trips and required slack or layover. A high level of complexity is caused by considering transfers between routes with minimum waiting times [24].

The purpose of operational planning is to determine how resources can be used in the most cost-efficient way to fulfill the previously described service. The set of resources consists of the vehicle fleet located in one or multiple depots and the driver crew. The service trips with a defined start/end location and time comprise the input of this process, and the outcomes regard a comprehensive set of schedules which describe the entire transport system during regular operation. However, the process is not strictly straightforward. Because resources are limited, infeasible or too costly, solutions may arise which require feedback loops to previous steps, as highlighted in Figure 2-4.

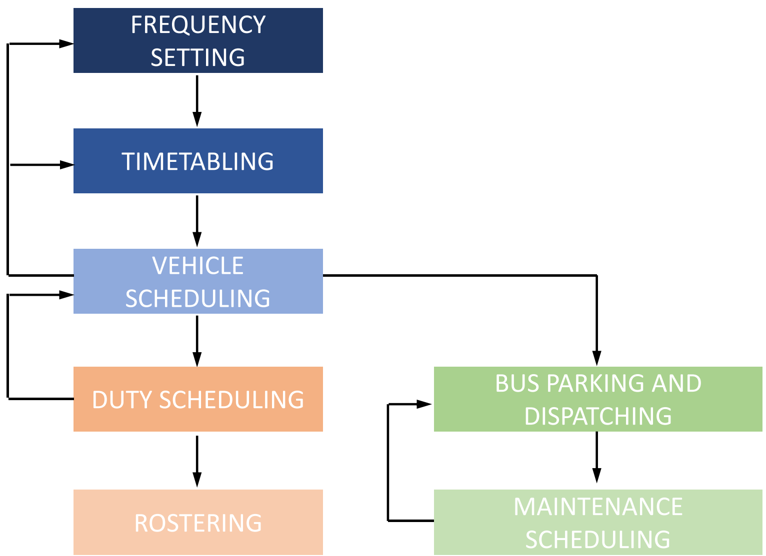

Figure 2-4: Processes in tactical and operational planning by Desaulniers and Hickman [17]

Vehicle scheduling represents a crucial step in operational planning as it introduces a strong cost focus and determines the acquisition costs by defining the required fleet size as well as the operational costs of the buses. Research investigates the single depot vehicle scheduling problem (SDVSP) consisting of a set of service trips, a single depot and only one vehicle type [25]. The SDVSP can be represented by various models, and Table 2-2 gives an overview of the most commonly used by providing a brief characterization according to Bunte and Kliewer [26].

Problem	Modelling approach	Characterization
SDVSP	Minimal Decomposition Model	Consists of a partially ordered set of trips according to their starting and ending times. It focuses on solving the minimum fleet size problem and excludes operational cost considerations as well as upper limits for the fleet size.
	Assignment Model	Can be represented by a bipartite graph with start and end nodes for each trips and arcs for the trip as well as for connections among them. Incompatible trips are connected with arcs, but the costs for these arcs represent a new vehicle. It extends the minimal decomposition model by operational costs. However, a fixed limit for the fleet size is not included.
	Transportations Model or Quasi-Assignment Model	Compared to the assignment model, only feasible arcs are considered. Additional nodes are added for the depot. It introduces an upper limit for the fleet size. Solutions could represent an under coverage if the vehicle number is not sufficient.
	Network flow model	Each trip is represented by a start and end node and the connecting trip arc. Further arcs are introduced for deadheading and depot trips.

Table 2-2: Modelling approaches for the VSP and characterization according to Bunte and Kliewer [26]

These models are used within a mixed integer linear problem (MILP) formulation to determine feasible and optimized operating schemes. However, the SDVSP represents a simplified version of the real problem. PTOs usually operate more than one depot, which results in a multi depot vehicle scheduling problem (MDVSP) with increased complexity. In addition, the vehicle fleet rarely consists of a single vehicle type. Buses with different lengths and therefore different capacities are operated to match the varying passenger demand within the network. The varying bus types can for example be managed by introducing additional pseudo depots of each type to allow the problem to be solved like an SDVSP.

The level of detail within the vehicle scheduling process is limited to bus types. Dedicated vehicles are considered afterwards within vehicle dispatching which is conducted depot-wise on a daily basis. The parking of vehicles must be performed in such a way that the following day can begin smoothly. The second reason for this short-term planning regards the scheduling of maintenance events. Vehicles must be checked on a regular basis based on driven mileage or after problems occur. Due to the varying daily assignments, the exact mileage of the vehicles is difficult to predict, which impedes long-term planning. More details of this problem and solution methods are provided in the work of Haghani and Shafahi [27].

Like vehicle scheduling and dispatching, crew planning is also divided into two procedures, namely duty scheduling and crew rostering. Duty scheduling creates general duties by considering all safety regulations such as required brakes or maximum driving time. Several additional rules must be considered in order to compose duties which fit the working conditions agreed by the drivers, such as a minimum shift duration. Because wages represent one of the highest costs of bus operators, optimization strategies focus on cost minimization. The high number of rules, which are sometimes non-linear, cause the duty scheduling problem to be more complex than the MDVSP.

Duty scheduling is followed by crew rostering which focuses on individual drivers and their particularities. For example, drivers must have sufficient recuperation time between two duties and the maximum number of duties per period must not be exceeded. This process is executed according to the operator's policy. An aim for example could regard the equal spread of workload among all drivers.

The previously described procedure featuring a separation of vehicle scheduling and crew rostering regards the usual practice for bus operations in urban areas, where many relief operations for drivers enable room for improvements. However, this is different in rural bus operation where the limited relief options entail a strong linkage between driver and vehicle. In this case it can be useful to consider vehicle and duty scheduling in an integrated process.

By introducing electric vehicles into the overall planning scheme, some processes – e.g., vehicle scheduling - must be revised or adjusted due to technical and operational constraints. The main constraint of a BEB regards the limited battery capacity limiting the operational range, which is a critical measure for an efficient bus operation. The range becomes furthermore dependent on the local situation, as the energy demand varies according to track characteristics (slope, position, and number of stops), operational characteristics (commercial speed, dwell times) and weather conditions (summer, winter). Besides the range, the charging time also regards a dominating constraint. The minimum charging time differs concerning the power level of the chargers and charging capabilities of the bus.

Current planning solutions such as IVU.run[1] offer the possibility to handle mileage and time-related constraints. Mileage-related constraints are for example utilized for the scheduling of maintenance events or refueling. Time constraints mainly relate to driver scheduling, with a maximum constraint on driving hours and working time. Both options allow a simplified BEB scheduling with fixed and constant energy demand, range, and refueling/charging time. However, a combined consideration of mileage and time-related constraints is not possible which clearly limits the scope of this approach.

[1] IVU.run is a product of the IVU Traffic Technologies AG and embedded in the toolchain IVU.suite

2.3 Planning Approaches and Methods for Fleet Electrification

The cost-efficient electrification of entire fleets represents a multidisciplinary topic that affects a wide range of thematic areas, including BEB technology, operational planning, strategic fleet management, life cycle cost calculation and environmental impact assessment, as shown in Figure 2-5. All thematic pillars must be addressed within a planning process in order to derive implementable concepts.

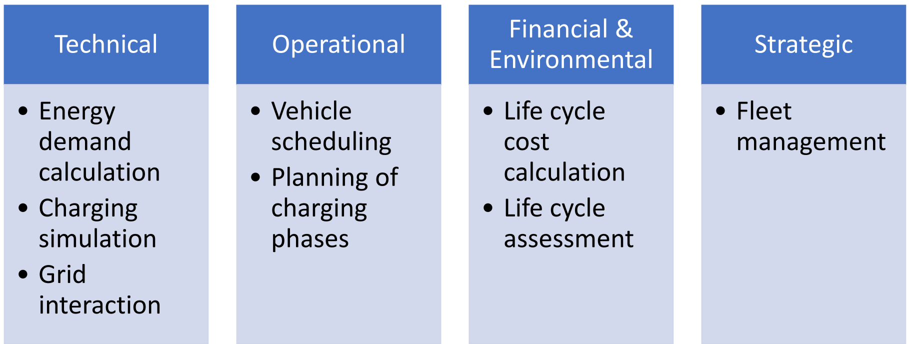

Figure 2-5: Thematic areas addressed in fleet electrification planning

Each thematic area listed in Figure 2-5 regards a scientific research discipline due to its complexity and depth. Simplifications are required in order to manage the high complexity. However, depending on the degree of simplification, e.g., generalized route characteristics or operational conditions, the focus could shift from the local situation of a PTO to a generalized statement for a specific technology or concept, which needs to be avoided.

Applying simplifications, especially regarding local conditions, leaves a gap between the analysis outcomes and realization in practice. Thus, a core topic of this work regards the conflict between the necessary depth of detail and the simplifications required in considering an entire bus network. The following subchapters introduce the current literature related to fleet electrification planning, beginning with on overview of general planning approaches.

2.3.1 General Electrification Planning

Fleet operators are confronted nowadays with the electrification challenge, especially those handling regular transport with fixed routes, which are particularly suited for electrification. One example regards the postal delivery service which was analyzed by Kleindorfer et al. who have investigated the electrification of the French postal fleet [28]. Their focus was on minimizing the life-cycle costs in the transition process by considering future price developments. Electrification was however assumed to be technically feasible since the daily routes of delivery vehicles are less than 44 km. This assumption does not apply in the public transport sector where a one-by-one replacement is limited by technical constraints such as range and charging time. As a result, the technical as well as economic situations must be evaluated.

The work published by Kunith entitled "Elektrifizierung des urbanen öffentlichen Busverkehrs" focuses on such a technical and economic analysis and aims to evaluate a broad spectrum of different technical concepts for urban, road-based public transport [29]. Kunith introduced a system-based life cycle cost calculation and enlarged the scope via a cost-efficient positioning of infrastructure. The overall complexity is reduced by performing simplifications regarding energy consumption and operational schemes. The modelling of the operation scheme focuses on the main service trips of a bus route which are operated several times a day. The shortening of bus routes, route variations and vehicles operated on several bus routes are neglected, which limits the analysis to single routes. It is not possible to consider bus runs covering multiple routes, which is the standard situation in the current operational planning of public transport operators.

The work of Berthold “Techno-ökonomische Auslegungsmethodik für die Elektrifizierung urbaner Busnetze” also provides a detailed life cycle cost calculation [30] and extends the work of Kunith by introducing a detailed vehicle simulation. However, an optimization of the operational planning is excluded from its scope, which limits the application to technical feasible scenarios.

The aim of this thesis is to close the gap between the outcomes of an analysis and their implementation by providing a software solution capable of considering the current operating scheme in detail. This includes an evaluation of technical feasibility as well as the ability to adjust or redo the operational planning while considering technical constraints. A software tool and holistic process covering these core topics have thus far not been published, as existing literature mainly focuses on isolated aspects such as energy demand determinations or operational planning. The following subchapters address these areas and provide an overview of the current state of research.

2.3.2 Energy Demand Calculation

Energy demand calculation represents an essential element in the electrification planning process, because the energy demand influences both technical feasibility and operational costs. General figures are not available since energy demand depends on the operating and route characteristics as well as on the technical configuration of the vehicle [31]. One option for energy demand determination regards a measurement campaign in which every eligible bus is operated under worst-case conditions on the potential bus routes. However, such a test operation would lead to horrendous execution costs. Furthermore, since worst-case conditions are not present throughout the entire year, the validity and transferability of the results are highly questionable.

Instead of conducting a measurement campaign locally, another option is to gather measurement data from existing BEB operations and transfer them to the local situation [6, 32]. The major challenge thereby is to identify and evaluate the energy demand-affecting parameters, as for example the speed profile [33]. The use of generalized and averaged figures could exclude significant influences. One example regards the average commercial speed, as there are several issues causing for example a low average speed such as several bus stops along the route or a low speed limit on inner-city routes. This results in dynamic or constant speed profiles for an identical distance driven, as shown in Figure 2-6. Due the losses in acceleration and deacceleration, the dynamic speed profile leads to a higher energy demand.

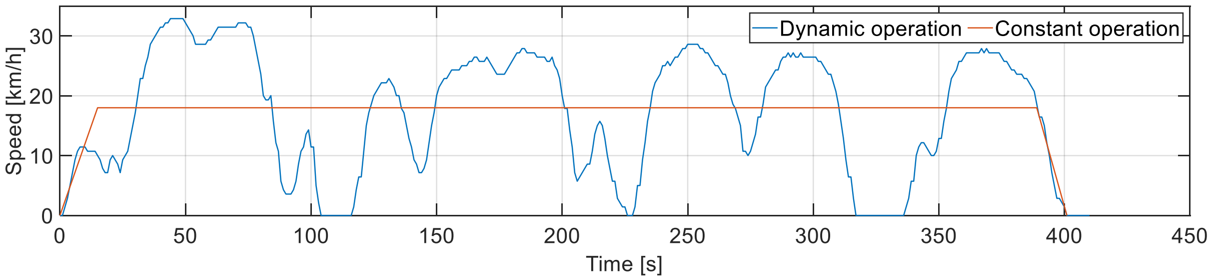

Figure 2-6: Example of dynamic and constant operation of a BEB with an identical commercial speed on a given distance

Another example where an aggregated figure reduces the information quality concerns the topography. If for example only the height difference between the start and end point of a trip is considered, the effect of a hilly road is hidden.

A higher level of detail and consideration of the respective route characteristics are enabled by utilizing simulation models which represent the physical conditions [9, 31, 34, 35]. Examples in literature include a track model, a vehicle model, and a driver model. The published energy demand calculation models base on the same physical principles. The track model is parameterized using characteristic data obtained from measurements or geodatabases such as topography and the position of traffic lights, intersections, and curve radii. The vehicle model is parameterized using technical specs describing vehicle performance and constraints. The major difference between the published modelling approaches regards the driver model which influences the universal applicability of the entire model.

While the driver model in the work of Gao is parametrized using a measured speed profile or with standard driving cycles [35], Sinhuber utilized a more open approach based on a driver model which reacts to operational parameters [31] consisting of the speed limit, position of bus stops and timetable of the service trip. Using such input data allows simulating the current operation without conducting measurement campaigns. Following the requirements of universal applicability for large scenarios, a methodology following the approach of Sinhuber is applied within this work as described in Section 4.4.1.

2.3.3 Life Cycle Costs and System Design

A life cycle cost (LCC) calculation is a common methodology for evaluating technological concepts in public transport and is already applied in diesel bus procurement and recommended for evaluating tender bids [36, 37]. While the calculations for diesel buses focus on a single bus, the focus in BEB shifts to the system level. In addition to the procurement of vehicles, the investments in charging infrastructure and grid connection must be considered [38]. Furthermore, the replacement costs of components receive attention since battery replacements could especially lead to substantial investments in the future, because battery lifetime is usually less than vehicle lifetime [39]. As a result, two uncertainties become part of the LCC calculation: First, the lifetime of a battery is determined by complex aging effects (see Section 3.5.3), forcing the integration of aging models in the calculation [40]. Furthermore, component prices are expected to decrease due to the market uptake and scaling effects. Therefore, predicting future cost developments is required [29].

Among the general LCC calculation, the minimization is the main goal for any PTO. This is done by adapting the technical configuration to meet a minimum operational requirement [41]. The technical design of BEB systems is mainly concerned with the dimensioning of batteries [42, 43], the location and dimensioning of charging infrastructure [44] as well as the effects of charging on the power supply system [45, 46]. LCC are usually defined as the objective and evaluation criteria.

In contrast to studies in the passenger car sector, the location and dimensioning of charging infrastructure for BEB is usually jointly considered with the dimensioning of batteries. Regarding battery sizing, a distinction can be made between publications that determine the minimum battery size on the basis of technical feasibility and initial investments [44] and those that include aging considerations to formulate the most viable solution in terms of LCC [41].

In addition to the minimization of LCC via improvements to the technical system design, cost cuts can also be enabled by vehicle scheduling as introduced in Section 2.2. However, a joint planning process covering technical system design and vehicle scheduling for entire fleets has not been published so far.

2.3.4 Environmental Impact

Emission mitigation represents a major topic of the 21st century. Negative consequences of continuously increasing output can be observed on global and local scales. The main driver of global warming regards greenhouse gas emissions (GHG) as CO_2. Due to their global impact, it does not matter where they are produced, which requires the consideration of the production of vehicles and energy supply. Nitrogen oxides (NO_X) and particular matter (PM) emissions entail direct consequences on local air quality, which brings vehicle operation into focus.

The transport sector is requested to contribute to mitigation initiatives by increasing the efficiency of conventional fuel-powered drivetrains and by introducing electric vehicle concepts powered by renewable energy sources. Life cycle assessment (LCA) has become the standard for the quantification and evaluation of achievable environmental benefits, the principle and framework of which is described by ISO 14040:2006 [47].

Several studies have been published focusing on the comparison of electric and conventional vehicles. The papers of Hawkins, Nordelöf and Nealer aim at a synthesis of the current literature [48–51]. These authors independently conclude that most studies are difficult to compare due to their individual scope and methods. A comprehensive goal and scope formulation, as recommended in the ISO 14040:2006, is rarely provided [50]. However, the synthesis highlights that the use phase dominates the environmental impact of electric vehicles [51]. The use phase describes the actual operation as shown in Figure 2-7.

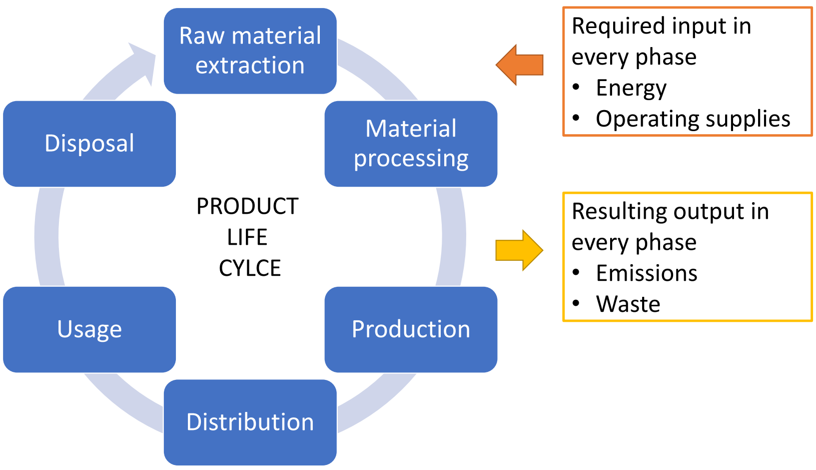

Figure 2-7: Product life cycle considered in the life cycle assessment – beginning with raw material extraction and ending with disposal / recycling

Battery production is especially relevant in the case of battery electric vehicles [52, 53]. A synthesis of studies analyzing the environmental impact of batteries is provided by the Swedish Environmental Research Institute IVL [54]. The authors conclude that the calculated emissions significantly vary between individual studies and stated that additional research is needed to provide robust information. However, their synthesis indicates that the ecological footprint of a battery is determined to a great extent by the footprint of the electricity used during the production phase.

Due to the lack of a comprehensive database regarding the ecological footprint of battery production, the focus of this work lies on emissions calculation during the use phase. However, the general framework is designed in such a way, that the ecological footprint of the battery production can be included.

2.3.5 Operational Planning with Electric Vehicles

The strategic planning of electric public transport bus fleets in conjunction with vehicle scheduling refer to the “Fleet Size and Mix Problem,” which is analyzed in operations research and forms a subcategory of the “Vehicle Routing Problem” in which routing is performed jointly with determining the required number of vehicles [55]. Fleets can consist of single vehicle types (homogeneous fleet) or multiple vehicle types (heterogeneous fleet). Recent work has mainly referred to the area of goods distribution. A comprehensive review focusing on electric vehicles in this field is provided by Pelletier, Jabali and Laporte [56]. The discussed approaches differ regarding the considered vehicle types (homogeneous or heterogeneous electric vehicle fleet as well as with and without conventional combustion engine vehicles) and the methodology concerning charging events. Goeke et al. and Lebeau et al. extensively studied the routing of mixed fleets composed of conventional and electric vehicles [57, 58]. They emphasized the need to consider vehicle types’ specific energy consumptions, especially for vehicles with varying weights; this consideration motivates the energy consumption simulation in this thesis. Van Duin et al. did not consider battery charging [59], whereas Gonçalves et al. suggested that charging could occur at every customer’s location [60]. In another study, Hiermann et al. included an insertion of charging events so that vehicles could drive to charging stations when needed [61]. However, none of these authors considered investments in charging infrastructure or usage fees. Sassi et al. included usage fees as time-dependent charging costs for a “Mixed Fleet Routing Problem,” [62] however the number of chargers in their model was predefined and fixed.

By focusing on public transport buses, the routing problem becomes a scheduling problem since service trips are fixed concerning time and location. Routing alternatives are limited to deadhead trips which regard the connecting elements between service trips. The electric vehicle scheduling problem can be viewed as a “Vehicle Scheduling Problem with Route and Fueling Time Constraints”. The objective is to minimize fleet size and operational expenses. Regarding vehicle routing, previous studies differ in how they consider battery charging. Li proposed a methodology for scheduling a fleet of BEB with battery renewal or fast charging [63]. The implemented truncated column generation with variable fixing and local search is highly competitive, but the durations of charging events are not linked to the energy consumption, and charging costs are defined at a fixed value per event. Other approaches considering the charging in greater detail are based, for example, on ant colony optimization [64, 65]. However, these approaches are not able to address heterogeneous fleets. In contrast, Paul and Yamada focused on the problem of fast-charging bus operations and scheduling charging events [66], however their implemented k-greedy algorithm can be viewed as lacking solution quality since it fails to focus on a global optimum. In another study, Chao et al. established a multi-objective optimization for the scheduling of battery exchange buses operated in Shanghai [67]. Their approach aims to minimize the fleet size and number of standby batteries, which are both related to investment costs as well as the grid load, however their considerations are limited to homogeneous fleets. Ke et al. introduced the scheduling of BEB, the handling of charging events and the consideration of entire system costs [68]. They analyzed a suburban bus network in Taiwan and utilized a scheduling approach based on a sequential process, however in their approach the assignment of bus types to routes is pre-defined and the number of chargers always equals the number of buses, which is an overestimation. Wen et al. developed an adaptive large neighborhood search to minimize investment and operational expenses of homogeneous electric vehicle fleets [69]. Their approach analyzes the consequences of locating charging stations using an artificial dataset, however the authors do not consider investments in charging infrastructure.

3 Technical Fundamentals of BEB

The technical setup of electric buses is characterized by a wide range of different topologies ranging from trolley to hybrid to BEB. The differences between the topologies can be explained by differentiating between the consumer and supply sides. The consumer side consists of an electric drivetrain, which is responsible for the prolusion, and auxiliaries required for the remaining vehicle functions such as lighting, doors, and air condition.

The setup of the supply side characterizes the electric bus type. Various technologies (individually or combined) can be used to supply electricity to operations as shown in Figure 3-1. The term electric bus is often used as a synonym for the BEB. In the following however, a distinction is made between electric bus and the BEB as a specific type of electric bus.

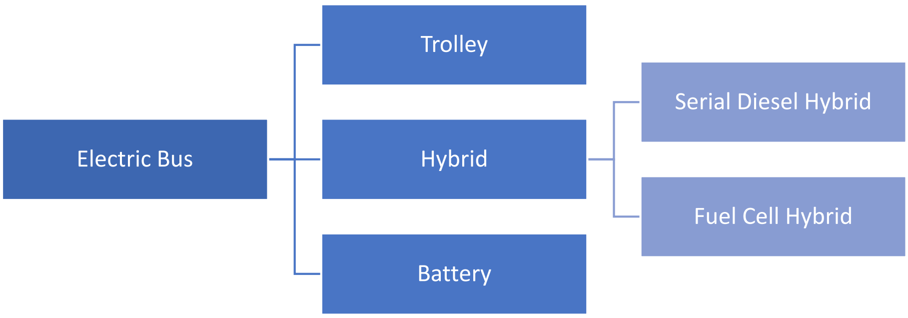

Figure 3-1: Electric bus concepts utilizing a full electric drivetrain clustered by their energy supply

A common electric bus concept regards the trolley bus, whose supply side consists of a direct connection to overhead catenaries which ensure sufficient energy supply at any time; however, the continuous connection severely limits flexibility. This issue is addressed by integrating energy storages in the buses, which enables partial operation without overhead catenaries [70]. Depending on the size of the energy storage, this configuration is also considered as a BEB with a charging possibility during driving.

Hybrid electric buses are characterized by the availability of two independent energy supply systems. The most common configurations regard the serial diesel hybrid and fuel cell hybrid, which are equipped with energy storage and internal combustion engine or fuel cell. A parallel diesel hybrid is excluded here due to the absence of a full electric drivetrain.

The availability of energy storage in a hybrid bus enables energy recovery during braking. The electric motor of the drivetrain operates as a generator in this case and charges energy for storage. This operating mode defines the minimum capacity of the energy storage following the available kinetic energy. The energy storage of the MAN Lion's City Hybrid for example has a capacity 0.4 kWh [71], which is sufficient to store the energy of braking from 50 km/h to standstill. In addition to regenerative braking, an energy storage can also be utilized to homogenize the load of the engine or fuel cell, which increases efficiency and enables downsizing.

The BEB regards the basic variant of an electric bus and is characterized by a comparatively small number of required components: drivetrain, auxiliaries, battery as the energy storage and a charging option. These components are introduced in the following subchapters.

3.1 Electric Drivetrain

The electric motor in BEB is usually designed as a central motor or wheel hub motor. Figure 3-2 provides an illustration of both configurations. By using a central motor, the electric drivetrain becomes similar to the diesel engine drivetrain, whereas wheel hub motor configurations utilize new degrees of freedom since the absence of a mechanical link between the driven wheels increases the low floor capabilities, which is one of the major optimization goals for public transport buses.

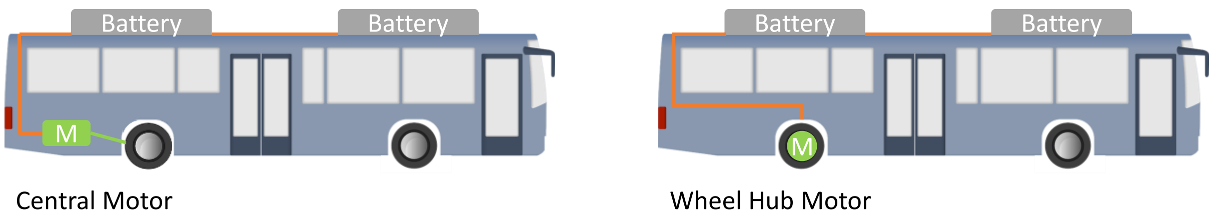

Figure 3-2: Schematic representation of a BEB with central and wheel hub motor configurations – electrical links are displayed with orange lines, mechanical with green

The central motor acts on the axle in the same way as a diesel engine via a transmission (fixed ratio for BEB in most cases) and differential. Wheel hub motors are mounted near or as part of the wheels (external rotor motor), which offers reduced space requirements and greater efficiency. Several components of the classic drivetrain (e.g., differential, gearbox etc.) are not required. However, wheel hub motors are much more exposed to environmental influences and physical stress compared to central motors, and the high weight of the wheels is disadvantageous since they are only cushioned by tire air. Such unsprung masses, including axles, shock absorbers and brakes, are usually kept as low as possible to ensure high comfort.

Central as well as wheel hub motor configurations are available in the current BEB market. The modeling of the drivetrain is described in Section 4.4.1.

3.2 Auxiliary Consumer

Besides the drivetrain, several additional components are required to operate a BEB. They can be divided into two categories based on their input voltage level – high voltage above 400 V and low voltage of about 24 V (standard voltage of the electrical system in a public transport bus). A general overview and assignments are provided in Figure 3-3.

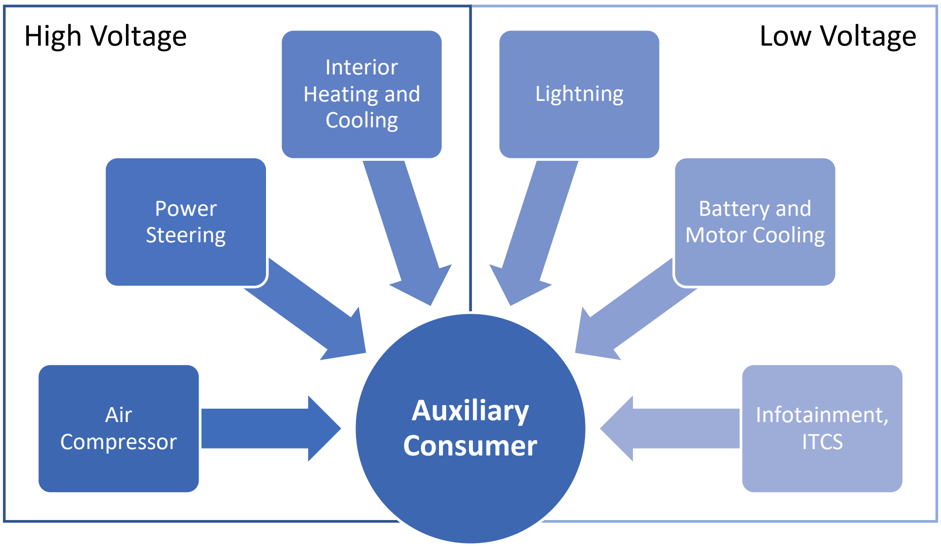

Figure 3-3: Auxiliary setup in a BEB with components clustered by voltage level

The different voltage levels indicate the varying power demand among the components. The main consumers fall in the high voltage category. In a diesel bus setup, air compressors or power steering are mechanically linked to the engine to satisfy the high power demand. In a BEB, they are powered by electric motors which require an input voltage in the range of 400 V to 800 V.

A further primary consumer regards the interior heating and cooling which is also named the heating ventilation and air conditioning system (HVAC). The heating during low outside temperatures entails high thermal demands and due to the absence of waste heat from a combustion engine, a powerful heating system is required, which in the case of pure electric heating systems cause significant range reduction [9]. This could be alleviated by utilizing heat pumps or a fuel heater. More details are provided in the model description in 4.4.2.1.

Components in the low voltage category are connected to the 24 V on-board supply which is buffered by standard lead acid batteries, closely corresponds to the diesel bus system. This power supply is required in every BEB for the startup process during which the high voltage system is switched off, however after it is switched on, the 24 V system is powered via a DC/DC converter from the higher voltage level. Further insight is provided in the description of the modeling approach in 4.4.2.2.

3.3 Charging Concepts

Every BEB requires an external energy supply to charge its batteries. Depending on the charging frequency and the charging power, two concepts can be distinguished: depot charging and opportunity charging. Figure 3-4 illustrates the infrastructure configuration with a single charging location for depot charging and three charging locations for opportunity charging. Both concepts not only entail operational constraints, they also determine the technical setup of the bus and design of the battery as explained in the following.

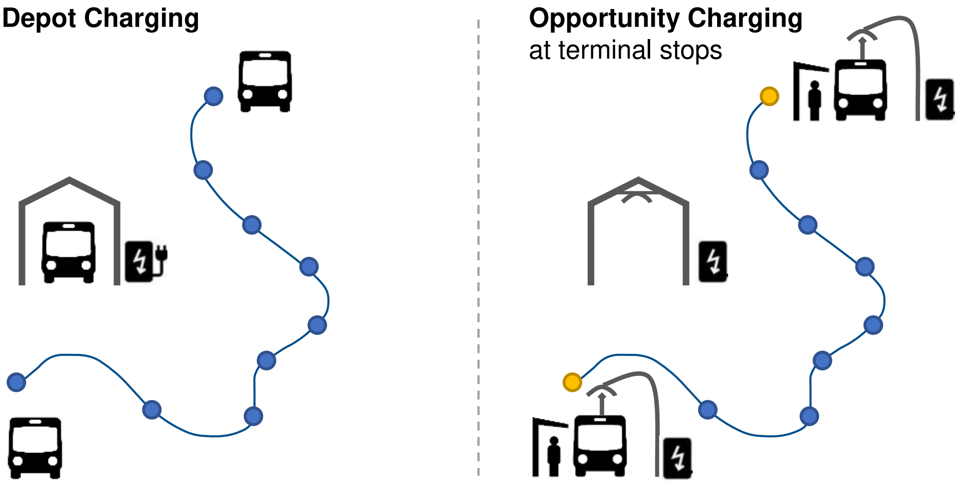

Figure 3-4: BEB charging concepts - Depot charging with charging infrastructure exclusively in the bus depot and opportunity charging with infrastructure at terminal stops and depot

3.3.1 Depot Charging

Depot charging describes exclusive charging in the bus depot, mainly overnight but also during longer dwell times throughout the day. This charging concept and its operating scheme closely correspond to diesel bus operations, however shortened bus runs may be required due to the limited range of a BEB.

The depot charging concept enables a concentration of infrastructure in the depot. The charging is mostly performed at moderate power levels (up to 150 kW) so that the battery stress on the one hand is relatively low. On the other hand, the infrequent charging (for example only once per day) increases the cycle depth of the battery.

The technical design aims at maximizing the range of the bus, which is achieved by minimizing electricity consumption, such as by using fuel heaters, and by maximizing the energy capacity of the battery. Therefore, batteries with high energy density are utilized. Nevertheless, there is always a tradeoff between battery capacity and passenger capacity due to gross vehicle weight limitations.

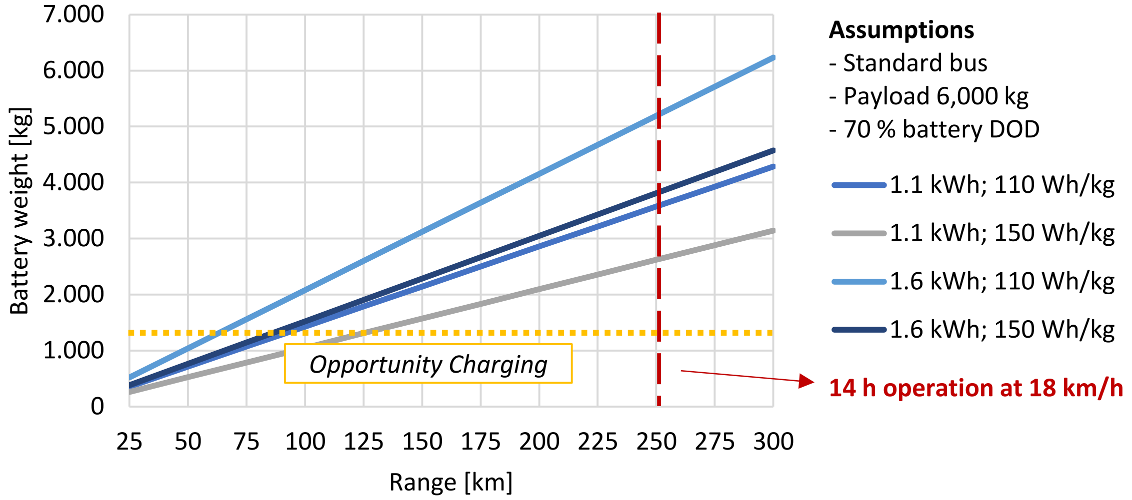

Figure 3-5: Exemplary battery weights of depot-charging BEB for varying energy demands and battery energy densities

Exemplary battery weights are illustrated in Figure 3-5 for the presented assumptions. The weight is calculated based on a given DOD, energy demand of the vehicle and energy density of the battery. The weight of a battery required for a 14 h operating day ranges from 2.6 t to 5.2 t and could therefore significantly reduce the passenger capacity of a standard bus. Using opportunity charging decouples the range from the required battery capacity, enables smaller batteries, and offers a potentially higher passenger load.

The operational efficiency of exclusive depot-charging operation is largely determined by the operating conditions. Bus routes with varying vehicle demand during peak and off-peak hours are potentially suited since off-peak hours can be utilized for longer charging breaks in the bus depot. However, as discussed in Section 1.1, achieving an entire fleet electrification without operational changes is highly unlikely.

3.3.2 Opportunity Charging

Opportunity charging extends depot charging by also charging the battery during the regular dwell times at stops, and it is particularly suitable for terminal stops due to the longer dwell times. Nevertheless, a high charging power of usually more than 300 kW is required to recharge from the previous trip during the available timeframe. This frequent charging makes the range and duration of the route operation independent of the installed battery capacity, as highlighted in Figure 3-5.

The high-power requirements of opportunity charging dominate the technical design. In contrast to depot charging, the entire system is optimized for high-power capability, requiring fast-charging batteries with efficient cooling.

The implementation of opportunity charging faces challenges in integrating infrastructure in public spaces such as the lack of space or complex construction measures. The lower flexibility of opportunity charging with deviating bus routes represents a significant hurdle as well, visiting terminals with charging infrastructure with regular frequency must be ensured. This underlines the strong linkage to the operational planning which defines the duration and frequency of dwell times at stops.

3.4 Charging Infrastructure

The charging infrastructure plays an important role in ensuring and increasing the daily range of BEB. A distinction is made between slow and fast chargers. Fast chargers are usually installed at terminal stops to enable opportunity charging, however standard chargers with lower outputs of up to 150 kW are used in depot charging.

The charging infrastructure considered in this thesis can be divided into three main components: the coupling system, charger itself and grid connection, as shown in Figure 3-6. The components are introduced in the following subchapters.

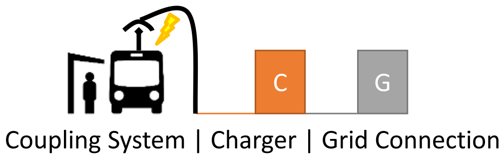

Figure 3-6: Charging infrastructure components considered in the thesis

3.4.1 Coupling System

The coupling system connects the bus with the charger (dc-connection) or directly to the grid (AC-charging). Various systems are available on the market, however conductive variants are the most widespread. In contrast to inductive charging, which is characterized by non-contact energy transfer, conductive charging utilizes a physical connection such as a plug or a pantograph.

Conductive Charging (manual plug)

Conductive charging via manual plug is familiar from the passenger car sector. Bus sector systems adopt the existing norms and utilize mostly identical plugs such as the Type 2 (AC connection) or Combo Type 2 (DC connection) also known as CCS plug (Combined Charging System) suited for charging according to IEC61851-1/23/24 [72–74]. Both plugs are shown in Figure 3-7.

Figure 3-7: Type 2 (AC-charging) and Combo Type 2 (DC-charging) plugs utilized as coupling system for BEB

The CCS plugs of coupling systems for BEB are limited to a charging current of about 200 A. Depending on the voltage of the battery system, the charging power can be up to 150 kW (in case of 750 V maximum voltage). Higher charging currents can only be achieved via liquid cooled plugs and cables, which are not currently applied in the bus sector.

The usage of standardized plugs entails interoperability between different manufacturers of vehicles and infrastructure. However, not only must the plug be compatible, but the communication protocol also needs to be standardized. The majority of bus manufacturers and infrastructure suppliers nowadays utilize a communication protocol according to ISO 15118, with cable-bound power-line-communication (PLC) [75, 76]. However, a few bus manufacturers have developed slightly different communication protocols which are not entirely compatible with ISO 15118 and require the charging system to be purchased with the bus and be bound to the bus, which thus reduces the interoperability.

Conductive Charging (automated)

In the case of fast charging, the conductive energy transfer is usually conducted through an automated contact via a pantograph as shown in Figure 3-8. The pantograph can be mounted on the vehicle roof or at the infrastructure side on the charging mast. Such systems are suitable for installation at bus stops to allow charging with high performance during operation within a brief dwell time.

Depending on the number of contact pins and the safety concept, the automated conductive coupling systems are divided into two categories:

- Grounded systems with four or five contact pin systems, which utilize two contacts for the energy transfer DC, one contact for the grounding and one or two contacts for the pilot lines PP-(Proximity-Pilot), CP (Control Pilot)
- Ungrounded systems with two contact pins solely for the DC energy transfer

Figure 3-8: Charging pantographs at terminal stops – stationary-mounted inverted pantograph (left), vehicle-mounted pantograph with charging hood (center) and vehicle-mounted pantograph with catenaries[2] (right)

In case of the four or more pin systems as shown in the left and center of Figure 3-8, charging according to IEC61851-1/23/24 and ISO 15118 is possible. However, this is not possible using only two contact pins such as with the Siemens Rampini buses in Vienna. Charging via two pins is comparable to trolley bus operation which requires additional safety measures such as doubled insulation.

In the case of automated depot charging, the vehicle roof-mounted pantograph is advantageous since the constructional measures for the installation of stationary-mounted inverted pantograph would be costly. Automated conductive coupling systems are for example used in the use cases Eindhoven and Amsterdam (see also Section 2.1.2).

Inductive Charging

Induction enables energy transfer without physical contact between the charging station and the bus. A street-side primary coil generates a magnetic field which is then converted into electricity by a secondary coil on the vehicle side and stored in the battery. At present, outputs up to 200 kW can be achieved with an efficiency of more than 90 % [77]. However, the actual charging capacity and efficiency depend on environmental conditions as well as the position and distance of the two coils. Due to the comparatively high costs and long-term nature of the structural measures at terminal stops, inductive charging is thus far not widespread in Europe.

Another reason for the limited adoption of inductive charging regards the depot charging situation which would require coils at every parking lot, which requires high investments. Therefore, the depot charging of such buses is performed via cable connection.

[2] Photography of Julian Ryf, 2017

3.4.2 Charger

The charger is responsible for the conversion from AC to DC or in special cases from DC to DC, allowing the battery to be charged with a full adjustable current. This is required since the battery voltage increases while charging and the current must be controlled to prevent exceeding power and voltage limits.

Internal and external chargers are used in the bus sector depending on the charging concept and desired charging power; however, their internal setup is comparable. A simplified schematic diagram of a charger is provided in Figure 3-9.

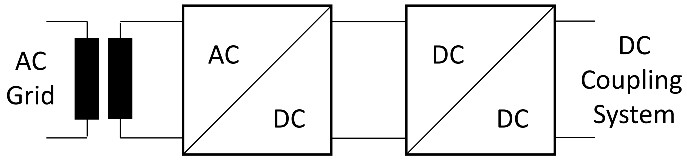

Figure 3-9: General setup of a DC-Charger for electric vehicles consisting of a transformer, a rectifier and a DC/DC converter

The transformer shown in Figure 3-9 is required due to IEC61851-1 which regards galvanic insulation between the AC input and DC output. The transformer contributes significantly to the weight of the charger and furthermore causes high charging power levels to only be realized using external chargers.

Figure 3-10: Mobile DC-charger from Ekoenergetyka and stationary charger from Jema

The product range offered by manufacturers begins at a charging power level of about 20 kW for mobile solutions and ends up to 600 kW for ultra-fast charging stations utilized in opportunity charging. Figure 3-10 provides an example of a mobile charger from Ekoenergetyka and stationary charger from Jema.

3.4.3 Grid Connection

The electricity grid connection ensures a continuous energy supply for the charging infrastructure. The three relevant options for the bus sector in Europe are shown in Figure 3-11. Further technical details are provided in Section 4.3.3 of this thesis.

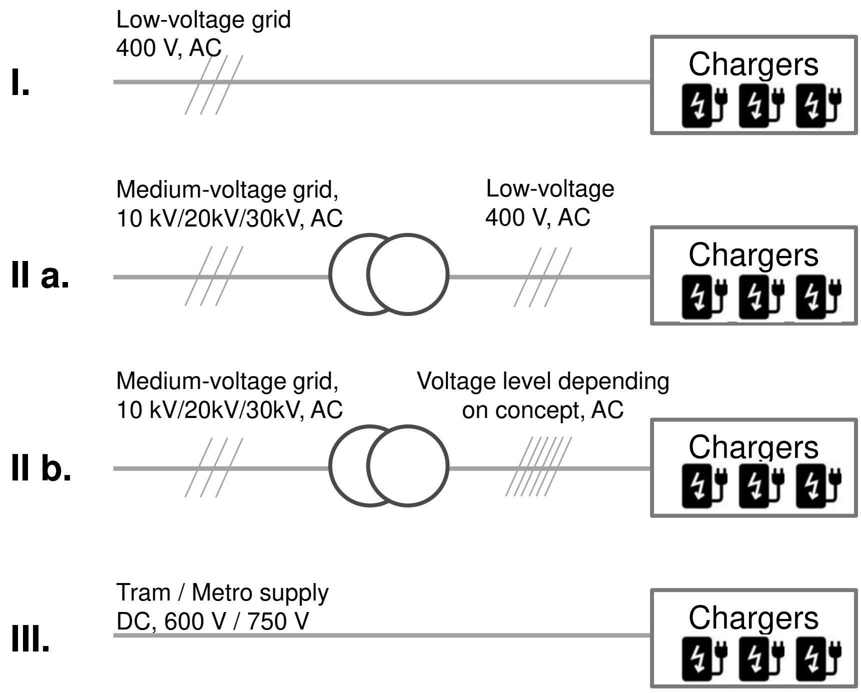

Figure 3-11: Charging infrastructure grid connection options

A connection to the - in most-cases - existing low-voltage grid (option I) has the advantage of relatively low investment requirements. However, the power which can be drawn is strictly limited and often insufficient for the charging of BEB (< 100 kW).

The supply for several chargers or even single fast chargers requires the medium-voltage grid connection (option II). The voltage level depends on the local network and ranges from 10 kV to 30 kV [78]. Such high voltage levels are not directly fed to the charger, but instead a transformation to the standard low-voltage level (II a) or to a specific voltage level defined by the charger (II b) is performed. The advantage of the standard low-voltage transformation (II a) is that standard transformers can be utilized. The alternative of transforming to a specific voltage level and potentially a higher number of phases provides the advantage of reduced interferences in the supply grid.

Direct DC supply is advantageous in some cases since transport companies often operate a DC grid for the supply of their trams or trolleybuses. Depending on the grid capacity, chargers can be connected to overhead catenaries or the supply station. However, although such systems have been implemented successfully such as in Oberhausen, suppliers are rare. An open topic in this matter regards additional galvanic insulation between the DC grid and the vehicle.

3.5 Energy Storage

The battery provides the namesake of the BEB and defines its characteristics to a large extent. The technical constraints of its performance determine the possible applications, and its costs largely determine the economic efficiency of the overall system.

Batteries for BEB are specially tailored to the respective application of obtaining the optimal system under given constraints. The following chapter discusses the demand of the BEB application, wherein the battery types utilized thus far are introduced and their general properties are explained. Finally, battery aging effects and their significance for BEB application are discussed.

3.5.1 Requirements from the Public Transport Application

In contrast to the passenger car sector, the operation of BEB in public transport is characterized by a long daily service and significant mileage despite low speeds. The yearly mileage of a public transport bus ranges from 50,000 km up to 80,000 km per year. In addition to intensive use, there is also high demand for reliability. The diesel buses currently used in public transport entail a high uptime due to their mature technology. A similar availability is also demanded for BEB [79], which highlights the demand for durable, high-quality batteries requiring minimal maintenance.

Depending on the charging concept, two properties are of importance. The exclusive charging in the depot requires a high energy density of the battery to ensure a long range. In the case of opportunity chargers, where the battery is charged at high power levels at the terminal stops of a route, the focus lies on the charging performance. Due to the frequent charging processes during the day, an ongoing operation with theoretically unlimited range can be achieved. Nevertheless, the energy density is not to be neglected here either since in the event of operational delays, charging times can be shortened or even eliminated in cases of defects in the infrastructure. The extent and duration of compensation in such cases depend on the range of the vehicles and thus on the energy content of the battery.

Depending on the location of operation and parking situation in the bus depot, the thermal behavior is also relevant. For example, fast charging must be ensured even at low temperatures such as when a vehicle is parked outdoors at night. These properties can be achieved either by a suitable choice of chemistry (e.g., Lithium-ion battery with LTO anode) or by appropriate measures at the battery system level such as heating systems [80, 81].

In the opposite situation such as in southern Europe, the energy storage system must also function under high temperatures, particularly regarding fast charging with high power levels. The temperature must be kept under a certain threshold in order to avoid exceeding stability limits and accelerating aging.

The major requirement for public transport buses regards high transport performance, i.e., the highest possible passenger capacity per vehicle. The transport capacity is primarily limited by the possible payload, and a low weight thus represents an essential requirement for energy storage systems. Modularity is mandatory to enable a certain weight distribution between the axles of a BEB, as the volume is furthermore limited depending on the installation location, e.g., in the former engine compartment. Safety and crash protection requirements correspond to the passenger car sector. Monitoring the energy storage ensures that critical conditions are quickly detected and safely addressed, and corresponding requirements from standards such as the ECE R 100 apply for BEB as well.

3.5.2 Energy Storage Types

One of the first BEB prototypes was introduced in 1970 and operated in Düsseldorf, Koblenz and Munich [82]. The electric-powered bus was based on a MAN metro bus powered by a lead-acid battery from Varta. The vehicle is shown in Figure 3-12.

Figure 3-12: BEB prototype of MAN operated in Düsseldorf (Germany) by the PTO Rheinbahn

The battery with a weight of more than 4 t and an energy content of about 160 kWh was accommodated using a separate trailer (visible behind the BEB in Figure 3-12), which offered advantages in terms of weight restrictions and simple battery replacement. During operation in Düsseldorf, the batteries were firstly charged overnight at the depot and later at a terminal stop. Due to its limited life span, high costs and limited energy content of the battery, the operation was discontinued in 1988. This underlines the dependence of the success of a BEB concept on the battery.

A few years later in 1993, a MAN midibus was tested in Munich [82]. Instead of a lead-acid battery, a sodium nickel chloride battery was utilized, which is a so-called zebra high-temperature battery. Zebra batteries were also used in hybrid buses by the bus manufacturer Daimler in the 1990s [83], and this battery type is currently used in the Irizar i2e with a capacity of 376 kWh [84]. However, the moderate energy density of zebra batteries and the measures for thermal conditioning hinder their broad use in mobile applications [85].

Nickel-metal hydride batteries (NiMH), which have been used in large quantities in the passenger car sector, e.g., in the Toyota Prius, are of minor importance in the field of BEB. They were mainly used in hybrid systems such as the H2-Bus NRW in combination with double-layer capacitors [86]. The so-called supercapacitors were installed to improve the performance of the overall system.

The majority of today's BEB are equipped with lithium-ion batteries, whose design and performance are characterized by a wide range of possible solutions as shown in Figure 3-13. The areas marked in the figure represent possible design variants of lithium-ion batteries, whose systems can be optimized for either high performance or high energy density. There is no optimal variant maximizing both requirements, which means that a compromise must be found for each application.

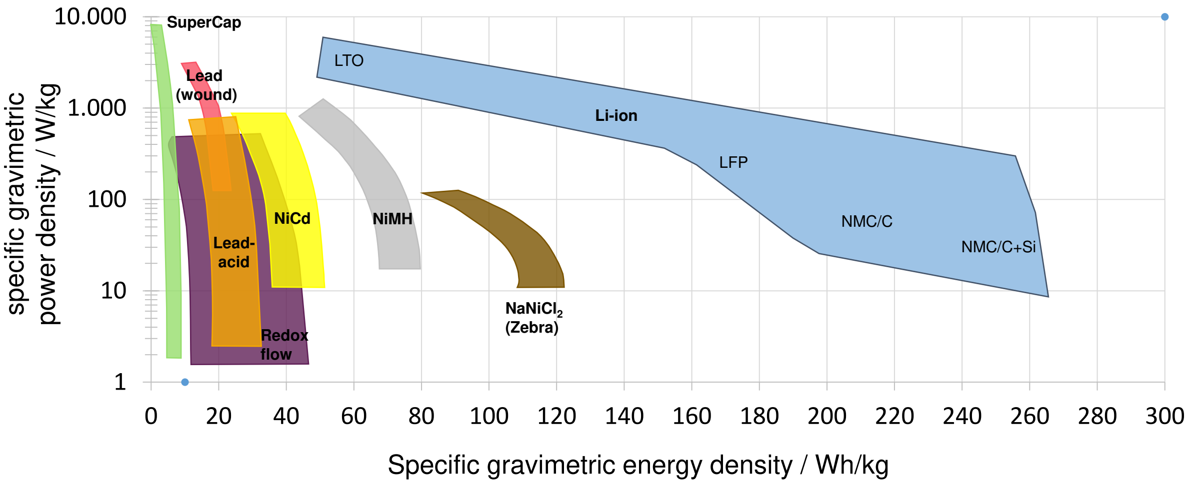

Figure 3-13: Specific power and energy density of current battery technologies

Lithium-ion regards the collective term for different cell chemistries and describes the principle of energy storage in which positively charged ions are exchanged between electrodes. The cathode and anode of a lithium-ion battery are separated by an ion-permeable separator surrounded by electrolytes, and the active material required for the general function of the cell is applied to the electrodes. In common cells, a combination of materials is used as listed in Figure 3-14. Common cathode materials are nickel manganese cobalt (NMC) and lithium iron phosphate (LFP). Graphite and lithium titanate (LTO) are the common anode materials for batteries utilized in BEB.

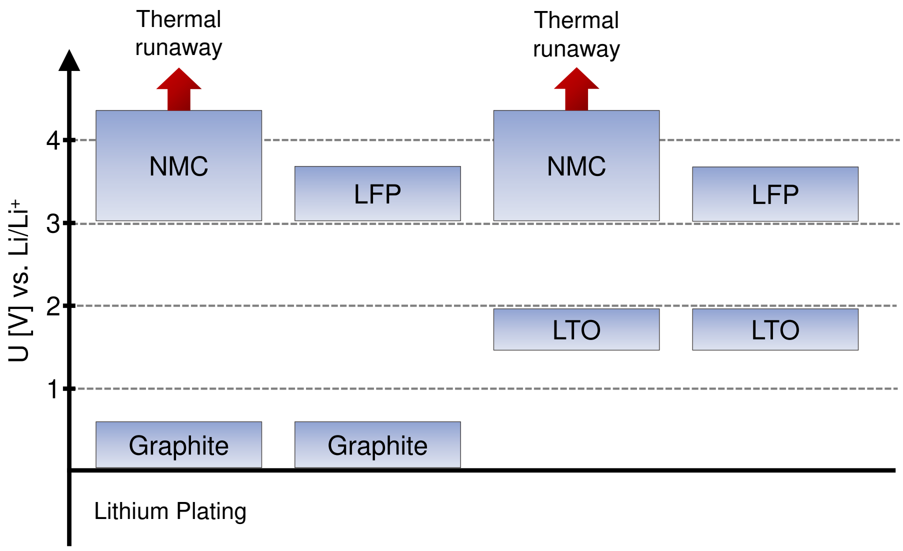

Figure 3-14: Voltage level of common active materials in lithium-ion batteries

The different voltage levels of the combinations shown in Figure 3-14 lead to different energy densities. The clearest difference lies between NMC/Graphite and NMC/LTO cells. The advantage of the lower anode potential of graphite positively affects energy density, however there are negative consequences regarding performance at low temperatures and fast-charging capability due to the low voltage gap towards lithium metal (Li/Li^+). The anode potential can drop below 0 V at high currents and low temperatures, which induces aging effects as lithium plating [87]. The maximum charging performance is therefore reduced for NMC and LFP cells with graphite anode compared to cells with lithium titanite anode.

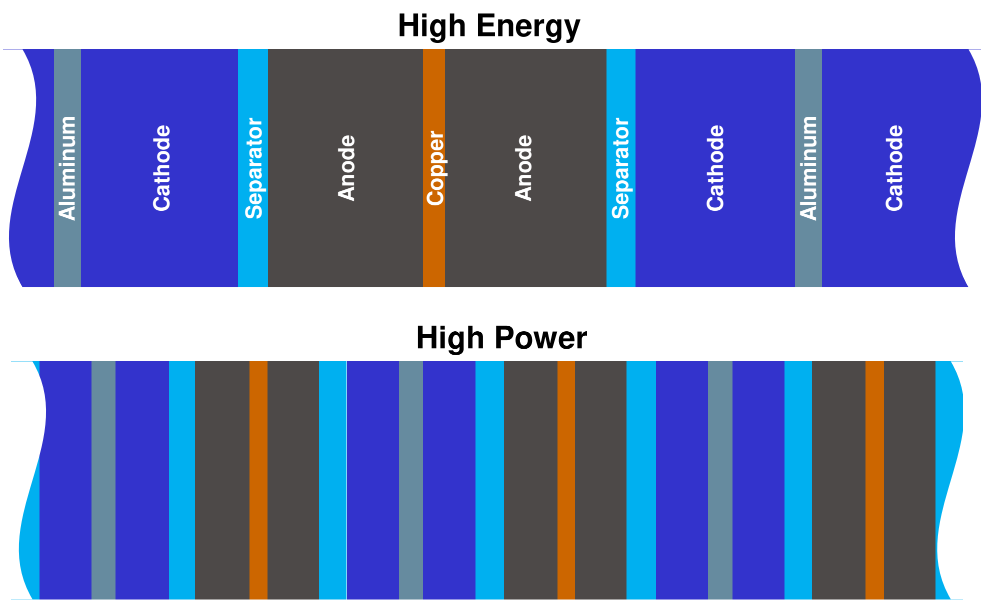

Figure 3-15: Schematic structure of high energy and high power lithium-ion batteries

In addition to the cell chemistry, the internal structure of the cell represents a further decisive factor. Characteristic at the cell level is the ratio of active to passive material, such as current conductors and connectors. High performance requires high currents which in turn require appropriately dimensioned conductors, which results in an increased proportion of passive materials in the cell. Figure 3-15 shows the schematic structure and illustrates the thickness of the individual layers.

Thermal management is important on the battery pack level, as sufficient cooling must be provided to dissipate heat, especially in the case of a fast-chargeable batteries. Three different systems are currently used for cooling:

- air cooling
- water cooling
- coolant cooling

Air and water cooling represent the most common systems in today's BEB. Water cooling enables a compact design whereas air cooling is robust and simple. The additional elements of a cooling system increase the proportion of passive components in the system and reduce energy density.

The selection of cell chemistry, cell design and battery pack design highlight the conflicting requirements of a battery which can be optimized either for high energy density or high charging power. This must be considered in electrification concept development. However, in the actual design and sizing of components it is important to focus on the relative load. For example, fast charging with 300 kW induces relatively moderate battery stress for a 400 kWh battery.

3.5.3 Aging Effects and their Significance for the Application

The aging mechanisms of batteries are highly complex and strongly depend on operational conditions. This subchapter discusses the general aging effects, the consequences of aging on the technical performance of the cell and the effects on the BEB application.

In the case of lithium-ion batteries, a distinction is generally made between calendar and cyclic aging [88]. Calendar aging occurs without usage of the battery and thus regards degradation during storage. The effect is influenced by storage conditions, especially by temperature and SOC [89–92], where the higher the storage temperature, the higher the aging rate [93].

The cyclic aging of a lithium-ion battery results from its actual use and depends on the energy throughput [88]. The literature also studies the dependence on the cycle depth, i.e., the depth of discharge (DOD) between two charging processes in relation to the total capacity [94]. Special situations, such as the charging of a lithium-ion battery with graphite anode at temperatures below 0° C, can significantly contribute to aging due to lithium plating, which occurs when the anode potential becomes negative [95].

Such effects are however excluded from the scope of this thesis since they do not represent normal operation where the battery management system prevents problematic low-temperature charging.

The consequences resulting from the various aging mechanisms can be divided into two categories. Aging firstly reduces the amount of free lithium in the cell which reduces its capacity. A typical capacity curve over full cycle equivalents (FCE), based on the energy throughput divided by the initial cell capacity, is shown in Figure 3-16 for an LTO cell analyzed in the framework of this thesis [96].

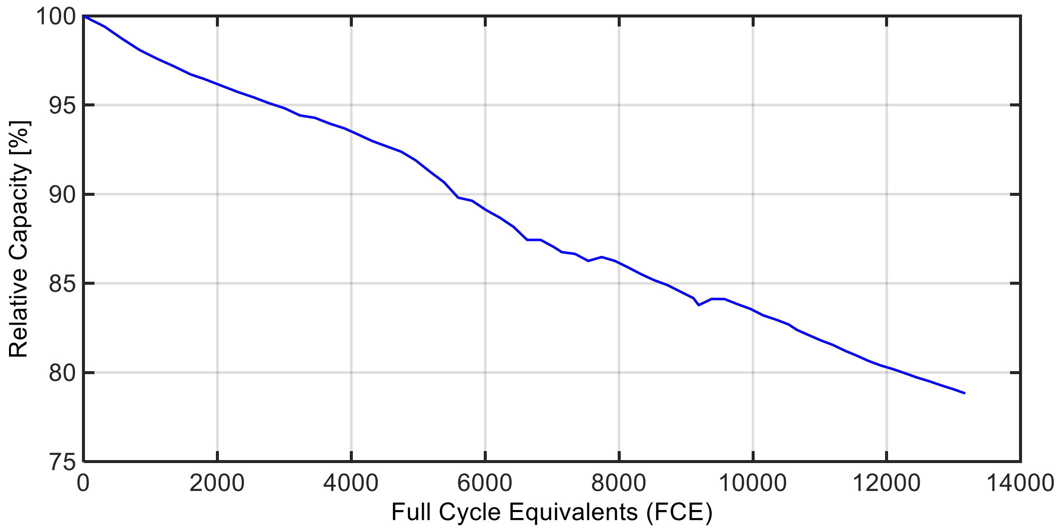

Figure 3-16: Aging Test Results - Capacity fade of a LTO battery cell over Full Cycle Equivalents (FCE)

The LTO cell has its full capacity (100 %) at the beginning of the aging test with 5C full cycles. The capacity diminishes over time due to cyclic and calendar aging. A residual capacity of 80 % is usually defined as the end-of-life, at which point a battery in the bus would be replaced. The LTO cell tested provided 12,000 FCE, which regards a competitive value compared to the lifetime of tested NMC cells, which is about 4,000 FCE.

The reduced capacity causes a decreased range of the BEB. There are two options to consider this effect in the planning and operation of the buses. Either the PTO uses the full capacity of the battery and adapts its operation to the decreasing range, or a capacity reserve is included in the planning to ensure that the BEB has a constant range over the entire lifetime of the battery. The latter option is usually chosen in current implementations to achieve stable operation throughout the year.

The second aging effect regards the increase of the internal resistance of the cell, which is partly due to the increase of the solid-electrolyte-interface (SEI) layer. The internal resistance defines the voltage drop during discharge and therefore the losses.

The increase leads to higher losses and a reduced usable energy capacity. Furthermore, it influences also the charging by increasing charging time and cooling demand.

A doubling of the internal resistance is often used as a criterion for determining the end-of -life. Figure 3-17 shows the course of the internal resistance over usage at various SOC for the tested LTO cell. When designing fast-charging solutions and thermal management, the losses at the end-of-life must be considered in order to prevent overheating, otherwise the charging current must be reduced which prolongs the charging process.

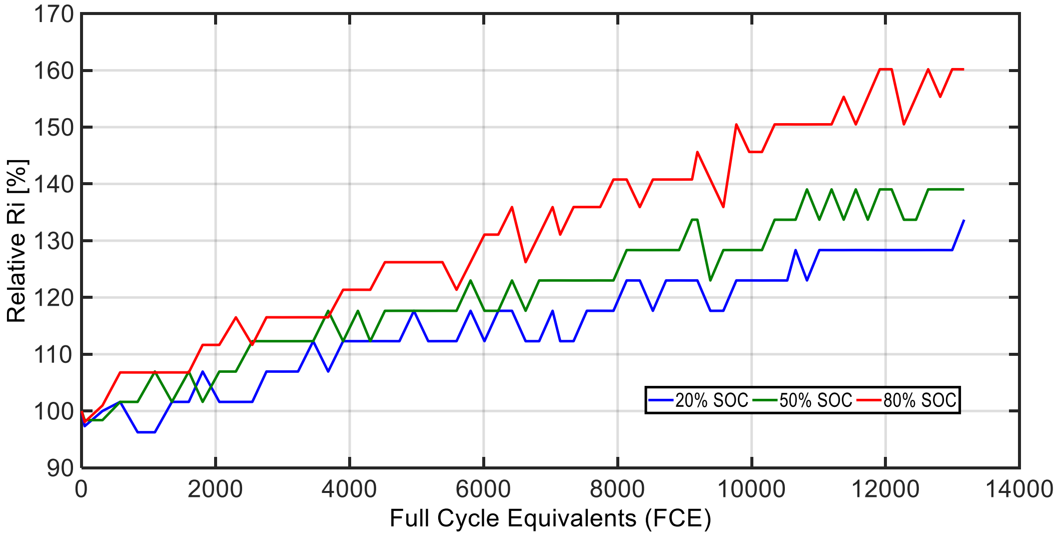

Figure 3-17: Aging Test Results – Internal resistance increase of a LTO battery cell over Full Cycle Equivalents (FCE)

4 BEB System Model

The software toolchain developed in this thesis builds on the technical fundamentals introduced in the previous section, which are modeled within the BEB system model and enlarged regarding LCC and emission calculations. This core functionality is tailored for usage within the technical operational analysis (Section 1) and provides all required measures to assess and evaluate the electrification potential of a bus network, from the assessment of the general technical feasibility to the calculation of costs and mitigation potential. Furthermore, this work provides the framework for an in-depth analysis and modification of the operational scheme within the technical and operational analysis.

The modeling approach is designed to analyze entire bus networks with several hundred vehicles. Therefore, efficient data gathering, and modular modeling are crucial. A strict separation between the general modeling of a BEB system and scenario-specific input is applied. Figure 4-1 provides an overview of the modular structure of the model and its interfaces. The model and the entire software toolchain are based on Matlab [97].

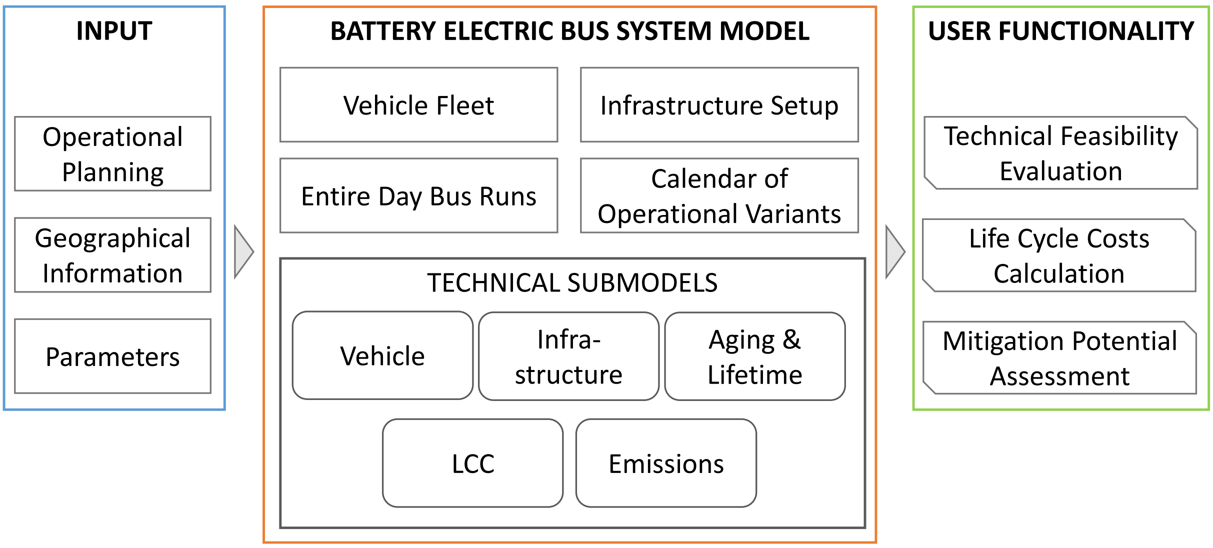

Figure 4-1: Modular structure of the BEB system model, the required input data and the offered functionality for the user

Three main inputs are required to setup the BEB system model. The entire operation of the BEB system is defined by its operational planning, which corresponding data-gathering procedure is described in Section 4.2.1. Geographical information regarding the bus route and position of bus stops is crucial for the vehicle simulation. Available data sources and data extraction methods are introduced in Sections 4.2.2 to 4.2.4. The third input named "model parameters" summarizes all input data required to initialize the technical submodels. These parameters are stored in editable Excel files to allow simple adjustment and exchange between different projects. The individual parameters are introduced in the submodel description.

4.1 Modeling Framework

The aim of the BEB system model is to analyze the BEB operation at a PTO over the entire usage period. Since these periods usually span twelve or more years, a continuous time simulation is not useful. So recurring operational scenarios must be instead identified, which can be analyzed separately and afterwards combined. This functionality is provided by the developed modeling framework.

The central element in the planning of PTOs regards the bus run which sums individual trips to determine an entire day's operating profile of a vehicle, beginning and ending at the bus depot. Thus, the time and locations of the vehicle operation are defined. Bus runs are furthermore clustered into day types which regard recurring daily planning scenarios for the entire fleet. The assignment of day types to dates in the calendar defines the operation, whose structure is illustrated in Figure 4-2.

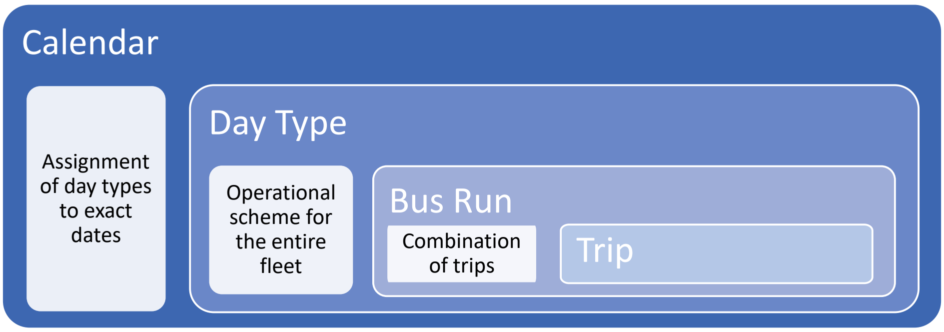

Figure 4-2: Separation of planning data at PTOs

The modeling framework adapts the structure of bus runs and day types. However, instead of focusing on individual dates in a calendar, the number of occurrences of day types within one year is set as an attribute of each day type, as illustrated in Figure 4-3. This model reduction significantly reduces the number of scenarios but disables the ability to consider individual days with varying temperature conditions throughout the year. Instead, a general average case is introduced based on the temperature distribution histogram of an entire year (see Section 4.2.5). Furthermore, the minimum and maximum temperature levels are identified and used for the worst-case definition. The number of temperature conditions can therefore be reduced to three (average, minimum and maximum).

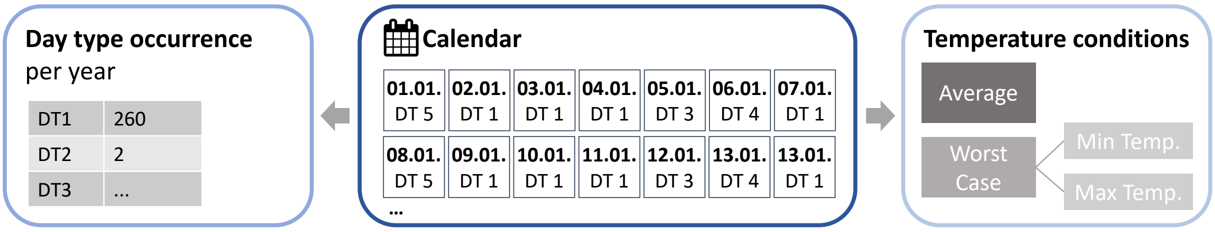

Figure 4-3: Model reduction by the extraction of day type occurrence and temperature conditions

The core of the modeling framework is shown in Figure 4-4 which highlights the input data setup with the bus run defined as the root. In this representation, neither the fleet size nor the actual number of charging stations are provided as fixed input, but instead both figures are determined based on the input data during initialization.

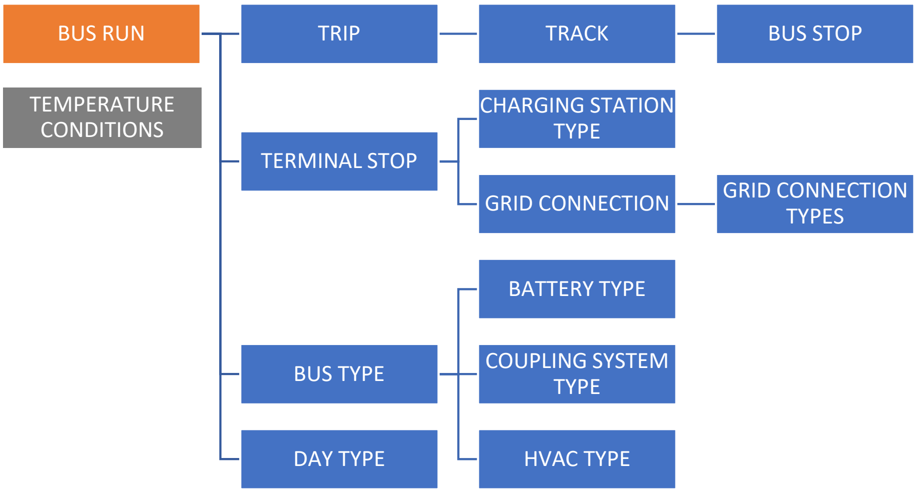

Figure 4-4: Elements of the modeling framework with the bus run as root

The bus run consists of several trips (in passenger service or deadheading), and each trip has a defined start and end time as well as a start and end location at terminal stops. The course of each trip is stored in the track element which is linked to the individual bus stops visited during operation. In addition to start and end locations, the bus run also defines the presence of vehicles at terminal stops. The terminal stop element consists of a name, a classification of whether the terminal stop is a bus depot or not, the number of directions at each stop and the maximum number of charging locations allowed for each direction. It is furthermore lined to a charging station type and a grid connection. The element charging station type contains the technical parameters describing the charging station, parameters for the aging simulation and financial figures utilized in the LCC. The element grid connection consists of a link to grid connection types along with the technical, aging, and financial figures for the different grid connection options.

Each bus run is linked to a single bus type. Basic technical specifications of each bus type e.g., size (e.g., length), weight and the installed traction system, represent attributes of the bus type element. Additional technical parameters are implemented as references to the elements battery type, coupling system type and HVAC type.

The reference of each bus run to a certain day type regards two functionalities. Firstly, the actual number of operations in one year can be determined for each bus run since the occurrence of day types in one year is extracted from the calendar and set as an attribute of each day type. This figure is required to calculate energy consumption, aging, and costs. The second functionality relates to the simultaneity of bus runs as all bus runs linked to the same day type are operated in parallel on one day. This information is necessary to assign charging stations and to verify the technical feasibility in fleet operation, which can for example be challenged by infrastructure shortages.

The bus runs are processed during initialization of the BEB system model. First the bus fleet is generated and the required number of buses of each type are determined based on the maximum number of bus runs simultaneously operated for all day types, as illustrated in Figure 4-5. An additional vehicle reserve is considered based on the desired reserve defined in the scenario parameters.

Bus run	Day type	Bus type
Bus run 1	Monday - Thursday	A
Bus run 2	Monday - Thursday	A
Bus run 3	Friday	A
Bus run 4	Monday - Thursday	B

Two BEB of bus type A required

One BEB of bus type B required

Figure 4-5: Fleet generation in the initiation of the modeling framework based on simultaneous day types

During this process, the bus run focus shifts towards the bus fleet and individual buses. A bus run assignment is generated which links the individual vehicles with bus runs. For each bus, the number of operations on a certain bus run per year is defined based on the occurrence of day types. The modeling framework is initiated using a uniform distribution so that each bus of a certain bus type operates the bus runs at the same frequency. An exemplary assignment is illustrated in Figure 4-6. This distribution can be manually adjusted by the user to account for bus-run- or route-specific assignments of individual vehicles.

The next step in initializing the modeling framework covers the infrastructure setup. The number of charging stations at the terminal stops are determined based on the simultaneity information provided regarding the bus runs. The required number of charging stations results from the maximum number of vehicles present at the terminal stop at the same time for all day types.

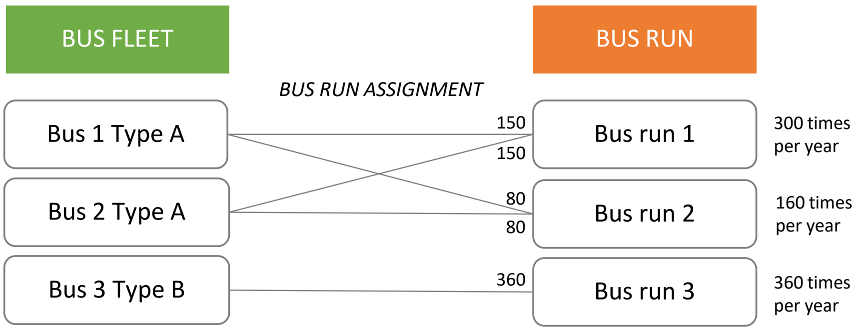

Figure 4-6: Assignment of individual buses to bus runs and definition of the operational frequency

This process considers constructional constraints such as the limited number of charging stations for one direction. Terminal stops not suited for the installation of charging infrastructure can be excluded by defining zero possible charging stations per direction. Charging stations are assigned to the actual charging phases in the bus runs by the infrastructure submodel.

4.2 Preparation of Input Data

The efficient operation of several thousand bus trips per day represents a major planning task for which transport companies utilize software tools. Basic operational data are therefore digitally available and can be used as the basis for the BEB system model.

The data gathering methods developed in this thesis utilize existing digital data. At first, the general basis is established by identifying tracks, trips and bus runs using the provided operational data. The input data gathered in the process are characterized by a high quantity describing every potential operational scenario. However, the data quality is not sufficient for direct usage in models and simulation, and therefore the following subsections describe an enhancement of the raw data.

4.2.1 Operational Data Acquisition

Operational planning at PTOs is characterized by high diversity. The individual planning clustered into day types differs regarding operational adjustments such as due to weekdays but also school holidays, public holidays or similar. Depending on the size of the transport operation and continuity of the planning, the number of day types varies significantly.

Figure 4-7: Relevant elements of the VDV public transport data model and their relation

All planning variants and corresponding day types must be included to develop a sophisticated electrification concept, for which purpose manual data processing is limited. Therefore, a data interface was developed for existing software solutions. The interface is based on the VDV public transport data model which follows VDV publications no. 451, 452 and 455 [98–100]. Almost all operational planning software (e.g., IVU Plan and Giro Hastus) can provide data in this format with minimal user effort.

Figure 4-7 shows the relation between the different data elements. The VDV public transport data model was designed for the exchange of planning scenarios between different software tools rather than explicitly for the BEB operation. Therefore, additional sources must be utilized to model the real-world operation especially regarding:

- Vehicle weight (passenger occupancy)
- Deviations from the planned operation, especially delays

The vehicle weight is relevant for the energy consumption calculation and directly linked to the occupancy of the buses. Transport companies determine the occupancy of their vehicles by counting buses and register all entries and exits via counting devices at the doors. These data are however not available in a standardized export format and therefore manual data processing is required. The vehicle occupancy is modeled tripwise as an upper bound considering the maximum occupancy measured for the entire trip.

Deviations from the planned operation must be considered to determine a robust solution which fulfills the requirements of the real-world operation. Delays are especially critical since they extend the trip duration and potentially reduce the charging time available after the trip. The missing standard for the exchange of such data also requires a manual data processing. The developed data model can handle route-, direction- and time-specific delay information.

4.2.2 Routing of Deadhead Trips

Deadhead trips regard the binding elements between service trips in bus runs. At least deadhead trips are required to pull-out from the depot at the beginning of the shift and pull-in at the end of the shift. The limited range of the BEB and required charging times make it necessary in many cases to modify the operational planning in the process of electrification. The adjustments could require additional deadhead trips potentially not included in the raw data.

The determination of the distance and travel time of additional deadhead trips requires a routing. Two well-known providers of such point-to-point routing are Google Maps[3]

[3] https://maps.google.com

and Bing Maps.[4] Given the geo coordinates of the start and end locations they can compute the path based on cartographic material.

Because a bus network consists of several terminal stops with a high number of potential connections, a manual route-by-route routing would be highly time consuming. For this purpose, providers (e.g. Google Maps, Bing Maps and Graphhopper) offer matrix routing, which computes all possible routes within an NxN matrix. An interface to the commercial Graphhopper routing API has been developed in this thesis to utilize such functionality.

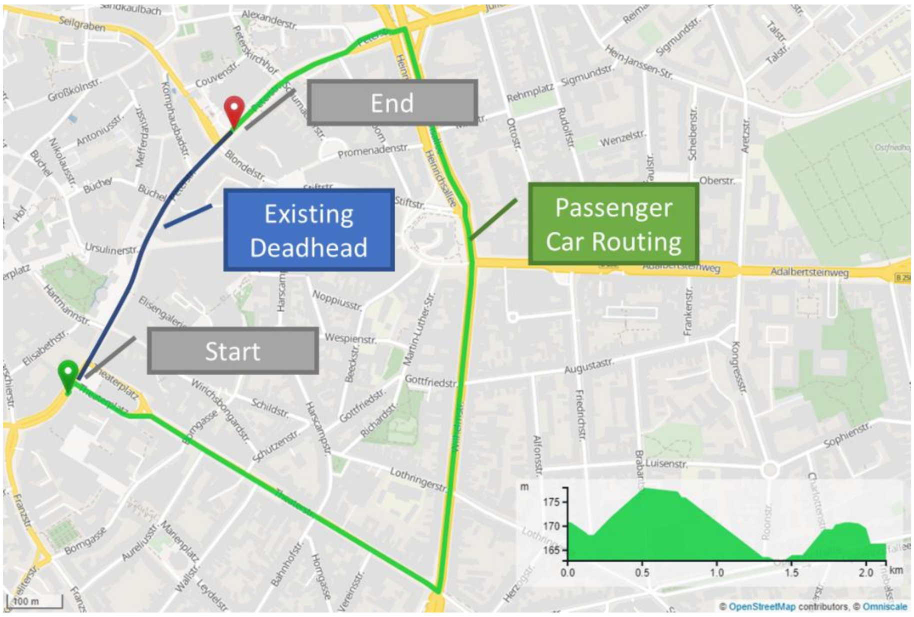

Figure 4-8: Comparison of a deadhead trip routing between two geographical locations and the original deadhead trip as operated today in the city of Aachen. The routing in this example does not make use of bus lanes causing that the distance is significantly longer.

By default, the routing in Graphhopper[5] considers passenger cars. It is furthermore possible to change the vehicle type to truck or bicycles. However, there is no routing option for public transport buses, which means that routing may not use dedicated bus lanes or similar. An example is shown in Figure 4-8, highlighting the significant difference between the existing deadhead trip in the raw data and the result of a Graphhopper routing for passenger cars in the city center of Aachen.

The example in Figure 4-8 reveals the necessity to evaluate and improve the results of the matrix routing, which is performed via an automatized process using the data of existing service and deadhead trips which serve as an upper bound. The procedure is

[4] https://www.bing.com/maps
[5] https://graphhopper.com/maps/

subsequently described for the distance of the deadhead trip and is applied for the duration as well within the software.

In an initial step, the matrix routing results are compared with the distances of existing routes and deadhead trips. If the distance of the matrix routing exceeds the distance of the raw data trips, it is replaced by this value, which could cause inconsistencies in the matrix. Inconsistencies are present when a point-to-point connection can be reached via different paths with different total distances. A simplified example is shown in Figure 4-9 where the distance from B to C was reduced from 10 to 8 via the raw data comparison. The path from A via B to C now has a value of 10, whereas the direct distance from A to C is 12.

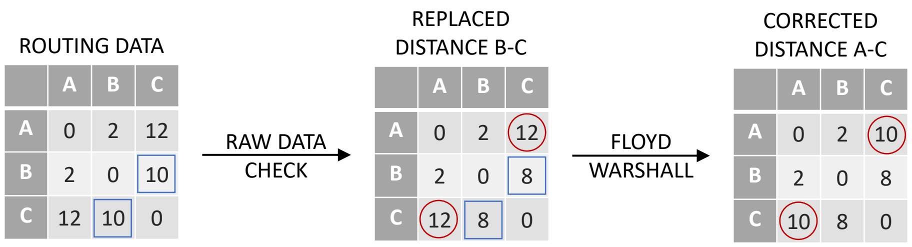

Figure 4-9: Process of improving distance data obtained from the Graphhopper matrix routing - Distances are replaced by values from the raw data followed by a check and repair of inconsistencies using the Floyd-Warshall algorithm

The repair of the adapted matrix is performed using the Floyd-Warshall algorithm [101, 102], which determines the shortest paths between all node pairs of a graph. Deviating elements of the matrix are replaced by the shortest distance, which in Figure 4-9 concerns the paths between A and C. The result is a consistent distance matrix for all routes validated by the raw data. This adjustment is especially important for the preparation of energy-based vehicle scheduling in order to avoid implausible conditions during the creation of bus runs. The resulting deadhead distances and durations are stored in a matrix and assessed during the energy-based vehicle scheduling.

4.2.3 Track Model

The energy consumption of BEB is influenced by the track characteristics. All tracks operated on a certain day type can be identified in the operational data, however the track details offered are limited as the track is only represented by a few intermediate points, which is insufficient to simulate the energy demand. Therefore, a more sophisticated track modeling is required.

The developed track modeling approach in this thesis is based on open-source routing data from Openstreetmap[6] and is universally applicable to any location worldwide. Openstreetmap regards an open database in which users can enter geoinformation and includes a built-in feature for the mapping of bus routes, which is utilized in this work's modeling approach.

Urban areas are characterized and modeled in high detail in Openstreetmap. However, the data quality must always be questioned since each user can upload content without a review process. This threatens the general validity of the data as well as the format due to unstrict conventions for the tagging and naming of elements. Therefore, a software toolbox has been developed which combines the data extraction with replace and repair functions.

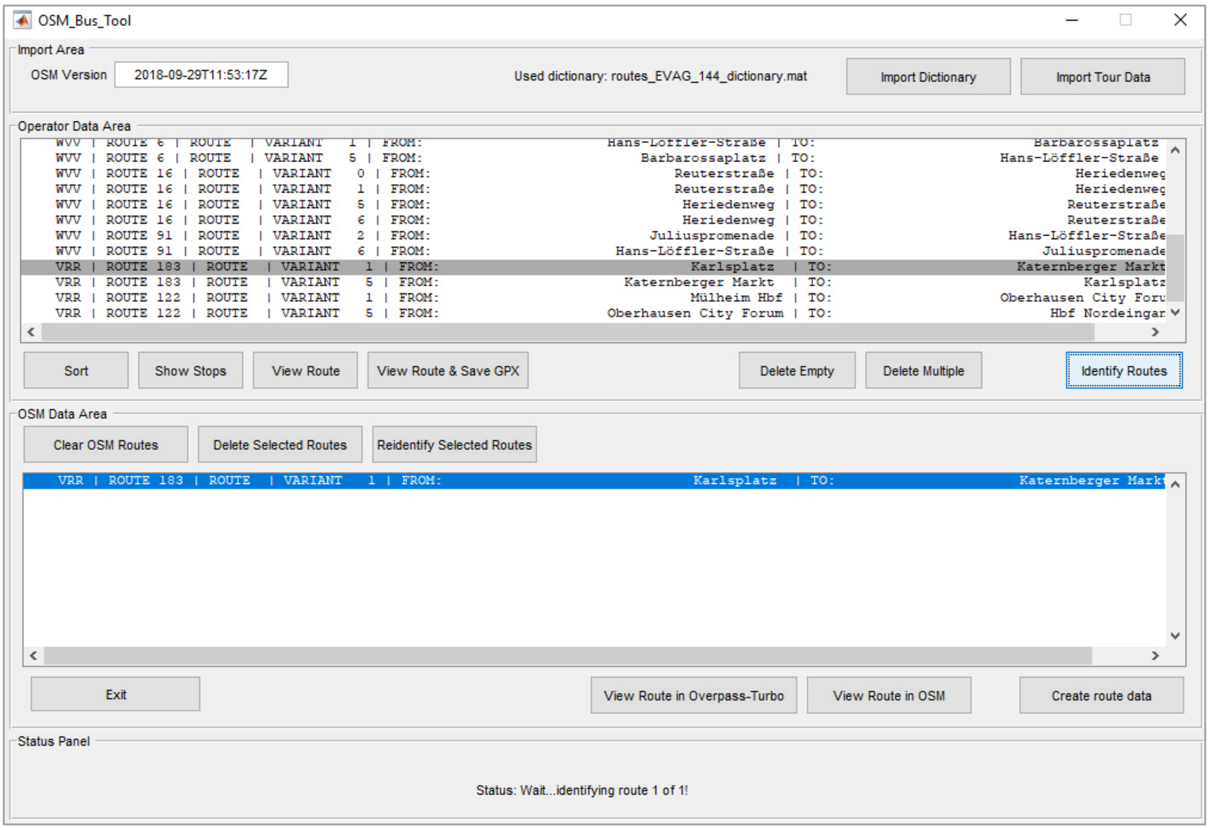

Figure 4-10: GUI of the OSMBusToolbox enabling an identification of bus routes in Openstreetmap

The entire process of the track modelling has been integrated in a guided user interface (GUI) called the OSMBusToolbox shown in Figure 4-10. Available information from the raw data is combined with the Openstreetmap geo data and prepared for manual

[6] https://www.openstreetmap.org

review by the user, who can verify and improve the data using the graphical editor JOSM[7] (Java-OpenStreetmap-Editor) shown in Figure 4-11.

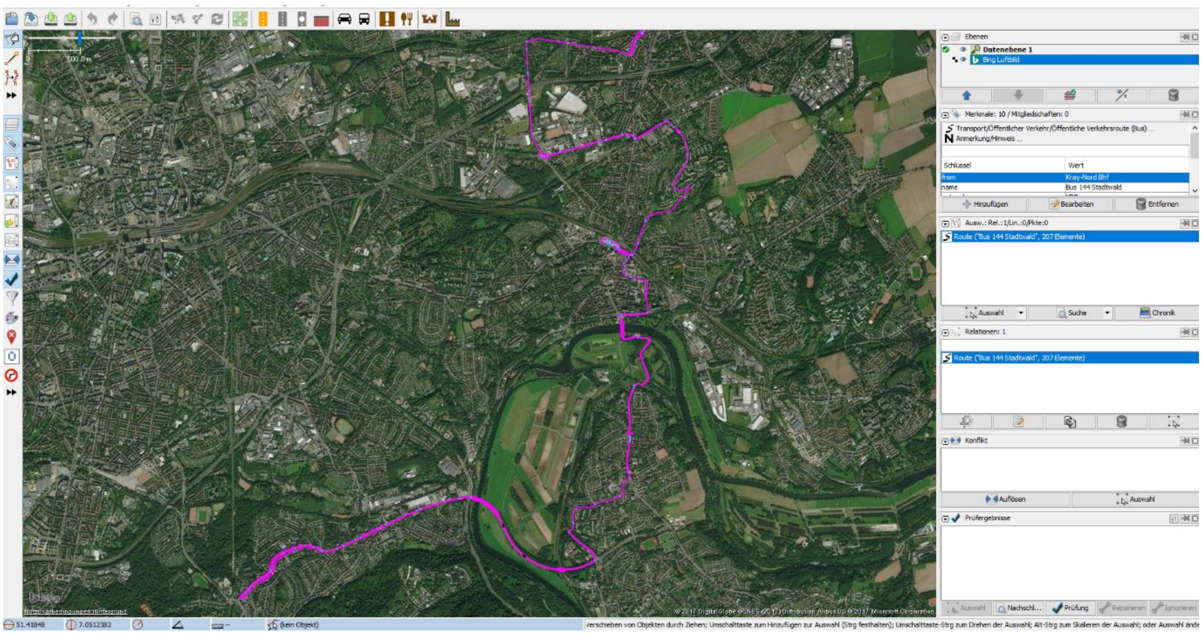

Figure 4-11: JOSM editor utilized within the OSMBusToolbox for the modeling of tracks

A first indication of the track is provided by the geocoordinates of the bus stops from the operational data. The OSMBusToolbox enables the user to conduct a Graphhopper routing based on these data which results in a rough approximation of the track. The user can afterwards display the routing in the JOSM editor and adjust the track. Once the track is completely modeled in the editor, it can be saved locally or directly in the Openstreetmap database.

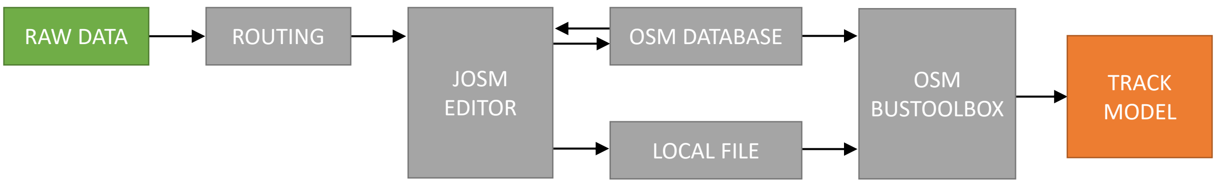

Figure 4-12: Track-modeling process implemented in the OSMBusToolbox

The track can be read by the OSMBusToolbox from a local file or the public database. The toolbox performs consistency checks in addition to data extraction and, if necessary, informs the user of implausible data. Because Openstreetmap regards a 2D mapping platform, the height is not included in the output. The toolbox provides two options for adding height data in an automatized process: either SRTM elevation data

[7] https://josm.openstreetmap.de/

from NASA [103] or elevation data from Google Maps. A flowchart of the entire process is shown in Figure 4-12.

The track model created with this procedure can be used in the vehicle model to simulate the energy demand. In addition to the physical modeling of the track and the slope of the bus route, the model provides data for the driver model regarding the location of bus stops and traffic signals as well as the permissible maximum speed for every section.

4.2.4 Bus Stop Modelling

Each route begins and ends at a terminal stop. Because these stops are frequently visited and vehicles often have a certain dwell time there, they are potentially suited for installing charging infrastructure to enable opportunity charging.

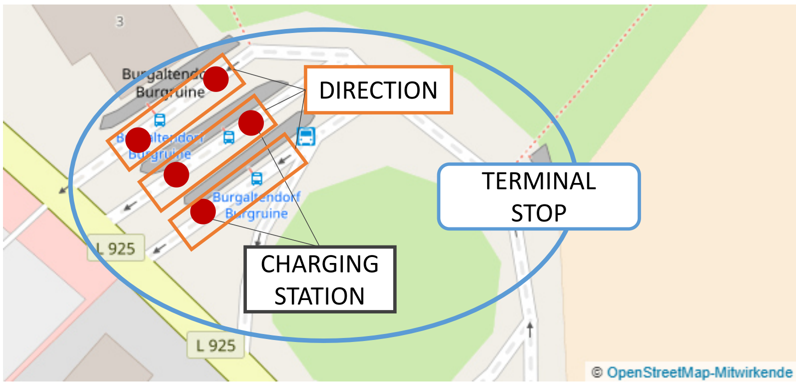

Figure 4-13: Structure of the bus stop modeling with three levels – charging station, direction and terminal stop

The geographical model represents terminal stops on three detail levels as shown in Figure 4-13. The terminal stop represents the highest level and consists of several directions which furthermore summarize individual stop positions where charging stations can be constructed. The technical modeling follows the described aggregation of individual charging stations. The grid connection is therefore not defined individually for each charging station but is instead defined for the entire terminal stop.

4.2.5 Environmental Model

In order to describe the entire local scenario, the local climate conditions must be determined. Therefore, an interface to the online service "OpenWeatherMap"[8] has been developed, which enables an import of historic temperature data for a given city or region.

[8] https://openweathermap.org/

The data are provided in hourly increments for the entire year. An example is shown in Figure 4-14 in which the maxima and minima are highlighted. The figure reveals that it is not sufficient to evaluate only one year, especially when the maxima and minima are considered. Depending on the historic data available, the user can evaluate several years and identify the global maxima and minima. These values are then utilized for the worst-case calculation to ensure technical feasibility under all conditions.

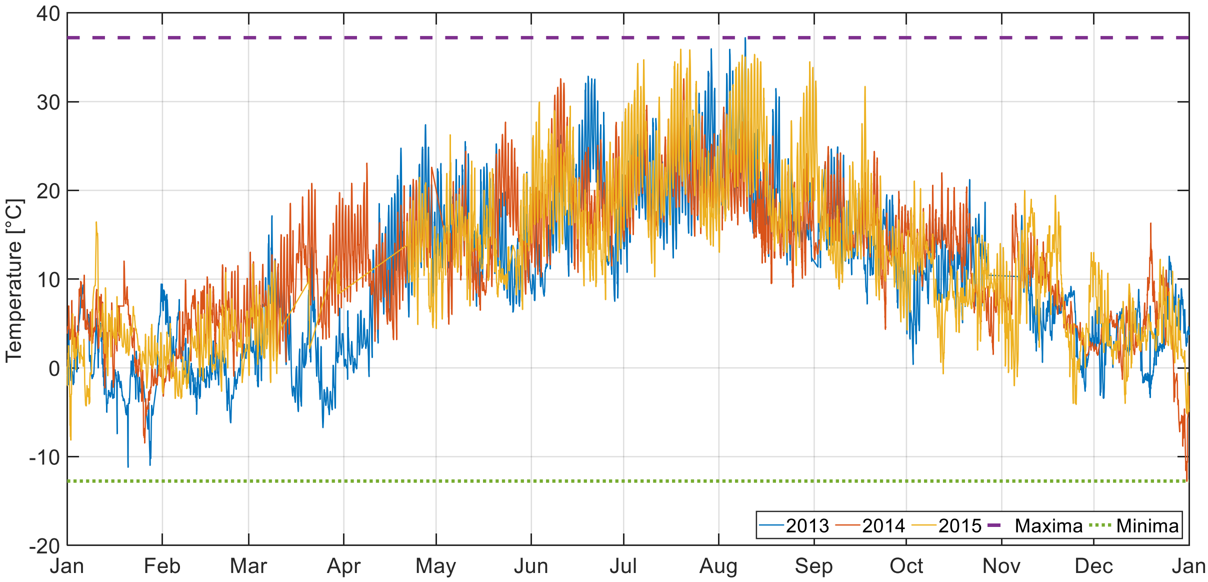

Figure 4-14: Exemplary temperature profile for entire years with maxima and minima temperatures highlighted

Whereas the maxima and minima enable an evaluation of the technical feasibility, requires the cost calculation the average case. However, considering only one general average temperature is not practicable, because the HVAC energy consumption varies significantly based on the temperature level. Instead, the hourly values are utilized to compute a histogram describing the relative share of a temperature level per year, see Figure 4-15. This histogram serves as the basis for the auxiliary power calculation in the vehicle submodel.

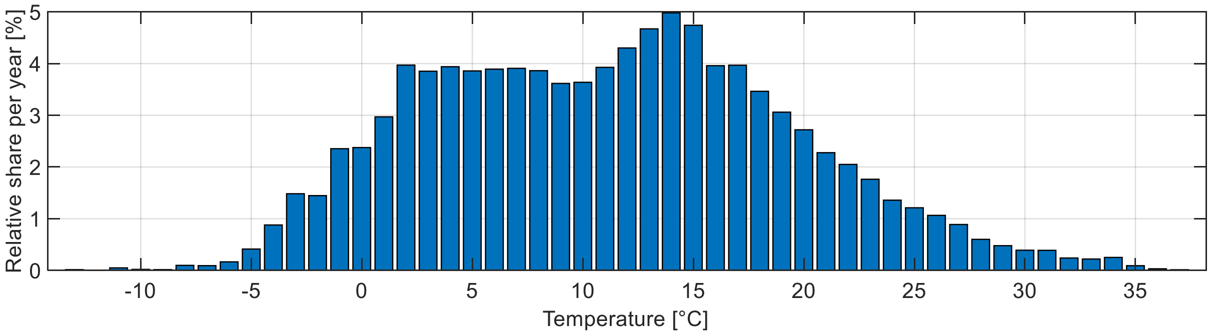

Figure 4-15: Exemplary temperature histogram for an entire year based on hourly temperature levels

4.3 Infrastructure Submodel

The bus runs define the occurrence of vehicles at charging stations, however the assignment of charging stations to individual buses is not predefined. The infrastructure model thus provides the functionality of charging station assignment, called charging management, which is executed during the initialization of the BEB system model.

After the assignment of charging stations to dwell times, time-based charging profiles are generated with the technical model. These profiles represent the maximum output power of the charging station during the timeframe considered and serve as an input for the energy management of the vehicle submodel. The further functionality of the infrastructure model regards the technical modeling of charging stations and their corresponding grid connection, whose output is provided as time-based vectors and aggregated for each terminal stop and grid connection.

4.3.1 Charging Management

The points in time at which a bus is present at a terminal stop are defined in the bus runs. They also contain information regarding direction (exact stop position) to allow occupancy determination of the charging stations. However, it could be the case that several vehicles visit a terminal stop at the same time. This situation is addressed in the infrastructure model by implementing two possible charging management strategies:

[A] First come, first served assignment and blocking of a charging station for the entire dwell time of the bus.

[B] First come, first served assignment and release of the charging station after the battery is fully charged.

The chosen charging strategy directly impacts the required number of chargers. The main difference between strategy A and B is revealed by the operational measures, whereas in strategy A the vehicle can remain at the charging location, strategy B requires a movement.

Since strategy A relies only on vehicles presences, the required number of chargers concludes directly from the operational planning and can be calculated during initialization of the BEB system model. Strategy B instead demands a calculation of charging demand and duration to determine the point in time a charging station is available for the next vehicle. It has the be applied during the runtime of the BEB system model.

4.3.2 Technical Modeling of Charging Systems

The technical modeling focuses on the technical performance of the charging system in order to calculate the charging ability within this determined timeframe. Three figures are especially relevant to this task:

- Maximum charging power
- Efficiency of the entire system
- Coupling and decoupling durations

The maximum charging power of a charging station $\mathrm{p}_{\mathrm{cstation,offered}}$ is defined as the charger DC output. The calculation of the grid load requires a consideration of the efficiencies of the involved components. The grid connection efficiency determined by the losses occurring in the medium-voltage switchgear, transformer and low-voltage distribution is summarized in $\eta_{grid\ connection}$. The charger efficiency $\eta_{charger}$ results from the losses of the power converter, and the efficiency of the coupling system $\eta_{coupling}$ describes the losses in power transmission. The resulting grid load can be described as:

$$p_{grid}(t) = \frac{p_{cstation,offered}(t)}{\eta_{grid\ connection}\ \eta_{charger}\ \eta_{coupling}}. \tag{4.1}$$

Because the modular structure of the BEB system model allows a combined simulation of various coupling systems, it is furthermore important to check the compatibility of the stationary and bus-mounted parts of the coupling system. In case of incompatibility, the charging power is set to zero.

Besides the charging power, the available charging time determines the amount of energy that can be charged. The actual timeframe of the energy transfer is reduced by the initialization time:

$$t_{init,charging} = t_{coupling,connect} + t_{init,charger}. \tag{4.2}$$

The charging period is determined by the time required for the coupling $t_{coupling,connect}$ and the initialization of the charger $t_{init,charger}$ including safety checks as insulation tests. At the termination of the charging the decoupling $t_{coupling,disconnect}$ must be considered:

$$t_{end,charging} = t_{coupling,disconnect}. \tag{4.3}$$

4.3.3 Grid Connection

The grid connection aggregates the power demand at the highest level. Several terminal stops and depots can be linked to one grid connection, as shown in Figure 4-16.

The grid connection itself does not entail further technical parameters besides efficiency which is addressed in the technical model.

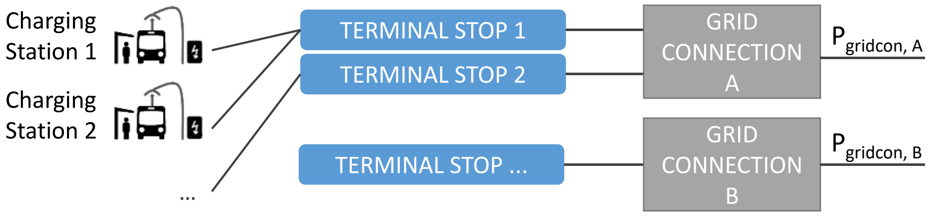

Figure 4-16: Aggregation of charging stations to terminal stops and further on to grid connections

4.4 Vehicle Submodel

The vehicle submodel describes the technical characteristics of the BEB. The traction power calculation utilizes a simulation to determine the energy consumption for the movement. The time-based energy consumption of the auxiliaries is added within the auxiliary power calculation and thereby defines entirely the consumer side of the BEB. The supply side is modeled by the energy management and technical battery model.

4.4.1 Traction Power Calculation

The traction power demand significantly relies on the local conditions and operational requirements, making the use of general figures impractical [9]. The traction power calculation in this thesis builds instead on a simulation model based on the methodology of Sinhuber [31]. The initial model of Sinhuber was enhanced and improved to become universally applicable to large scenarios. The upcoming subchapters provide a brief introduction to the model and describe the enhancements. An overview of the simulation model implemented in Matlab Simulink is shown in Figure 4-17.

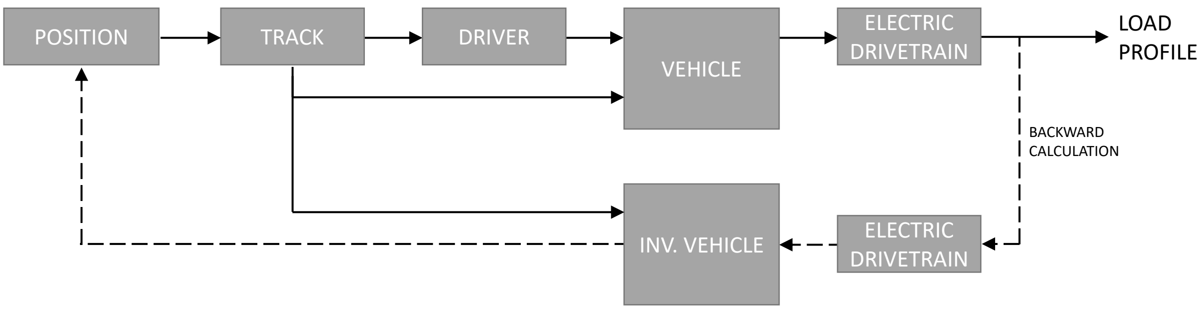

Figure 4-17: Closed-loop energy demand calculation model proposed by Sinhuber [31]

The ability to consider the local specific situation is established by the track model that provides the characteristic parameters (slope, maximum speed and stop position) according to the position of the vehicle on the track. The track model serves as an input for the driver model to set desired speeds and stop the vehicle at bus stops. Furthermore, the track model is an input to the vehicle model to calculate driving resistances. Based on the calculated resistances the electric drivetrain model is applied to determine the electric load profile. The following backward calculation is utilized to determine the resulting speed and position on the track by considering any saturations/limitations caused by the drivetrain.

The traction power calculation is applied for every characteristic trip identified by the track, the trip duration and the passenger occupancy. The characteristic trips are afterwards combined to entire day-load profiles representing the bus runs and stored as time-based vectors in the data structure.

4.4.1.1 Driver

The traction power calculation in this thesis is designed on the one hand for an application to large scale scenarios by considering on the other hand the detailed characteristics of each bus route. Therefore, a universally applicable driver model is required. The input for the driver model regards the desired speed and locations of bus stops. Based on this, the task of the bus driver model is to control the acceleration of the vehicle to meet the desired speed threshold or to stop the vehicle at bus stops when needed. The desired speed is set to the maximum admissible speed of the road segment limited by a parameterizable upper speed limit for each bus type.

In addition to the general speed limit of the road segment a driver must reduce his speed during curves or while turning in order to avoid unstable driving situations. Based on the work of Sinhuber et. al, a curve detection with a reduction of the permissible maximum speed depending on the curve angle is applied [31]. The curve is represented by three points through which two straight routes are drawn, and the angle between the two straight routes is the curve angle. The stored upper limits for the maximum permissible speeds in curves are shown in Table 4-1. Based on this specification, a target acceleration is determined in the driver model and applied to the vehicle model.

Angle [degree]	**Maximum permissible speed [km/h]**
$30 \leq \alpha$	10
$20 \leq \alpha < 30$	30
$10 \leq \alpha < 20$	40
$\alpha < 10$	No reduction

Table 4-1: Maximum permissible speed according to the curve angle defined by three points

The driver behavior is modeled by lookup tables which define a target acceleration for a given speed delta. The accelerations are derived from the SORT cycles (Standardized on Road Tests Cycles) published by the UITP and frequently used in public transport [104]. In the recommendation published by the UITP, three characteristic cycles (SORT1, SORT2 and SORT3) are defined which reflect different driving situations ranging from heavy urban traffic to interurban traffic.

A characteristic feature of the profiles regards an acceleration dependent on the speed delta. Sinhuber derived an acceleration reference according to the accelerations used in the SORT cycles (see Figure 4-18). The data are stored in lookup tables allowing an easy adaptation [31].

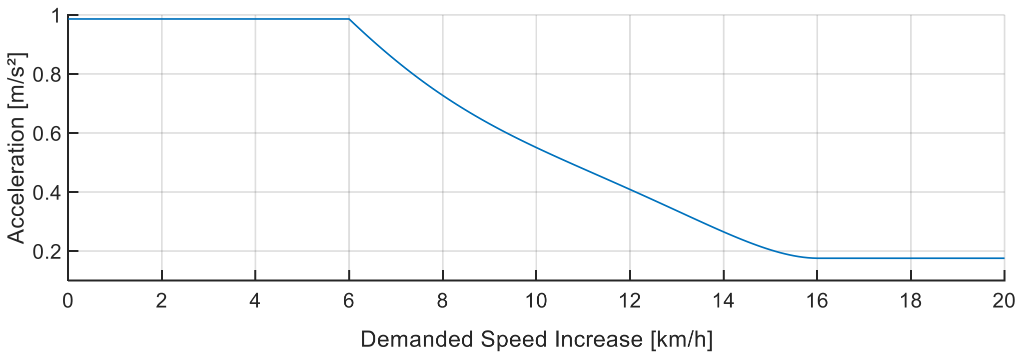

Figure 4-18: Acceleration determined in the driver model according to the demanded speed increase

4.4.1.2 Driving Resistances

The traction power to accelerate the bus is determined by the driving resistances which must be overcome. An overview of the four driving resistances (air drag, gradient, rolling and acceleration resistance) and their effective direction are provided in Figure 4-19.

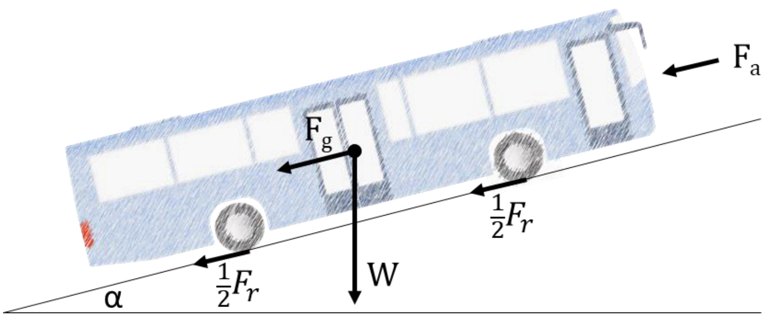

Figure 4-19: Driving resistances considered in the vehicle model

Air Drag Resistance

Air resistance primarily results from the dynamic pressure in front of the vehicle. In addition, the flow resistance and frictional resistance on the bus surface play a role [105]. Due to the dynamic pressure, the resistance depends on the front surface A of the bus. The velocity v influences the resistance quadratically and depends on the air density ρ and drag coefficient c_w. The air density in turn depends on several factors such as air humidity and temperature. The drag coefficient c_w is determined by the vehicle type. The air drag resistance is calculated with this input according to:

$$F_a = \frac{1}{2}\, v^2\, A\, c_w\, \rho. \tag{4.4}$$

Gradient Resistance

The gradient resistance is determined by the weight force represented by mass m and gravitational constant g and the slope described by the angle α. The angle α can become positive or negative, which results in a positive or negative gradient resistance:

$$F_g = W\, sin(\alpha) = m\, g\, sin(\alpha). \tag{4.5}$$

Rolling resistance

The rolling resistance results from the elastic deformation of the tire on a solid road and is described by:

$$F_r = m\, g\, cos(\alpha)\, c_R. \tag{4.6}$$

Like the gradient resistance, the rolling resistance also depends on the weight force and angle of the gradient. Another factor regards the rolling resistance coefficient c_R, which changes depending on the nature of the ground and the speed [106].

Acceleration Resistance

The force representing acceleration resistance is caused by the inertia during acceleration and is opposite to the movement. In addition to acceleration a, it depends on the mass m and can become positive or negative. The acceleration resistance results in:

$$F_{acc} = m\, a. \tag{4.7}$$

4.4.1.3 Electric Drivetrain

The electric drivetrain model utilizes the calculated driving resistances as an input. The torque of the motor M_{motor} is determined based on the wheel diameter. The modeling approach regards a combined efficiency factor for inverter and motor. The maximum power of the traction system is modeled as a saturation which serves as an upper barrier for acceleration and deacceleration.

According to the sign of the requested traction power, either the efficiency (deacceleration) or inverted efficiency (acceleration) must be utilized to calculate the electrical power request $P_{el,req}$. This principle is shown in Figure 4-20.

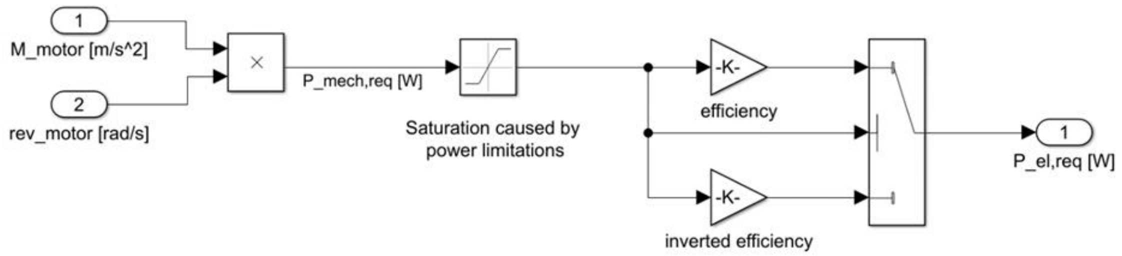

Figure 4-20: Drivetrain model with power limitation and efficiency

Using the inverted models in the backward calculation, it is possible to consider the influence of power limitations on the acceleration, which at the same time ensures that only technical feasible values are used for calculation. Further details on this modeling approach are available in the publication of Sinhuber [31].

4.4.2 Auxiliary Power Calculation

The energy demand of a BEB is not solely defined by the drivetrain as the auxiliaries also play a significant role, especially in the public transport application featuring low commercial speeds and high levels of passenger comfort. The following subsections introduce the heating and air conditioning system as the major consumer, describe its modeling and the consideration of further auxiliaries.

4.4.2.1 Interior Heating and Cooling

The interior heating and cooling system regards one of the main auxiliary consumers in a BEB. The developed modeling approach is divided into two modules. The first provides the thermal heating or cooling demand for a given outside temperature while the second represents the technical systems which cover this thermal demand. An overview is given in Figure 4-21.

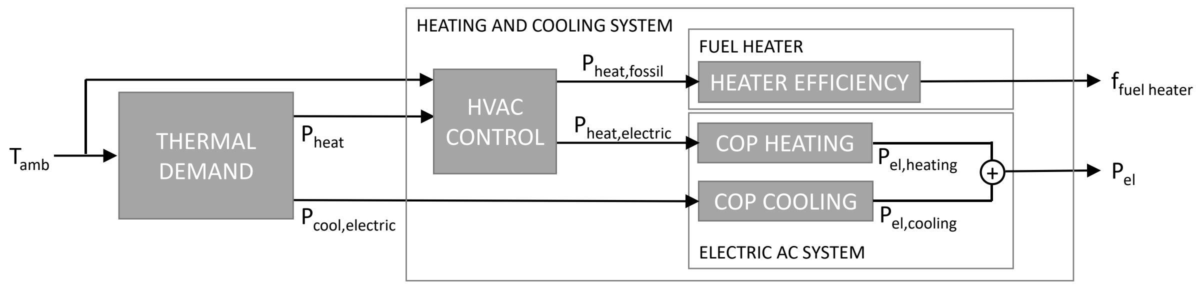

Figure 4-21: Interior heating and cooling modelling approach based on a separation of thermal demand and technical model

Thermal Demand

The determination of the thermal demand and simulation of the heating and cooling system performance regard subjects of current research [107, 108]. The main factors influencing the thermal demand include:

- Insulation of side panels, roof and windows
- Fresh air supply for driver and passengers
- Frequency of door openings
- Number of passengers in the vehicle
- Desired interior target temperature

Comprehensive simulation models offer the possibility to determine detailed temperature distributions and thermal demand figures, however they require significant effort concerning parameterization and computational time [109]. An alternative regards the usage of characteristic figures parameterized using experimental data.

Because this thesis focuses on the assessment of a conservative upper limit of the thermal demand rather than the dynamic behavior, the modeling approach using characteristic figures has been selected. This approach and the parametrization method are introduced in the following.

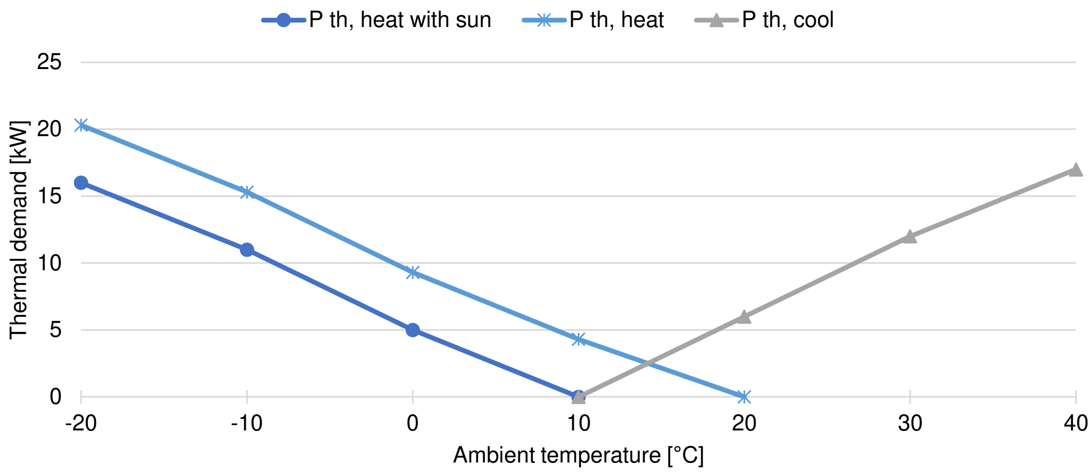

Figure 4-22: Thermal energy demand for the heating and cooling of the interior of a 12 m bus determined by simulation [110]

Figure 4-22 shows the simulated thermal demand of a standard public transport bus with a length of 12 m published by Konvekta (Sonnekalb) [110]. The heating or cooling demand is shown for varying ambient temperatures and a fixed temperature threshold for the interior temperature. Solar radiation is assumed in the publication to be continuous, which could lead to an underestimation of the thermal demand especially during winter conditions. Aiming at a conservative assumption, the thermal demand without direct sunlight is utilized for heating operation. The thermal demand with direct sunlight, which increases the total thermal demand, is set for the summer conditions.

The demand is modeled by lookup tables indicating the continuous demand in heating and cooling operations. The worst-case consideration without solar radiation causes the absence of a point at which the power is 0 kW, as shown in Figure 4-22. Thus, a distinction must be made between heating and cooling demand in the temperature window between 10 °C and 20 °C. The threshold can be parameterized for each vehicle type and for example set at the intersection of both demand figures.

The modeling approach using lookup tables according to Figure 4-22 allows for easy customization. An individual lookup table can be manually defined for every bus type by the user so that their own measurement results or values from literature can be used.

Heating and Cooling Systems

Thermal energy can be provided by different systems. The most common technical combinations currently on the market are:

- Fuel heating; no air conditioning
- Fuel heating and air conditioning
- Hybrid heating system consisting of a heat pump with additional fuel heating and air conditioning
- All-electric heating (PTC and heat pump) and air conditioning

The main differentiating criteria between the systems regard their electrical energy demand and maximum thermal output. The objective of the modelling is to determine an electrical power requirement for the respective technical solution via a stringent procedure for each selected operating point based on the thermal requirements of the respective vehicle type. For this purpose, the COP (Coefficient of Performance) of the individual components is modeled as a function of the outdoor temperature.

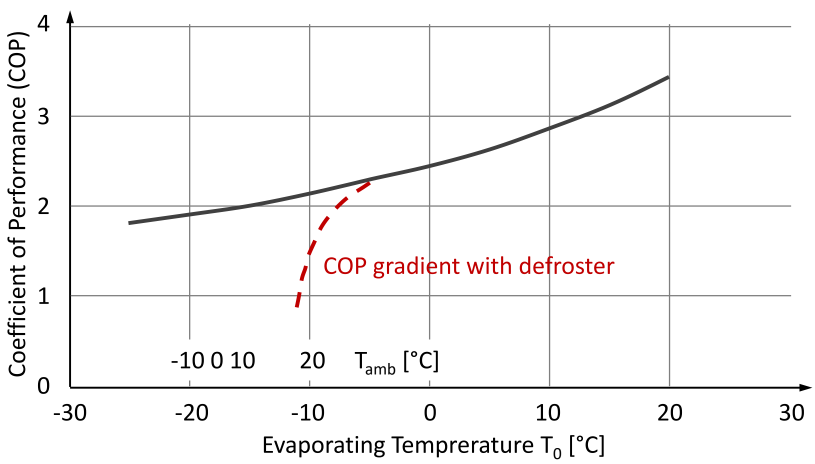

Figure 4-23: Heat pump COP with and without defrosting according to Basile [108]

Figure 4-23 shows the COP of a heat pump with standard refrigerant R134a, which considerably decreases with the temperature. Furthermore, defrosting at temperatures below 5 °C reduces the overall performance to where a heat pump operation with

R134a is not practicable [111]. In this case, an additional heating device (fuel or PTC heater) is required to fulfill the thermal demand. A further alternative regards the use of CO_2 (R744) as a refrigerant, which enables an improved performance at low temperature levels [111].

The modeling approach enables a consideration of combined heating systems whose application is controlled via a temperature threshold. The determination of a reasonable switchover temperature depends on the thermal capacity of the heating systems and their efficiency and can be defined by the user during the parameter setup.

The total electric load profile of the interior heating and cooling $p_{HVAC,r}$ is calculated for every bus run r based on the time t and temperature condition T, which determine the thermal demand p_{th} and the COP of the selected heating and cooling system:

$$p_{HVAC,r}(t) = p_{th,heat,r}(t,T)\ COP_{heat}(T) + p_{th,cool,r}(t,T)\ COP_{cool}(T). \quad (4.8)$$

For systems which utilize a fuel heater, the fuel consumption is computed based on the integral of thermal demand p_{th}, the available heat of combustion of the selected fuel type hc and the heater efficiency η_{heater}:

$$f_r = \frac{\int_{t=0}^{T} p_{th,heat,fossil,r}(t)\ dt}{hc\ \eta_{heater}}. \quad (4.9)$$

4.4.2.2 Further Auxiliaries

In addition to the interior heating and cooling system, there are further auxiliary consumers in a BEB which contribute to overall energy demand. The developed modeling approach does not account for the dynamic behavior of these auxiliaries and instead focuses on the average load in predefined modes of operation.

The average load within a bus run r is computed based on the sum of the maximum loads of all components P_{total} multiplied with the duty cycle of auxiliary operation in each bus run d_r defined by the vehicle status (Section 4.4.2.3). The result regards a time-based vector for each bus run representing the average power demand of the further auxiliaries:

$$p_{aux,r}(t) = P_{total}\ d_r(t). \quad (4.10)$$

4.4.2.3 Operation Dependent Usage

The auxiliaries are considered in different modes of operation described by the vehicle status defined as a time-based vector for each bus run. The vehicle status is set during the initialization of the BEB system model. Table 4-2 shows the different vehicle status defined in the current implementation as well as the individual modes of operation of the heating and cooling system and further auxiliaries.

Vehicle status no.	Description	Heating and cooling system operation	Further auxiliaries [Exemplary duty cycles]
1	Driving	On	50 %
2	Charging at terminal stops	On	25 %
3	Charging in bus depot	Off	5 %
4	Pause at terminal stop	On	20 %
5	Vehicle switched off	Off	0 %

Table 4-2: Auxiliary modes of operation according to the vehicle status

Since some auxiliaries, as for example the steering support, are only active during driving, the vehicle status distinguishes between driving and parking. However, further scenarios occur depending on the parking position, such as at a charging station, at terminal stops without charging infrastructure or in the bus depot.

The consideration of driving and idling is enabled by the usage of entire day bus runs. The output of the auxiliary power calculation regards the electric load profile as a time-based vector. The combination with the traction power load profile forms the total demand profile of the bus and is utilized in the battery and energy management models.

4.4.3 Energy Management

The energy management system (EMS) controls the energy flow in the BEB system model and ensures that the power demand (positive and negative) of the traction system and auxiliaries is fulfilled at any time. The availability of power is however determined by the battery, and thus the EMS model requires the subsequently introduced battery model.

The modeling of management routines and control strategies can be conducted with specialized toolboxes, as for example Matlab Stateflow, in which every state and possible transitions are described. Such implementation would however lead to a time step simulation, with drawback on the computational time. A reduction in computational time compared to a Stateflow implementation is achieved by utilizing a vector-based approach according to the work of Klawikowski [112]. The EMS model utilizes the capability of the battery model to return the battery load profile within the technical limits for a given power demand vector.

The internal calculation procedure is divided into three steps:

1) Compose the total load profile including traction system power demand, the auxiliaries power demand and potential charging power offered by an external power supply.
2) Utilize the battery model to assess the battery power profile following from the total load profile
3) Evaluate the battery power profile, asses the consequences for the traction system as well as for auxiliaries and calculate the resulting load profile for the charging stations.

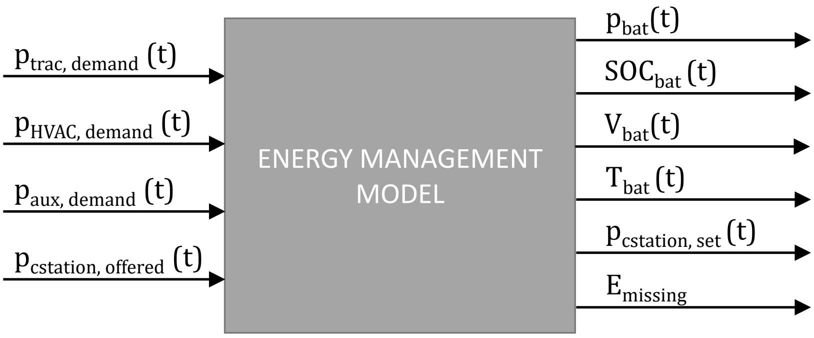

Figure 4-24: In- and output of the energy management model

The in- and output parameters of the EMS model are shown in Figure 4-24. The input variables represent the required DC link power of traction system, HVAC and further auxiliaries and charging power offered by charging stations visited. The vector $p_{cstation,offered}$ combines the time- and position-based availability of charging power for a specific vehicle. The actual charging station supplying this power can differ. A direct link is established by the usage of a time-based charging station vector, which contains the respective charging station ID on vehicle presence.

The output variables describe the battery behavior and the resulting power profile of the charging stations visited by the considered vehicle. In case of any shortages in the power supply for the traction system or auxiliaries, the missing energy is calculated which enables an evaluation of shortages during postprocessing.

The calculation of the total demand profile combines the demanded and offered power profiles as:

$$p_{bat,demand}(t) = p_{cstation,offered}(t) - p_{trac,demand}(t) - p_{HVAC,demand}(t) - p_{aux,demand}(t). \tag{4.11}$$

The battery model handles $p_{bat,demand}$ and provides the resulting power profile p_{bat}. Based on this, the assessment of shortages is performed. In order to detect power shortages, the missing energy is calculated when the energy demand of the traction system and auxiliaries is not supplied by the battery or charging station. The following formula is applied:

$$E_{missing} = \int_{t=0}^{T} \Big(max\Big(0, p_{trac,demand}(t) + p_{HVAC,demand}(t) + p_{aux,demand}(t)\Big) + min\big(0, p_{bat}(t)\big) - p_{cstation,offered}(t)\Big)\, dt. \tag{4.12}$$

Furthermore, the calculation of the charging station load profile $p_{cstation,set}(t)$ is performed, which describes the charging power utilized by the considered bus run at all charging stations visited. The vector for each bus run results in:

$$p_{cstation,set}(t) = min(p_{cstation,offered}(t), max\,(0, p_{bat}(t) + p_{trac,demand}(t) + p_{HVAC,demand}(t) + p_{aux,demand}(t))). \tag{4.13}$$

After the computation of all bus runs, charging-station-specific load profiles are derived. The bus run vector $\mathrm{p_{cstation,set}}(\mathrm{t})$ is divided and assigned based on the charging station ID vector. The procedure is illustrated in Figure 4-25.

$p_{cstation,set}(t)$	0	...	0	50	50	50	50	50	50	0	...	0	50	50	50	50	50	50	50	0	...	0	80	80	80	80	80	80	0	...
$cstation\_ID(t)$	0	...	0	1	1	1	1	1	1	0	...	0	1	1	1	1	1	1	1	0	...	0	2	2	2	2	2	2	0	...

$p_{cstation\,1}(t)$	0	..	0	50	50	50	50	50	50	0	...	0	50	50	50	50	50	50	50	0	...	0	0	0	0	0	0	0	0	...
$p_{cstation\,2}(t)$	0	..	0	0	0	0	0	0	0	0	...	0	0	0	0	0	0	0	0	0	...	0	80	80	80	80	80	80	0	...

Figure 4-25: Generation of charging station load profiles based on bus-run-specific values and the charging station ID vector

4.4.4 Battery Model

The battery model in this section models the technical battery performance. The task is to calculate the resulting power profile given a demanded load profile by considering the technical constraints of the battery such as maximum power levels and capacity limits. The model is designed for efficient calculation with minimum computational time and thus utilizes time-based vectors and an energy-based SOC [112].

The input is described by a demand profile and an initial value of the SOC as shown in Figure 4-26. The output consists of time-based vectors according to the format of the demand profile for the resulting battery power p_{bat}, SOC, open-circuit voltage V and temperature T.

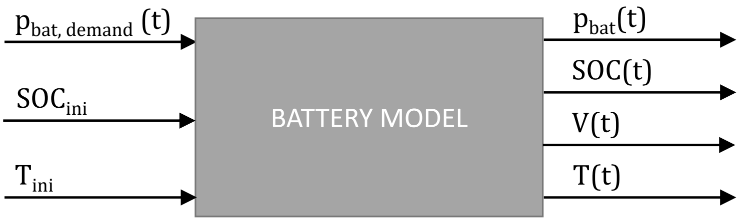

Figure 4-26: In- and output of the battery model

The direct calculation of a technically feasible output power profile indicates that the battery model exceeds the scope of a classical physical model. It includes management routines and simulates an ideal cooperation of the internal management of the battery with the energy management of the vehicle. The calculation procedure is presented in Figure 4-27.

The vector of the demand profile is firstly divided into sections based on the sign, which is required since the battery behavior varies depending on whether it is charging or discharging. The battery behavior is afterwards calculated in chronological order for these sections.

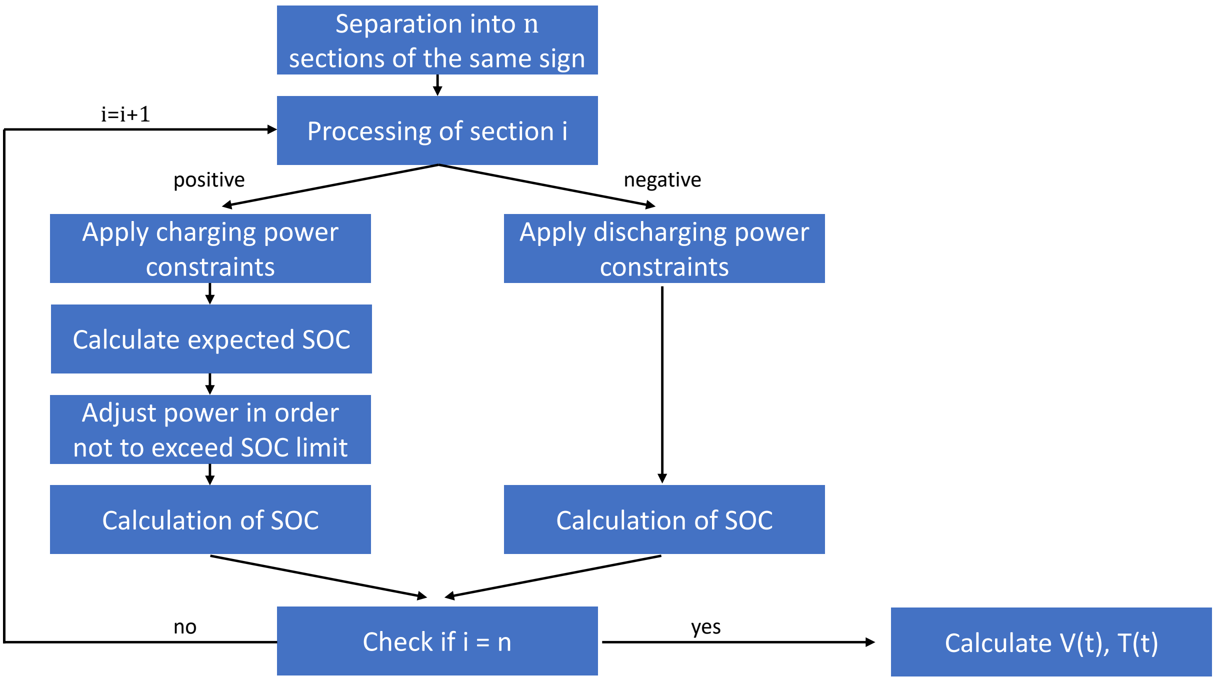

Figure 4-27: Calculation procedure of the battery model for fast processing of given power profiles

Charging

When charging (positive sign), the requested charging power is compared with the maximum charging power of the battery. The maximum power is defined by the maximum c-rate for charging c_{cha} and energy content E_{bat} and is parametrized for every bus type and thus for every BEB in the fleet. In the event of exceeding power limitations, the demanded battery power is limited to the maximum power:

$$p_{bat,lim}(t) = min\ (p_{bat,demand}(t), c_{cha} \cdot E_{bat}). \tag{4.14}$$

The expected SOC can be calculated based on the SOC of the previous section and adjusted power demand $p_{bat,lim}$. Ignoring the upper SOC limit SOC_{max} of the battery, the expected SOC is described by:

$$SOC_{expected}(t) = SOC_{-1} + \frac{\eta_{bat,cha}}{E_{bat}} \int_{t_{period}} p_{bat,lim}(t)\, dt. \tag{4.15}$$

The energy charged within the period t_{period} is determined by the integration of $p_{bat,lim}$ and multiplied with the charging efficiency of the battery. The delta SOC is determined by setting the charged energy in relation to the energy content of the battery and added to the previous value SOC_{-1}. However, $SOC_{expected}$ exceeding SOC_{max} must be avoided. The charging power is therefore set to zero so that charging is terminated at SOC_{max}:

$$p_{bat,lim}(SOC_{expected} > SOC_{max}) = 0. \tag{4.16}$$

The modified requested battery power can now be charged to the battery without limitation so that the following applies:

$$p_{bat}(t) = p_{bat,lim}(t), \tag{4.17}$$

$$SOC(t) = SOC_{-1} + \frac{\eta_{bat,cha}}{E_{bat}} \int_{t_{period}} p_{bat}(t) \cdot dt. \tag{4.18}$$

Discharging

The modeling of the discharge process (negative sign) follows the same principle as for the charging process. Given the maximum c-rate for discharge c_{dch} and the SOC of the previous period, the resulting SOC is calculated:

$$p_{bat}(t) = max\ (p_{bat,demand}(t), -c_{dch} \cdot E_{bat}), \tag{4.19}$$

$$SOC(t) = SOC_{-1} + \frac{1}{\eta_{bat,dch}\ E_{bat}} \int_{t_{period}} p_{bat}(T) \cdot dT. \tag{4.20}$$

In contrast to the charging where the SOC faces an upper limit, during discharge no lower SOC limit is considered in the battery model. The SOC can therefore become negative which enables an assessment of the actual required battery capacity in the further analysis. However, because the result indicated a technically non-feasible configuration, any further calculations regarding lifetime and costs are skipped and the operation is marked as technically non-feasible.

Voltage and temperature profiles for aging calculation

The general battery behavior is described by the SOC. However, the aging model requires a voltage input. Therefore, the open circuit voltage (OCV), which describes a steady state of the battery without an applied current, is calculated based on the SOC. The determination of the OCV is performed using a lookup table based on the SOC vector.

The temperature profiles are also generated for a steady state. Fixed temperature values are defined for the different vehicle statuses (driving, pause time at terminal stops, parking overnight) and considered for each bus run.

4.5 Aging and Lifetime Submodel

The introduced vehicle and infrastructure models allow a detailed analysis of the technical performance of BEB. The availability of long-term planning data enables furthermore profound aging consideration. The purpose of the aging consideration in this thesis regards determining component-specific lifetimes in order to calculate required replacements within the planning horizon.

The aging and lifetime calculations are performed for the relevant components of the BEB system based on the bus runs, and special focus is given to the innovative components: battery, coupling system and charger. The life of these components is usually shorter than the planning horizon and the battery especially contributes to the overall costs. Further components are considered in aggregated categories such as basic vehicle and grid connection, which represent standard components whose lifetimes are expected to exceed the planning horizon. Thus, a detailed aging consideration of standard components is excluded from the scope of this thesis.

The usage intensity of the vehicle and its components is described by the bus runs and their operating frequency. The latter is defined by the bus run assignment to day types as introduced in the modeling framework. In the following, the number of operations of bus b^k of bus type k on bus run r in time period q are referred to as $n_{q,r}^{b^k}$. The set of buses of bus type k is defined as B^k and the set of bus runs operated in time period q by R_q. A further declaration of individual sets for battery types and coupling system types is avoided in the mathematical formulation, although it is used in the modeling framework. Battery-specific or coupling-type-specific values are therefore only labeled with k.

The set of charging stations p^h of charger type h is defined as P^h. Charging stations are assigned to grid connections g^u of grid connection type u, and the set of all grid connections is G. The set of all chargers of type h at grid connection g is defined as P_g^h.

4.5.1 Standard Components

The lifetime of the standard components is considered to be independent of the actual usage, and therefore only time-dependent aging is considered for the basic vehicle and grid connection. The basic vehicle element summarizes the standard components; bus chassis including the electric drivetrain with motor and inverter but without the battery. The lifetime of the basic vehicle is defined-usage independent, meaning only the depreciation period $D^k_{vehicle}$ of bus type k specified by the user is considered:

$$L^{b^k}_{vehicle} = D^k_{vehicle}. \tag{4.21}$$

The grid connection components have been introduced in 3.4.3. In the aging and lifetime calculation, these components are considered standard components of one unit with a lifetime limited by the depreciation period $D_{grid\ connection}$. Therefore, the lifetime is defined as:

$$L^g_{grid\ connection} = D_{grid\ connection}. \tag{4.22}$$

4.5.2 Innovative Components

Innovative components can reach their end-of-life in the modelling approach in two ways. Either the component age exceeds a specified depreciation period as with standard components, or the useful life ends prematurely due to aging processes. The aging processes depend on the actual vehicle use which is determined in the operational model based on bus runs and their number of operations within a considered time period.

4.5.2.1 Battery

The lifetime of the battery is determined using the aging model of a lithium-ion battery developed at ISEA. A detailed explanation of all modeled processes and the derivation of formal relationships can be found in the work of Müller and Sistig [113, 114]. This section summarizes the most important equations and explains their application in the context of this thesis.

Each battery is subject to both calendric and cyclic aging processes which result in a loss of capacity and an increase in internal resistance. While cyclic aging processes are caused by charging or discharging the battery, calendar aging also occurs during standstill. The aging model uses the approach described by Ecker et al. [115], according to which both the capacity loss and increase in internal resistance can be modelled as a superposition of calendric and cyclic aging. The intensity of these aging processes is described by the aging rates α_C, α_R, β_C and β_R.

The concept of bus runs representing entire-day vehicle operations enables an aging modeling based on days, which can afterwards be combined according to the actual operation. BEB are operated on bus runs or parked in the bus depot on each day. A three-step process is applied to calculate the aging, whereby bus-run-related aging rates are firstly computed [112]. In the second step, the average aging rates are determined which result from the bus-run-related aging rates and number of operations of a BEB on the corresponding bus runs. In the third and final step, the battery lifetime is determined for each BEB based on the average aging rates.

The relative battery capacity C_{rel} and relative internal resistance R_{rel} of the battery over time d in days are defined as:

$$C_{rel}(d) = \frac{C(d)}{C_0} = 1 - \alpha_C \cdot \sqrt{d} - \beta_C \cdot d, \tag{4.23}$$

$$R_{rel}(d) = \frac{R(d)}{R_0} = 1 - \alpha_R \cdot \sqrt{d} - \beta_R \cdot d. \tag{4.24}$$

α_{C} Calendric aging rate describing capacity fade.
α_{R} Calendric aging rate describing rise of internal resistance.
β_{C} Cyclic aging rate describing capacity fade.
β_{R} Cyclic aging rate describing rise of internal resistance.
C_0 Battery capacity at $d = 0$
R_0 Internal resistance at $d = 0$

The individual aging rates $\alpha_{C,r}^k$, $\alpha_{R,r}^k$, $\beta_{C,r}^k$ and $\beta_{R,r}^k$ are calculated separately for each bus run due to the varying operation and the varying technical performance of the bus types. The calculation of the calendric and cyclic aging rates for the processes' capacity and fade and rise of internal resistance are conducted according to the same principle. Therefore, this section merely presents the determination of the two aging rates that parameterize aging through capacity loss.

The calendric aging is determined by the voltage $V(t)$ and temperature level $T(t)$ of the battery [115]. The reference value $\alpha_{\mathrm{C,ref}}^{\mathrm{k}}$ is utilized for the calculation of the calendar aging rate $\alpha_{\mathrm{C,operation,r}}^{k}(V,T)$ of bus run r operated with vehicle type k:

$$\alpha_{C,operation,r}^{k}(V,T) = \alpha_{C,ref}^{k} \cdot c_V^{k\,\frac{V_{operation}^k(t) - V_{ref}^k}{\Delta V^k}} \cdot c_T^{k\,\frac{T_{operation}^k(t) - T_{ref}^k}{\Delta T^k}}. \tag{4.25}$$

V_{ref}^k and T_{ref}^k are the reference voltage and temperature of bus type k. The variables ΔV and ΔT define the voltage and temperature deviation at which the aging increases by c_V^k and c_T^k.

For all downtimes in the depot, it is assumed that the battery is not exposed to cyclic loads and the cell voltage corresponds to its reference value. For this reason, the battery is only subject to calendar aging processes during these periods, and the aging is therefore solely determined by the temperature level. The calendric aging rate during downtimes is calculated as:

$$\alpha_{C,parking}^{k}(T) = \alpha_{C,ref}^{k} \cdot c_T^{k\,\frac{T_{parking}^{k}(t)-T_{ref}^{k}}{\Delta T^{k}}}. \tag{4.26}$$

The results from the bus-run-related aging rates and calendar aging rate at standstill are weighted by the period of use and downtime within the period q according to:

$$\alpha_C^{b^k} = \sqrt{\frac{\sum_{r\in R_q} \alpha_{C,operation,r}^{k}{}^2 \cdot t_{operation,r} \cdot n_{q,r}^{b^k} + \alpha_{C,parking}^{k}{}^2 \cdot t_{parking,total,q}}{t_q}}. \tag{4.27}$$

$\alpha_{C,q}^{\mathrm{b^k}}$	Combined calendric aging rate within time period q for bus b^k
t_q	Duration of time period q

The cyclic aging rate of bus run r is modeled based on the depth of discharge DOD^k and the factors ρ^k and σ^k by:

$$\beta_{C,r}^{k}(DOD) = \rho^k\, e^{\sigma^k\, DOD^k}. \tag{4.28}$$

The DOD^k is computed in the aging calculation with the rainflow-counting algorithm for the technical parameters of bus type k for each bus run r [116].

The actual cyclic aging rate corresponds to the average of all bus-run-related cyclic aging rates, which are scaled with the number of bus run operations of the considered bus b^k and divided by the number of days d_q in time period q:

$$\beta_C^{b^k} = \frac{\sum_{r\in R_q} \beta_{C,r}^{k}\, n_{q,r}^{b^k}}{d_q}. \tag{4.29}$$

The battery life is determined based on the actual calendar and cyclic aging rates. The service life accordingly can be calculated based on the capacity reduction and internal resistance increase. The final calculation of the battery lifetime requires a threshold describing the end-of-life of the battery, which is defined as a remaining relative capacity EOL_C (often set to a remaining capacity of 80 %) or a relative increase of the internal resistance EOL_R (often defined as an increase by 100 %):

$$EOL_{C,rel} = 0{,}8 = 1 - \alpha_C^{b^k} \cdot \sqrt{d_C^{b^k}} - \beta_C^{b^k} \cdot d_C^{b^k}, \tag{4.30}$$

$$EOL_{R,rel} = 2 = 1 - \alpha_R^{b^k} \cdot \sqrt{d_R^{b^k}} - \beta_R^{b^k} \cdot d_R^{b^k}, \tag{4.31}$$

$$L_{battery}^{b^k} = min\left(d_C^{b^k}, d_R^{b^k}\right). \tag{4.32}$$

4.5.2.2 Coupling System

The usage intensity of the coupling system varies based on the charging strategy. Whereas depot charging operation requires one or two coupling events per day, opportunity charging can require multiple per hour, which directly impacts the lifetime of the coupling system.

The coupling system aging model distinguishes between two elements: one moving part of the coupling system mounted on the bus and its stationary counterpart at the charging station. The modeling approach for the moving part is introduced in the following and required substitutions for the stationary counterpart are highlighted at the end of this section.

The aging model considers the varying number of coupling events defined as coupling cycles. A cycle of a coupling system summarizes the entire couple and decouple processes that occur before and after charging. In the case of plug connections for example, this coupling process consists of two plug operations (connect and disconnect).

The number of coupling cycles $O^{b^k}_{cpl\ cycles,q}$ of a BEB b^k in time period q depends on the bus runs operated and follows from the number of coupling cycles in each bus run $O^{k}_{\mathrm{cpl\ cycles},r}$ and the number of operations of BEB b^k on the bus run r in the time period q defined as $n^{b^k}_{q,r}$ by:

$$O^{b^k}_{cpl\ cycles,q} = \sum_{r \in R_q} O^{k}_{cpl\ cycles,r} \cdot n^{b^k}_{q,r}. \tag{4.33}$$

The lifetime calculation regards the average number of couplings per day, which follow from the number of days d_q in time period q:

$$O^{b^k}_{cpl\ cycles,average} = \frac{O^{b^k}_{cpl\ cycles,q}}{d_q}. \tag{4.34}$$

For a given maximum number of coupling cycles until end-of-life $O^{k}_{cpl\ cycles,max}$ the specific lifetime corresponds to:

$$L^{b^k}_{coupling\ bus,cyc} = \frac{O^{k}_{cpl\ cycles,max}}{O^{b^k}_{cpl\ cycles,average}}. \tag{4.35}$$

The calendric lifetime of the coupling system is given by the depreciation period $D^{k}_{coupling}$:

$$L^{b^k}_{coupling\ bus,cal} = D^{k}_{coupling}. \tag{4.36}$$

The resulting lifetime is defined as the minimum of cyclic and calendric lifetime:

$$L^{b^k}_{coupling,k} = min\left(L^{b^k}_{coupling\ bus,cyc,k}, L^{b^k}_{coupling\ bus,cal}\right) . \tag{4.37}$$

The same calculation method is also used for the lifetime calculation of stationary coupling systems, in which case the number of coupling cycles in a bus run $O^k_{\text{cpl cycles},r}$ is replaced by the number of couplings with the specific charging station p in bus run r represented by $O^k_{\text{cpl cycles},r,p}$.

4.5.2.3 Charger

Each charger consists of semiconductors which are supposed to calendric and cyclic aging determined by the temperature level and usage. Current chargers for BEB are usually equipped with heating and cooling systems for active temperature control, and as a result the average temperature can be expected to fall within its optimal window ensuring a sufficient calendric lifetime for the planning horizon. A detailed modeling of the calendric aging effects and their temperature dependency are therefore excluded from the scope of this thesis. Thus, the calendric lifetime equals the depreciation period:

$$L^{p^h}_{charger,cal} = D^h_{charger} . \tag{4.38}$$

Despite being equipped with a cooling system, the power electronics experience a temperature increase during charging. The resulting temperature and power cycles could critically influence the charger lifetime and are therefore considered in the cyclic aging calculation [117].

The operating scheme of charging stations regards the bus runs and their number of operations during time period q. The aging model corresponds to the model of the stationary part of the coupling system. For charger p^h and the maximum number of cycles $O^h_{cha\ cycles,max}$ follows a lifetime of:

$$L^{p^h}_{charger,cyc} = \frac{O^h_{cha\ cycles,max}}{\sum_{b^k \in B^k} \sum_{r \in R_q} O^{p^h}_{cha\ cycles,r} \cdot n^{b^k}_{q,r}}\ d_q . \tag{4.39}$$

The combination of calendric and cyclic lifetimes provides the total lifetime of charger j:

$$L^{p^h}_{charger} = min\left(L^{p^h}_{charger,cal}, L^{p^h}_{charger,cyc}\right) . \tag{4.40}$$

4.6 Life Cycle Cost Calculation

The main goals of the BEB system model include the assessment and comparison of technical alternatives. Although all alternatives deliver the same service to passengers, namely the operation of service trips, their individual characteristics can differ significantly, which compromises the technical design (e.g., different components, battery capacities and charging power levels), the operation (e.g., varying number of vehicles and deadhead mileage) and financial figures (e.g., cost breakdown in upfront investment and operating expenses). This underlines the need for an aggregated figure to assess technical alternatives on a common basis.

The technical design as well as the operational characteristics of each BEB concept can be converted into costs, which enables usage of the net present value (NPV) of an investment calculation as the aggregated figure. All payments and revenues in the planning horizon are discounted and related to the time of the investment decision. This accounts for initial investments, replacements and residual values as well as continuous expenses in the form of energy or maintenance costs, which are summarized as operational costs in Figure 4-28.

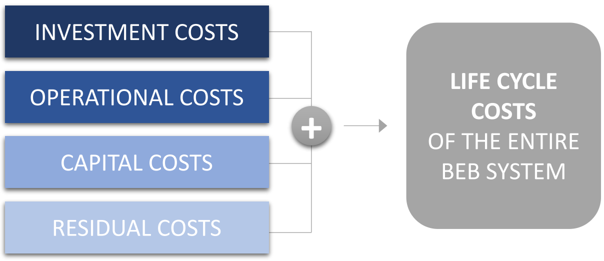

Figure 4-28: Cost figures included in the life cycle cost calculation

The total NPV regards the sum of investment and operational costs of the entire BEB system:

$$NPV_{total} = NPV_{invest} + NPV_{operation} \tag{4.41}$$

which are defined in the following subchapters. Revenues generated by ticket sales are excluded from the calculation since they are equal for all considered bus concepts.

4.6.1 Investment Costs

The NPV of investments in an BEB system divides in the NPV of bus and infrastructure, which are furthermore composed of sub elements:

$$NPV_{invest} = NPV_{bus} + NPV_{inf}, \tag{4.42}$$

$$NPV_{bus} = NPV_{basic\ vehicle} + NPV_{battery} + NPV_{coupling\ bus}, \tag{4.43}$$

$$NPV_{inf} = NPV_{grid\ connection} + NPV_{power\ electronics} + NPV_{coupling\ stat}. \tag{4.44}$$

The lifetime calculation for each component considered in the NPV calculation has already been introduced. Based on the computed lifetime, replacements within the planning horizon could be required. The point in time at which a replacement is required t is set to the computed lifetime L.

Figure 4-29 provides an overview of the methodology for a general component X. The initial investment at t_0 undergoes no discounting, whereas the replacements at t_1 and t_2 are discounted with interest rate i. The same accounts for the residual value at RV at the end of the planning horizon T.

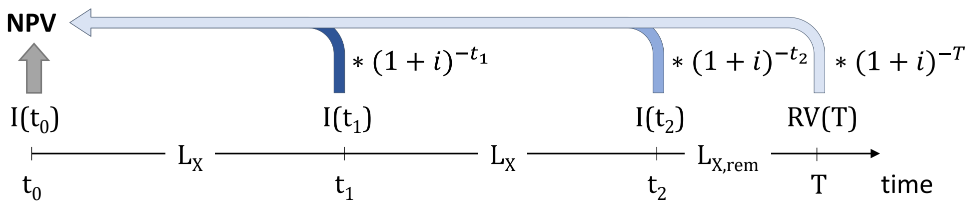

Figure 4-29: Calculation of the NPV of investments considering replacements and residual value

In this case, the NPV calculation is defined by:

$$NPV_X = \sum_{t=1}^{T} \frac{I(t)}{(1+i)^t} - \frac{RV(T)}{(1+i)^T}. \tag{4.45}$$

The investments I are determined by the quantity of elements purchased at the considered point in time $n(t)$ and price level $p(t)$, so that the following applies:

$$I(t) = n(t) \cdot p(t). \tag{4.46}$$

The dynamic price level can be defined by growth or decline functions given a current price level at t_0 and a growth/decline rate. Linear and exponential rates can be applied.

The price level is furthermore relevant to calculating the residual value at the end of the period under consideration. The following applies by taking into account linear depreciation:

$$RV(T) = \frac{L_{X,rem}}{L_X} p(T). \tag{4.47}$$

4.6.2 Operational Costs

The costs of operating a BEB system can be divided into energy-, mileage- and time-related expenses. Whereas energy-related costs are directly caused by the energy demand of vehicle and infrastructure operations, mileage-related costs summarize a group of cost figures related to maintenance. Time-related costs regard the driving time required to operate the vehicles. Although such expenses occur on a regular basis, they cannot be defined as constant throughout the period under investigation due to cost developments.

Following the principle introduced in the aging and lifetime submodel, cost determining figures are calculated on the level of bus runs. Based on this and the planned operation, the actual figures are computed by considering cost developments. Finally, discounting is applied to determine the net present value consisting of:

$$NPV_{operation} = NPV_{energy} + NPV_{maintenenace} + NPV_{driver}. \tag{4.48}$$

4.6.2.1 Energy Costs

Energy-related costs result from the electricity demand of the charging infrastructure and the consumption of fuel if a fuel heater is installed. Electricity costs are determined for an aggregated energy demand at the grid connections, whereas fuel consumption is computed on the level of bus runs.

The modelling of electricity costs follows the composition of the electricity price and consists of expenses for electricity generation, grid utilization, electricity tax, EEG levy and value-added tax. The price for electricity generation $l_{gen,q}$ represents the payments to the electricity producers, and the grid utilization price for the upstream electricity grid must be paid to the grid operator. This price is modeled as energy price $l_{grid,q}$ linked to the amount of electricity purchased. The electricity tax and EEG levy regard taxes that are levied on the electricity price without relation to other prices.

This results in the electricity costs at the grid connection g^u in time period q of:

$$J^{g^u}_{electricity,q} = (l^u_{gen,q} + l^u_{grid,q} + l^u_{tax,q} + l^u_{EEG,q}) \cdot E_{q,g^u}. \tag{4.49}$$

The energy demand E_{q,g^u} during time period q at grid connection g^u results from the vehicle and infrastructure model. It follows from the sum of all buses and their frequency of operation on bus runs provided as $n^{b^k}_{q,r}$ in time period q.

Fuel consumption over time is computed using the auxiliary model of the vehicle. The fuel consumption of all bus runs operated in time period q is F_q. With the fuel price of $l_{fuel,q}$ the fuel costs during a certain time period result in:

$$J_{fuel,q} = l_{fuel,q} \cdot F_q. \tag{4.50}$$

The NPV of the energy-related costs is defined by:

$$NPV_{energy} = \sum_{g^u \in G} \sum_{q=1}^{T} \frac{J^{g^u}_{electricity,q}(q)}{(1+i)^q} + \sum_{q=1}^{T} \frac{J_{fuel,q}(q)}{(1+i)^q}. \tag{4.51}$$

4.6.2.2 Maintenance Costs

The mileage-related costs represent maintenance expenses which are the sum of all expenses of daily routine inspections and minor spare parts which are not treated separately. In the calculation of the total mileage, no distinction is made between service and deadhead operation. The total maintenance costs per bus b^k during time period q are calculated based on the specific maintenance costs $j^k_{maintenance}$ of bus type k, the total mileage per bus run m_r and the operational frequency of the bus run $n^{b^k}_{q,r}$:

$$J_{maintenance,q} = \sum_{r \in R_q} j^k_{maintenance} \cdot m_r \cdot n^{b^k}_{q,r}, \tag{4.52}$$

$$NPV_{maintenenace} = \sum_{q=1}^{T} \frac{J_{maintenance,q}(q)}{(1+i)^q}. \tag{4.53}$$

4.6.2.3 Driver Costs

Driver costs are incurred whenever a vehicle is operated. Time-related costs are identical if only technical alternatives with identical operating schemes are compared. However, these costs gain importance when bus-run adjustments are performed such as in depot charging operation with a limited range. Considering the personal costs allows assessing the additional expenses incurred by a modified operating scheme, which are then fully charged to the technical alternative to allow a neutral comparison.

The driver costs calculation bases on the operating hours within a bus run. Deviations caused by driver shifts are excluded from the scope. The cost figure NPV_{driver} is calculated following the methodology introduced for the mileage-related costs, with the difference that the total operation time t_r is considered and multiplied with the hourly rate j_{driver}:

$$J_{driver,q} = \sum_{r \in R_q} j_{driver} \cdot t_{operation,r} \cdot n^{b^k}_{q,r}, \tag{4.54}$$

$$NPV_{driver} = \sum_{q=1}^{T} \frac{J_{driver,q}(q)}{(1+i)^q}. \tag{4.55}$$

4.7 Emission Calculation

The previous sections describe the technical and economical modeling of the BEB system. A detailed cost-benefit analysis of an electrification furthermore requires an assessment of the positive outcome for the environment, namely the mitigation potential.

Two measures are required to assess the mitigation potential of BEB. Firstly, the actual emissions of the BEB operation must be calculated, and secondly a reference representing the conventional bus operation is needed. Both calculations are performed within the emission calculation submodel.

The developed emission calculation focuses on the operation phase of the product since this phase dominates the overall emissions footprint as discussed in Section 2.3.4. Emissions occur during the operation phase from the actual vehicle operation (driving) and, in the case of BEB, from the electricity generation and from upstream refinery processes in the case of conventional buses. The quantification of these emissions is introduced in the following.

4.7.1 Operational Emissions

The reduction of operational emissions represents one of the main drivers of the BEB application. The assessment of mitigation potential requires a calculation of operational emissions of electric and conventional bus operation and is performed in the BEB system model individually for each bus run and afterwards combined as the total sum of the entire fleet by considering the frequency of bus-run operations.

4.7.1.1 BEB Operation

In contrast to the internal combustion engine, the electric motor enables local emission-free operation, i.e., no inner-city air pollution by nitrogen oxides (NO_X) and fine dust (Particulate Matter, PM). However, fine dust may be emitted by the braking system during mechanical braking, but due to recuperative braking it can be assumed that these emissions fall below the level of a conventional diesel bus. Therefore, no explicit consideration is conducted.

Depending on the heating system, it is possible that a BEB releases local emissions. This is always the case when using a fuel heater operated using fossil fuel such as diesel. The implemented emission calculation is based on reported figures of a study published by Shancita et al, who compared different methods for reducing the emissions of trucks during idling [118]. The emissions are provided as the average fuel consumption and average emissions per hour so that the total emissions per liter can be calculated. The NO_X emissions range from 0.47 g/l [119] to 1.40 g/l [120] and the PM10 emissions range from 0.29 g/l [121] to 0.39 g/l [122].

For each bus run, the thermal demand regarding the fuel heating system and fuel consumption F_r^k is computed via the auxiliary power calculation in the vehicle model. Based on the emission parameter em_{CO_2}, em_{NO_X} and em_{PM}, the emissions of the fuel heater operation during time period q are:

$$EM_{BEB,CO_2,q} = em_{CO_2} \sum_{r \in R_q} F_r^k \, n_{q,r}^{b^k} , \tag{4.56}$$

$$EM_{BEB,NO_X,q} = em_{NO_X} \sum_{r \in R_q} F_r^k \, n_{q,r}^{b^k} , \tag{4.57}$$

$$EM_{BEB,PM,q} = em_{PM} \sum_{r \in R_q} F_r^k \, n_{q,r}^{b^k} . \tag{4.58}$$

4.7.1.2 Conventional Bus Operation

Diesel combustion in conventional bus operation causes global as well as local emissions. The emission quantification methodology applied in this thesis is based on the work of Puetz, who developed an approximation method for generalizing emission measurements for public transport buses [6].

The method is based on a characteristic map describing the fuel consumption as well as CO_2, NO_X and PM emissions based on the commercial speed during operation. An exemplary map for a constant vehicle weight is provided in Figure 4-30. The methodology of Puetz has been extended via a factor describing the relative weight difference in order to account for varying weights in the bus operation which are considered in the BEB modeling.

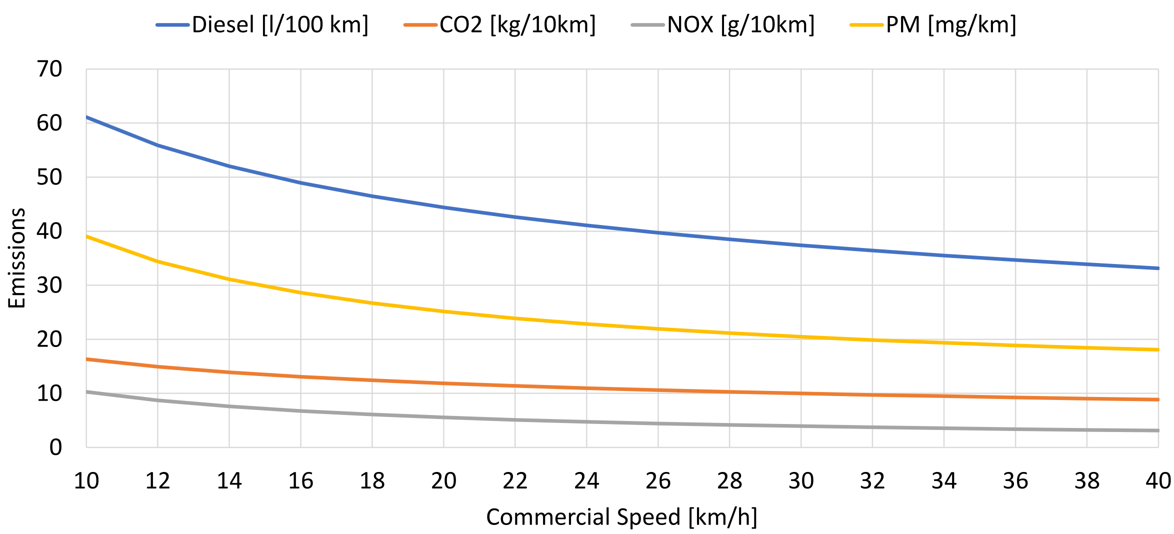

Figure 4-30: Exemplary fuel consumption and emissions (CO_2,NO_X and PM) of diesel buses over commercial speed

A linear relation is introduced for the weight difference, because the weight regards a linear factor in the dominating driving resistances (see Section 4.4.1.2). The fuel consumption and emissions are calculated based on:

$$em_{conv,trip} = ((a \cdot log(v) + b) \cdot (1 + \frac{c}{v}) \cdot d) \cdot \frac{m}{m_{ref}}. \tag{4.59}$$

$em_{conv,trip}$: Emission in l/100km or g/km
a, b, c, d: Characteristic curve-fitting parameters based on measurement data
m: Vehicle weight including passengers
m_{ref}: Reference vehicle weight in the measurement campaign
v: Vehicle speed

The calculation is conducted trip-wise for each bus run by considering the vehicle weight and average passenger load of each trip. The results are aggregated per bus run to $em_{conv,r}$ and the total emissions are computed based on the number of times each bus run is operated in time period q:

$$EM_{conv} = \sum_{r \in R_q} em_{conv,r} \, n_{q,r}^{b^k} . \tag{4.60}$$

4.7.2 Emissions of Energy-Supply

As the primary energy source in BEB, electricity enables a further environmental advantage via the usage of renewable energy and therefore a CO_2-neutral energy supply. However, if the electricity is generated by conventional power plants such as those fired with coal, substantial CO_2 emissions can occur. This underlines the necessity of also considering global emissions from energy supply during the mitigation potential assessment. CO_2 is especially highly relevant in this matter due to its global impact and is therefore calculated in the model.

4.7.2.1 Electricity

The electricity used for charging BEB could incur an ecological footprint depending on the way the electricity is generated. Due to the geographical separation of bus operation and electricity generation, the globally impacting CO_2 emissions are especially relevant and are modelled using separate electricity tariffs for each grid connection type with constant emission factor per kWh consumed electricity $e_{elec,CO_2}^{g^u}$.

The total emissions are calculated by:

$$EM_{BEB,CO_2,q} = \sum_{g^u \in G} e_{elec,CO_2}^{g^u} E_{q,g^u}. \tag{4.61}$$

4.7.2.2 Fuel

In addition to the emissions caused by the combustion of fossil fuel, the refinery process and transportation also contribute to its ecological footprint. As for the electricity, the focus lies on globally effective CO_2 emissions. With the emission factor e_{fuel,CO_2} the emissions are calculated by:

$$EM_{fuel,CO_2} = e_{fuel,CO_2} \cdot \sum_{r \in R_q} F_r^k \, n_{q,r}^{b^k} . \tag{4.62}$$

The same equation is applied in order to determine the emissions of the fossil fuel supply in case of a fuel heating system in a BEB.

5 Technical and Operational Analysis

The technical and operational analysis represents the core element in the electrification potential assessment. The technical feasibility assessment describes the application of the BEB system model for a given operational planning. Building on this, a methodology for the analysis of technical and operational constraints is introduced. The purpose of the analysis is to enable in-depth insight into the linkage between the operating scheme and the consequences of the technical design of the system, which is of special interest in the allocation of infrastructure for opportunity-charging BEB.

Operational changes required by technical constraints are addressed for depot-charging BEB. The solution approach consists of a methodology for the energy-based vehicle scheduling, determines optimized operational scenarios and reveals the operational consequences in the form of additional vehicles, increased deadhead mileage and rising driver time.

5.1 Technical Feasibility Assessment

The introduced BEB system model enables an efficient calculation of entire bus operations. By considering existing bus runs, the performance of a BEB can be evaluated and its technical feasibility assed.

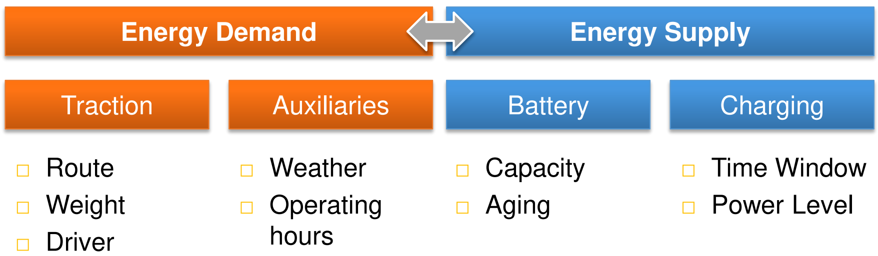

Figure 5-1: Relevant influencing factors for energy demand and supply

The technical feasibility is determined by the balance of energy demand and energy supply as illustrated in Figure 5-1. The energy demand results from the demand of the traction system and of the auxiliary consumers. Using the energy demand calculation in the vehicle model, the demand side can be determined for various scenarios. In this process, local-specific conditions are considered as dependencies regarding route characteristics, weight, and driver behavior as well as climatic conditions.

In addition to the demand side, the supply side also needs to be evaluated. It is important to distinguish between internal energy supply, namely energy stored in the battery, and external energy supply by charging infrastructure. The positive effect of energy gained via regenerative braking system is located on the demand side with a negative sign and reduces the traction energy demand.

The technical feasibility is assessed based on the minimum SOC while operating a certain bus run in the worst-case scenario. The BEB system model's ability to manage negative values for the SOC enables an evaluation of the severity of energy shortages.

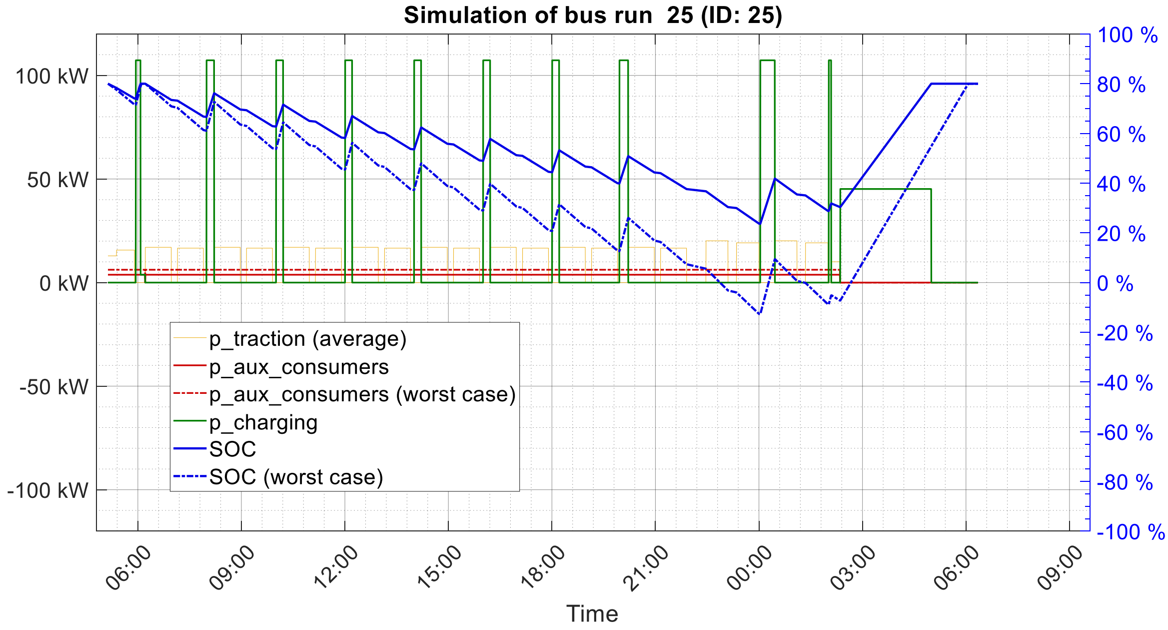

Figure 5-2: Simulation results of an exemplary bus run for the average and worst case - Both scenarios reveal an insufficient charging, however, only the worst case regards a technically non-feasible scenario

Figure 5-2 provides an example by showing the SOC in opportunity-charging operation for the average and worst cases, which is characterized by a high auxiliary energy demand and an aged battery at end-of-life. The vehicle begins the operation with a SOC of 80 %. The operation of the first service trip is followed by a charging phase which enables a charging of the entire energy consumed. However, this is not the case for the subsequent charging events since the SOC gradually fades and reaches negative values in the worst case. The occurrence of a fading SOC reveals a shortage in the energy supply, despite frequent charging.

The technical feasibility can be achieved in this case via operational or technical measures. Operational measures describe the adjustments in the bus runs aimed to increase charging time at the charging locations, whereas technical measures regard the increase in charging power or increasing battery capacity.

The shown bus run simulation can be conducted in the technical feasibility evaluation for a large amount of different bus runs in various scenarios, which could represent either the current operating scheme of the bus operator or adjusted scenarios with operational changes. The feasibility is assessed by comparing the minimal SOC in operation with a predefined lower bound which can regard a fixed SOC value or an SOC value determined by the average energy demand and a required buffer in terms of time or mileage.

A batch processing has been implemented to achieve an efficient calculation, which allows for example assessing the performance of various bus types on the provided bus runs. The output is provided in a standardized format while indicating the technical feasibility evaluated based on the SOC lower bound.

5.2 Analysis of Technical and Operational Constraints

Bus runs, especially within the opportunity charging operation, are characterized by complex linkages between the operational planning and technical feasibility. Based on the results of the technical feasibility assessment introduced in the previous section, the bus runs can be clustered into the following categories:

- [A] Technically feasible without adjustments
- [B] Technically feasible without adjustments, however with low utilization of charging infrastructure
- [C] Technically non-feasible due to insufficient charging caused by limited charging power or dwell time
- [D] Technically non-feasible without regular dwell times at potential fast-charging locations

Bus runs assigned to category A require no adjustment to the operational planning since they are already technically feasible. The category B bus runs can also be electrified, but one or more charging stations are used only at a low utilization. However, these charging stations could be required to ensure technical feasibility. Thus, it is useful to assess operational measures to avoid this due to the negative impact on economic efficiency. Category C describes technical non-feasible bus runs with insufficient opportunity charging. In this case, operational as well as technical measures needs to be assessed. Bus runs that do not visit opportunity charging infrastructure at all are assigned to category D.

It requires significant effort to manually assign bus runs to categories and derive the necessary measures for a bus network with several hundred bus runs per day type, especially for categories B and C. For this reason, a tool for bus run analysis was developed which utilizes the BEB system model.

5.2.1 Problem Formulation

The aim of the bus run analysis is to identify problems caused by operational constraints which occur when designing opportunity charging bus systems. In general, two decisions must be made when dimensioning the BEB system: The battery capacity of each bus type must be selected as well as the location and power level of charging stations.

A determining criterion in this process regards the minimum required battery capacity of each bus type. Figure 5-3 highlights the dependencies of this value on the trips and charging time available in the bus runs. If the bus type is operated on several bus runs, the minimum battery capacity is described by the highest demand of these bus runs.

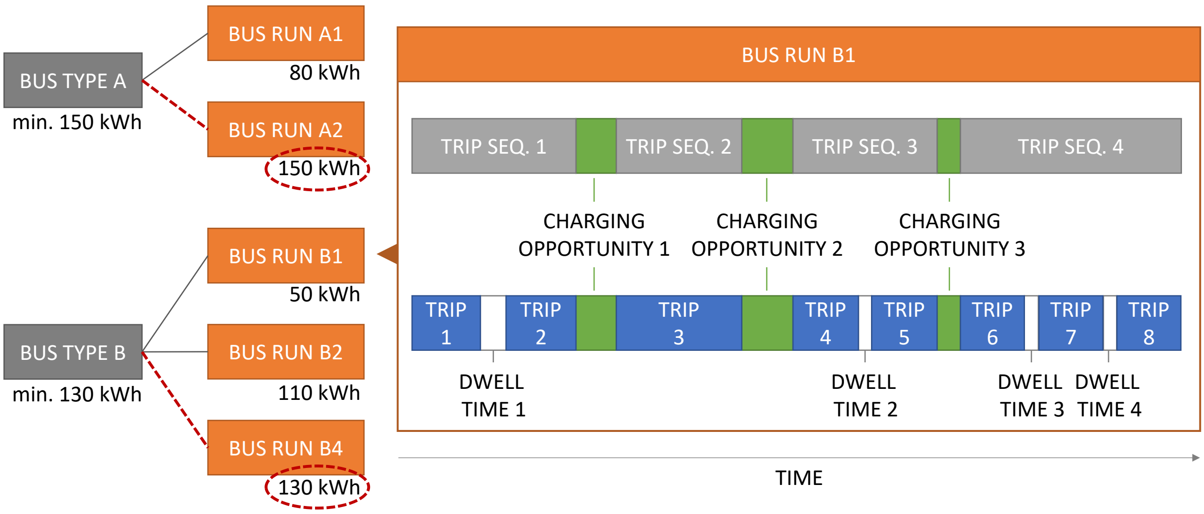

Figure 5-3: Constraints for the minimal battery capacity of a bus type determined by its linkage to bus runs

A bus run is composed of single-service and deadhead trips, which are operated subsequently. The consumed energy in trip operation can be charged within the dwell times between the trips. Without a charging in between, the energy demand of service trips accumulates. This is defined in the following as a trip sequence during which no charging is possible (grey blocks in Figure 5-3). Depending on the consumed energy and the available charging power and time, it is not guaranteed that an entire charging is performed between trip sequences. The missing energy caused by the partial charging must be added at following sequences.

The bus run describes the connection of service trips and therefore trip sequences. The minimum battery capacity is defined by the energy demand of trip sequences and their linkage. Charging opportunities can decouple trip sequences and therefore reduce the minimal battery capacity. Bus runs are linked by their assignment to bus types, and the minimum battery capacity is determined based on the highest demand of the assigned bus runs to a bus type.

The second major decision in the design process regards dimensioning the charging infrastructure. Regarding cost efficiency, it makes sense to only build charging stations with a high utilization. Figure 5-4 shows the utilization of two charging stations serving different bus runs.

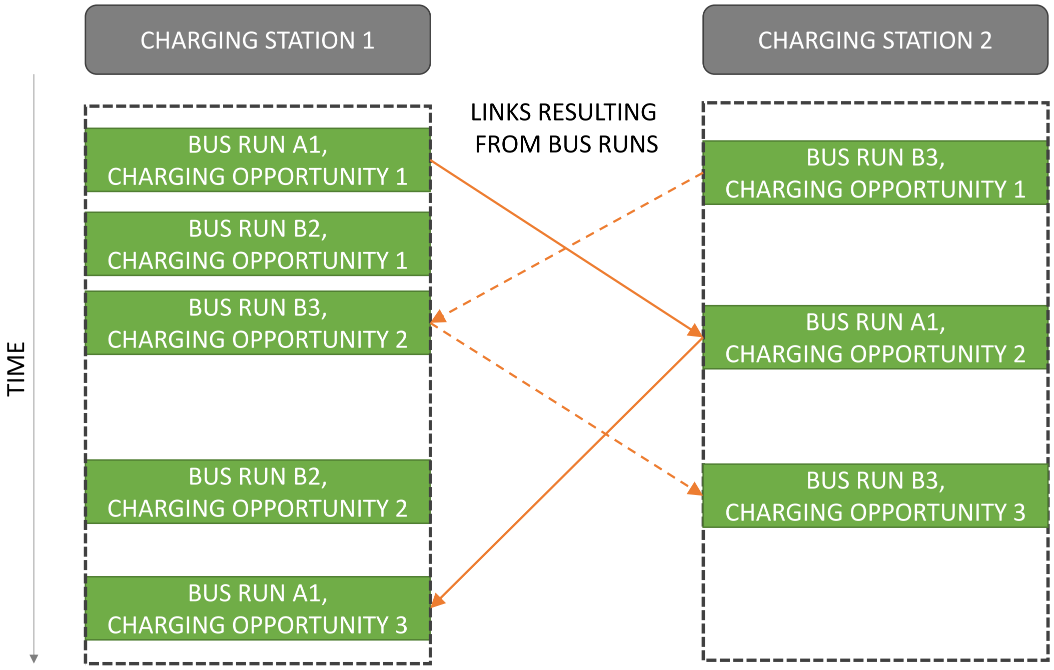

Figure 5-4: Exemplary utilization of charging stations by various bus runs – Both charging stations are linked by bus run A1 and B3

The example in Figure 5-4 indicates that charging station 1 claims a higher utilization than charging station 2 and can therefore be more economically operated. This observation however does not cover the full scope of the problem, as the linkage of charging events by bus runs must be considered.

The utilization depends on the actual energy transferred to the vehicle at a certain time during a certain bus run operation and furthermore depends on the energy drawn at other charging stations visited during the same bus run. The decision to establish a charging station with a certain power level is therefore influenced by the setups of other charging stations.

Charging stations can serve multiple bus runs and thereby link bus types as shown in Figure 5-5. The strength of the linkage is determined by the relevance of the charging time at the considered station within the bus run. If the bus run served by the charging station defines the minimum battery capacity of a bus type, changes to the power level could significantly affect the system dimensioning.

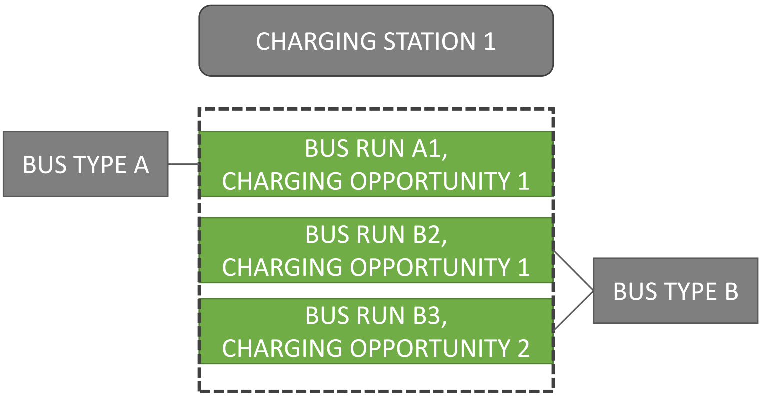

Figure 5-5: Relation of bus types and charging stations – Charging station 1 sets constraints for the technical design of bus type A and B

5.2.2 Bus Run Analysis

The problem definition revealed the complexity of the bus run analysis. The heavily linked and interacting constraints impede an effective manual analysis. However, a fully automatized analysis is also prevented by the high number of special cases which must be evaluated based on experience and expert knowledge. Therefore, a software tool based on the BEB system model has been implemented, which supports users in the analysis process.

A major task of the software tool is to enable the user to interpret the interdependencies between operational planning and technical design, which is achieved by introducing two KPIs: The first regards the minimal battery capacity, whose calculation method is introduced in Section 5.2.2.1. The minimal battery capacity serves as a lower bound, enables an in-depth analysis of bus runs and directly visualizes the effect of missing or insufficient energy supply such as when a charging station is removed. The second KPI aims at assessing the relevance of individual charging stations regarding the technical feasibility of the BEB system, which is determined in a stepwise process via recurring simulations with the BEB system model as described in Section 5.2.2.2. The overlaying GUI and its application are finally explained in 5.2.2.3.

5.2.2.1 Minimal Battery Capacity

The minimum battery capacity required to operate a given bus run depends on the energy demand of the BEB, which is influenced by the weight of the battery and therefore by the battery capacity. This loop impedes a straightforward calculation and requires an approximation method.

The approximation method in this thesis is based on the work of Sistig, who presents an iterative approach in his master's thesis which considers different cases for the sign of the traction power and its dependency on the battery capacity [123]. The weight loop is dissolved in an iterative approach and the minimal battery capacity of a single trip is provided.

In order to determine the minimal battery capacity for a trip sequence, the energy demand of the individual service trips is firstly calculated. Groups of service trips without charging time between are then aggregated to trip sequences, which is accomplished by querying the charging time and charging power between the individual trips. If the charging time or charging capacity between the trips is zero, the service trips are aggregated to a trip sequence. The energy demand of the individual trips is then summed up to calculate the energy demand of the trip sequence.

In addition to the minimal battery capacity of the trip sequences, the minimal battery capacity of the entire bus run is calculated. This value could exceed the minimal battery of the trip sequences when charging between the trip sequences is insufficient. An example is shown in Figure 5-6.

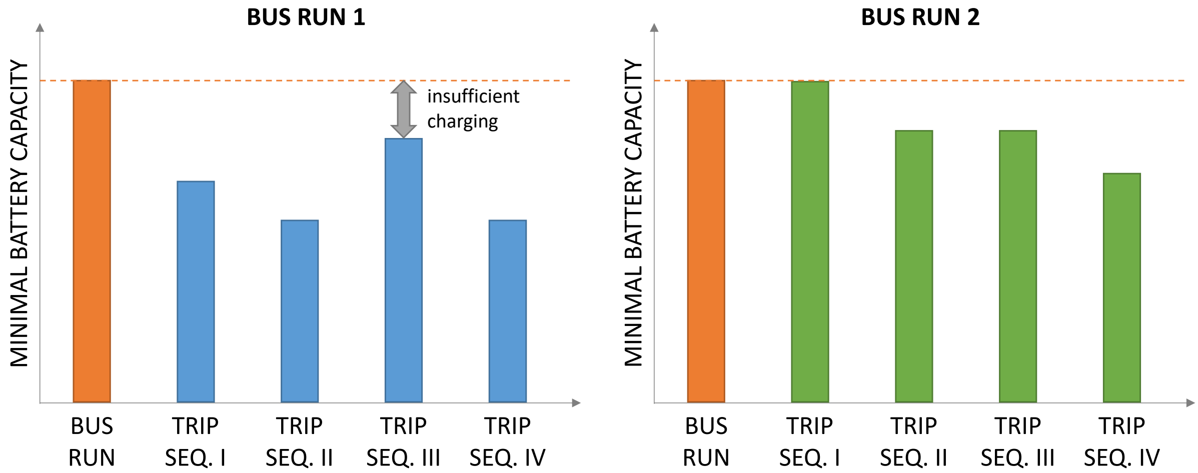

Figure 5-6: Minimal battery capacities of two bus runs and comparison with the minimal battery capacities of the corresponding trip sequences.

The minimal battery capacities of the trip sequences in bus run 1 (Figure 5-6) fall below the minimal battery capacity of the entire bus run, which is the consequence of an insufficient charging throughout the bus run operation. Through an improved charging, the bus run's minimal battery capacity could be reduced to the level of trip sequence III, which is the case for bus run 2 whose minimal battery capacity equals the minimal battery capacity of trip sequence I. Modifications of trip sequence I are required for a further reduction, which could be an integration of a charging event or the deletion of single trips in the trip sequence.

5.2.2.2 Relevance of Charging Stations

In some scenarios, dwell time occurs at stops far from the city center. Charging stations at these stops are often characterized by low utilization and could potentially negatively influence the system's economic efficiency. However, their absence could result in increased minimal battery capacities or in the infeasibility of scenarios. Therefore, the second KPI aims at identifying such critical charging stations via a two-step process. First the economic viability is approximated by computing the utilization, while in the second step the consequences of the absence of a single critical charging station are assessed via simulation using the BEB system model. The consequences are assessed and rated based on the rise in minimal battery capacity.

Economy

A charging station is uneconomical if its contribution to the overall system performance is rather low compared to the costs. The cost structure of charging stations is determined by the fixed values for the construction and purchasing of components. The following criteria have been selected to evaluate the economically viable operation of charging stations following the approach of Sistig [123].

Utilization
The utilization is described based on the time period during which a present bus can be charged at a charging station regardless of the current battery SOC. Under real world conditions, it is always possible that the bus does not require the entire period for charging. Thus, the benefits of lengthy but seldom stops could be reduced, which further reveals that this criterion is not sufficient on its own and that additional indicators are needed.

Number of charging events
The number of charging events indicates how frequently a charging station is visited. It extends the scope of the timely utilization.

Approximated energy-related costs
Energy-related expenses for charging at a certain station provide a further criterion to evaluate economic usefulness since they directly reveal cost-critical stations with low energy throughput or high costs. However, the charged energy depends on the dimensioning of all charging stations and batteries, and the absence of one charging station can cause that another charges significantly more. In addition, the costs for installing the charging station are influenced by the selected power level. Thus, the energy-related costs can only be approximated in the bus run analysis. The implemented approximation only includes fixed costs independent of the power level.

A further approximation is required for the energy charged at the particular charging station. Therefore, the assumption is made that all potential charging stations are installed and operated at maximum power, which could result in an over- or underestimation. However, the gap for the critical charging stations is expected to be rather low.

System relevance

Charging stations with limited economic viability could still be relevant for the system. Their absence may lead to infeasible system configurations or to strongly overdimensioned batteries.

The assessment of the system relevance of charging stations is performed in two steps: First, the scenario is simulated with the all potential charging stations at maximum power. In the second step, charging stations that were identified as uneconomical are excluded stepwise while it is analyzed how the minimal battery capacity develops and whether the energy charged at another uneconomical charging station rises. If one of the two criteria is applicable, the uneconomical charging station is labeled as critical.

5.2.2.3 GUI and Application

The entire functionality of the bus run analysis is integrated in a GUI, which enables a visualization of operational and technical constraints and their interdependencies. The GUI is divided into three areas as shown in Figure 5-7.

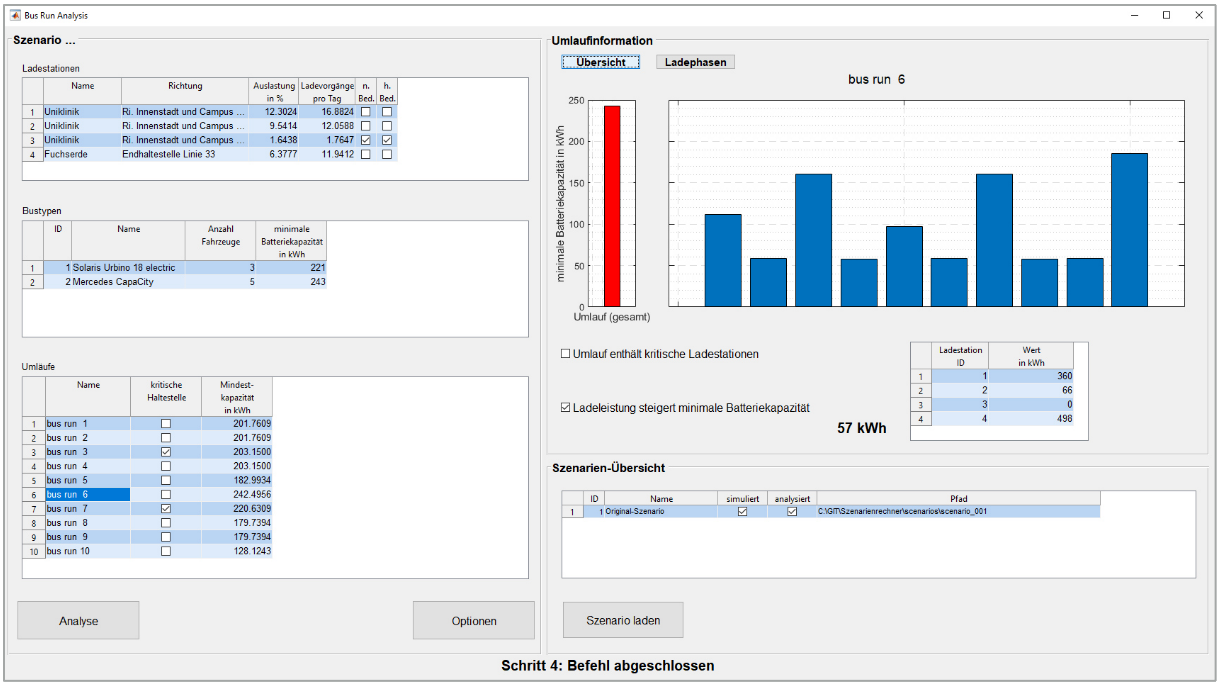

Figure 5-7: Bus Run Analysis GUI enabling users to assess the structure of bus runs and their linkage by charging events

The left part of the GUI displays the scenario with the identified charging stations, bus types and bus runs. The listing of elements is extended by the KPI introduced in the previous sections. The right part of the GUI shows details for the selected element in the left part. In Figure 5-7 for example bus run 6 is selected. The lower part on the right of the GUI enables the user to select different scenarios. The linkage of critical charging stations and bus runs is highlighted with markers.

The general workflow in the bus run analysis begins with loading the scenario which can consist of several bus runs and charging stations. The KPI are automatically evaluated and displayed in this process. Based on the information provided, the user can identify critical charging stations and dominating operational constraints which increase the minimal battery capacity. Afterwards manual changes can be applied to the operational scenario. One measure to remove a critical charging station regards for example assigning trips to this charging station to other bus runs. For widely varying minimal battery capacities, an introduction of an additional bus type could be advantageous so that not all buses have to be equipped with the maximum battery capacity. After applying the manual changes, the user can load the scenario again and evaluate the improvements.

5.3 Operational Adjustments for Depot Charger

The bus run analysis methods introduced in the previous section are less useful for depot-charging operations since no opportunity charging events at terminal stops occur. Therefore, an alternative measure is needed to improve infeasible bus runs, which is achieved by conducting a rescheduling of service trips under consideration of technical constraints regarding energy demand and charging time. The resulting problem is named Electric Vehicle Scheduling Fleet Size and Mix Problem with Optimization of Charging Infrastructure (EVS-FMC). The problem definition and solutions method have been published by the author in 2018 in the Applied Energy Journal [124].

The formulation of the EVS-FMC is introduced in Section 5.3.1. The developed solution approach for the problem combines a genetic algorithm and a MILP solver. Section 5.3.2 presents the structure of the genetic algorithm and the application. Using the described methodology, technically feasible bus runs can be generated which fulfill the respective constraints of a defined BEB type. Besides the bus runs, relevant output parameters regard the additional vehicle requirements, deadhead mileage and driver time.

5.3.1 Problem Formulation

The vehicle scheduling of depot-charging BEB must consider bus-specific and trip-dependent energy demands, energy limitations and required charging times. It is crucial for the TCO of the entire system since the required number of buses and chargers as well as the deadhead mileage and driver time directly follow from the schedule.

Figure 5-8 sketches the EVS-FMC that determines bus runs, fleet composition and charging infrastructure. The input consists of a given set of service trips (blue blocks in the right part of the figure), a set of BEB types (e.g., “white” and “grey” buses), one charging station type and a bus depot. Output, as depicted on the top right, assigns a subset of trips to a bus of a specific type, together referred to as the bus run, and includes charging time. Furthermore, the number of chargers is determined as well, and the usage of these charges over time directly follows from the bus runs.

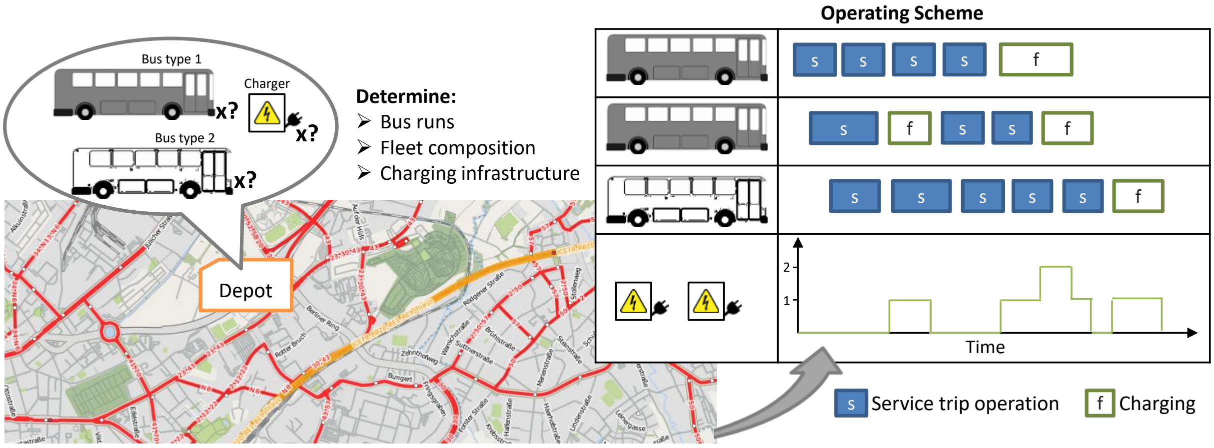

Figure 5-8: Overview of the Electric Vehicle Scheduling Fleet Size and Mix Problem with Optimization of Charging Infrastructure

The selection of bus types and quantities must be jointly executed with the scheduling of service trips to ensure that the particularities of each bus type are considered. Buses with a small battery capacity for example require several charging events during the daytime, whereas high-battery-capacity buses are mainly charged at night, which directly influences the fleet size and number of required chargers.

Each service trip in the EVS-FMC is defined by a starting time and location, an ending time and location and a set of route characteristics. The trip must be operated by exactly one bus of the given bus type. Each bus type has a limited battery capacity, a specific energy demand depending on the operational conditions, a fixed cost for the purchase of the bus and energy-related costs for the battery usage, which represent the replacements costs for a degraded battery or battery leasing. Each bus must begin and end its shift at the depot.

The total energy demand during operations is limited to the allowed range for the state of charge of the battery defined by SOC_{min} and SOC_{max}. It is assumed that the state of charge equals SOC_{max} when the bus begins its shift, which implies a full charging during the night. Charging occurs each time a bus visits a charging station and is conducted until the SOC reaches SOC_{max} with constant power.

5.3.1.1 Mathematical Model

For a set of n service trips S, a set of possible charging events F and a depot represented by a source node 0 and sink node $n + 1$, the model of the EVS-FMC is defined on the directed multigraph $G = (N, A)$ depicted in Figure 5-9.

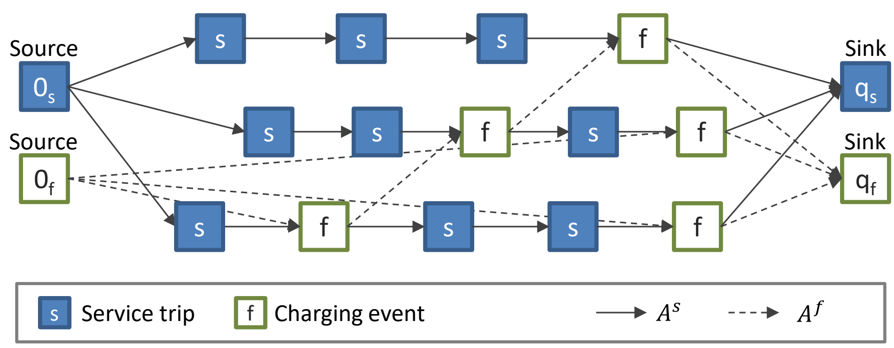

Figure 5-9: Directed multigraph of the EVS-FMC with arcs A^s connecting service trips and charging events operated by the same vehicle, and arcs A^f connecting charging events operated by the same charger.

The set of nodes N is defined as $N \coloneqq S \cup F \cup 0_s \cup 0_f \cup q_s \cup q_f$. Thus, the set N contains a node for each service trip $i \in S$ represented by blue nodes; it contains a node for each possible start of a charging event $f \in F$ represented white nodes in Figure 5-9; and it also contains source nodes $0_s, 0_f$ and sink nodes q_s, q_f representing the depot for both the set of service trips and set of charging events respectively. The set of arcs A, $A \coloneqq A^s \cup A^f$ consists of the set of all feasible deadhead trips A^s, represented by solid arcs, and the set of arcs A^f that connects charging events serviced by the same charger, represented by dashed arcs in Figure 5-9. A deadhead trip represents a non-service trip in which a bus drives from either the terminal stop of one service trip to the start of the next service trip; from the terminal stop of a service trip to a charger; or from a charger to the start of a service trip. Furthermore, S_0 denotes the union of the set of service nodes S and the source node 0_s; S_{n+1} denotes the union of the set of service nodes S and the sink node q_s; and $S_{0,n+1}$ denotes the union of the set of service nodes N^s, the source node 0_s and the sink node q_s. Similarly, the set F_0 (F_{n+1}) denotes the union of F and the source node 0_f (sink node q_f). The solution to the EVS-FMC defines a set of paths in the graph G depicted so that all (blue) service nodes are contained in exactly one path. Charging events are inserted in the paths to ensure sufficient charge for the entire trip and a fully charged battery of each bus by the end of the day.

A service trip $i \in S$ is defined by a start time β_i, a duration t_i and a set of trip characteristics relevant for the energy demand simulation within the BEB system model. Let V be the set of bus types. Each bus type $k \in K$ is represented by a usable battery capacity E^k in the range from SOC_{max} to SOC_{min}, a charging capability o^k and a specific energy demand of y_{ij}^k representing the energy demand of servicing trip $j \in S_{n+1}$ after trip $i \in S_0$ using vehicle type $k \in V$, including costs of servicing trip i and deadheading from i to j. Let m^k be the purchasing cost of a bus of type $k \in K$ and c_e^{k*} be the bus-specific energy costs.

The time-related operational costs of a bus (mainly driver salary) are represented by c_t. The time required for the subsequent execution of event $j \in S_{n+1}$ after $i \in S_0$ is expressed by t_{ij}. A supplement is added to all trips coming from and going to the depot in order to consider the required handling for parking and connecting to the charging infrastructure. The charging time is not considered as in-service time costs in the operational costs since the charging is not monitored by the driver. The purchasing costs of charging infrastructure are defined per charger as v.

Let the binary decision variable x_{ij}^{k} equal 1 if a bus of type $k \in K$ is operated on arc $a \in A^{s}$, which means that service trips or charging events are performed subsequently with the same bus type. Let the binary decision variable z_{lm} equal 1 if charging event $m \in F$ occurs after charging event $l \in$; thus, the arc $(l, m) \in A^{f}$ connects the charging events. The current energy level of a bus after executing trip $i \in S_{0,n+1}$ is defined by e_{i}^{k}. Let a_i be the starting time of event $i \in S \cup F$ (service trip or charging event) and $a_i = \beta_i$ for all $i \in S$. The starting time a_i for charging events $i \in F$ must fall in the range of the first possible charging time γ and the last possible charging time δ. The constant $M \gg a_i$ is used to avoid nonlinearities.

Objective Function

$$
\begin{aligned}
min \quad & \sum_{k \in K} \sum_{j \in N} m^{k} x_{0j}^{k} \\
& + \sum_{k \in K} \sum_{i \in S_0, j \in N, i \neq j} (t_i + t_{ij})\, j_{driver}\, x_{ij}^{k} \\
& + \sum_{k \in K} \sum_{i \in N, j \in F, i \neq j} c_{e}^{k*}\, (E^{k} - e_{j}^{k})\, x_{ij}^{k} \\
& + \sum_{j \in N} v\, z_{0j}
\end{aligned}
\tag{5.1}
$$

The objective (5.1) is to minimize the TCO, which is split into four sums. This simplified representation of the LCC model enables cost focus at an early stage, and the linearization ensures appropriate calculation speed.

In the first sum, the bus investment is calculated based on the arcs leaving the depot from the source node. Secondly, in-service costs unrelated to energy demand such as bus driver costs are accumulated and multiplied with a time-dependent cost factor. The third term represents the bus-specific costs related to energy demand and considers the accumulated energy demand whenever a bus visits a charging station, multiplied by an energy-dependent and bus-specific cost factor. Finally, the last part of the sum represents the investments in charging infrastructure.

Vehicle Scheduling Constraints

$$\sum_{k\in K}\sum_{j\in S_{n+1},i\neq j} x_{ij}^k = 1 \qquad \forall i \in S \qquad (5.2)$$

$$\sum_{k\in K}\sum_{j\in S_{n+1},i\neq j} x_{lj}^k \leq 1 \qquad \forall l \in F \qquad (5.3)$$

$$\sum_{i\in S_{n+1},i\neq j} x_{ji}^k - \sum_{i\in S_0,i\neq j} x_{ij}^k = 0 \qquad \forall j \in N, \forall k \in K \qquad (5.4)$$

$$a_i + t_i + t_{ij} \leq a_j + M\,(1 - \sum_{k\in V} x_{ij}^k) \qquad \forall k \epsilon K, \forall i \in S, \forall (i,j) \in A \qquad (5.5)$$

$$x_{ij}^k \in \{0,1\} \qquad \forall k \epsilon K, i \in S_0, j \in S_{n+1}, i \neq j \qquad (5.6)$$

Constraint (5.2) ensures that each service trip is covered by exactly one bus, while constraint (5.3) ensures that each copy of a charging station can maximally be visited once. Constraint (5.4) represents the flow constraints of the vehicle network. Next, constraint (5.5) ensures that events assigned to one vehicle do not overlap in time – that is, the starting time of the next service trip or charging event for a vehicle is greater or equal to the sum of the starting time of the previous trip, the trip or charging duration, and the deadheading time. In vehicle scheduling, the start time of service trips is pre-defined by the timetable while the start time of charging events is determined in the model. Constraint (5.6) defines the binary nature of the decision variables x_{ij}^k, representing that a vehicle of type k visits event i after event j. Events could regard both service trips and charging events. Individual bus runs are obtained from the x_{ij}^k variables of a solution.

Energy Constraints

$$0 \leq e_j^k \leq (e_i^k - h_{ij}^k)x_{ij}^k + E^k(1 - x_{ij}^k) \qquad \forall k \epsilon K, \forall i \in S, \forall j \in S_{n+1}, i \neq j \qquad (5.7)$$

$$e_0^k = E^k \qquad \forall k \epsilon K \qquad (5.8)$$

$$0 \leq e_j^k \leq E^k - y_{lj}^k\, x_{lj}^k \qquad \forall k \epsilon K, \forall l \in F, \forall j \in S_{n+1}, i \neq j \qquad (5.9)$$

Constraint (5.7) ensures that the required energy level for the assigned trips to a vehicle never exceeds the usable battery capacity. Furthermore, constraints (5.8) and (5.9) ensure that buses are fully charged when leaving the depot and after charging respectively – that is, that the battery energy level e_0^k is set to the maximum.

Charger Scheduling Constraints

$$\sum_{l,\in F_{n+1},l\neq m} z_{ml} - \sum_{l\in F_0,l\neq m} z_{lm} = 0 \qquad \forall m \in F \tag{5.10}$$

$$\sum_{m\in F_0} z_{lm} = \sum_{k\in V} \sum_{i\in S} x_{il}^k \qquad \forall l \in F \tag{5.11}$$

$$\sum_{k\in V} \sum_{i\in S} x_{il}^k \left(a_i + t_i + t_{il} + o^k\left(E^k - e_i^k\right)\right) \leq \sum_{k\in V} \sum_{j\in S} x_{jm}^k\left(a_j + t_j + t_{jm}\right) + M\,(1 - z_{lm}) \qquad \forall l,m \in F \tag{5.12}$$

$$\gamma \leq a_m \leq \delta \qquad \forall m \in F \tag{5.13}$$

$$a_l + o^k(E^k - e_l^k) + t_{lj} \leq a_j + M\,(1 - \sum_{k\in V} x_{lj}^k) \qquad \forall k \in K, \forall l \in F, \forall (l,j) \in A \tag{5.14}$$

$$z_{lm} \in \{0,1\} \qquad \forall\, l,m \in F, l \neq m \tag{5.15}$$

Constraint (5.10) represents the flow constraints of the charging infrastructure network, while constraint (5.11) ensures that each charging event includes a corresponding ingoing trip. Next, constraint (5.12) defines that the starting time of the next charging event must be greater or equal to the ending time of the previous charging event. Constraint (5.13) ensures that the charging can only be conducted within the predefined time window. Moreover, constraint (5.14) ensures that no charging events for a single charger overlap in time. Finally, constraint (5.15) defines the range of the binary decision variable z_{lm} indicating whether two charging events are scheduled sequentially.

5.3.2 Energy-based Vehicle Scheduling using Genetic Algorithms

The developed approach is based on a grouping genetic algorithm (GGA) that evaluates alternatives regarding fleet composition and scheduling. The overall framework is illustrated in Figure 5-10.

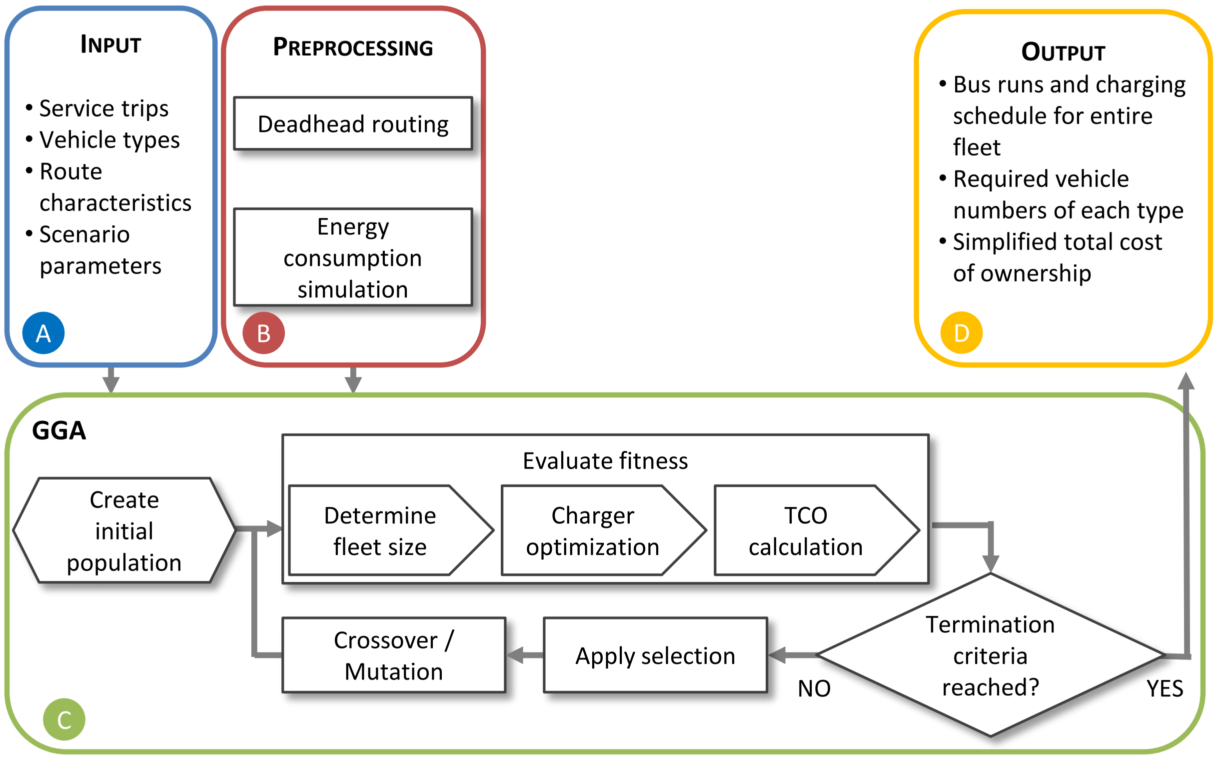

Figure 5-10: Framework of the energy-based vehicle scheduling with genetic algorithms

The input data (A) consist of operational and technical information and are utilized in the preprocessing (B) to calculate the values, which are not influenced by the vehicle scheduling, such as the deadhead mileage between terminal stops, with the functionality provided by the BEB system model. The route determination ensures that all distances of potential deadhead trips between service trips and between a service trip and charging station at the depot are realistic. The data prepared in the preprocessing are used within the GGA (C), which generates a population in which each individual describes a feasible assignment of an entire set of service trips to blocks starting and ending at the depot. In the following charger optimization phase, bus runs including charging times are designed based on these blocks. Individuals in the population are evaluated regarding their generalized TCO, consisting of BEB procurement costs (including determination of fleet size and mix), charging infrastructure investments and operational costs consisting of energy and personnel costs. After reaching a termination criterion, the GGA delivers the required fleet size and mix, the corresponding bus runs and the TCO of ownership as output (D). The individual steps are described in further detail in the following.

The heuristic is based on Falkenauer's concept describing the GGA [125] and emphasizes the grouping aspect of a scheduling problem – in this case, the assignment of a set of service trips to blocks. This clustering represents the core part of the EVS-FMC problem, as the locations and times of service trips are already fixed and the assignment of a feasible set of service trips $s \in S$ to blocks uniquely defines the tour. The GGA has been chosen due to its ability to identify high-quality solutions for comparable problems [126] and is furthermore well suited for parallel computing and offers several options for problem-specific customization.

The general procedure of the GGA is shown in step C of Figure 5-10 and begins by generating an initial population (set of individuals) that is afterwards evaluated by the fitness function. The process of evaluating an individual consists of three steps: 1) the determination of the fleet size by combining blocks defined by the chromosomes to bus runs, 2) the charger optimization and 3) the TCO calculation. If no termination criterion is reached, the process continues with the selection of competitive individuals which are modified during the crossover and mutation operations. After new genetic material has been created via crossover and mutation, the entire generation is evaluated again, and the loop continues until a termination criterion is reached. Termination criteria can for example be formulated as a maximum number of iterations, a limit for the change of the best fitness value over the last iterations and a lower bound of the diversity. The implementation in this work is terminated after a maximum number of iterations, but the extension to any of the other measures is straightforward.

The described procedure applies to the majority of genetic algorithms, but the particularity of the GGA regards its genetic representation of individuals. The genes of the GGA represent the characteristics of groups, which in this case regard blocks of service trips. The variable length of blocks implies chromosomes of a variable length. Furthermore, special operators are needed to perform crossover and mutation on the level of blocks.

5.3.2.1 Genetic Representation and Operators

The clustering of service trips within the GGA is conducted by creating blocks that define the genetic representation (chromosomes), as shown in Figure 5-11. A block represents a trip sequence operated by the same vehicle starting from and ending at the depot. Each block is followed by a charging event, and each individual in the population of the GGA covers the entire set of service trips divided into these blocks.

The block-based representation differs from other standards such as binary string chromosomes or arrays with real-valued numbers, as it is especially suited for clustering problems. The chromosome consists of different blocks to which service trips (represented as blue dots in Figure 5-11) can be assigned. The order of service trips within a block is uniquely defined by the starting time of the service trip. Each block is assigned to one bus type so that the specific usable battery capacity is respected given the bus type's specific energy demand. The blocks are furthermore characterized by a unique identifier (ID) that represents a consecutive numbering according to the earliest starting time of the covered trips.

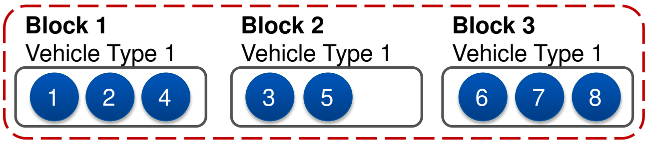

Figure 5-11: Genetic representation based on blocks containing service trips

The number of blocks in an individual and the number of trips assigned to a block can vary. Furthermore, the total number of required buses is not defined at this stage. It is computed afterwards in the fitness function by combining blocks and charging events to bus runs. This is executed jointly with the charger optimization, as described in Section 5.3.2.2. The GGA only allows the construction of feasible blocks in which the energy required to service all trips does not exceed the battery capacity and in which there is a feasible time ordering of the assigned trips. An ordering is feasible when the start time of the next trip is no earlier than the time required to service the previous trip and deadhead to the following one. The subsequently described construction heuristic ensures that only feasible blocks regarding time and energy exist in the population.

The population is divided into several subpopulations that are computed in parallel. After a predefined number of generations, a migration is performed in which individuals are exchanged among the subpopulations. The exchange strategy is to replace the worst individuals of one subpopulation with the best individuals of another. The separated treatment allows for promising solutions to be independently developed for a certain time, and the experiments conducted in this thesis reveal an improved stability of the algorithm.

Initial Solution

Both a random and greedy initialization are implemented and evaluated. In the random initialization, a trip is selected at random and inserted according to the insertion heuristic described in the next paragraph. In contrast, in the greedy initialization trips are inserted based on their starting time. Given a randomly selected first trip and a randomly selected direction (forward or backward in time), the trips to be inserted are ordered according to start time and selected in this order. Although the first random initialization leads to greater diversity, the quality of the initial solutions is generally worse as they may contain large gaps in time. Conversely, the diversity of the greedy initialization is lower, but solutions are generally of higher quality since the blocks are denser.

Figure 5-12 provides an exemplary overview of the quality of the initial solutions of both approaches. Experiments have shown that the greedy start enables the GGA to determine better overall solutions, and thus this methodology is set as the standard for this work.

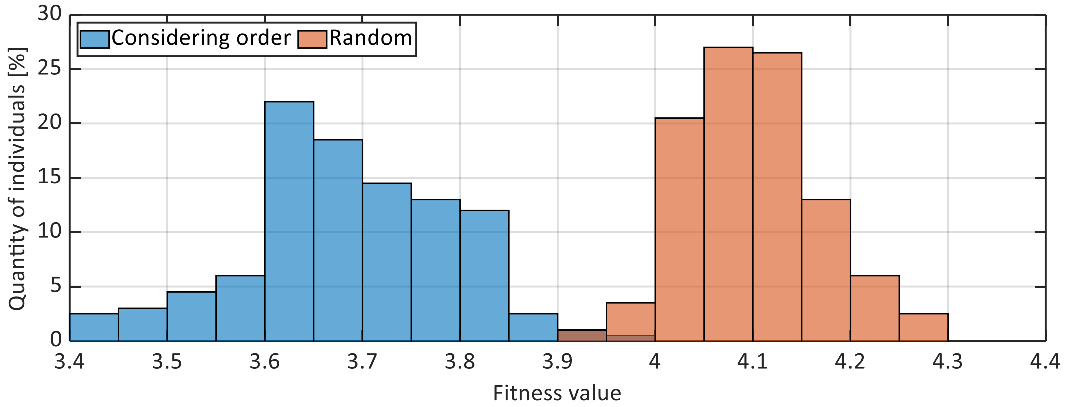

Figure 5-12: Distribution of fitness values (€ per service km) of the initial solutions for greedy and random start

Insertion Heuristic

The insertion heuristic, which is included in the crossover and mutation operators, assigns service trips to blocks based on operational costs. The service trip that should be inserted is selected beforehand by the calling function of the insertion heuristic. The heuristic inserts a service trip into a block for which the additional operational costs are the lowest.

For a given service trip, the insertion costs are calculated for all existing blocks as well as for an empty block. The costs consist of energy-related expenditures (electricity and battery usage) and the operational cost of deadheading to and from the service trip. Two scenarios could arise in which an insertion is impossible: First, the timing could be infeasible meaning that the existing and given service trip cannot be combined. Second, the required energy level could be insufficient. The new block considered by the insertion heuristic is empty and, in case of an assignment, would only cover the given service trip with its pull-out and pull-in deadhead trips plus a time buffer for handling at the bus depot. The consideration of an empty block ensures the existence of a feasible assignment.

Crossover

The crossover operation generates new genetic material by combining the chromosomes of selected parents. Blocks of the first parent are combined with blocks of the second parent to form an offspring. Figure 5-13 illustrates the crossover process.

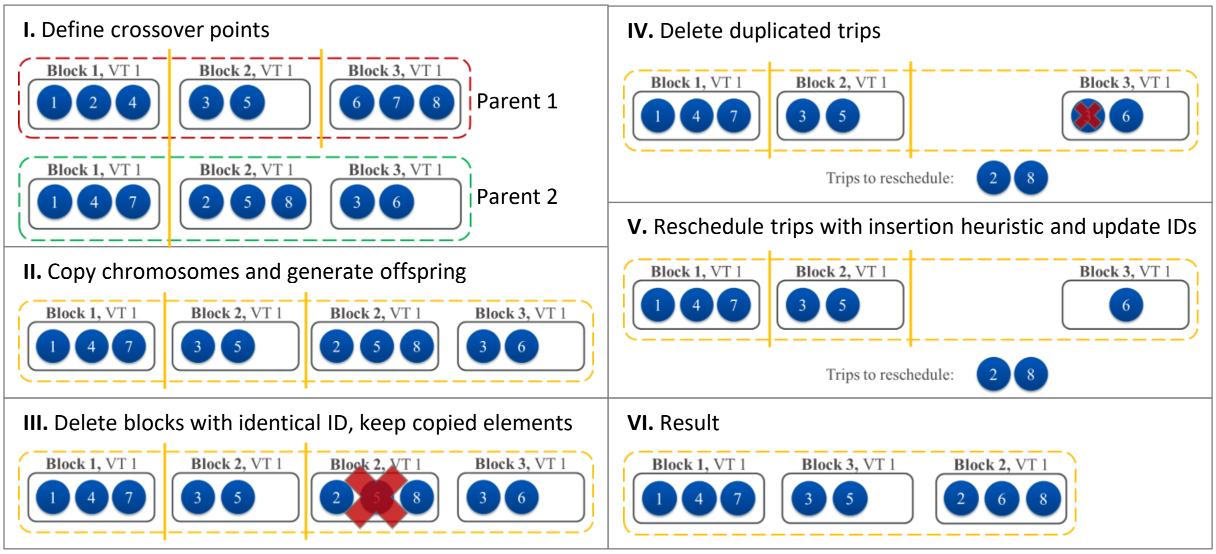

Figure 5-13: Overview of the implemented crossover

The first crossover points indicated by yellow vertical lines in Figure 5-13 are defined for both parents: two for the donating parent and one for the receiving parent. In the second step, the blocks between the two crossover points of parent 1 are copied to parent 2 at the position of the defined crossover point. The resulting child in stage II is infeasible, because the insertion from parent 1 has led to the issue of trips occurring twice in the child. Therefore, a repair is conducted in steps III to VI. In step III, blocks of parent 2 with an ID equal to the inserted blocks of parent 1 are removed. Step IV removes remaining duplicate service trips from parent 2, i.e., trips that are contained in the inserted blocks of parent 1. Then, in step V any service trips that are not contained in the child (as a result of step III) are re-inserted in random order according to the insertion heuristic. The result in step VI regards the new feasible offspring produced from the genetic material of both parents.

Mutation

The mutation aims to generate new genetic material to increase diversity. Instead of combining chromosomes of individuals as in the crossover, it modifies only single individuals. The mutation deletes one block selected at random and then reinserts the deleted service trips in random order. The feasibility of the solution is ensured by the usage of the insertion heuristic.

Fitness Function and Selection

Only operational costs are considered in the construction of blocks. The fitness function evaluates the solution with regard to the TCO, consisting of operational costs, number of required buses and number of required chargers.

The fitness function is divided into three steps as shown in part C of Figure 5-10. First, the fleet size is determined, which comprises the calculation of charging time required after completion of one block and the assignment of blocks to buses. It is assumed that each bus can start charging immediately after arriving at the depot. The assignment is performed based on a “first charged first out” strategy, which means that the first bus to be fully charged serves the next block. This defines the fleet size and composition.

However, when charging occurs immediately after a bus arrives at the depot, several simultaneous charging events can occur. This especially occurs in the evening when the passenger service is gradually reduced, and the buses return to the depot. Therefore, charging events are rescheduled in the second step of the fitness function in order to reduce the number of chargers and overall power level at the bus depot. Section 5.3.2.2 describes how the rescheduling is implemented and discusses further strategies for integration in the overall framework.

Finally, the TCO is calculated for each individual in step three and sums up the investment depreciations and operational expenses of a given time period. Within the GGA, the TCO characterizes the quality of an individual and is therefore called the fitness value.

In the selection process, individuals are ranked based on their fitness value. A stochastic uniform selection process is used to select individuals for reproduction, who form the input for the next generation and are modified via crossover or mutation. The selection process can be described using the example of a line on which each parent has a share according to the square root of its rank. A selector proceeds along the line in equal step sizes and selects parents according to the sections, beginning with a random point smaller than the step size. This concept can also be described as a roulette wheel with several pointers at an even distance.

5.3.2.2 Optimization of Charging Infrastructure

The objective of the charger optimization is to reduce the number of chargers and therefore charger investments. The input is described by a set of charging events F which have an earliest possible starting time b_l and a duration d_l. The charger optimization assigns charging events to chargers. The rescheduling of the charging events to reduce the number of chargers and the grid load regards a complex scheduling problem. However, the number of charging events in F is significantly lower than the number of service trips described by the set S.

Thus, common MILP solution approaches can be utilized. The mathematical model is derived from the network flow problem formulation presented in Section 5.3.1, uses the already introduced notation and is parameterized during runtime in Matlab [97] and solved by CPLEX [127]. Penalties for shifting a charging event in time are included since this has been found to decrease computation time. However, the weighting factor w is defined to ensure that a reduction in the number of chargers always dominates potential shift penalties.

$$min \sum_{m \in F} z_{0m} + w \sum_{l \in F} u_l \tag{5.16}$$

$$s.t. \sum_{l \in F_{n+1}, l \neq m} z_{ml} - \sum_{l \in F_0, l \neq m} z_{lm} = 0 \qquad \forall m \in F \tag{5.17}$$

$$\sum_{l \in F} z_{lm} = 1 \qquad \forall m \in F \tag{5.18}$$

$$a_l + d_l \leq a_m + M(1 - z_{lm}) \qquad \forall m, l \in F \tag{5.19}$$

$$\gamma_l \leq a_l + d_l \leq \delta_l \qquad \forall l \in F \tag{5.20}$$

$$a_l - b_l \leq u_l \qquad \forall l \in F \tag{5.21}$$

$$u_l \in \mathbb{R}_+ \qquad \forall l \in F \tag{5.22}$$

$$z_{lm} \in \{0,1\} \qquad \forall\, l \in F, m \in F, l \neq m \tag{5.23}$$

The objective in (5.16) minimizes the number of chargers (first term) as well as the amount of time-shift (second term). Constraint (5.17) regards the flow conservation constraint, while constraint (5.18) ensures that every charging event is scheduled. The linkage of charging events and therefore usage of the same physical charger are handled by constraint (5.19), which ensures that the subsequent charging event can only be linked if the starting time a_j is greater than the ending time of the previous event. Furthermore, constraint (5.20) limits the overall time window of charging events. Finally, the shift penalties are defined by constraint (5.21) as a supplement u_i added to the starting time and added for faster convergence.

Several measures are introduced to accelerate the computation of the model to allow an integration into the fitness function. The number of connection arcs is reduced by using ordered sets and only allowing forward assignments $z_{lm} = 0 \; \forall \; l \in F, m \in F, l \geq m$. The weighting factors are configured in such a way that the charger costs always dominate the shift penalties. A limit on the optimality gap is used to halt the computation if the number of chargers cannot be further reduced. In addition, a time limit of 5 s is introduced, which stops the solving and uses the best solution found at that point even if optimality is not proven. Instances with up to 70 charging events are solved in less than 1 s with CPLEX.

Including the MILP formulation in the fitness function enables the genetic algorithm to evaluate and select individuals based on the TCO, which includes the costs of charging infrastructure. An alternative strategy would be to approximate or ignore the number of chargers in the fitness function and to conduct the charger optimization afterwards.

An approximation could be realized by disabling the rescheduling of charging events in the fitness function, as shown by strategy I illustrated in Figure 5-14. This would lead to every charging event starting immediately after a bus finishes a block and arrives at the depot. In the example in Figure 5-14, both charging events can be operated by one charger. However, due to the reassignment of the initial trip of the first bus during mutation or crossover, the charging time of the second bus increases. The consequence is an overlap and the conclusion that two chargers are required. Thus, the number of chargers is overestimated since the potential shift forward in time is not utilized. The problem also occurs for improvements in the scheduling of service trips that would enable a reduction in the number of chargers. The improvements could be hidden and therefore not considered by the genetic algorithm if the number of chargers is approximated with an overestimation.

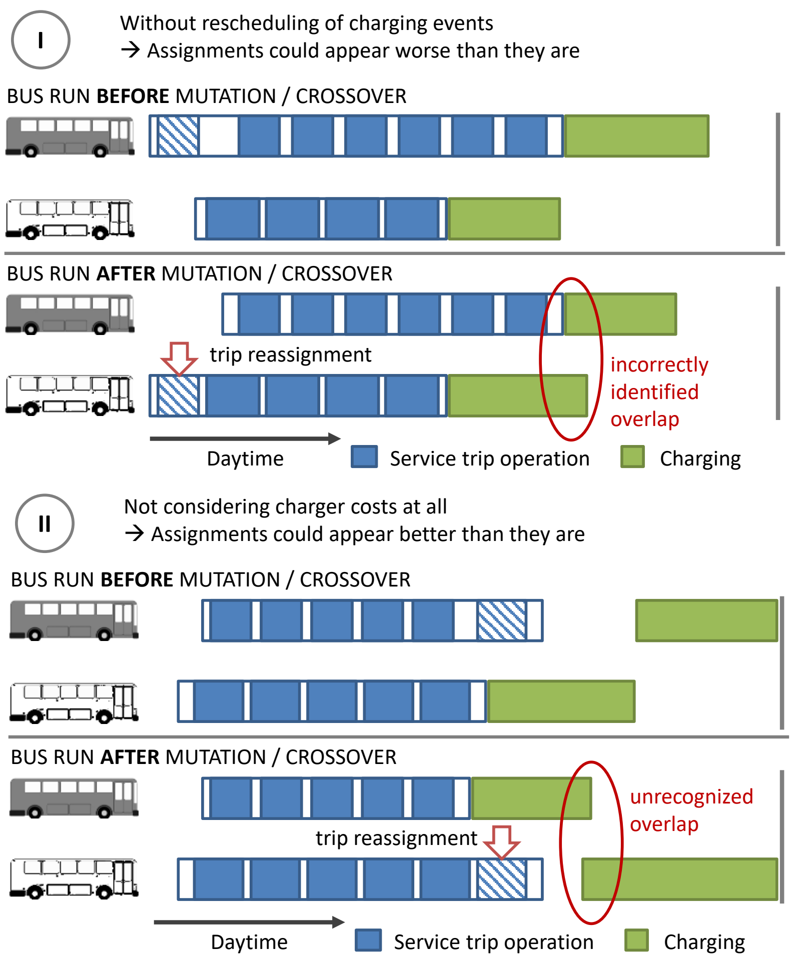

Figure 5-14: Illustration of problem cases that occur when using approximation strategies for determining the number of chargers

Not considering charging investments at all during the GGA runtime would lead to the opposite problem (strategy II, Figure 5-14). Unfavorable assignments of service trips that would cause an increased number of chargers would appear better than they are which could be misleading for the genetic algorithm. This example highlights how the reassignment of the last trip of the first bus during mutation or crossover leads to an increased charging time of the second bus and a shift forward in time of the entire charging event since the bus arrives later at the depot. Depending on the reduction of the charging time of the first bus, which is influenced by the charging power capabilities of the bus type and difference in energy demand before and after the reassignment, it is possible for the two charging events to overlap. This overlap would not be visible for the GGA when using this approximation, and a subsequent charging optimization could not fix this issue.

6 Case Study – Electrification of the Bus Network in Essen

The BEB system model in combination with the technical and operational analysis tools forms a comprehensive toolchain for the electrification potential assessment. Its application is demonstrated in this case study for the bus network of Essen, a city in western Germany with a population of more than 500,000 people. The case study represents a modified excerpt of the ebusplan project (ebusplan GmbH, Aachen) “Studie Zero Emission - Elektrifizierung des Bedienungsgebiets der Via Verkehrsgesellschaft” conducted by the author in 2017 for the PTO Via Verkehrsgesellschaft mbH (nowadays Ruhrbahn GmbH).

The case study follows a four-step planning process, starting with the database preparation during which the operational data are read and processed (Section 6.2). The database is afterwards enriched using geographical models of the track and a manual evaluation of charging opportunities. In addition to the local specific parameters, general technical parameters defining technology (vehicles and infrastructure) and costs are added. At the end of step one, the entire planning basis is established and the BEB system model is parameterized.

The utilization of the databases is conducted in step two within the technical and operational analysis (Section 6.3). For a set of BEB and charging infrastructure types, the general technical feasibility is evaluated and, where necessary, changes to the operational planning are executed. After step two, a large variety of different bus runs especially tailored for the considered BEB types have been developed. Depending on the user’s preferences and the local situation, the bus runs can be generated for a single bus route, a part of or for the entire bus network. For the case study, a route-wise analysis has been selected.

Given the large set of different technologies and their individually optimized operational planning, a further step is required to identify suitable solutions. Therefore, the technical and operational consequences are monetarized in step three (Section 6.4) within the LCC calculation for every scenario derived in step two, and furthermore the emissions of the BEB and conventional diesel bus operation are computed (Section 6.5). Both figures enable the user to conduct a cost-benefit analysis, which forms the basis for step four.

Step four regards the final step of the case study. Firstly, a technology recommendation is derived (Section 6.6.2) based on the cost-benefit analysis of step three. This recommendation includes the selection of a limited number of suitable BEB types and the determination of an infrastructure setup. The recommendation focuses on a full electrified bus fleet and thereby defines the goal of the entire electrification process. The final electrification concept describes the path towards this goal using stepwise vehicle procurements and infrastructure roll-out.

6.1 Scenario Description

Ruhrbahn is a community-owned PTO in Essen responsible for the operation of trams and buses in the densely populated city area. Ruhrbahn operates in total 49 bus routes in Essen, which divide into 31 regular routes, 2 sprint bus routes and 16 night routes. Further information regarding the routes is provided in Table 6-1.

Route	Category	Depot	Yearly mileage [km]	Route	Category	Depot	Yearly mileage [km]
14	Sprint	Stadtmitte	22,520	**180**	Regular	Ruhrallee	418,152
15	Sprint	Ruhrallee	575,532	**183**	Regular	Stadtmitte	347,543
140	Regular	Stadtmitte	336,276	**184**	Regular	Ruhrallee	301,167
141	Regular	Ruhrallee	459,464	**185**	Regular	Stadtmitte	310,238
142	Regular	Ruhrallee	871,964	**186**	Regular	Stadtmitte	568,631
143	Regular	Stadtmitte	461,153	**190**	Regular	Ruhrallee	250,023
144	Regular	Ruhrallee	167,802	**194**	Regular	Ruhrallee	667,445
145	Regular	Stadtmitte	550,749	**196**	Regular	Stadtmitte	446,151
146	Regular	Stadtmitte	665,271	**401**	Night	Ruhrallee	35,932
147	Regular	Stadtmitte	203,638	**402**	Night	Stadtmitte	26,689
154	Regular	Stadtmitte	166,567	**403**	Night	Stadtmitte	34,392
155	Regular	Ruhrallee	652,094	**404**	Night	Stadtmitte	50,973
159	Regular	Ruhrallee	16,622	**405**	Night	Stadtmitte	43,611
160	Regular	Ruhrallee	542,865	**406**	Night	Stadtmitte	40,442
161	Regular	Ruhrallee	184,648	**407**	Night	Stadtmitte	40,154
162	Regular	Stadtmitte	93,188	**408**	Night	Stadtmitte	71,348
164	Regular	Ruhrallee	302,037	**409**	Night	Stadtmitte	22,838
166	Regular	Stadtmitte	926,055	**410**	Night	Stadtmitte	36,974
167	Regular	Ruhrallee	22,709	**411**	Night	Stadtmitte	58,501
169	Regular	Ruhrallee	677,297	**412**	Night	Stadtmitte	61,218
170	Regular	Stadtmitte	1,024,703	**413**	Night	Stadtmitte	55,378
172	Regular	Stadtmitte	89,269	**414**	Night	Ruhrallee	48,040
173	Regular	Stadtmitte	126,214	**415**	Night	Stadtmitte	63,491
174	Regular	Ruhrallee	223,437	**416**	Night	Ruhrallee	48,206
177	Regular	Ruhrallee	404,775				

Table 6-1: Bus routes of the bus network in Essen operated by Ruhrbahn in 2017

In total 189 diesel buses are required to operate the bus routes, not including spare vehicles. Because the night route operation starts after the termination of most regular routes, the same vehicles can be utilized. The total yearly mileage in route service is about 13.8 million km or approximately 73,000 km per vehicle (without considering spare vehicles), which underlines the intensive usage of public transport buses.

The buses are located in two bus depots in Essen, *Ruhrallee* and *Stadtmitte*. Each route is dedicated to one bus depot as shown in Table 6-1. The locations of the bus depots are shown in Figure 6-1.

Figure 6-1: Locations of the bus depots of Ruhrbahn in Essen

6.2 Database Preparation and Parameter Definition

Local-specific operating schemes as well as general technical figures need to be gathered and defined for the electrification concept development. The processing of the PTO existing planning basis is described in Section 6.2.1. Relevant technical and financial figures are introduced in the following Sections 6.2.2 and 6.2.3.

6.2.1 Operational and Geographical Model

As a first step, the input for the operational and geographical model is derived from an export of the current planning basis. The export of Ruhrbahn consists of 12 individual day types covering the entire planning horizon. The most challenging day type regarding daily service mileage has been selected for further analysis, which is a weekday without school holiday.

On the selected day type, 3,645 trips (including 3,041 service trips) with a total mileage of 42,997 km are operated. The individual mileage of the service trips ranges from about 2 km to 27 km, revealing strong deviations between the routes. The demand regarding the route modeling is described by the number of route variants with the same track and bus stops. In total 238 variants of service trips were identified. Because this number still entails significant efforts regarding the track modeling, a further reduction regarding the main variants is conducted. Main variants describe the full track of the bus route from which subvariants can be derived. Figure 6-2 highlights the reduction and extraction of the proportion of main variants.

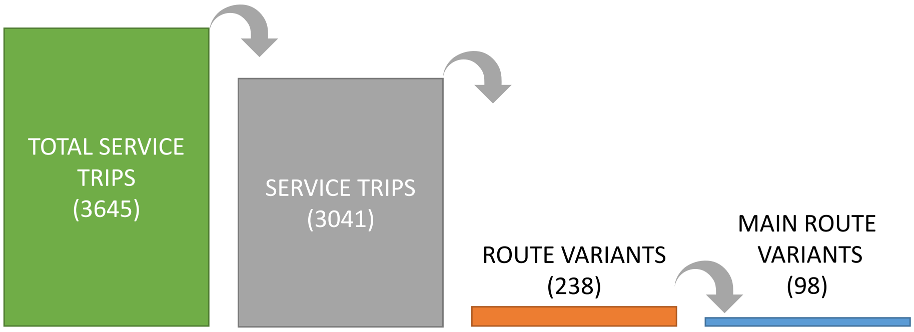

Figure 6-2: Overview on the number of operational elements and the proportion of main route variants required for the track modeling

The variant reduction enables a minimization of the efforts required for the track modeling. Results from the energy demand simulation of the main variants are transferred to the total number of variants based on the distance.

Figure 6-3 shows the model of bus route 142 starting at depot *Ruhrallee*. The markers highlight the stop positions on the track. Even though departure and arrival stop approximately have the same elevation, the total height difference of the route (difference between minimum and maximum elevation) is about 100 m.

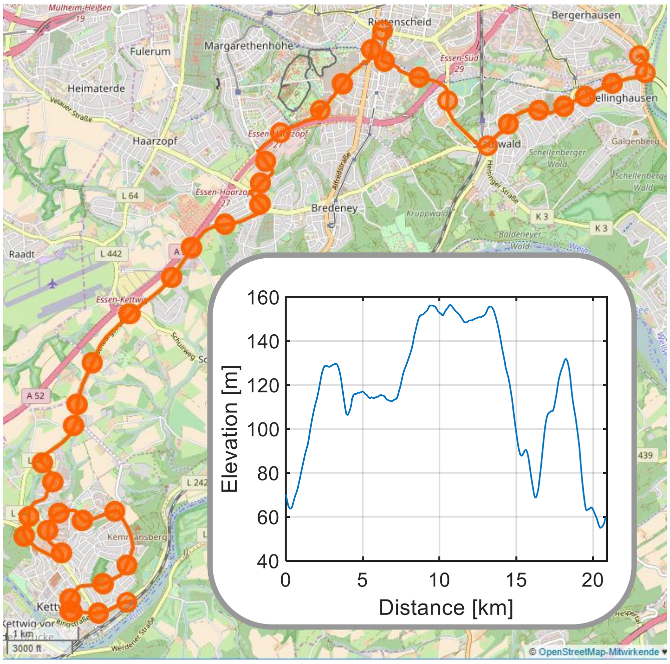

Figure 6-3: Track model of route 142 highlighting stop positions and elevation profile

In addition to the service trips, the deadhead trips also need to be identified. The total number of potential deadhead trips is defined by the quantity of terminal stops visited. Because this analysis focuses on the strategic planning, single stop positions at the same location are clustered to terminal stops, which is performed automatically based on the operational data acquisition routines.

In total 66 terminal stops (including both depots) were identified leading to 4,356 potential deadhead trips. While considering data already available in the PTO planning basis, the routing of these trips is executed using the input data preparation methods of the BEB system model. After completing this step, the operational and geographical model is completely defined for the further analysis covering operational data, routing of deadhead trips and track models.

6.2.2 Vehicles and Infrastructure

The current BEB market is characterized by a large variety of technical solutions. The aim of this case study is to derive a strategic decision for the electrification of the entire bus network. It is therefore not useful to focus on a specialized bus concept only offered by a single supplier. Instead, reference bus types are defined which summarize the main characteristics of the available solutions. The two dominating BEB concepts, depot and opportunity charging, are considered in the case study.

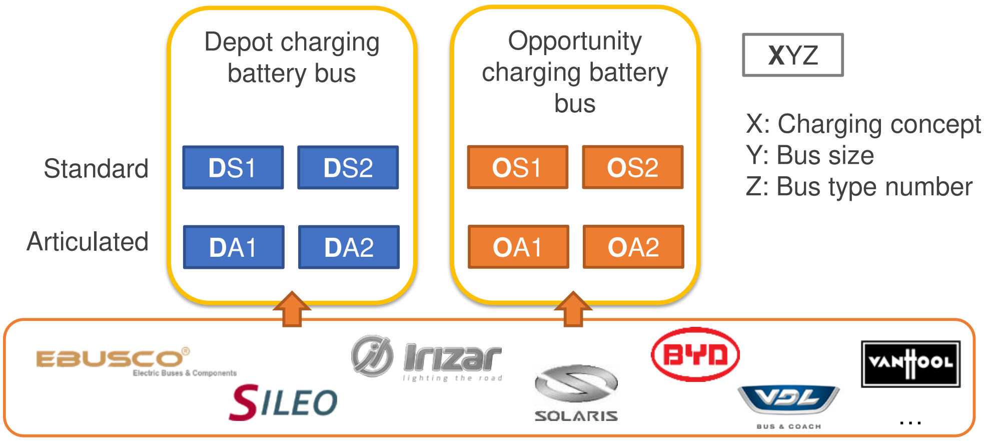

Figure 6-4: Reference bus types defined for the case study

Figure 6-4 provides an overview of the defined reference bus types. For each BEB concept, four bus types are derived, which differ regarding bus size (standard/articulated) and their technical parameters shown in Table 6-2. It is assumed that every bus is equipped with a pantograph coupling system.

The parameters provided in Table 6-2 represent the scenario “Current Technology” with technology currently available on the market. Furthermore, a scenario with improved technology (scenario “Advanced Technology”) is generated. The battery capacity and maximum charging power in the “Advanced Technology” scenario are increased by 20 % while the battery weights remain constant, and thus the energy and power density increase by 20 %.

Parameter	**Depot charger Type 1**		**Depot charger Type 2**		**Opportunity charger Type 1**		**Opportunity charger Type 2**	
	Stand. DS1	Artic. DA1	Stand. DS2	Artic. DA2	Stand. OS1	Artic. OA1	Stand. OS2	Artic. OA2
Battery capacity (installed) [kWh]	250	300	350	400	180	220	180	220
Battery capacity (useable) [kWh]	180	216	252	288	108	132	108	132
Maximum continuous charging power [kW]	80	80	80	80	300	300	450	450

Table 6-2: Technical parameters of the reference bus types – Scenario "Current Technology"

In addition to the bus types, two HVAC concepts are considered, namely:

[Aux-A] Full electric heating with heat pump and PTC heater

[Aux-B] Hybrid heating system with heat pump and fuel heater

The heat pumps utilized in both concepts serve as heating units in winter and as air condition in summer. The main difference between the concepts regards their additional heater (PTC or fuel heater). The performance at the relevant operating points is shown in Figure 6-5. Because concept B utilizes a fuel heater at low temperature, its electricity demand is significantly lower than using a PTC heater which generates heat from electricity in concept A. The worst case for concept B is therefore described as the air conditioning in summer, whereas the worst case of concept A regards winter operation with interior heating.

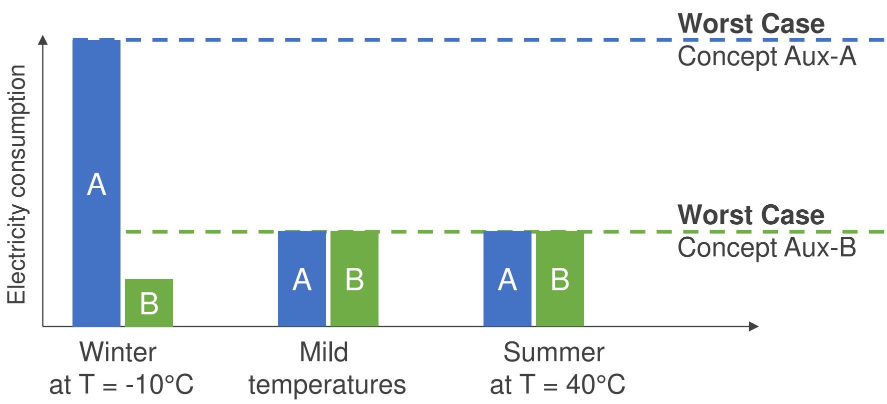

Figure 6-5: Exemplary electricity demands of the two cooling and heating concepts analyzed

The technical parameters of the charging infrastructure are provided in Table 6-3. The standard charger is relevant for charging in the depot, while the fast and ultra-fast chargers are installed at the terminal stops and only considered for opportunity charging BEB. The "Advanced Technology" scenario for the charger parameters is defined only for the fast and ultra-fast chargers, allowing an interoperable infrastructure in the depot.

Parameter	Standard charger	Fast charger	Ultra-fast charger
Located at	Depot	Terminal stop	Terminal stop
Coupling system	Coupling hood	Coupling hood	Coupling hood
Maximum charging power [kW]	80	300	450
Grid connection	Low voltage	Mid voltage	Mid voltage

Table 6-3: Technical parameters of the charging infrastructure types – Scenario “Current Technology”

Besides the technical parameters, the installation options of charging infrastructure must be evaluated, which is achieved via a manual process supported by statistical information extracted from the operational planning. The aim of this evaluation to increase the efficiency of the analysis by excluding stops which are rarely visited and at which no grid connection is available.

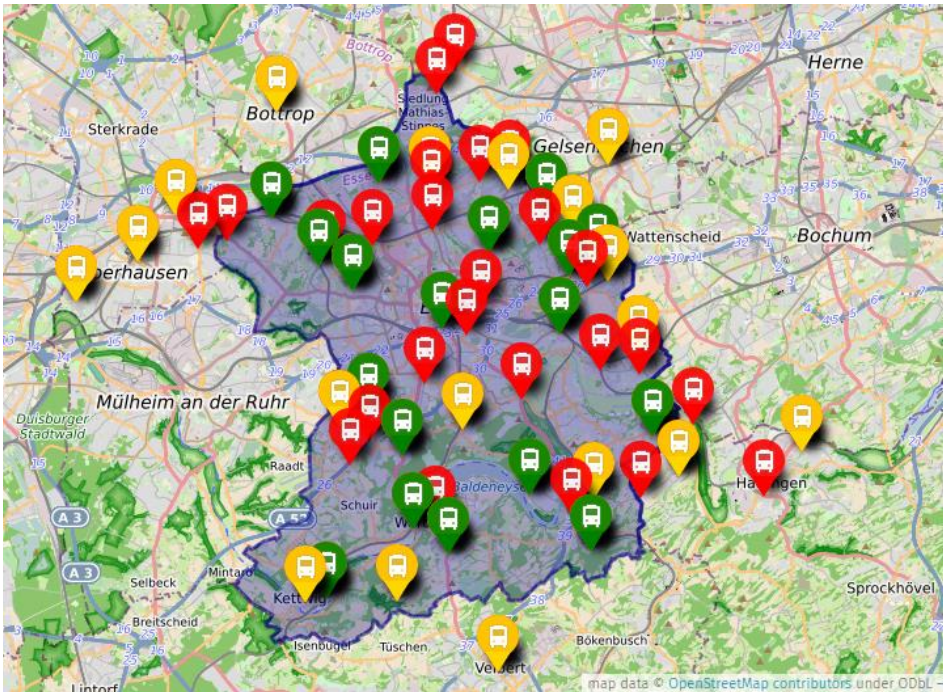

Figure 6-6: Terminal stops of the bus network – red and yellow markers reveal locations which were excluded from the scope of the analysis, whereas green indicators highlight potentially suitable charging locations

Figure 6-6 provides a visualization of the applied reduction. A favorable indication regarding the usefulness of installing charging infrastructure at a terminal stop is determined by the number of visits per day linked to the distance of the incoming trip. With a lower bound of 100 km per day, 28 terminal stops can be excluded, which reduced the total number from 64 to 36. The excluded terminal stops are highlighted in red in Figure 6-6. The manual assessment of the local conditions at the remaining locations enables a further reduction by 18 terminal stops (yellow). The final list of 18 terminal stops potentially suited as charging locations (green) is considered in the case study.

6.2.3 Costs Assumptions

LCC have been chosen as the comparative criterion between the technical solutions considered. The calculation includes cost assumptions for the basic vehicle, batteries, charging infrastructure, energy and personnel, which are introduced in the following subchapters. In addition, an interest rate of 2 % and an observation period of twelve years is chosen. All depreciations are assumed to be linear.

6.2.3.1 Basic Vehicle

The vehicle costs considered in the case study refer to the investment costs for the basic vehicle without battery but including the electric drivetrain. The additionally required battery and its replacement are considered separately. Table 6-4 gives an overview of the assumed investment and maintenance costs for the defined bus concepts and sizes.

Description	**Bus size**	**Bus type**	**Vehicle price [€]**	**Maintenance costs [€/km]**
DS1, DS2	Standard	Depot charger	300,000	0.35
DA1, DA2	Articulated	Depot charger	400,000	0.45
OS1, OS2	Standard	Opportunity charger	300,000	0.38
OA1, OA2	Articulated	Opportunity charger	400,000	0.48
RDS	Standard	Diesel reference	250,000	0.35
RDA	Articulated	Diesel reference	340,000	0.45

Table 6-4: Investments (without battery) and maintenance costs for the basic vehicle

A standard depot-charging bus with a basic vehicle price of 300,000 € equipped with a 350 kWh battery costing 262,500 € (Section 6.2.3.2) leads to a total investment of 562,500 €, which depicts the current market [128]. This price level is more than twice as high as the price level of a standard diesel bus, highlighting the importance of an LCC calculation within the electrification concept development to determine if high upfront invests can be compensated by lower operational costs.

Whereas purchase prices of BEB are available from ongoing procurements, maintenance costs regard empirical values and are not yet available due to the emerging technology. Although the electric drive offers the potential of low-maintenance operation, a significant part of the maintenance costs results from components that are not directly assigned to the electric drivetrain (doors, air compressor, etc.). Furthermore, the coupling system to the charger adds new components to the vehicles that require regular maintenance, and for this reason maintenance costs are estimated conservatively and for depot chargers are equal to the level of diesel buses. Due to the heavy utilization of the coupling systems in opportunity charging operation, maintenance costs are assumed to increase by 0.03 €/km for this bus type.

The useful life of the diesel buses is assumed to be 12 years with a residual value of 10 % at end-of-life. For BEB, a useful life of 15 years is assumed with a residual value of 4 %. The higher service life is expected due to the low-vibration drivetrain and can be observed in trolleybus fleets for example.

6.2.3.2 Batteries

The main component in the BEB regards the battery, which determines the technical performance and to a large extent the costs. The requirements for batteries differ according to the bus type. In the case of batteries for depot chargers, a high energy density is important. Such batteries therefore have lower specific costs than batteries for opportunity chargers, which are optimized for high charging power. The cost assumptions for batteries and the parameters for the lifetime calculation are shown in Table 6-5.

Bus type	Price in [€/kWh]	Cyclic lifetime in full cycle equivalents [FCE]	Calendric lifetime at 25 °C [years]
Depot charger	750	2,500	20
Opportunity charger	1000	5,000	20

Table 6-5: Specific price level and cyclic as well as calendric lifetimes of batteries

In order to consider the current market ramp-up for BEB, a linear price drop of 30 % is assumed for batteries in the 12-year planning horizon. Replacements are also procured at these reduced cost rates. Replacement batteries that are still functional at the end of the observation period are included in cost accounting with their residual values determined based on the remaining lifetime.

6.2.3.3 Charging Infrastructure

Charging infrastructures for BEB are offered in various configurations. A basic distinction can be made between chargers for the depot and fast chargers for installations at terminal stops. The cost assumptions listed in Table 6-6 are derived from current market prices.

Charger type	Power output [kW]	Price [€]	Maintenance [€/year]	Lifetime [years]
Standard	80	62,400	500	15
Fast charger	300	234,000	3,000	15
Ultra-fast charger	450	351,000	3,000	15

Table 6-6: Purchase prices, maintenance expenses and lifetime of charging infrastructure

A fully automatized charging system with a vehicle-mounted pantograph is assumed for both depot and opportunity chargers. The defined cost assumptions include the complete hardware, its installation and commissioning of a charging station. The high-power levels demand a new grid connection to the medium voltage grid. The establishing of the grid connection and the electric network at charging locations are considered with specific costs of 350 €/kVA.

6.2.3.4 Energy

The case study compares BEB with conventional diesel buses which serve as the reference, and therefore, three energy sources (diesel, electricity, and heating oil) must be considered. The values assumed for the case study are summarized in Table 6-7.

Energy source	Price	Annual price increase
Diesel	0.875 €/l	2.24 ct/l
Electricity	0.14 €/kWh	0.55 ct/kWh
Heating oil for fuel heater	0.60 €/l	1.54 ct/l

Table 6-7: Energy price levels and assumed annual developments in the planning horizon

The price level of diesel is based on procurements of the PTO, and value-added tax (VAT) in not included in the listed values. The assumed electricity price models the supply of electricity from renewable energy sources. The price level of heating oil for the fuel heater is comparable to diesel but using a different tax situation since it is not used for propulsion, which leads to a lower price per liter. The annual price increase is assumed based on the price development since 2000. The resulting price levels in the planning horizon are shown in Figure 6-7.

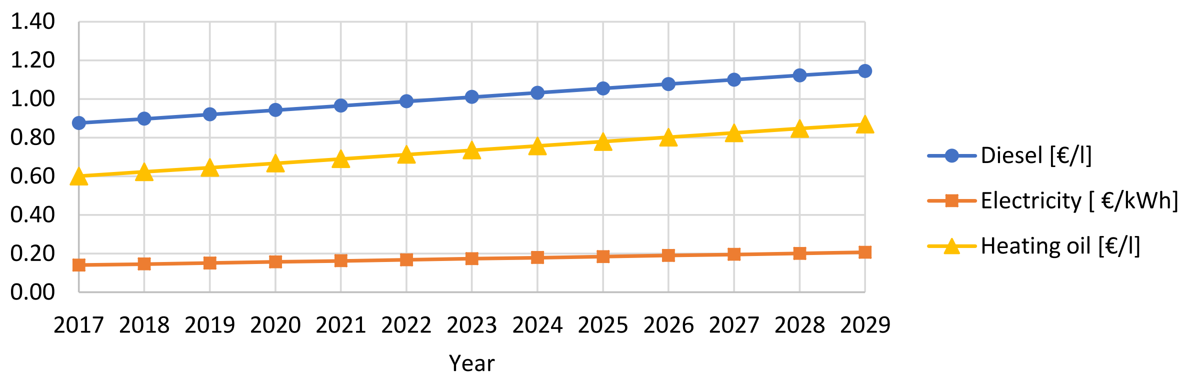

Figure 6-7: Assumed energy price levels in the planning horizon

6.2.3.5 Personnel

The operational changes caused by the operation of BEB with a limited range could lead to additional vehicles and additional deadhead mileage. Besides the consumed energy in deadheading, personnel expenses for the driver need to be considered. The personnel cost calculation in the BEB system model is based on a fixed hourly rate which is assumed to 28 €/h.

6.2.4 Robustness

A major concern of PTOs regards the robustness of their operation. Time buffers are already included in the diesel bus operation to compensate delays caused by traffic jams or high passenger utilization. However, for opportunity-charging BEB, delays are even more critical since they reduce the charging time at terminal stops if subsequent trips are started without delay. Delays on the routes are manually evaluated based on data from the PTO and modeled per route and direction.

Charging infrastructure malfunctions represent a further issue with direct consequences on the performance of opportunity-charging BEB. Due to the high utilization of fast-charging stations, a malfunction affects several buses. The robustness is ensured in this case by an energy reserve in the batteries. Such buffers can be defined as a fixed value or by requesting an autonomy in time or mileage (see Section 5.1).

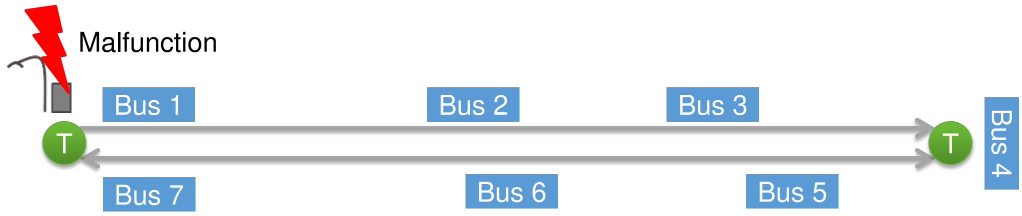

Figure 6-8: Situation in the event of charging infrastructure malfunction at arrival of bus 7

A minimum autonomy time of one hour is defined for the case study, during which route operation can be maintained even if all charging stations fail. An example is shown in Figure 6-8 in which bus 7 represents the most critical one. The autonomy defines the timeframe in which a repair must be conducted, or the affected buses must be replaced. Due to the demanded autonomy, opportunity-charging BEB always run with an energy reserve, which also enables compensating reduced dwell times or slightly changed routes.

6.3 Technical and Operational Analysis

The BEB system model and analysis tools are utilized in technical and operational analysis to determine the technical feasibility of an electrification and, where required, generate adjusted operating schemes for the various BEB concepts. The technical and operational analysis is conducted using the proviso that reliable operation under all conditions must be guaranteed. On the one hand, this specification refers to the operational conditions, such as the worst-case conditions for auxiliary consumers, and on the other hand to the technical condition of the vehicles such as the capacity loss of the battery due to aging. The most unfavorable combination is therefore assumed, which consists of maximum energy demand of the auxiliaries and an aged battery at the end-of-life (80 % residual capacity).

The energy demand of the traction system is determined by simulation with the vehicle model for each technology and the main route variants, and the results are afterwards transferred to the other route variants by considering mileage and trip duration. The transfer also considers the height difference between the varying terminal stops, which is obtained from the geographical model.

Because the operational consequences vary based on the technical performance, the results become sensitive towards the technical development, and as a result the entire analysis is performed twice: once with the reference vehicle types representing the current market and a second time for a scenario six years into the future with an expected increase of battery energy and power density. This enables a general classification of routes appropriate for a short or long term electrification.

The analysis is conducted route-wise, however by including the operational planning in the solution approach, the solution space widely expands. Therefore, a preselection of suitable operational schemes is performed. For depot-charging BEB this selection is already included in the algorithm based on the fitness function. For opportunity-charging BEB the preselection is performed based on the number of required buses, number of charging stations and additional deadhead mileage. In total, operating schemes for 784 configurations (49 bus routes, 4 bus types, 2 auxiliary configurations and 2 technology levels) are determined. Figure 6-9 highlights number of permutations for each route.

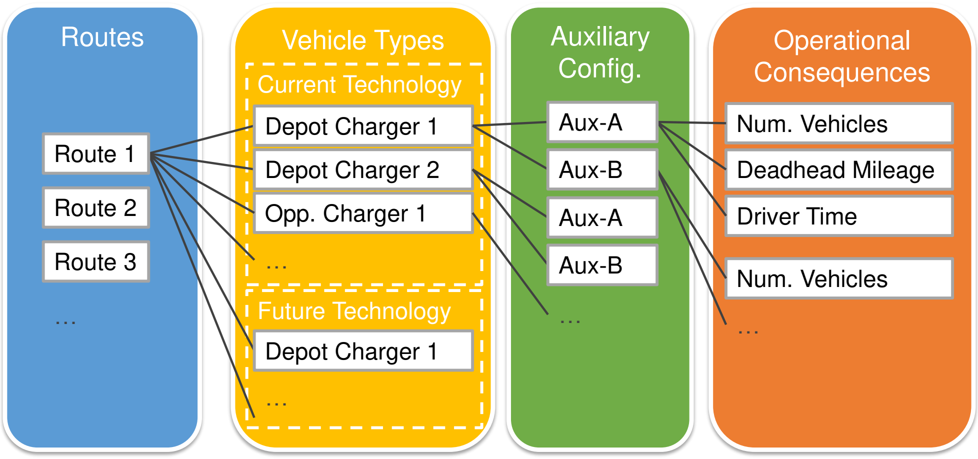

Figure 6-9: Overview of the determined configurations for each route

6.3.1 Detailed Results

The outcome of the route-wise technical and operational analysis is discussed in this section for route 140 and 144 in detail. Beginning with the current diesel bus operation, the required adaptations for the operational planning are introduced and discussed on the level of bus runs.

6.3.1.1 Route 140

Route 140 is currently operated using four standard diesel buses out of the depot *Stadtmitte*. The diesel bus runs shown in Figure 6-10 regard a mileage ranging from 216 km (bus 2) to 288 km (bus 1). Each blue block represents a service trip. The deadhead trips, not shown in the figure, have a total distance of 41.8 km.

The current bus runs have been assessed for both depot charger types and both auxiliary configurations. The SOC of the battery becomes negative in any simulation, pointing out that the mileages of the bus runs do not allow an electrification without operational adjustments. The final operating schemes derived for depot and opportunity charging are introduced in the following.

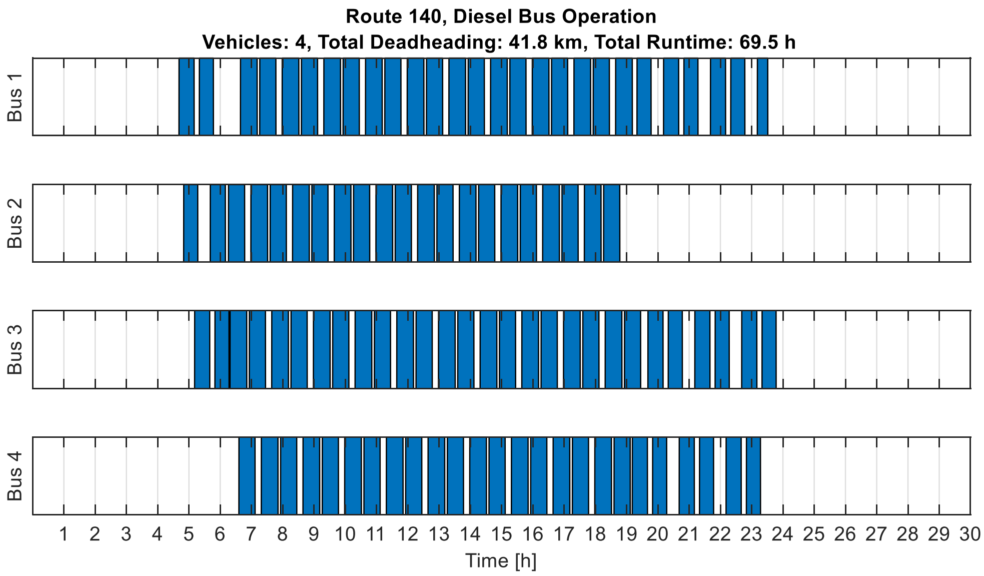

Figure 6-10: Route 140 – Bus runs in diesel bus operation

Opportunity Charging

Route 140 is characterized by regular dwell times at the terminal stop *Borbeck Bf*. With a 450 kW ultra-fast charging station at this terminal stop, route 140 can be electrified without adjustments to the original bus runs. Figure 6-11 highlights the bus runs of Opportunity Charger Type 2 (OS2) with electric heating (Aux-A). The charging time windows displayed in red are located at *Borbeck Bf*.

An operation with the original diesel bus runs is not possible for the 300 kW fast-charging station due to the limited dwell time. An additional bus becomes necessary, which is used to generate an overlay at *Borbeck Bf*. This overlay adds charging time according to the timetable interval of the route (20 minutes), which is sufficient for a charge sustaining operation.

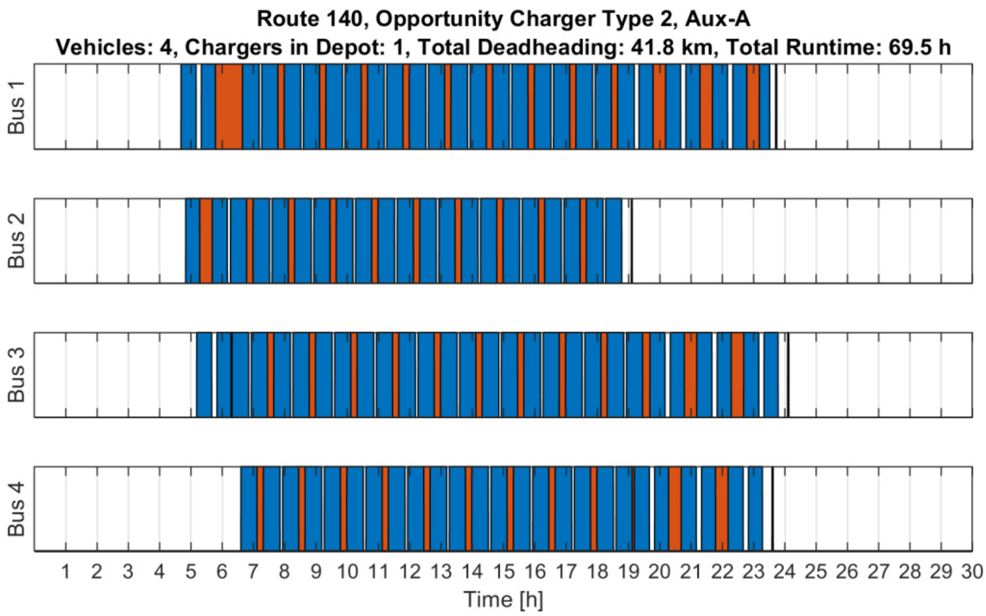

Figure 6-11: Route 140 – Bus runs of Opportunity Charger Type 2 Aux-A operation

Depot Charging

Figure 6-12 shows the generated bus runs for the Depot Charger Type 2 (DS2) with fuel heating (Aux-B). Service trips are marked as blue and charging phases in the depot as red blocks. Due to the large battery (350 kWh) and the low electricity demand of the hybrid heating system in winter, this type of depot charger provides the longest range. However, it is still necessary to cut existing bus runs and add charging time windows, which requires the usage of an additional vehicle.

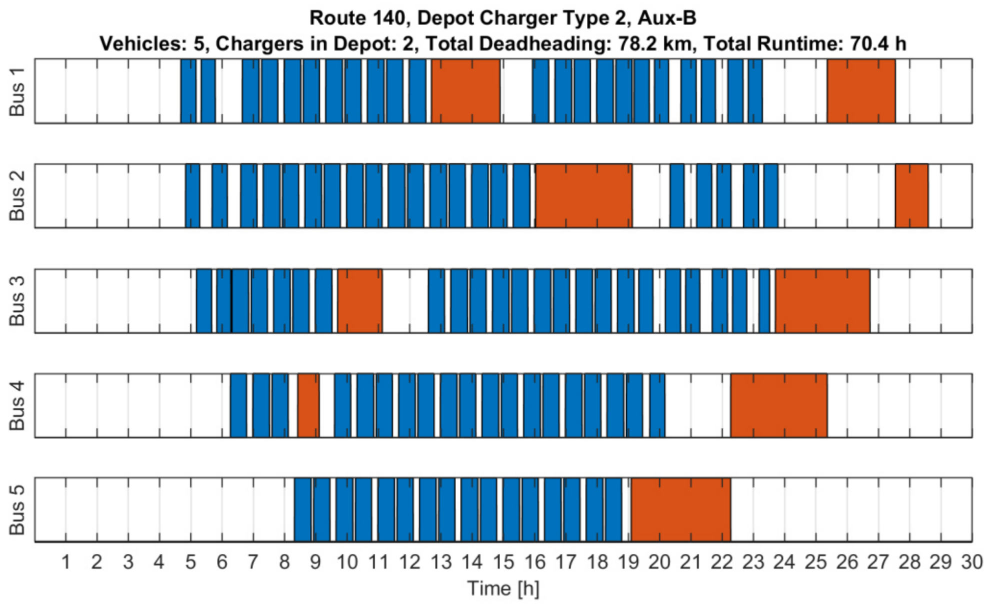

Figure 6-12: Route 140 – Bus runs of Depot Charger Type 2 Aux-B operation

Although five buses are operated in this scenario, two chargers are sufficient. This is enabled by the shifting of charging events, whose positive effect can be viewed in Figure 6-12 at the end of the bus runs as the final charging events of bus 1, bus 2 and bus 4 are shifted forward in time.

A further redistribution of trips becomes necessary if a full electric heater (Aux-A) is selected instead of the hybrid heating system (Aux-B). The higher electricity demand in the worst-case limits the individual applications of the vehicles even further and causes an increased charging time, which is illustrated by the number of bus runs shown in Figure 6-13. Instead of the four diesel buses, six BEB are now required. The deadhead mileage increases by 22 % compared to the operation with the same bus type and fuel heating. Compared to the diesel reference case, the deadhead mileage has more than doubled.

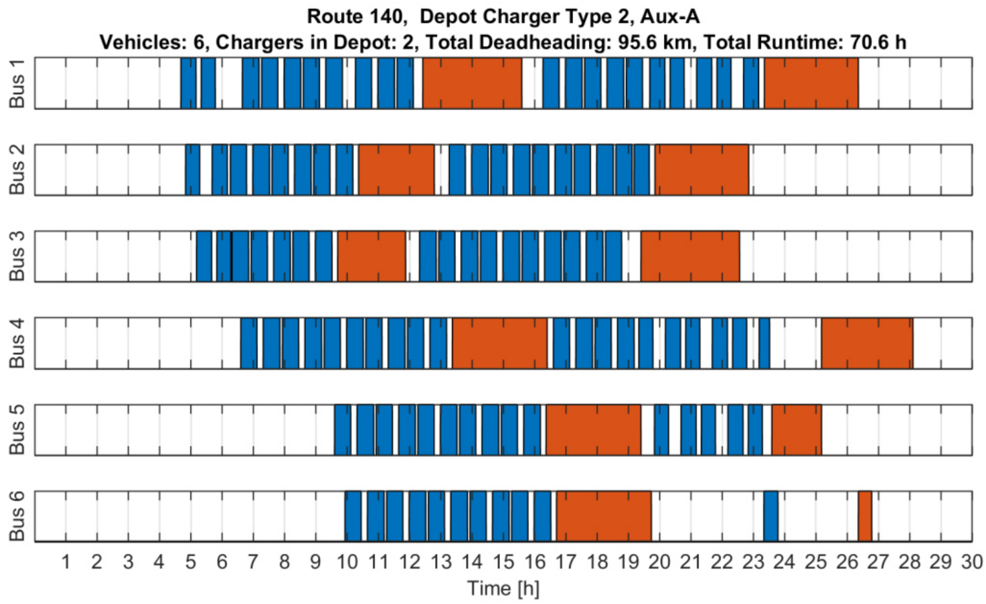

Figure 6-13: Route 140 – Bus runs of Depot Charger Type 2 Aux-A operation

6.3.1.2 Route 144

Route 144 operated from depot *Ruhrallee* is selected as a further example since its operational characteristics differ significantly from route 140. The vehicle requirement shown in Figure 6-14 is not constant over the entire operating day in contrast to route 140. During peak hours in the morning and afternoon five vehicles are operated and only two in the remaining morning.

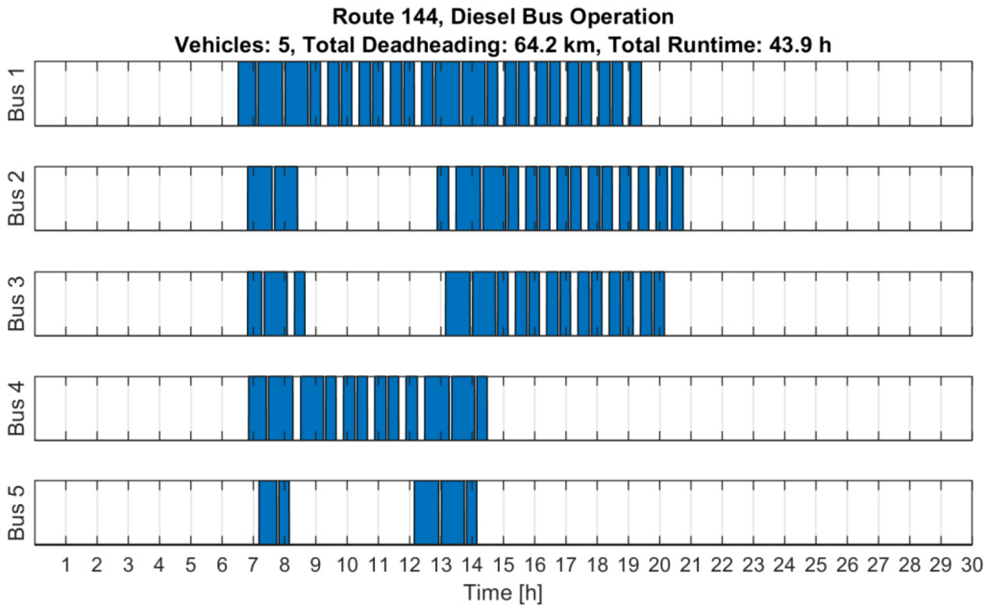

Figure 6-14: Route 144 – Bus runs in diesel bus operation

Opportunity Charging

Route 144 can be electrified with opportunity chargers and hybrid heating without operational changes compared to the diesel bus operation. The operating scheme for these buses is identical to the operating scheme of the diesel buses shown in Figure 6-14, however this changes when a full electric heating is requested. The dwell time and therefore the charging are not sufficient, thus an additional vehicle is needed. However, this mode of operation does not seem to be favorable since it does not utilize the varying vehicle demand between peak and off-peak hours.

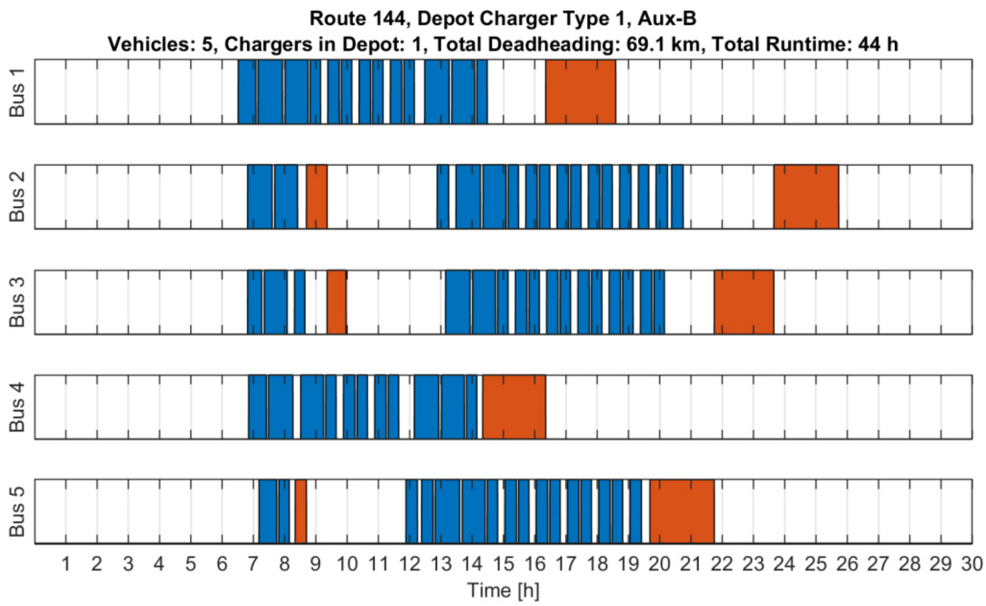

Figure 6-15: Route 144 – Bus runs of Depot Charger Type 1 Aux-B operation

Depot Charging

The interruptions of bus runs 2, 3 and 5 in the given operating scheme provide an initial indication of the potential suitability for depot chargers. Due to the high mileage of bus 1, minor adjustments to the operational planning are nevertheless necessary, as shown in Figure 6-15 for an operation with Depot Charger Type 1 Aux-B. The mileage of bus 1 in its original operating mode cannot be operated with a BEB due to the limited battery capacity. However, a redistribution of service trips and increased utilization of the vehicles allow electrification without additional vehicles in the case of Depot Charger Type 1, with only slightly increased deadhead mileage from 64 to 69 km.

The operating scheme for an electrification with Depot Charger Type 1 and a full electric heating (Aux-A) is illustrated in Figure 6-16. On the one hand, the operation can still be performed without additional vehicles, whereas on the other hand significant operation changes are introduced which increase the deadhead mileage by more than 45 %.

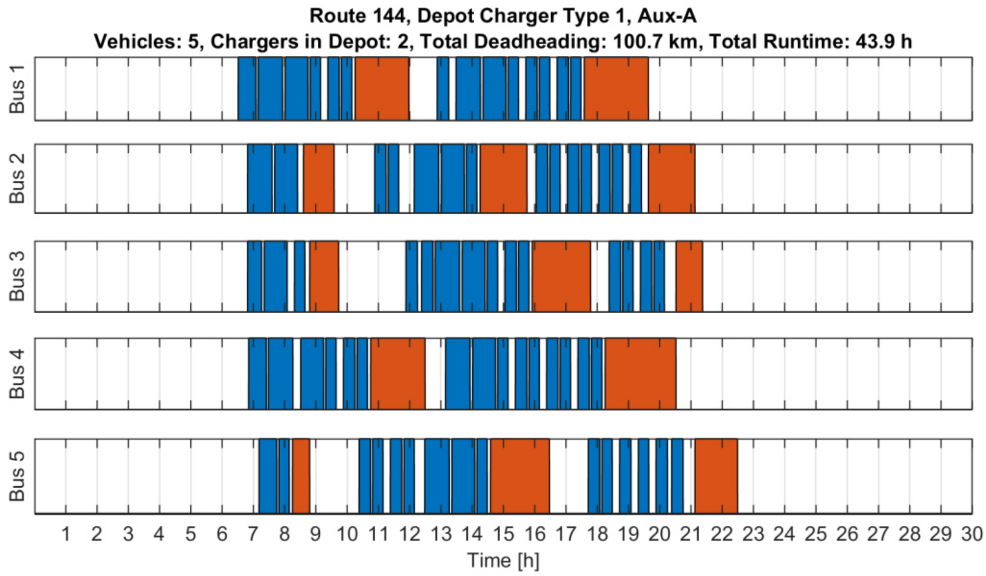

Figure 6-16: Route 144 – Bus runs of Depot Charger Type 1 Aux-A operation

6.3.2 Results Overview and Discussion

The detailed analysis presented for route 140 and 144 is conducted for all routes of the bus network. Considering the technical parameters of the BEB systems, operating concepts are derived and evaluated regarding vehicle demand, deadhead mileage and driver time. Diesel bus operation is used as the reference. Due to their long range, diesel buses entail few operational restrictions, which is why the diesel bus operating concept defines the lower bound in terms of the number of vehicles.

Table 6-8 shows the results regarding vehicle demand for each route in the entire network, and additional vehicle demand is highlighted with a color coding. Routes without additional vehicles compared to diesel bus operation are marked in green, routes with one to two additional vehicles in yellow and routes with three or more additional vehicles in red.

The plausibility of the results can be verified based on the technical assumptions. Depot Charger Type 1 is equipped with the smallest battery, and the additional vehicle demand for this bus type is therefore comparatively the highest. Furthermore, the influence of the heating systems becomes clear as the full electric heater (Aux-A) often requires a higher number of vehicles than hybrid heating system (Aux-B), which can be explained by the higher energy demand which reduces the range and causes longer charging phases and therefore downtimes. The battery capacity of Depot Charger Type 2 is higher than that of Type 1, which increases the range so that the additional vehicle requirements can be reduced for some routes.

In the case of opportunity chargers, the permitted additional vehicle requirements are limited due to limited space at terminal stops and since charging stations cannot be built at all locations. As a result, not all routes can be electrified with opportunity charging. Respective routes are highlighted in red and marked with "-" such as route 166.

The detailed examination of the results has already shown that depot charging is particularly suitable for routes whose vehicle requirements vary during the day, such as with route 144. Necessary charging phases can thus be integrated into the operating scheme with little effort. Routes with similar characteristics include 142, 146, 154, 161, 166, 170, 172, 174 and 180, but routes 146 and 170 still require additional vehicles.

The results furthermore reveal that where opportunity charging is possible, it can often be accomplished without additional vehicles when a hybrid heating strategy is applied. In comparison to the depot-charging operation, the consequences of a full electric heating (Aux-A) are lower regarding the vehicle demand. In most cases, one additional vehicle is sufficient, which is enabled by frequent charging during operation.

Route	Bus Type	Num. Vehicles Diesel Reference	Additional Vehicle Demand (Scenario Current Technology)								Additional Vehicle Demand (Scenario Advanced Technology)							
			Depot Charger Type 1		Depot Charger Type 2		Opportunity Charger Type 1		Opportunity Charger Type 2		Depot Charger Type 1		Depot Charger Type 2		Opportunity Charger Type 1		Opportunity Charger Type 2	
			Aux-A	Aux-B	Aux-A	Aux-B	Aux-A	Aux-B	Aux-A	Aux-B	Aux-A	Aux-B	Aux-A	Aux-B	Aux-A	Aux-B	Aux-A	Aux-B
14	Articulated	2	0	0	0	0	0	0	0	0	0	0	0	0	0	0	0	0
15	Articulated	6	7	6	6	4	2	1	1	1	6	4	6	3	1	1	1	1
140	Standard	4	3	2	2	1	1	0	0	0	2	2	2	1	0	0	0	0
141	Standard	5	4	2	4	2	-	-	-	-	3	2	3	1	-	-	-	-
142	Standard	12	3	0	1	0	-	1	1	1	2	0	1	0	1	1	1	1
143	Standard	6	5	3	4	2	-	1	1	1	4	2	3	1	1	1	1	1
144	Standard	5	0	0	0	0	1	0	1	0	0	0	0	0	0	0	0	0
145	Articulated	7	7	5	7	4	-	1	1	1	7	4	6	3	1	1	1	0
146	Articulated	10	5	2	4	1	-	-	-	1	5	2	3	1	-	1	-	1
147	Articulated	3	3	2	3	1	0	0	0	0	3	2	2	1	0	0	0	0
154	Standard	5	2	0	0	0	1	0	1	0	0	0	0	0	1	0	0	0
155	Articulated	7	7	5	7	4	-	-	-	-	7	4	6	4	-	-	-	-
159	Standard	1	1	0	0	0	0	0	0	0	0	0	0	0	0	0	0	0
160	Articulated	7	7	5	7	4	1	0	1	0	7	4	6	3	1	0	1	0
161	Articulated	6	2	0	1	0	0	0	0	0	1	0	0	0	0	0	0	0
162	Standard	2	1	1	1	0	-	0	-	0	1	1	1	0	0	0	0	0
164	Articulated	4	4	3	4	2	-	1	1	1	4	2	4	2	1	1	1	1
166	Articulated	15	6	2	4	0	-	-	-	-	5	1	3	0	-	-	-	-
167	Standard	1	1	0	1	0	0	0	0	0	1	0	1	0	0	0	0	0
169	Articulated	7	7	6	8	5	-	1	1	1	9	6	7	4	2	1	1	0
170	Articulated	16	11	5	9	3	-	-	-	-	9	4	6	2	-	-	-	1
172	Standard	2	1	0	0	0	-	-	-	-	1	0	0	0	-	-	-	0
173	Standard	2	1	1	1	1	-	-	-	-	1	1	1	0	-	0	-	0
174	Standard	5	1	0	1	0	1	0	0	0	1	0	0	0	0	0	0	0
177	Standard	4	4	3	4	3	1	1	1	1	4	3	4	2	1	1	1	1
180	Standard	6	2	1	2	0	1	0	0	0	2	1	1	0	0	0	0	0
183	Standard	4	3	2	2	1	-	-	-	-	2	1	2	1	-	-	-	-
184	Standard	5	3	2	3	1	1	0	0	0	3	2	2	1	0	0	0	0
185	Standard	4	3	2	2	1	1	1	1	1	3	1	2	1	1	1	1	1
186	Standard	7	4	3	4	2	-	-	-	-	5	3	4	2	-	-	-	-
190	Standard	4	3	2	2	1	-	-	-	-	2	1	2	1	-	-	-	-
193	Standard	1	0	0	0	0	0	0	0	0	0	0	0	0	0	0	0	0
194	Standard	8	9	5	8	4	-	-	-	-	8	5	7	4	-	-	-	-
196	Standard	6	6	4	6	3	1	1	1	1	6	3	5	3	1	1	1	1
401	Articulated	2	0	0	0	0	1	1	1	1	0	0	0	0	1	1	1	1
402	Articulated	2	0	0	0	0	1	0	1	0	0	0	0	0	1	0	0	0
403	Standard	2	0	0	0	0	0	0	0	0	0	0	0	0	0	0	0	0
404	Standard	3	1	0	0	0	1	0	0	0	0	0	0	0	0	0	0	0
405	Articulated	3	0	0	0	0	1	0	1	0	0	0	0	0	1	0	0	0
406	Standard	2	0	0	0	0	1	1	1	1	0	0	0	0	1	1	1	1
407	Standard	2	0	0	0	0	1	1	1	1	0	0	0	0	1	1	1	0
408	Articulated	3	1	1	1	0	-	-	-	1	1	1	1	0	-	1	-	1
409	Articulated	2	0	0	0	0	1	0	1	0	0	0	0	0	1	0	0	0
410	Articulated	3	0	0	0	0	0	0	0	0	0	0	0	0	0	0	0	0
411	Articulated	3	1	0	0	0	-	1	-	1	1	0	0	0	-	1	1	1
412	Articulated	3	1	0	1	0	0	0	0	0	1	0	0	0	0	0	0	0
413	Standard	3	0	0	0	0	1	0	1	0	0	0	0	0	0	0	0	0
414	Standard	2	1	0	1	0	1	0	0	0	1	0	0	0	0	0	0	0
415	Standard	2	2	1	2	1	0	0	0	0	2	1	1	0	0	0	0	0
416	Standard	3	0	0	0	0	1	1	1	1	0	0	0	0	1	1	1	0

Table 6-8: Additional vehicle demand in BEB operation compared to the diesel reference for the scenario "Current Technology" with available technology on the market and the scenario "Advanced Technology" with an assumed technology improvement

Route	Bus Type	Num. Vehicles Diesel Reference	Relative Additional Vehicle Demand (Scenario Current Technology)								Relative Additional Vehicle Demand (Scenario Advanced Technology)							
			Depot Charger Type 1		Depot Charger Type 2		Opportunity Charger Type 1		Opportunity Charger Type 2		Depot Charger Type 1		Depot Charger Type 2		Opportunity Charger Type 1		Opportunity Charger Type 2	
			Aux-A	Aux-B	Aux-A	Aux-B	Aux-A	Aux-B	Aux-A	Aux-B	Aux-A	Aux-B	Aux-A	Aux-B	Aux-A	Aux-B	Aux-A	Aux-B
14	Articulated	2	0%	0%	0%	0%	0%	0%	0%	0%	0%	0%	0%	0%	0%	0%	0%	0%
15	Articulated	6	117%	100%	100%	67%	33%	17%	17%	17%	100%	67%	100%	50%	17%	17%	17%	17%
140	Standard	4	75%	50%	50%	25%	25%	0%	0%	0%	50%	50%	50%	25%	0%	0%	0%	0%
141	Standard	5	80%	40%	80%	40%	-	-	-	-	60%	40%	60%	20%	-	-	-	-
142	Standard	12	25%	0%	8%	0%	-	8%	8%	8%	17%	0%	8%	0%	8%	8%	8%	8%
143	Standard	6	83%	50%	67%	33%	-	17%	17%	17%	67%	33%	50%	17%	17%	17%	17%	17%
144	Standard	5	0%	0%	0%	0%	20%	0%	20%	0%	0%	0%	0%	0%	0%	0%	0%	0%
145	Articulated	7	100%	71%	100%	57%	-	14%	14%	14%	100%	57%	86%	43%	14%	14%	14%	0%
146	Articulated	10	50%	20%	40%	10%	-	-	-	10%	50%	20%	30%	10%	-	10%	-	10%
147	Articulated	3	100%	67%	100%	33%	0%	0%	0%	0%	100%	67%	67%	33%	0%	0%	0%	0%
154	Standard	5	40%	0%	0%	0%	20%	0%	20%	0%	0%	0%	0%	0%	20%	0%	0%	0%
155	Articulated	7	100%	71%	100%	57%	-	-	-	-	100%	57%	86%	57%	-	-	-	-
159	Standard	1	100%	0%	0%	0%	0%	0%	0%	0%	0%	0%	0%	0%	0%	0%	0%	0%
160	Articulated	7	100%	71%	100%	57%	14%	0%	14%	0%	100%	57%	86%	43%	14%	0%	14%	0%
161	Articulated	6	33%	0%	17%	0%	0%	0%	0%	0%	17%	0%	0%	0%	0%	0%	0%	0%
162	Standard	2	50%	50%	50%	0%	-	0%	-	0%	50%	50%	50%	0%	0%	0%	0%	0%
164	Articulated	4	100%	75%	100%	50%	-	25%	25%	25%	100%	50%	100%	50%	25%	25%	25%	25%
166	Articulated	15	40%	13%	27%	0%	-	-	-	-	33%	7%	20%	0%	-	-	-	-
167	Standard	1	100%	0%	100%	0%	0%	0%	0%	0%	100%	0%	100%	0%	0%	0%	0%	0%
169	Articulated	7	100%	86%	114%	71%	-	14%	14%	14%	129%	86%	100%	57%	29%	14%	14%	0%
170	Articulated	16	69%	31%	56%	19%	-	-	-	-	56%	25%	38%	13%	-	-	-	6%
172	Standard	2	50%	0%	0%	0%	-	-	-	-	50%	0%	0%	0%	-	-	-	0%
173	Standard	2	50%	50%	50%	50%	-	-	-	-	50%	50%	50%	0%	-	0%	-	0%
174	Standard	5	20%	0%	20%	0%	20%	0%	0%	0%	20%	0%	0%	0%	0%	0%	0%	0%
177	Standard	4	100%	75%	100%	75%	25%	25%	25%	25%	100%	75%	100%	50%	25%	25%	25%	25%
180	Standard	6	33%	17%	33%	0%	17%	0%	0%	0%	33%	17%	17%	0%	0%	0%	0%	0%
183	Standard	4	75%	50%	50%	25%	-	-	-	-	50%	25%	50%	25%	-	-	-	-
184	Standard	5	60%	40%	60%	20%	20%	0%	0%	0%	60%	40%	40%	20%	0%	0%	0%	0%
185	Standard	4	75%	50%	50%	25%	25%	25%	25%	25%	75%	25%	50%	25%	25%	25%	25%	25%
186	Standard	7	57%	43%	57%	29%	-	-	-	-	71%	43%	57%	29%	-	-	-	-
190	Standard	4	75%	50%	50%	25%	-	-	-	-	50%	25%	50%	25%	-	-	-	-
193	Standard	1	0%	0%	0%	0%	0%	0%	0%	0%	0%	0%	0%	0%	0%	0%	0%	0%
194	Standard	8	113%	63%	100%	50%	-	-	-	-	100%	63%	88%	50%	-	-	-	-
196	Standard	6	100%	67%	100%	50%	17%	17%	17%	17%	100%	50%	83%	50%	17%	17%	17%	17%
401	Articulated	2	0%	0%	0%	0%	50%	50%	50%	50%	0%	0%	0%	0%	50%	50%	50%	50%
402	Articulated	2	0%	0%	0%	0%	50%	0%	50%	0%	0%	0%	0%	0%	50%	0%	0%	0%
403	Standard	2	0%	0%	0%	0%	0%	0%	0%	0%	0%	0%	0%	0%	0%	0%	0%	0%
404	Standard	3	33%	0%	0%	0%	33%	0%	0%	0%	0%	0%	0%	0%	0%	0%	0%	0%
405	Articulated	3	0%	0%	0%	0%	33%	0%	33%	0%	0%	0%	0%	0%	33%	0%	0%	0%
406	Standard	2	0%	0%	0%	0%	50%	50%	50%	50%	0%	0%	0%	0%	50%	50%	50%	50%
407	Standard	2	0%	0%	0%	0%	50%	50%	50%	50%	0%	0%	0%	0%	50%	50%	50%	0%
408	Articulated	3	33%	33%	33%	0%	-	-	-	33%	33%	33%	33%	0%	-	33%	-	33%
409	Articulated	2	0%	0%	0%	0%	50%	0%	50%	0%	0%	0%	0%	0%	50%	0%	0%	0%
410	Articulated	3	0%	0%	0%	0%	0%	0%	0%	0%	0%	0%	0%	0%	0%	0%	0%	0%
411	Articulated	3	33%	0%	0%	0%	-	33%	-	33%	33%	0%	0%	0%	-	33%	33%	33%
412	Articulated	3	33%	0%	33%	0%	0%	0%	0%	0%	33%	0%	0%	0%	0%	0%	0%	0%
413	Standard	3	0%	0%	0%	0%	33%	0%	33%	0%	0%	0%	0%	0%	0%	0%	0%	0%
414	Standard	2	50%	0%	50%	0%	50%	0%	0%	0%	50%	0%	0%	0%	0%	0%	0%	0%
415	Standard	2	100%	50%	100%	50%	0%	0%	0%	0%	100%	50%	50%	0%	0%	0%	0%	0%
416	Standard	3	0%	0%	0%	0%	33%	33%	33%	33%	0%	0%	0%	0%	33%	33%	33%	0%

Table 6-9: Relative additional vehicle demand in BEB operation compared to the diesel reference for the scenario "Current Technology" with available technology on the market and the scenario "Advanced Technology" with an assumed technology improvement

The positive effect of further technical developments is revealed by comparing the "Current Technology" and "Advanced Technology" scenarios in Table 6-8. The number of additional vehicles can be reduced for several routes, especially for depot charging, which makes the routes suitable for a long term implementation. An example regards route 170, where with current technology and depot charger type 2, nine additional vehicles are required for full electric heating (Aux-A). The increased battery capacity in the "Advanced Technology" scenario enables a longer range and therefore an improved scheduling. The additional vehicle demand can be reduced from three vehicles to six, which is however still an increase of about 37 % compared to the diesel bus operation. Alternatives such as hybrid heating or opportunity charging in the "Advanced Technology" scenario are thus more suitable.

In addition to the absolute numbers of additional vehicles in Table 6-8, Table 6-9 highlights the relative increase of the vehicle demand. The color coding reveals the strong influence of the full electric heating which increases the vehicle demand for certain routes by up to 117 % in depot-charging operation (Depot Charger Type 1). The highest increase for opportunity charging on the regular bus routes is limited to 33 %. The high relative values for the night routes (4XX) are caused by the limited number of vehicles per route and can be neglected here.

6.4 Life Cycle Cost Calculation

The technical and operational analysis revealed the operational consequences of an electrification with the different BEB concepts. Recommendations regarding the preferable concept should however not solely regard operational performance, as the costs need to be considered in order to derive the most economical solution. The costs are quantified based on the LCC calculation methodology described in the BEB system model including aging and lifetime calculation.

The LCC are determined route-wise based on the outcome of the technical and operational analysis. The major cost categories include the purchase of vehicles and batteries, maintenance expenses, charging infrastructure investments as well as energy costs. In addition, personnel costs for additional driver time are considered, resulting from the adjusted operating scheme compared to the diesel reference. An overview of the color scheme used in the results graphics is shown in Figure 6-17.

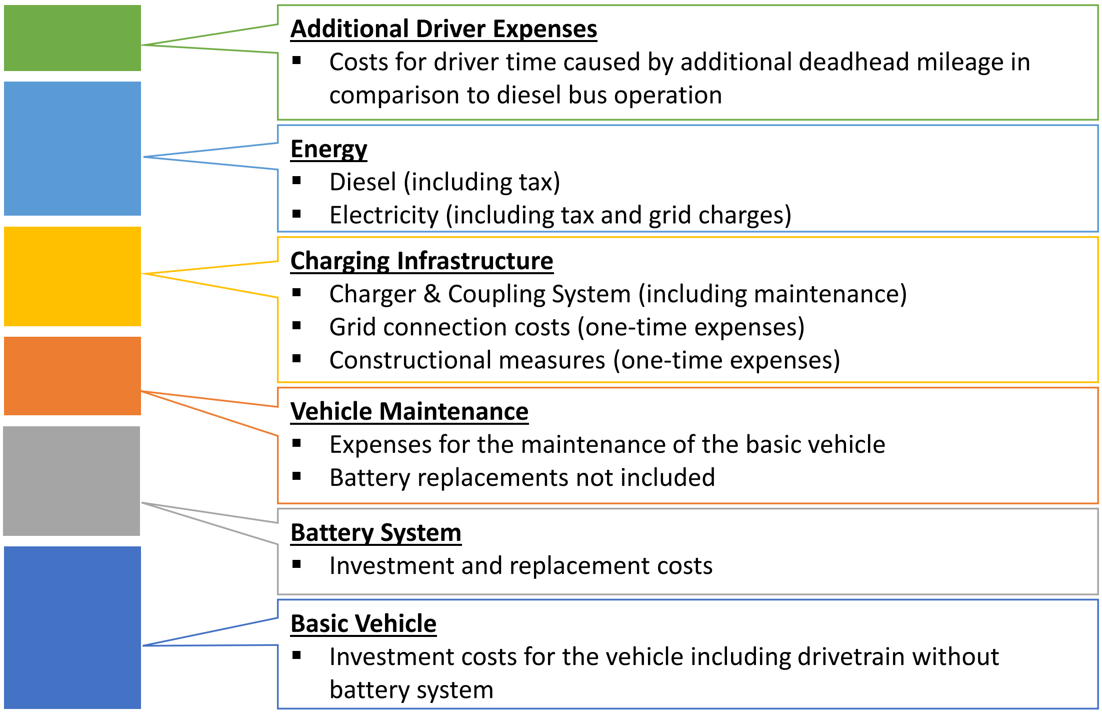

Figure 6-17: Cost categories of the LCC calculation

The LCC are provided in the following as annuities per service kilometer. This normalization enables a neutral comparison of different BEB concepts with potentially varying total mileages, caused for example by additional deadhead kilometers in depot-charging operation.

The route-specific LCC are determined for both technology scenarios ("Current Technology" and "Advanced Technology"). This procedure makes it possible to assess whether the electrification of a route can be implemented more cost-efficiently via further technical developments, which enables the selection of the most economical technical solution and an allocation of implementation periods.

6.4.1 Detailed Results

The detailed results provide insight into the cost structure of the introduced routes 140 and 144 and show that their varying operating scheme has a direct consequence on the LCC and their distribution among the different cost categories.

6.4.1.1 Route 140

Figure 6-18 highlights the results of the LCC calculation of route 140 as single bars per BEB concept, beginning with the diesel reference on the left. The diesel bus operation is shown to not only be the reference in terms of minimum vehicle requirements but also leads to the lowest LCC. The BEB operation increases the LCC in the range of 24 % to 72 % depending on the bus concept.

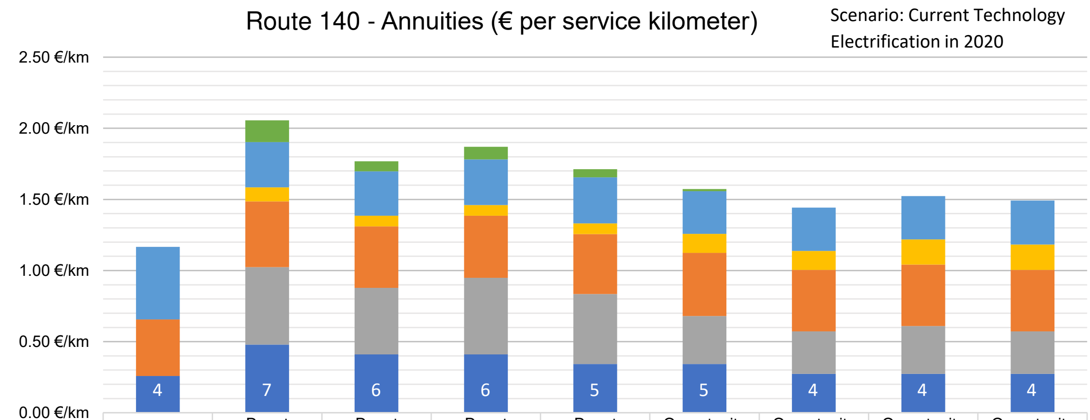

	Diesel Reference	Depot Charger 1 Aux-A	Depot Charger 1 Aux-B	Depot Charger 2 Aux-A	Depot Charger 2 Aux-B	Opportunity Charger 1 Aux-A	Opportunity Charger 1 Aux-B	Opportunity Charger 2 Aux-A	Opportunity Charger 2 Aux-B
Add. Driver Expenses	0.00	0.15	0.07	0.09	0.06	0.01	0.00	0.00	0.00
Energy	0.51	0.32	0.31	0.32	0.32	0.30	0.30	0.30	0.31
Cha. Infrastructure	0.00	0.10	0.07	0.07	0.07	0.13	0.13	0.18	0.18
Veh. Maintenance	0.40	0.46	0.43	0.44	0.42	0.44	0.43	0.43	0.43
Battery	0.00	0.55	0.47	0.54	0.49	0.34	0.30	0.34	0.30
Basic Vehicle	0.26	0.48	0.41	0.41	0.34	0.34	0.27	0.27	0.27
TOTAL	1.17	2.06	1.77	1.87	1.71	1.57	1.44	1.52	1.49

Figure 6-18: LCC comparison for bus route 140 in the scenario “Current Technology” and electrification in 2020

By comparing the sum of basic vehicle and battery costs with the infrastructure costs, the difference between the depot- and opportunity-charging concepts became clear. Whereas the additional vehicles in depot-charging operation contribute significantly to the overall costs (number of vehicles required is displayed in the basic vehicle bar), the share of infrastructure investments increases for the opportunity-charging concepts. Among the different bus concepts, the consequences of the varying auxiliary configurations can be also assessed. Especially in depot-charging operation, the full electric heating (Aux-A) increases the costs significantly compared to a hybrid heating (Aux-B), however this effect fades for opportunity charging due to frequent charging. Only Opportunity Charger Type 1 requests an additional vehicle.

Depot charging always requests at least one additional vehicle with direct consequences on the LCC. Furthermore, the additional deadheading leads to higher energy costs per service kilometer and causes increased driver expenses. Therefore, depot charging is not the ideal electrification concept for bus route 140.

The most cost-efficient BEB concept for route 140 is Opportunity Charger Type 1 with Aux-B. The LCC reaches 1.46 €/km in contrast to 1.17 €/km for diesel bus operation. The higher charging power of Opportunity Charger Type 2 does not entail any economic advantages since the number of vehicles already meets the lower bound. However, when a full electric heating is required this represents the preferable concept.

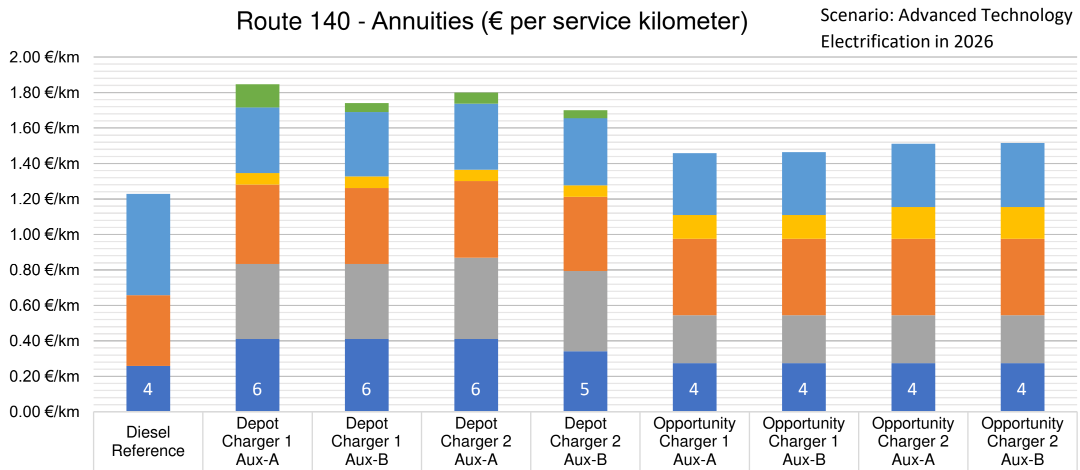

	Diesel Reference	Depot Charger 1 Aux-A	Depot Charger 1 Aux-B	Depot Charger 2 Aux-A	Depot Charger 2 Aux-B	Opportunity Charger 1 Aux-A	Opportunity Charger 1 Aux-B	Opportunity Charger 2 Aux-A	Opportunity Charger 2 Aux-B
Add. Driver Expenses	0.00	0.13	0.05	0.06	0.05	0.00	0.00	0.00	0.00
Energy	0.57	0.37	0.36	0.37	0.38	0.35	0.36	0.36	0.36
Cha. Infrastructure	0.00	0.06	0.06	0.06	0.06	0.13	0.13	0.18	0.18
Veh. Maintenance	0.40	0.45	0.43	0.43	0.42	0.43	0.43	0.43	0.43
Battery	0.00	0.42	0.42	0.46	0.45	0.27	0.27	0.27	0.27
Basic Vehicle	0.26	0.41	0.41	0.41	0.34	0.27	0.27	0.27	0.27
TOTAL	1.23	1.85	1.74	1.80	1.70	1.46	1.46	1.51	1.52

Figure 6-19: LCC comparison for bus route 140 in the scenario “Advanced Technology” and electrification in 2026

Figure 6-19 shows the LCC results for the “Advanced Technology” scenario and electrification in 2026. The costs for electric operation decrease compared to the scenario with current technology and electrification in 2020. The increasing diesel costs and expected decrease in battery and infrastructure prices lead to a shrinking of the gap between conventional diesel and BEB operational costs. Besides the price developments, a major influencing factor regards the lower vehicle demand in the “Advanced Technology” scenario such as for Opportunity Charger Type 1 Aux-A.

The Opportunity Charger Type 1 with Aux-B still represents one of the most-cost effective concepts in this scenario to where there is no need to postpone the electrification. Route 140 could therefore be integrated in the first electrification phase utilizing current technology available on the market.

6.4.1.2 Route 144

The operation of route 144 is characterized by varying vehicle demand throughout the day with peaks in the morning and evening hours. The technical and operational analysis has indicated its suitability for depot-charging operation, which is also confirmed by the LCC shown in Figure 6-20.

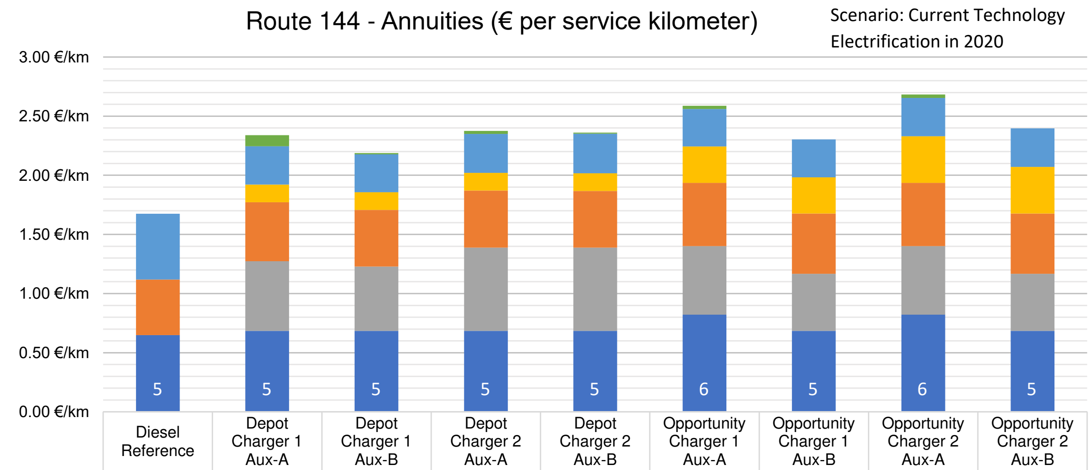

	Diesel Reference	Depot Charger 1 Aux-A	Depot Charger 1 Aux-B	Depot Charger 2 Aux-A	Depot Charger 2 Aux-B	Opportunity Charger 1 Aux-A	Opportunity Charger 1 Aux-B	Opportunity Charger 2 Aux-A	Opportunity Charger 2 Aux-B
Add. Driver Expenses	0.00	0.09	0.01	0.02	0.01	0.03	0.00	0.03	0.00
Energy	0.56	0.32	0.32	0.33	0.33	0.32	0.32	0.32	0.33
Cha. Infrastructure	0.00	0.15	0.15	0.15	0.15	0.31	0.31	0.39	0.39
Veh. Maintenance	0.47	0.50	0.48	0.48	0.48	0.54	0.51	0.54	0.51
Battery	0.00	0.59	0.54	0.70	0.70	0.58	0.48	0.58	0.48
Basic Vehicle	0.65	0.69	0.69	0.69	0.69	0.82	0.69	0.82	0.69
TOTAL	1.67	2.34	2.19	2.37	2.36	2.59	2.30	2.68	2.40

Figure 6-20: LCC comparison for bus route 144 in the scenario "Current Technology" and electrification in 2020

The most cost-efficient electrification concept regards Depot Charger Type 1 with Aux-B. For route 140, the hybrid heating enables a significant cost reduction compared to the full electric heating by avoiding additional deadheading, as discussed in Section 6.3.1.2. The increased battery capacity of Depot Charger Type 2 does not provide significant operational benefits (identical vehicle demand and deadhead mileage), meaning the LCC are increased by the higher battery investments.

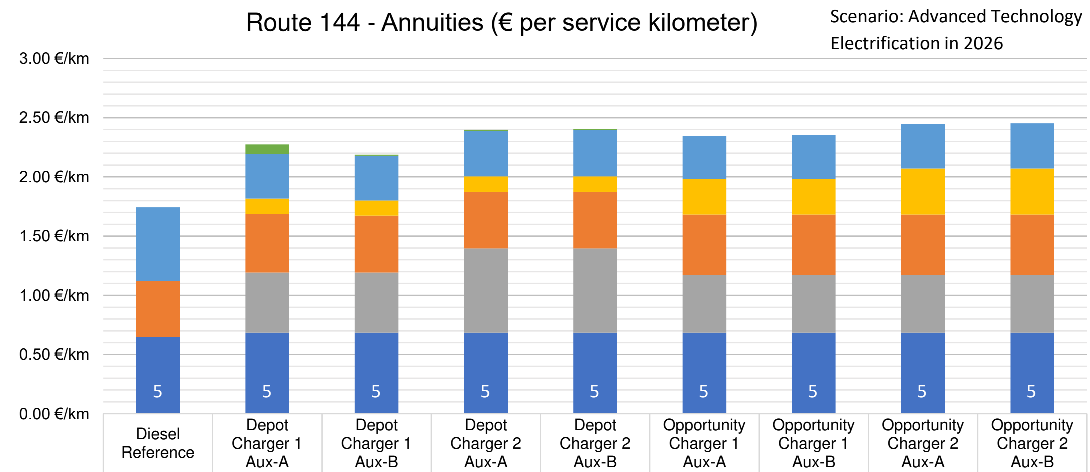

	Diesel Reference	Depot Charger 1 Aux-A	Depot Charger 1 Aux-B	Depot Charger 2 Aux-A	Depot Charger 2 Aux-B	Opportunity Charger 1 Aux-A	Opportunity Charger 1 Aux-B	Opportunity Charger 2 Aux-A	Opportunity Charger 2 Aux-B
Add. Driver Expenses	0.00	0.08	0.01	0.01	0.01	0.00	0.00	0.00	0.00
Energy	0.62	0.38	0.38	0.38	0.39	0.37	0.37	0.38	0.38
Cha. Infrastructure	0.00	0.13	0.13	0.13	0.13	0.30	0.30	0.39	0.39
Veh. Maintenance	0.47	0.49	0.48	0.48	0.48	0.51	0.51	0.51	0.51
Battery	0.00	0.51	0.51	0.71	0.71	0.49	0.49	0.49	0.49
Basic Vehicle	0.65	0.69	0.69	0.69	0.69	0.69	0.69	0.69	0.69
TOTAL	1.74	2.27	2.19	2.40	2.41	2.35	2.35	2.45	2.45

Figure 6-21: LCC comparison for bus route 144 in the scenario "Advanced Technology" and electrification in 2026

The highest LCC for route 144 are caused by the Opportunity Chargers and full electric heating (Aux-A) since an additional vehicle is required. This is however no longer the case with advanced technology in the future as shown in Figure 6-21. However, depot charging still represents the most cost-efficient solution. Like route 140, there is no need to postpone the electrification of route 144.

6.4.2 Results Overview and Discussion

The LCC calculation has been performed for every route under consideration. The overview in Table 6-10 lists the absolute costs for the diesel bus reference and relative additional costs of the BEB operation.

Route	Bus Type	LCC Diesel Ref. €/km	Relative Additional Costs (Scenario: Current Technology)								LCC Diesel Ref. €/km	Relative Additional Costs (Scenario: Advanced Technology)							
			Dep. Type 1		Dep. Type 2		Opp. Type 1		Opp. Type 2			Dep. Type 1		Dep. Type 2		Opp. Type 1		Opp. Type 2	
			Aux-A	Aux-B	Aux-A	Aux-B	Aux-A	Aux-B	Aux-A	Aux-B		Aux-A	Aux-B	Aux-A	Aux-B	Aux-A	Aux-B	Aux-A	Aux-B
14	Articulated	4.96	41%	42%	54%	54%	74%	46%	88%	46%	5.10	39%	39%	51%	51%	72%	43%	86%	44%
15	Articulated	1.41	92%	77%	82%	66%	38%	30%	32%	32%	1.49	68%	53%	68%	51%	28%	22%	27%	27%
140	Standard	1.17	76%	52%	60%	47%	35%	24%	31%	28%	1.23	50%	42%	46%	38%	19%	19%	23%	23%
141	Standard	1.11	83%	52%	75%	53%	-	-	-	-	1.17	55%	41%	52%	36%	-	-	-	-
142	Standard	1.19	40%	26%	37%	30%	-	22%	28%	24%	1.25	27%	19%	27%	21%	19%	16%	18%	18%
143	Standard	1.27	83%	56%	72%	47%	-	28%	31%	31%	1.34	57%	34%	51%	32%	20%	21%	25%	24%
144	Standard	1.67	40%	31%	42%	41%	55%	38%	60%	43%	1.74	30%	26%	38%	38%	35%	35%	40%	41%
145	Articulated	1.58	102%	80%	97%	68%	-	34%	43%	43%	1.67	91%	57%	78%	55%	29%	30%	37%	30%
146	Articulated	1.66	80%	58%	69%	47%	-	-	-	29%	1.74	65%	39%	53%	37%	-	20%	-	24%
147	Articulated	1.61	84%	66%	84%	55%	31%	31%	40%	37%	1.70	70%	53%	60%	44%	27%	27%	32%	32%
154	Standard	1.73	61%	28%	37%	38%	57%	40%	63%	45%	1.80	22%	22%	34%	34%	53%	25%	41%	26%
155	Articulated	1.49	92%	69%	87%	64%	-	-	-	-	1.57	79%	52%	68%	49%	-	-	-	-
159	Standard	2.42	187%	65%	83%	82%	141%	140%	178%	177%	2.48	63%	62%	80%	79%	140%	138%	177%	176%
160	Articulated	1.63	110%	78%	98%	67%	35%	27%	40%	36%	1.72	83%	57%	77%	51%	26%	22%	29%	26%
161	Articulated	2.51	59%	32%	50%	34%	42%	35%	49%	39%	2.61	37%	24%	31%	31%	39%	33%	36%	37%
162	Standard	1.47	78%	66%	79%	34%	-	42%	-	54%	1.54	62%	54%	73%	25%	38%	38%	49%	49%
164	Articulated	1.60	81%	68%	83%	59%	-	34%	41%	38%	1.69	69%	48%	69%	46%	29%	28%	33%	34%
166	Articulated	1.71	79%	58%	66%	48%	-	-	-	-	1.79	64%	39%	51%	34%	-	-	-	-
167	Standard	2.15	131%	43%	160%	58%	106%	40%	137%	40%	2.23	125%	40%	152%	54%	103%	37%	133%	37%
169	Articulated	1.45	105%	89%	110%	75%	-	38%	42%	42%	1.53	100%	70%	81%	58%	35%	31%	35%	32%
170	Articulated	1.73	78%	50%	71%	49%	-	-	-	-	1.82	59%	39%	46%	35%	-	-	-	24%
172	Standard	1.51	63%	31%	34%	27%	-	-	-	-	1.58	58%	18%	29%	25%	-	-	-	49%
173	Standard	1.26	69%	58%	66%	61%	-	-	-	-	1.32	55%	44%	62%	21%	-	30%	-	41%
174	Standard	1.42	54%	36%	56%	37%	42%	29%	34%	34%	1.49	41%	25%	37%	33%	27%	27%	32%	32%
177	Standard	1.09	80%	60%	75%	60%	30%	28%	34%	34%	1.15	58%	44%	60%	43%	23%	24%	26%	27%
180	Standard	1.25	67%	43%	58%	38%	30%	28%	34%	34%	1.32	46%	31%	40%	24%	23%	16%	30%	19%
183	Standard	1.14	67%	45%	54%	40%	-	-	-	-	1.20	43%	28%	41%	31%	-	-	-	-
184	Standard	1.30	65%	50%	69%	43%	32%	22%	28%	29%	1.37	52%	40%	51%	34%	18%	17%	22%	23%
185	Standard	1.20	79%	60%	65%	46%	36%	36%	40%	41%	1.26	64%	40%	50%	34%	29%	30%	34%	34%
186	Standard	1.20	66%	49%	65%	49%	-	-	-	-	1.27	59%	39%	52%	35%	-	-	-	-
190	Standard	1.29	112%	73%	85%	60%	-	-	-	-	1.35	77%	54%	70%	43%	-	-	-	-
194	Standard	1.18	121%	71%	104%	63%	-	-	-	-	1.24	86%	55%	75%	50%	-	-	-	-
196	Standard	1.20	102%	67%	94%	60%	28%	29%	32%	32%	1.26	77%	48%	75%	50%	22%	23%	27%	26%

Table 6-10: LCC of the diesel bus operation and relative additional costs for the BEB operation in the scenarios “Current technology” and “Advanced Technology”

The "Current Technology" scenario assumes that electrification will occur in 2020 using state-of-the-art technology. The “Advanced Technology" scenario on the other hand assumes electrification in 2026 using improved technology. For illustration purposes, the route-specific additional costs are classified by color, from the cheapest electrification concept (green) to the most expensive (red). As mentioned in the technical and operational analysis, due to a lack of space or dwell time it is not possible to perform opportunity charging at some terminal stops. The LCC for opportunity charger are therefore not calculated for the routes concerned.

The LCC of the diesel bus operation range from 1.09 €/km to 2.51 €/km, except for the sprint bus route 14 with 4.96 €/km. The exceptional high costs of route 14 are caused by the limited mileage per day as the two vehicles are only operated in the morning and evening hours. The additional costs for the BEB operation range from 21 % to 187 % in the "Current Technology" scenario, which underlines the relevance of proper technology selection and route prioritization.

The general results overview indicated that in most cases routes with high mileage can be operated more economically using opportunity charging rather than with depot charging, especially when investments in fast-charging infrastructure can be allocated to a high number of vehicles. In addition, opportunity charging through frequent charging enables the use of smaller batteries and increased battery life through moderate cycle depths.

Depot charging turns out to be the preferred concept for bus routes 14, 144, 154, 159 and 161. The operating scheme of these routes is characterized by varying vehicle demand (as shown in 6.3.1.2 for route 144), which enables an integration of charging phases within the regular dwell time at the depot and a depot-charging operation without a significant number of additional vehicles.

The LCC results must be interpreted in conjunction with the findings of the technical and operational analyses. In general, the more favorable BEB concept for each route is due to a lower vehicle demand. As soon as the use of Depot Charger Type 2 or Opportunity Charger Type 2 results in a lower vehicle requirement than Type 1, this variant represents the more economical solution. With the same operating scheme for both types, Type 1 concepts are more economical due to lower battery and charging infrastructure costs.

The same can also be observed when comparing electrification with the current state of the art to an advanced technology in the future scenario. As soon as advanced technology leads to lower vehicle demand or significantly reduced deadheading, this results in lower LCC in the future scenario.

6.5 Mitigation Assessment

The environmental benefits of an electrification are determined in the mitigation assessment. The status quo is described by the EURO VI diesel bus operation, whose emissions are calculated with the BEB system model. Global as well as local emissions are considered by focusing on CO_2, NO_X and PM.

Figure 6-22 illustrates the computed yearly emissions for the diesel reference and the BEB types for operations on route 140. It is assumed that emission-neutral electricity from renewables is used for the BEB, meaning that buses with full electric heating (Aux-A) cause zero emissions. BEB with a fuel heater installed in the hybrid heating system (Aux-B) are however not entirely emission free.

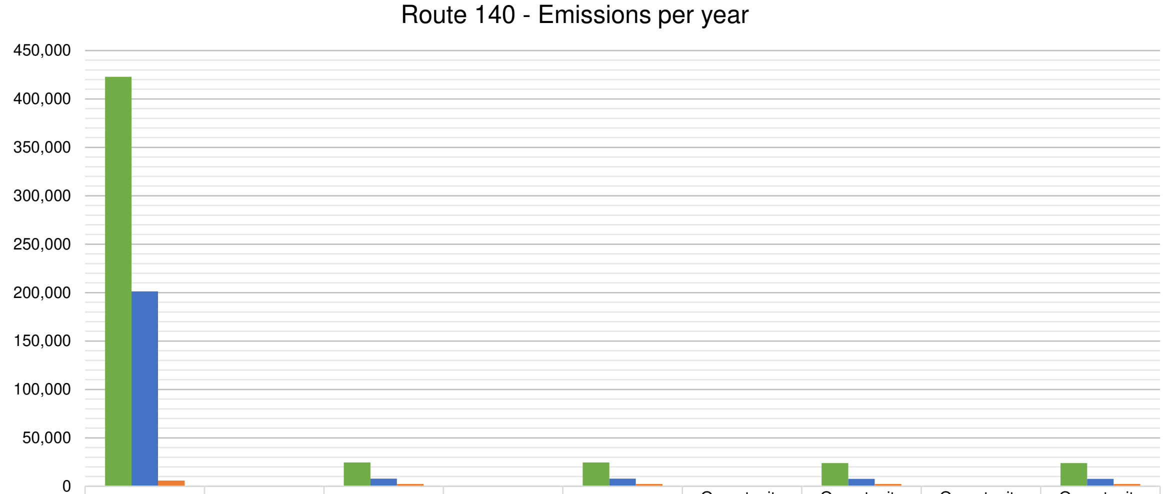

	Diesel Reference	Depot Charger 1 Aux-A	Depot Charger 1 Aux-B	Depot Charger 2 Aux-A	Depot Charger 2 Aux-B	Opportunity Charger 1 Aux-A	Opportunity Charger 1 Aux-B	Opportunity Charger 2 Aux-A	Opportunity Charger 2 Aux-B
CO2 [kg]	422,820	0	24,608	0	24,545	0	23,993	0	23,993
NOX [g]	201,237	0	7,967	0	7,946	0	7,768	0	7,768
PM [g]	5,897	0	2,390	0	2,384	0	2,330	0	2,330

Figure 6-22: Yearly emissions of the operation of route 140 in scenario “Current Technology”

The comparison of the diesel bus emissions with the emissions of the fuel heater reveals the strong reduction of CO_2 (about 95 %) and NO_X (about 96 %), however the mitigation potential regarding PM emissions of about 60 % is significantly lower, which is mainly caused by the absence of a particle filter in current fuel heaters. The minor variations in the results for the BEB are caused by the slightly varying operating schemes.

Assuming that the entire fleet of Ruhrbahn consists of diesel Euro VI buses, the yearly emissions are about 22,630 t CO_2, 8,290 kg NO_X and 283 kg PM (Table 6-11). A full mitigation can be achieved by replacing all buses with BEB and full electric heating (Aux-A). However, the implementation of BEB with hybrid heating (Aux-B) also enables a significant reduction to a total of about 1,200 t CO_2, 400 kg NO_X and 120 kg PM per year.

Route	Bus Type	CO2 in t					NOX in kg					PM in kg				
		Diesel Reference	Dep. Type 1 Aux-B	Dep. Type 2 Aux-B	Opp. Type 1 Aux-B	Opp. Type 2 Aux-B	Diesel Reference	Dep. Type 1 Aux-B	Dep. Type 2 Aux-B	Opp. Type 1 Aux-B	Opp. Type 2 Aux-B	Diesel Reference	Dep. Type 1 Aux-B	Dep. Type 2 Aux-B	Opp. Type 1 Aux-B	Opp. Type 2 Aux-B
14	Articulated	70	3	3	3	3	20	1	1	1	1	1	-	-	-	-
15	Articulated	960	51	50	48	48	287	16	16	16	16	12	5	5	5	5
140	Standard	470	25	25	24	24	201	8	8	8	8	6	2	2	2	2
141	Standard	598	28	28	-	-	234	9	9	-	-	8	3	3	-	-
142	Standard	1,150	54	54	54	54	460	17	17	17	17	14	5	5	5	5
143	Standard	716	40	39	38	38	321	13	13	12	12	9	4	4	4	4
144	Standard	256	13	13	13	13	112	4	4	4	4	3	1	1	1	1
145	Articulated	1,042	64	62	59	59	346	21	20	19	19	13	6	6	6	6
146	Articulated	1,244	73	71	-	68	403	24	23	-	22	16	7	7	-	7
147	Articulated	367	20	20	19	19	116	6	6	6	6	5	2	2	2	2
154	Standard	268	14	14	14	14	120	5	5	5	5	3	1	1	1	1
155	Articulated	1,191	70	68	-	-	384	23	22	-	-	15	7	7	-	-
159	Standard	24	1	1	1	1	9	-	-	-	-	-	-	-	-	-
160	Articulated	1,072	66	64	61	61	362	21	21	20	20	13	6	6	6	6
161	Articulated	435	24	24	24	24	150	8	8	8	8	5	2	2	2	2
162	Standard	145	8	8	8	8	67	3	3	3	3	2	1	1	1	1
164	Articulated	581	36	35	35	35	200	11	11	11	11	7	3	3	3	3
166	Articulated	1,741	101	98	-	-	556	33	32	-	-	22	10	10	-	-
167	Standard	39	2	2	2	2	18	1	1	1	1	-	-	-	-	-
169	Articulated	1,181	65	63	60	60	359	21	20	19	19	15	6	6	6	6
170	Articulated	2,037	117	117	-	-	681	38	38	-	-	26	11	11	-	-
172	Standard	140	8	7	-	-	64	2	2	-	-	2	1	1	-	-
173	Standard	174	9	9	-	-	72	3	3	-	-	2	1	1	-	-
174	Standard	310	16	16	16	16	131	5	5	5	5	4	2	2	2	2
177	Standard	543	28	28	27	27	227	9	9	9	9	7	3	3	3	3
180	Standard	593	30	29	29	29	245	10	9	9	9	7	3	3	3	3
183	Standard	472	24	24	-	-	198	8	8	-	-	6	2	2	-	-
184	Standard	440	25	25	24	24	199	8	8	8	8	6	2	2	2	2
185	Standard	430	22	21	21	21	177	7	7	7	7	5	2	2	2	2
186	Standard	829	45	45	-	-	364	15	14	-	-	10	4	4	-	-
190	Standard	347	17	16	-	-	136	6	5	-	-	4	2	2	-	-
194	Standard	943	52	50	-	-	403	17	16	-	-	12	5	5	-	-
196	Standard	619	34	33	32	32	266	11	11	10	10	8	3	3	3	3
401	Articulated	69	3	3	4	4	21	1	1	1	1	1	-	-	-	-
402	Articulated	48	2	2	2	2	15	1	1	1	1	1	-	-	-	-
403	Standard	45	2	2	2	2	17	1	1	1	1	1	-	-	-	-
404	Standard	74	3	3	3	3	29	1	1	1	1	1	-	-	-	-
405	Articulated	85	4	4	-	-	26	1	1	-	-	1	-	-	-	-
406	Standard	52	2	2	-	-	19	1	1	-	-	1	-	-	-	-
407	Standard	52	2	2	2	2	20	1	1	1	1	1	-	-	-	-
408	Articulated	132	6	6	-	6	37	2	2	-	2	2	1	1	-	1
409	Articulated	44	2	2	-	-	14	1	1	-	-	1	-	-	-	-
410	Articulated	73	4	4	-	-	23	1	1	-	-	1	-	-	-	-
411	Articulated	114	6	6	6	6	35	2	2	2	2	1	1	1	1	1
412	Articulated	110	6	5	5	5	33	2	2	2	2	1	1	1	1	1
413	Standard	77	3	3	3	3	28	1	1	1	1	1	-	-	-	-
414	Standard	66	3	3	3	3	26	1	1	1	1	1	-	-	-	-
415	Standard	82	4	4	4	4	32	1	1	1	1	1	-	-	-	-
416	Standard	76	3	3	4	4	29	1	1	1	1	1	-	-	-	-
Total per year		22,630	1,240	1,219	650	725	8,290	401	394	210	234	283	116	114	60	67

Table 6-11: Yearly CO_2, NO_X and PM emissions of operation of each bus route with the diesel reference and BEB with Aux-B – BEB with Aux-A are 100 % zero emission and therefore not mentioned here

The results reveal the high mitigation potential of BEB and a further cost benefit analysis can be conducted based on the emission cost rates published by the German Environment Agency (Umweltbundesamt – UBA) in the “Methodological Convention 3.0 for the Assessment of Environmental Costs” [129]. In terms of CO_2, climate costs of 187 €/t are proposed for the year 2020 (linear interpolation between 2016 and 2030) based on a 1 % pure rate of time preference[9]. Thus, operating a diesel Euro VI bus fleet in Essen incurs climate costs of about 4.2 million € per year. The average costs per service kilometer result in this case in 0.30 €/km. Lowering the pure rate of time preference to 0 % increases the climate costs to 649 €/t. This value leads to average costs per service kilometer of 1.06 €/km, which overcompensates the gap between diesel and BEB operation in the LCC.

The "Methodological Convention 3.0 for the Assessment of Environmental Costs" contains additional cost rates for NO_X (15,000 €/t) and PM (28,500 €/t) emissions in an urban environment. These cost rates cause average costs per service kilometer of 0.01 €/km.

6.6 Electrification Concept

The electrification concept development represents the final synthesis of the computed results. The aim is to provide the PTO a concrete plan for upcoming years with recommendations regarding technology choice, infrastructure establishment and operation. A general overview on the relevant steps and their linkage to the sections of this thesis is provided in Figure 6-23.

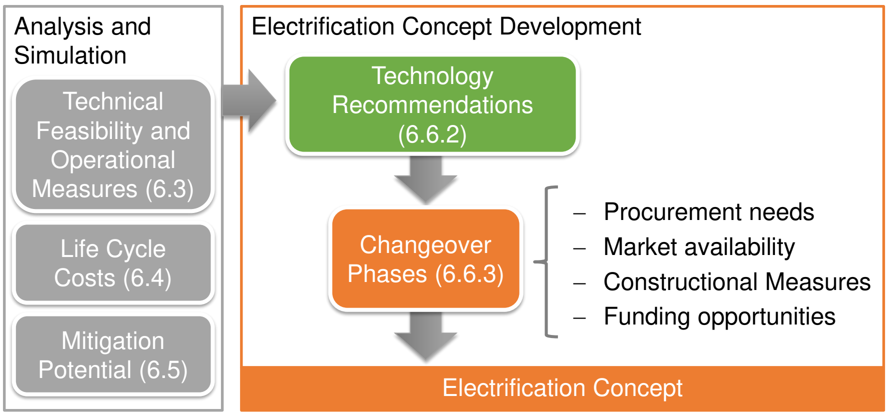

Figure 6-23: Relevant steps in the electrification concept development

The constraints for the concept development are introduced and discussed in 6.6.1 and are considered in the determination of technology recommendations (6.6.2), in which the previous line-specific focus is enlarged to the fleet level. Building on the BEB technology recommendations and required infrastructure measures, the final changeover phases are derived in 6.6.3.

[9] The pure rate of time preference determines how damages incurred for the next generations are considered. A value of 1 % weights the damages incurred in 30 years by 74 % and the damages incurred in 60 years by 55 %. An equal weight is given for 0 % pure rate of time preference.

6.6.1 Constraints for the Concept Development

The electrification concept development faces mutual constraints caused by external and internal effects. External effects mainly regard the maturity of technology and market availability. Furthermore, the possibilities and durations of constructional measures (e.g., establishment of a grid connection) play a significant role. Internal effects are mainly described by the current status at Ruhrbahn such as regarding the fleet composition and procurement strategy.

6.6.1.1 Maturity of Technology and Market Availability

BEB are not yet a standard product and are currently manufactured in small quantities. This causes consequences for the electrification concept development, the first of which is linked to the variety of technical solutions. Since PTOs in Germany are mostly owned by the community, they must run tenders for their procurements. A competitive tender can only be ensured when several potential bidders are available. Therefore, highly specialized BEB concepts which are only provided by single manufacturers need to be avoided.

However, the market availability only represents a snapshot. Each manufacturer aims at enriching his portfolio so that today's specialized systems could become the standard in the future. An example regards the installation of heat pumps. Evobus integrated a heat pump heating system in their eCitaro and set a standard which is now also adopted by Sileo, Solaris, VDL and further manufacturers. This technology forecast is already considered in the defined reference bus types. Furthermore, the scenario with advanced technology enables an assessment of the potential benefits, so that each recommendation in the electrification concept is linked to a time period.

The second consequence is linked to robustness. Considering the low availability from field trials and the fact that BEB technology that has not yet been tested to a great extent relative to diesel buses, it is assumed that the availability for scheduled operation at the beginning of the conversion to BEB is 20 % lower than that of the diesel reference. The availability should increase in the future with increasing experience and emerging technology, to where a similar reserve as for the diesel reference requirement is assumed for the subsequent changeover phases.

6.6.1.2 Procurement Needs and Time Horizon

The fleet of Ruhrbahn in Essen consists of several vehicles at different ages. Buses are replaced on a regular basis, after 12 years at the latest. Due to the fact the oldest buses usually have the lowest emission standard, the general procurement strategy of replacing old vehicles maximizes the mitigation.

Based on the usage period of conventional diesel buses, the time horizon for the electrification concept is set at 12 years. The earliest starting date is determined by the duration of the decision-making in the committees of Ruhrbahn, the application for funding, the tendering and the construction time. Therefore, the electrification of a first route cannot occur before 2021.

6.6.2 Technology Recommendations

The subsequent analysis steps generated a large solution space with route-wise results regarding the performance of the different BEB concepts. For each route, a suitable electrification concept must be chosen. The decision can be based on several criteria such as:

- Lowest LCC
- Lowest operational measures
- Lowest infrastructural measures

The user is guided through this process through supportive functions of the software toolchain. At first a list of recommendations is generated based on the criterion "lowest LCC". The list combines the given route parameters, such as the number of vehicles in diesel bus operation, with consequences of the selected BEB concept. An excerpt is provided in Table 6-12 showing the recommendations for routes 140, 141, 144 and 180.

Route	Adv. techn.	Num. diesel buses	Num. BEB	BEB concept	Charging station 1 at	Charging station 2 at	Annuities (€/km)
…							
140	no	4	4	OS1-Aux B	Borbeck Bf	-	1,442
140	yes	4	4	OS1-Aux B	Borbeck Bf	-	1,479
141	no	5	7	DS1-Aux B	-	-	1,691
141	yes	5	6	DS2-Aux B	-	-	1,629
144	no	5	5	DS1-Aux B	-	-	2,188
144	yes	5	5	DS1-Aux B	-	-	2,247
180	no	6	6	OS1-Aux B	Burgaltendorf Burgruine	Werden S	1,606
180	yes	6	6	OS1-Aux B	Burgaltendorf Burgruine	-	1,544
…							

Table 6-12: Excerpt of BEB concept recommendation list based on criterion "lowest LCC"

The technology recommendation for routes 140 and 144 is identical for the scenarios with current and advanced technology, meaning that the advantages of a higher battery capacity and charging power do not encourage a concept change. Both routes could therefore be electrified during an early state with current technology. The situation is however different for routes 141 and 180, as the high battery capacity of the depot charger type 2 in the advanced technology scenario reduces the required number of BEB on route 141. The improvements of the advanced technology regarding route 180 regard the reduction of charging locations. The charging infrastructure at *Werden S* becomes redundant, and thus the electrification of both routes should be postponed.

Based on the recommendation list, the user can determine an appropriate BEB concept and time horizon for the electrification of each route. In preparation of the electrification concept development, the route-wise focus however needs to be enlarged to the fleet level. This is mandatory since an individual technical configuration for each route limits the operational flexibility of the PTO. BEB must be able to serve several routes, thus the number of technical variants should be minimized.

The first measure of the variant reduction is already included in the recommendation list. The auxiliary setup Aux-B with a hybrid heating system is chosen for all concepts due to its lower LCC compared to Aux-A. The main reason for the cost advantage of this concept is that the fuel heater of the hybrid heating system enables a system design closer to the average operating conditions throughout the year. The number of vehicles and chargers do not have to be chosen for the worst-case winter day, which occurs only sporadically, and thus the over-dimensioning of the BEB system can be reduced. In addition, the mitigation potential compared to the diesel bus operation is still high.

The second measure is to limit the number of BEB variants in a single depot. Even if the cost efficiency of a single route benefits from a smaller battery capacity, it is advantageous to install a larger battery and enable the operation on various routes. An example regards route 154 operated with buses from the depot *Stadtmitte*, where the depot charger type 1 already provides a sufficient battery capacity so that the route can be electrified without additional vehicles. However, the majority of routes which can be electrified with current technology require a depot charger type 2, and therefore depot charger type 2 is set for route 154 as well.

The entire technology recommendations derived for the Ruhrbahn network are shown in Figure 6-24, and a visual distinction is made between regular routes (day routes) and night routes. Furthermore, a distinction is introduced between standard (orange) and articulated (blue) buses. In addition, the concept-specific vehicle requirements and required charging locations (in the case of opportunity charging) are given for each route.

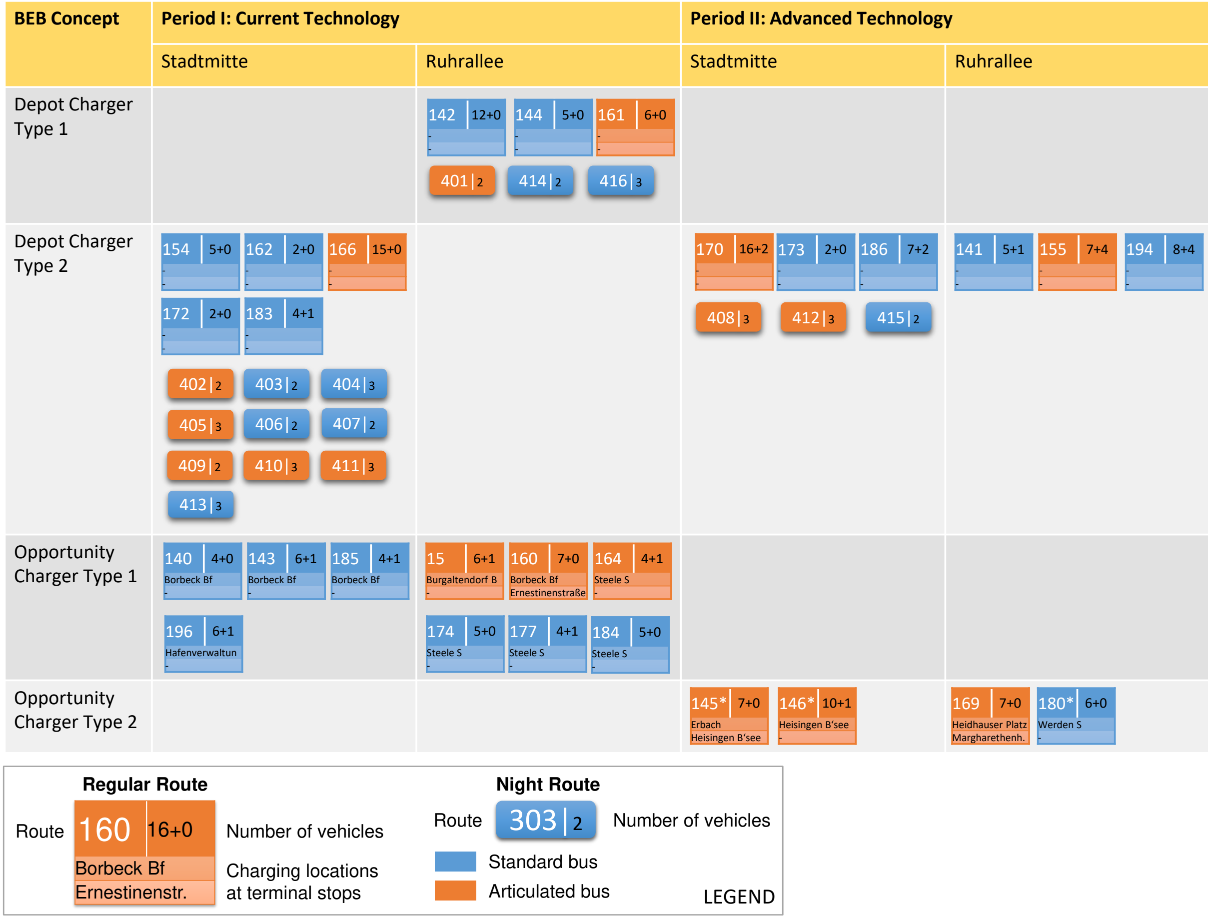

Figure 6-24: Technology recommendations for each route in the bus network of Ruhrbahn and assignment to realization periods with current or advanced technology

The considered route timetables are based on the status as of January 2017. To keep track of future developments, the planned future measures from the local transport plan were examined and considered. Routes that will be discontinued in the future (14, 147, 159, 167, 190) were excluded from the scope of the electrification concept and do not appear in the overview. Routes that are affected by changes but uninfluenced regarding technical feasibility appear unchanged in the overview. Finally, routes with extensive adaptation requirements are marked with an "*" and are postponed.

The technology recommendations result in a fleet mix of depot- and opportunity-charging BEB for both depots. Whereas opportunity charger type 1 with 300 kW charging power in the current technology scenario is recommended for both depots, the depot charger concept varies. A fleet of depot charger type 2 buses is recommended for *Stadtmitte* and depot charger type 1 for *Ruhrallee*. Opportunity charging in the advanced technology scenario is recommended with at least 540 kW charging power for the routes of both depots.

The depot *Stadtmitte* comprises 99 vehicles for operation of the considered routes after conversion to BEB (Table 6-13), including 48 standard buses and 51 articulated buses, not including spare vehicles. The additional vehicle requirement of the electrification resulted in 6 standard buses and 3 articulated buses compared to the diesel bus reference. Charging infrastructure must be installed in the depot and at the terminal stops *Borbeck Bf* and *Hafenverwaltung* in the first period (300 kW) and at *Heisingen Baldeneysee* and *Erbach* in period two (540 kW).

STADTMITTE	**Standard buses**	**Articulated buses**	**Total**
Depot charger Type 1	-	-	-
Depot charger Type 2	25	33	58
Opp. charger type 1	23	-	23
Opp. charger type 2	-	18	18
Total	48	51	99

Table 6-13: Fleet composition at depot *Stadtmitte* for a complete changeover (spare vehicles not included)

Table 6-14 lists the number of vehicles in depot *Ruhrallee*. For a complete changeover to BEB, 56 standard buses and 43 articulated buses are required, not including spare vehicles. The fleet size increases by 6 standard buses and 6 articulated buses compared to the diesel bus reference. The opportunity charging routes operated from *Ruhrallee* require charging infrastructure at the terminal stops *Steele S, Borbeck Bf, Burgaltendorf Burgruine, Ernestinenstraße* with 300 kW in the first period and 540 kW chargers at *Werden S, Heidhauser Platz* and *Margarethenhöhe* for the second period.

RUHRALLEE	**Standard buses**	**Articulated buses**	**Total**
Depot charger Type 1	17	6	23
Depot charger Type 2	18	11	29
Opp. charger type 1	15	19	34
Opp. charger type 2	6	7	13
Total	56	43	99

Table 6-14: Fleet composition at depot *Ruhrallee* for a complete changeover (spare vehicles not included)

6.6.3 Changeover Phases

The changeover phases are based on the technology recommendations and consider the constraints introduced in 6.6.1. The first phase starts in 2019 and ends in 2021, and subsequent phases have a duration of two years.

Figure 6-25 provides an overview and highlights the major steps in the changeover process. At first, a single bus route is electrified with depot charging in the bus depot *Ruhrallee*. The depot charging is extended in the next phase and then opportunity charging with a charging hub at *Steele S* is introduced. The electrification of the *Stadtmitte* depot begins in Phase C by establishing opportunity- as well as depot-charging buses.

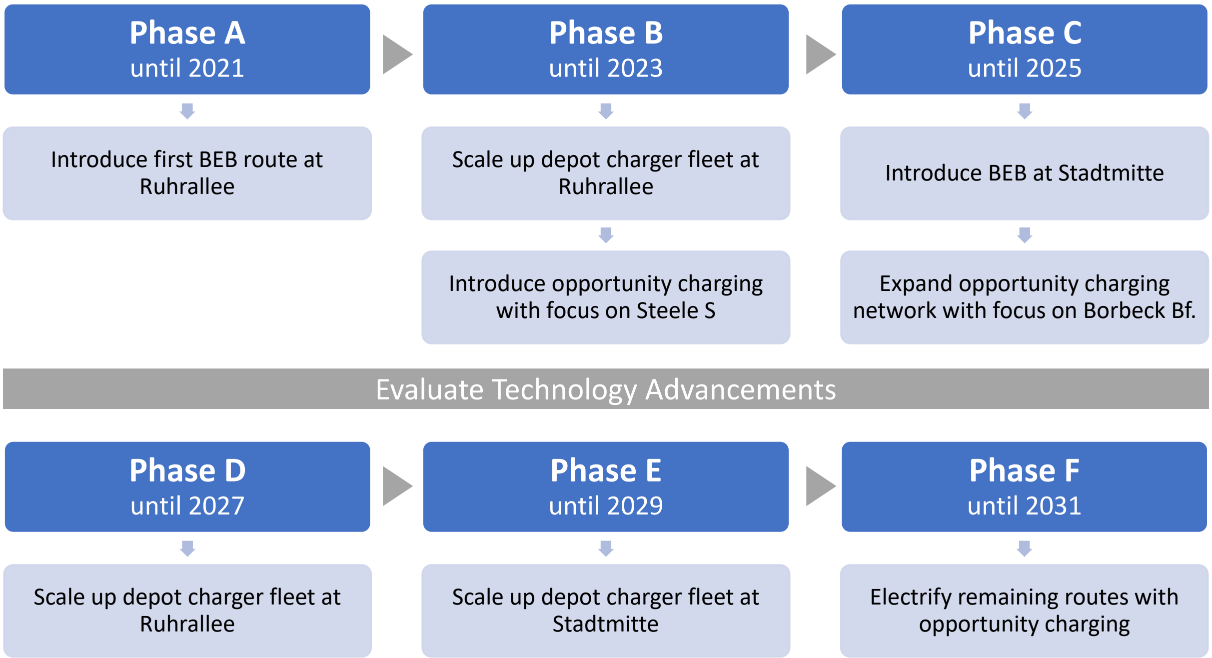

Figure 6-25: Changeover phases for the entire fleet electrification until 2031

If the future predictions are confirmed in the evaluation of technical advancements after Phase C, Phase D continues with the scaleup of the depot charger fleet at *Ruhrallee* and Phase E at *Stadtmitte*. The final conversion of the last routes with opportunity charging is scheduled for Phase F.

Table 6-15 provides further details regarding the individual changeover phases. Due to its low complexity and high market availability, the depot charger type 1 standard bus is recommended for the conversion of routes 144, 414 and 416 (phase A, until 2021). The battery is charged exclusively in the depot, and therefore additional infrastructure at terminals are not necessary. This simplifies the changeover in the first phase regarding implementation planning and makes it possible to run BEB on night routes at an early stage. In addition, buses with battery capacities of around 250 kWh can already be purchased from several manufacturers.

For changeover phase B until 2023, the expansion of the depot charger fleet at the *Ruhrallee* and the introduction of opportunity charging with a focus on *Steele S* are recommended. The expansion of the depot-charging fleet corresponds to the acquisition of 12 standard buses with a battery capacity of 250 kWh (depot charger type 1) and 6 articulated buses with a battery capacity of 300 kWh (depot charger type 1). The standard buses are assigned to route 142 and the articulated buses to route 161 and 401.

In addition to the scaleup of the depot charger fleet, the introduction of opportunity charging is also scheduled for Phase B, which requires the purchase of 10 standard buses and 12 articulated buses for operation on routes 164, 174, 177 and 184. The fast-charging infrastructure for these routes is concentrated at the terminal stop *Steele S*, where four 300 kW fast-charging stations need to be installed.

In phase C until 2025 the opportunity charger fleet at Ruhrallee is enlarged and the electrification is extended to the *Stadtmitte* depot by introducing depot and opportunity chargers. The additional 14 opportunity-charger type 1 articulated buses at Ruhrallee are operated on routes 15 and 160. A concentration of charging infrastructure at *Borbeck Bf.* (4 charging stations with 300 kW each) is enabled by the electrification of the *Stadtmitte* bus routes 140, 143, 185 and 196, and further charging stations are required at *Burgaltendorf Burgruine*, *Ernestienenstraße* and *Hafenverwaltung*.

The introduction of depot charging at *Stadtmitte* requires a total of 14 standard buses and 15 articulated buses. The standard buses serve routes 154, 162, 172 and 183 in regular operation and afterwards switch to night routes 403, 404, 406, 407 and 413. All 15 depot-charger type 2 articulated buses are intended for use on Line 166. In addition, the vehicles can also be used to cover the night services of routes 402, 405, 409, 410 and 411.

			Depot Charger			**Opportunity charger**			
Phase	**Year**	**Depot**	Routes	Num. stand. buses	Num. articul. buses	Routes	Num. stand. buses	Num. articul. buses	Charging stations at
A	2021	Ruhrallee	144, 414, 416	5					
B	2023	Ruhrallee	142, 161, 401	12	6	164, 174, 177, 184	15	5	Stelle S [4]
C	2025	Ruhrallee				15, 160		14	Burgaltendorf B. [1], Borbeck Bf. [1], Enestinenstr. [1]
C	2025	Stadtmitte	154, 162, 166, 172, 183, 402, 403, 404, 405, 406, 407, 409, 410, 411, 413,	14	15	140, 143, 185, 196	23		Borbeck Bf. [3], Hafenverwaltung [1]
D	2027	Ruhrallee	141, 155, 194	18	11				
E	2029	Stadtmitte	170, 173, 186, 408, 412, 415	11	18				
F	2031	Ruhrallee				169, 180	6	7	Heidhauser Platz [1], Werden S [1], Margarethenh. [1],
F	2031	Stadtmitte				145, 146		18	Erbach [1], Heisingen Baldeneysee [2]

Table 6-15: Changeover phases with vehicle numbers

Following the scenario with advanced technology, the second generation of depot charger type 2 are introduced in phases D and E. The depot-charger fleet at *Ruhrallee* is extended by 39 vehicles which are assigned to routes 141, 155 and 194. In phase E an additional 39 vehicles are required in the *Stadtmitte* depot to be operated on routes 170, 173, 186, 408, 412 and 415. The final changeover phase F contains the most challenging routes which require fast-charging infrastructure at five locations to electrify 31 BEB with opportunity charging.

The investments for each changeover phase are shown in Figure 6-26. It becomes clear that the purchase of the vehicle dominates the total costs. The comparison of the infrastructure investment indicates changeover phases with a focus on opportunity charging as B, C and F, and the higher costs are caused by the installations of fast-charging infrastructure.

The mitigation potential of each changeover phase is shown in Figure 6-27. A realization of phases A to C reduces the CO_2 emissions of the Ruhrbahn fleet by more than 50 %, proving that although a hybrid heating system with fuel heater is utilized, significant savings are ensured by replacing Diesel Euro VI buses.

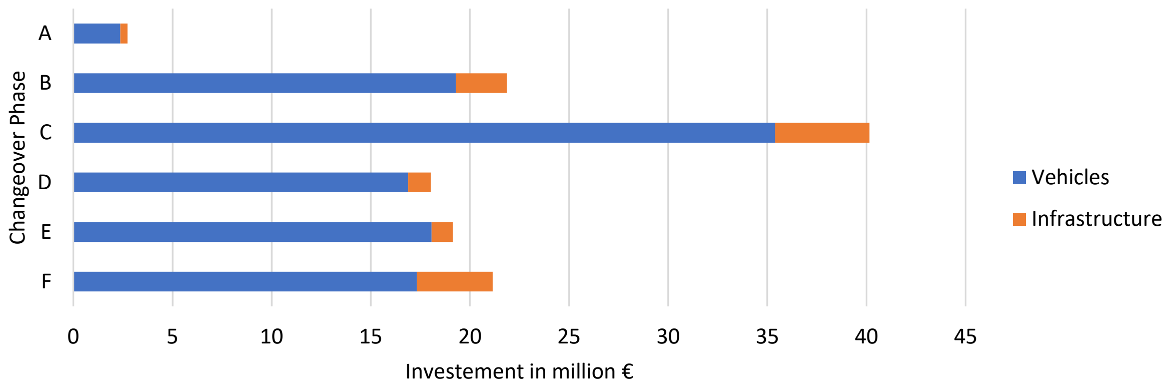

Figure 6-26: Initial investment for the changeover phases

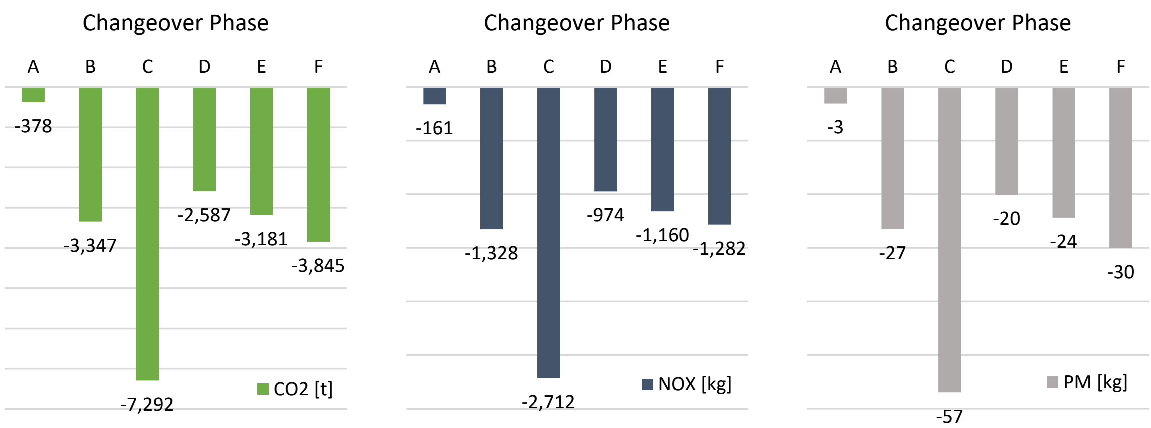

Figure 6-27: Mitigation potential of the changeover phases in the categories CO_2, NO_X and PM

The derived changeover phases provide Ruhrbahn a detailed path to fleet electrification with technology recommendations and a prioritization of routes. The high level of detail in the previous analysis ensures that the electrification concepts fulfill the technical and operational constraints and are tailored to the current market. A further advantage from the detailed analysis is that the consequences are transparent to the different departments of Ruhrbahn and external stakeholders. The operational planning department can for example consider the adapted bus runs in their planning, and the infrastructure department has a transparent scenario regarding when and where infrastructure is required. This high level of transparency reduces the hurdles to realization and fertilizes the larger roll-out of BEB.

7 Summary and Conclusion

One of the major challenges for public transport operators (PTO) in the coming years regards the substantial electrification of bus fleets. Among different technological alternatives, the battery electric bus (BEB) has especially gained substantial market shares in recent years and is viewed as the enabler for a larger rollout. However, its implementation entails several constraints regarding technical design and operational planning. The overall performance is determined to a large extent by the characteristics of the battery. The battery energy content defines the range of the BEB which is in most cases shorter than that of conventional buses. This requires frequent charging events whose duration are furthermore influenced by the charging capabilities of the battery. The limited range and additional downtimes due to charging determine the number of vehicles required for operation. This leads to the fact that operational constraints must be considered even during the early stage of strategic planning.

The general field of electrification planning comprises several research disciplines such as electrical engineering, operational research, or economics. However, a comprehensive planning approach combining the current state of research in the different disciplines is absent. The present thesis addresses this gap and provides a software-based planning approach for the strategic planning of BEB fleets in the public transport domain.

The BEB concepts available on the market share a common full electric drivetrain. The two dominant concepts are depot charging and opportunity charging, which differ in terms of their battery characteristics. While depot-charging BEB are optimized for a long range, opportunity-charging BEB are designed for high-charging capability and therefore reduced downtimes. Regardless of the charging strategy, a further distinguishing factor concerns the cooling and heating system. Heating at low temperatures entails a high thermal demand which can be covered by a full electric heating or a hybrid heating system with a fuel heater. While the heat generation by a fuel heater does not impact the range of the BEB, the full electric heating causes a significant range reduction. The planning complexity for PTOs is furthermore caused by the large variety of different technical solutions which differ for example regarding the manufacturer, vehicle size or current development status as well as dependence on the local situation in terms of route characteristics and climate conditions. Thus, simulation models are required which enable an analysis of the performance of a certain concept at the local scenario.

The simulation framework developed in this thesis is entitled the BEB system model and provides interfaces to planning tools currently used at PTO and further third party applications that provide required data for BEB simulation. The models can be divided into the categories technological (infrastructure, vehicle, and aging model), economical (life cycle cost calculation) and environmental (emission calculation). The vehicle and infrastructure models enable an analysis of the technical performance of a certain BEB on a defined route by considering the specific local situation. The results of the application of the vehicle and infrastructure model forms the input for the aging and lifetime model. The component lifetime is calculated based on the planned operation so that scenario-specific results are gained. The next step in the toolchain is described by the life cycle cost calculation (LCC) which enables a monetization of the technical configuration and operational consequences. In addition, the mitigation potential is assessed via the emission calculation. The final set of results enables a cost-benefit analysis and neutral comparison of BEB alternatives.

The developed technical and operational analysis build on the BEB system model and is applied in three scenarios: The first regards the general assessment of the technical feasibility of electrification. Batch processing enables a fast calculation even for large scenarios with several hundred vehicles and a wide range of considered BEB concepts. The second application aims at the detailed analysis of the technical and operational constraints and their interaction. The reasons for technically infeasible scenarios can be overserved and mitigation measures can be investigated such as the setup of charging infrastructure at terminal stops. The third application addresses operational adjustments for depot-charging battery buses. An energy-based vehicle scheduling enables the generation of tailored operating schemes for a given BEB type, ensuring that all technical constraints are fulfilled and that a technically feasible scenario is produced.

The application of the technical and operational analysis and the integrated BEB system within the case study has proven the functionality of the planning approach. A long-term electrification concept with technological recommendations and concrete changeover phases could be determined for the PTO Ruhrbahn. Beginning with an export of the diesel bus operational planning, the BEB system model has been applied to determine the energy demand, evaluate charging opportunities, and generate an adapted operating scheme for each considered BEB concept. The subsequent LCC calculation monetized the results and provided a comprehensive basis for the development of technological recommendations and changeover phases for about 200 vehicles in a 12-year planning horizon.

8 References

[1] S. Bakker and R. Konings, "The transition to zero-emission buses in public transport – The need for institutional innovation," *Transportation Research Part D: Transport and Environment*, vol. 64, pp. 204–215, 2018.

[2] IEA, "Global EV Outlook 2019: Scaling-up the transition to electric mobility," 2019.

[3] *Directive (EU) 2019/1161 of the European Parliament and of the Council of 20 June 2019 amending Directive 2009/33/EC on the promotion of clean and energy-efficient road transport vehicles (Text with EEA relevance.): PE/57/2019/REV/2*, 2019.

[4] A. A. Bertossi, P. Carraresi, and G. Gallo, "On some matching problems arising in vehicle scheduling models," *Networks*, vol. 17, no. 3, pp. 271–281, 1987.

[5] H. Fichtl and F. Steinert, "IVIsion and IVInet – Tool Chain for the Electrification of City Bus Routes," *Transportation Research Procedia*, vol. 14, pp. 2554–2563, 2016.

[6] R. Pütz, *Modell zur ökologischen und ökonomischen Analyse und strategischen Optimierung von Linienbusflotten*. Düsseldorf: DVV Media Group, 2010.

[7] Sean Lockie, *Municipal E-Bus Planner 2 (Munep2).* Available: https://www.climate-kic.org/success-stories/municipal-e-bus-planner-2-munep2/ (2019, Sep. 08).

[8] P. Sinhuber, D. U. Sauer, and A. Lohner, "Design of Energy Storage System for a Hybrid Electric Fuel Cell Bus," in *Proceedings of 18th World Hydrogen Energy Conference 2010 - WHEC 2010*, Jülich, 2010.

[9] A. Lajunen, "Energy consumption and cost-benefit analysis of hybrid and electric city buses," *Transportation Research Part C: Emerging Technologies*, vol. 38, pp. 1–15, 2014.

[10] D. Göhlich, A. Kunith, and T.-A. Ly, "Technology assessment of an electric urban bus system for Berlin," *WIT Transactions on the Built Environment*, vol. 138, 2014.

[11] J.-Q. Li, "Battery-electric transit bus developments and operations: A review," *International Journal of Sustainable Transportation*, vol. 10, no. 3, pp. 157–169, 2014.

[12] A. O'Donovan, J. Frith, and C. McKerracher, "Electric Buses in Cities: Driving Towards Cleaner Air and Lower CO2," Bloomberg New Energy Finance, Mar. 2018.

[13] P. Bruge, *ZeEUS Launch in Bonn: six e-buses to commence regular service: UITP*. Brussles, 2016.

[14] L. Mathieu, "Electric buses arrive on time: Marketplace, economic, technology, environmental and policy perspectives for fully electric buses in the EU," Transport & Environment, 2018.

[15] Royal Schiphol Group, *Europe's largest fleet.* Available: https://www.schiphol.nl/en/schiphol-group/page/europes-largest-fleet-of-fully-electric-buses/ (2019, Sep. 08).

[16] M. Rohs, "E-Bus-Radar," PricewaterhouseCoopers GmbH (PwC), 2019.

[17] G. Desaulniers and M. D. Hickman, "Chapter 2 Public Transit," in *Handbooks in Operations Research and Management Science*: Elsevier, 2007.

[18] A. Ceder and N. H.M. Wilson, "Bus network design," *Transportation Research Part B: Methodological*, vol. 20, no. 4, pp. 331–344, 1986.

[19] W. Lampkin and P. D. Saalmans, "The Design of Routes, Service Frequencies, and Schedules for a Municipal Bus Undertaking: A Case Study," *OR*, vol. 18, no. 4, p. 375–375, 1967.

[20] D. Hasselström, *Public Transportation Planning: A Mathematical Programming Approach*. Doctoral thesis: University of Gothenburg, 1981.

[21] R. van Nes, R. Hamerslag, and B. H. Immers, *Design of public transport networks*: National Research Council, Transportation Research Board, 1988.

[22] W. Fan and R. B. Machemehl, "Optimal Transit Route Network Design Problem: Algorithms, Implementations, and Numerical Results 6. Performing Organization Code," *Journal of transportation engineering*, vol. 132, pp. 40–51, 2006.

[23] V. M. Tom and S. Mohan, "Transit route network design using frequency coded genetic algorithm," *Journal of transportation engineering*, vol. 129, no. 2, pp. 186–195, 2003.

[24] A. Ceder, B. Golany, and O. Tal, "Creating bus timetables with maximal synchronization," *Transportation Research Part A: Policy and Practice*, vol. 35, no. 10, pp. 913–928, 2001.

[25] J. R. Daduna and J. M. Pinto Paixão, "Vehicle Scheduling for Public Mass Transit — An Overview," in *Sixth International Workshop on Computer-Aided Scheduling of Public Transport*, 1995.

[26] S. Bunte and N. Kliewer, "An overview on vehicle scheduling models," *Public Transport*, vol. 1, no. 4, pp. 299–317, 2009.

[27] A. Haghani and Y. Shafahi, "Bus maintenance systems and maintenance scheduling: Model formulations and solutions," *Transportation Research Part A: Policy and Practice*, vol. 36, no. 5, pp. 453–482, 2002.

[28] P. R. Kleindorfer, A. Neboian, A. Roset, and S. Spinler, "Fleet Renewal with Electric Vehicles at La Poste," *Interfaces*, vol. 42, no. 5, pp. 465–477, 2012.

[29] A. W. Kunith, *Elektrifizierung des urbanen öffentlichen Busverkehrs: Technologiebewertung für den kosteneffizienten Betrieb emissionsfreier Bussysteme*. Wiesbaden: Springer-Verlag, 2017.

[30] K. Berthold, "Techno-ökonomische Auslegungsmethodik für die Elektrifizierung urbaner Busnetze," Dissertation, Karlsruhe Institute of Technology (KIT).

[31] P. Sinhuber, W. Rohlfs, and D. U. Sauer, "Study on power and energy demand for sizing the energy storage systems for electrified local public transport buses," in *Proceedings of IEEE Vehicle Power and Propulsion Conference*, 2012.

[32] B. Zhou, Y. Wu, B. Zhou, R. Wang, W. Ke, S. Zhang, and J. Hao, "Real-world performance of battery electric buses and their life-cycle benefits with respect to energy consumption and carbon dioxide emissions," *Energy*, vol. 96, pp. 603–613, 2016.

[33] A. Braun, *Effiziente Elektrofahrzeuge*. Wiesbaden: Springer Fachmedien Wiesbaden, 2019.

[34] G. de Filippo, V. Marano, and R. Sioshansi, "Simulation of an electric transportation system at The Ohio State University," *Applied Energy*, vol. 113, pp. 1686–1691, 2014.

[35] Z. Gao, Z. Lin, T. J. LaClair, C. Liu, J.-M. Li, A. K. Birky, and J. Ward, "Battery capacity and recharging needs for electric buses in city transit service," *Energy*, vol. 122, pp. 588–600, 2017.

[36] UITP - International Association of Public Transport, *Bus Tender Structure*. Brussles, 2018.

[37] Verband Deutscher Verkehrsunternehmen (VDV), *VDV-Mitteilung 2315 Life Cycle Costs (LCC) bei Linienbussen: Bewertungskriterien bei Ausschreibungen*. Köln, 2010.

[38] Z. Bi, R. de Kleine, and G. A. Keoleian, "Integrated Life Cycle Assessment and Life Cycle Cost Model for Comparing Plug-in versus Wireless Charging for an Electric Bus System," *Journal of Industrial Ecology*, vol. 21, no. 2, pp. 344–355, 2017.

[39] M. Rogge, W. Rohlfs, and D. U. Sauer, "Fast charging of battery buses and its impact on the aging of various lithium-ion cell types," in *Proceedings of 10th Braunschweig Symposium Hybrid and Electric Vehicles*, Braunschweig, 2013.

[40] A. Lajunen, "Lifecycle costs and charging requirements of electric buses with different charging methods," *Journal of Cleaner Production*, vol. 172, pp. 56–67, 2018.

[41] M. Rogge, P. Sinhuber, and S. Dirk Uwe, "Development of Cost-Efficient Electrification Strategies for Public Transport Bus Networks," in *ICEEV 2015: Visions, Trends and Solutions for Energy Efficient Vehicle Systems*, 2015.

[42] S. Kukkonen, V. Erkkila, A. Manninen, J. Haavisto, and M. Pihlatie, "Method for Dimensioning Battery and Thermal Management Systems for Heavy-Duty Vehicle Applications Using Aged Battery Experimental Data and Advanced Modelling Techniques," *ECS Transactions*, vol. 68, no. 2, pp. 83–95, 2015.

[43] A. Ostadi and M. Kazerani, "A Comparative Analysis of Optimal Sizing of Battery-Only, Ultracapacitor-Only, and Battery–Ultracapacitor Hybrid Energy Storage Systems for a City Bus," *IEEE Transactions on Vehicular Technology*, vol. 64, no. 10, pp. 4449–4460, 2015.

[44] J. Chen, B. Atasoy, T. Robenek, M. Bierlaire, and M. Thémans, “Planning of feeding station installment for electric urban public mass-transportation system,” in *Proceedings of 13th Swiss Transportation Research Conference*, 2013.

[45] M. Dietmannsberger, M. Meyer, and M. Schumann, *Metastudie Elektromobilität Hamburg, 9. Dezember 2016: Anforderungen an das Stromnetz durch Elektromobilität, insbesondere Elektrobusse*: Helmut-Schmidt-Universität, Universität der Bundeswehr, Professur für Elektrische Energiesysteme, 2017.

[46] M. Ranta, V. Karvonen, J. J. Potter, R. Pasonen, E. Pursiheimo, T. Halmeaho, P. Ponomarev, and M. Pihlatie, “Method Including Power Grid Model and Route Simulation to Aid Planning and Operation of an Electric Bus Fleet,” in *Proceedings of IEEE Vehicle Power and Propulsion Conference (VPPC)*, 2016.

[47] *Environmental management - Life cycle assessment - Principles and framework*, 14040, 2006.

[48] T. R. Hawkins, O. M. Gausen, and A. H. Strømman, “Environmental impacts of hybrid and electric vehicles—a review,” *The International Journal of Life Cycle Assessment*, vol. 17, no. 8, pp. 997–1014, 2012.

[49] T. R. Hawkins, B. Singh, G. Majeau-Bettez, and A. H. Strømman, “Comparative Environmental Life Cycle Assessment of Conventional and Electric Vehicles,” *Journal of Industrial Ecology*, vol. 17, no. 1, pp. 53–64, 2013.

[50] A. Nordelöf, M. Messagie, A.-M. Tillman, M. Ljunggren Söderman, and J. van Mierlo, “Environmental impacts of hybrid, plug-in hybrid, and battery electric vehicles—what can we learn from life cycle assessment?,” *The International Journal of Life Cycle Assessment*, vol. 19, no. 11, pp. 1866–1890, 2014.

[51] R. Nealer and T. P. Hendrickson, “Review of Recent Lifecycle Assessments of Energy and Greenhouse Gas Emissions for Electric Vehicles,” *Current Sustainable/Renewable Energy Reports*, vol. 2, no. 3, pp. 66–73, 2015.

[52] J. B. Dunn, L. Gaines, J. C. Kelly, C. James, and K. G. Gallagher, “The significance of Li-ion batteries in electric vehicle life-cycle energy and emissions and recycling's role in its reduction,” *Energy Environ. Sci,* vol. 8, no. 1, pp. 158–168, 2015.

[53] G. Cooney, T. R. Hawkins, and J. Marriott, “Life Cycle Assessment of Diesel and Electric Public Transportation Buses,” *Journal of Industrial Ecology*, vol. 451, no. 7179, 2013.

[54] M. Romare and L. Dahllöf, *The Life Cycle Energy Consumption and Greenhouse Gas Emissions from Lithium-Ion Batteries: A Study with Focus on Current Technology and Batteries for light-duty vehicles*. Stockhol: IVL Swedish Environmental Research Institute, 2017.

[55] A. Hoff, H. Andersson, M. Christiansen, G. Hasle, and A. Løkketangen, “Industrial aspects and literature survey: Fleet composition and routing,” *Computers & Operations Research*, vol. 37, no. 12, pp. 2041–2061, 2010.

[56] S. Pelletier, O. Jabali, and G. Laporte, “50th Anniversary Invited Article—Goods Distribution with Electric Vehicles: Review and Research Perspectives,” *Transportation Science*, vol. 50, no. 1, pp. 3–22, 2016.

[57] D. Goeke and M. Schneider, "Routing a mixed fleet of electric and conventional vehicles," *European Journal of Operational Research*, vol. 245, no. 1, pp. 81–99, 2015.

[58] P. Lebeau, C. de Cauwer, J. van Mierlo, C. Macharis, W. Verbeke, and T. Coosemans, "Conventional, Hybrid, or Electric Vehicles: Which Technology for an Urban Distribution Centre?," (eng), *TheScientificWorldJournal*, vol. 2015, p. 302867–302867, 2015.

[59] J.H.R. van Duin, L. A. Tavasszy, and H. J. Quak, "Towards E(lectric)- urban freight: first promising steps in the electric vehicle revolution," *European Transport*, no. 54, p. 9–9, 2013.

[60] F. Gonçalves, Sónia R. Cardoso, Susana Relvas, and A. P. F. D. Barbosa-Póvoa, "Optimization of a distribution network using electric vehicles: A VRP problem," *In the Proceedings of the IO2011-15 Congresso da associação Portuguesa de Investigação Operacional, Coimbra, Portugal*, pp. 18–20, 2011.

[61] G. Hiermann, J. Puchinger, S. Ropke, and R. F. Hartl, "The Electric Fleet Size and Mix Vehicle Routing Problem with Time Windows and Recharging Stations," *European Journal of Operational Research*, vol. 252, no. 3, pp. 995–1018, 2016.

[62] O. Sassi, W. R. Cherif-Khettaf, and A. Oulamara, "Vehicle Routing Problem with Mixed Fleet of Conventional and Heterogenous Electric Vehicles and Time Dependent Charging Costs," *International Journal of Mathematical, Computational, Physical, Electrical and Computer Engineering*, no. 3, pp. 171–181, 2015.

[63] J.-Q. Li, "Transit Bus Scheduling with Limited Energy," *Transportation Science*, vol. 48, no. 4, pp. 521–539, 2014.

[64] H. Wang and J. Shen, "Heuristic approaches for solving transit vehicle scheduling problem with route and fueling time constraints," *Applied Mathematics and Computation*, vol. 190, no. 2, pp. 1237–1249, 2007.

[65] X. Hao, W. Jin, and M. Wei, "Max-Min ant system for bus transit multi-depot vehicle scheduling problem with route time constraints," in *Proceedings of 2012 10th World Congress on Intelligent Control and Automation (WCICA 2012)*, 2012.

[66] T. Paul and H. Yamada, "Operation and charging scheduling of electric buses in a city bus route network," in *Proceedings of IEEE 17th International Conference on Intelligent Transportation Systems (ITSC)*, 2014.

[67] Z. Chao and C. Xiaohong, "Optimizing Battery Electric Bus Transit Vehicle Scheduling with Battery Exchanging: Model and Case Study," *Procedia - Social and Behavioral Sciences*, vol. 96, pp. 2725–2736, 2013.

[68] B.-R. Ke, C.-Y. Chung, and Y.-C. Chen, "Minimizing the costs of constructing an all plug-in electric bus transportation system: A case study in Penghu," *Applied Energy*, vol. 177, pp. 649–660, 2016.

[69] M. Wen, E. Linde, S. Ropke, P. Mirchandani, and A. Larsen, “An adaptive large neighborhood search heuristic for the Electric Vehicle Scheduling Problem,” *Computers & Operations Research*, vol. 76, pp. 73–83, 2016.
[70] R. Kühne, “Electric buses – An energy efficient urban transportation means,” *Energy*, vol. 35, no. 12, pp. 4510–4513, 2010.
[71] P. Hofmann, *Hybridfahrzeuge*. Vienna: Springer-Verlag, 2014.
[72] *Electric vehicle conductive charging system*, IEC 61851-1, 2017.
[73] *Electric vehicle conductive charging system*, IEC 61851-23, 2014.
[74] *Electric vehicle conductive charging system*, IEC 61851-24, 2014.
[75] *Road vehicles - Vehicle to grid communication interface*, ISO 15118-1, 2019.
[76] *Road vehicles - Vehicle to grid communication interface*, ISO 15118-3, 2015.
[77] Bombardier Inc, *PRIMOVE E-BUS: Erstes Projekt mit induktiv geladenen E-Bussen für den Fahrgastbetrieb*, 2015.
[78] P. Konstantin, *Praxisbuch Energiewirtschaft: Energieumwandlung, -transport und -beschaffung im liberalisierten Markt*: Springer-Verlag, 2013.
[79] National Renewable Energy Laboratory (NREL), “King County Metro Battery Electric Bus Demonstration: Preliminary Project Results,” National Renewable Energy Lab. (NREL), Golden, CO (United States) NREL/BR-5400-68412; DOT/FTA-ZEB-FS1, 2017.
[80] N. Omar, M. Daowd, P. van den Bossche, O. Hegazy, J. Smekens, T. Coosemans, and J. van Mierlo, “Rechargeable Energy Storage Systems for Plug-in Hybrid Electric Vehicles—Assessment of Electrical Characteristics,” *Energies*, vol. 5, no. 12, pp. 2952–2988, 2012.
[81] S. Rothgang, M. Rogge, J. Becker, and D. Sauer, “Battery Design for Successful Electrification in Public Transport,” *Energies*, vol. 8, no. 7, pp. 6715–6737, 2015.
[82] D. Naunin, *Hybrid-, Batterie- und Brennstoffzellen-Elektrofahrzeuge: Technik, Strukturen und Entwicklungen*: Expert-Verlag, 2007.
[83] Daimler AG, *Alternative drive systems in Buses of Daimler AG – Part I.* Available: http://www.omnibusarchiv.de/include.php?path=content/articles.php&contentid=443 (2019, Sep. 29).
[84] M. Kane, *Irizar Introduces Electric Bus With 376 kWh Sodium Nickel Battery Pack.* Available: https://insideevs.com/irizar-introduced-electric-bus-376-kwh-sodium-nickel-battery-pack/ (2019, Sep. 29).
[85] O. Veneri, C. Capasso, and S. Patalano, “Experimental study on the performance of a ZEBRA battery based propulsion system for urban commercial vehicles,” *Applied Energy*, vol. 185, pp. 2005–2018, 2017.
[86] D. Kaup, R. Bouwman, G. Schädlich, D. U. Sauer, and A. Lohner, “H2 Bus NRW - The Hybrid Electric Fuel-Cell Bus,” in *18th World Hydrogen Energy Conference*, Forschungszentrum J¸lich GmbH, Ed, 2010.
[87] M. Ecker, P. Shafiei Sabet, and D. U. Sauer, “Influence of operational condition on lithium plating for commercial lithium-ion batteries – Electrochemical exper-

iments and post-mortem-analysis," *Applied Energy*, vol. 206, pp. 934–946, 2017.

[88] J. Vetter, P. Novák, M. R. Wagner, C. Veit, K.-C. Möller, J. O. Besenhard, M. Winter, M. Wohlfahrt-Mehrens, C. Vogler, and A. Hammouche, "Ageing mechanisms in lithium-ion batteries," *Journal of Power Sources*, vol. 147, no. 1-2, pp. 269–281, 2005.

[89] W. Bögel, J. P. Büchel, and H. Katz, "Real-life EV battery cycling on the test bench," *Journal of Power Sources*, vol. 72, no. 1, pp. 37–42, 1998.

[90] K. Ohue, T. Utsunomiya, O. Hatozaki, N. Yoshimoto, M. Egashira, and M. Morita, "Self-discharge behavior of polyacenic semiconductor and graphite negative electrodes for lithium-ion batteries," *Journal of Power Sources*, vol. 196, no. 7, pp. 3604–3610, 2011.

[91] A. Barré, B. Deguilhem, S. Grolleau, M. Gérard, F. Suard, and D. Riu, "A review on lithium-ion battery ageing mechanisms and estimations for automotive applications," *Journal of Power Sources*, vol. 241, pp. 680–689, 2013.

[92] S. Käbitz, J. B. Gerschler, M. Ecker, Y. Yurdagel, B. Emmermacher, D. André, T. Mitsch, and D. U. Sauer, "Cycle and calendar life study of a graphite|LiNi1/3Mn1/3Co1/3O2 Li-ion high energy system. Part A: Full cell characterization," *Journal of Power Sources*, vol. 239, pp. 572–583, 2013.

[93] M. Lewerenz, S. Käbitz, M. Knips, J. Münnix, J. Schmalstieg, A. Warnecke, and D. U. Sauer, "New method evaluating currents keeping the voltage constant for fast and highly resolved measurement of Arrhenius relation and capacity fade," *Journal of Power Sources*, vol. 353, pp. 144–151, 2017.

[94] M. Ecker, N. Nieto, S. Käbitz, J. Schmalstieg, H. Blanke, A. Warnecke, and D. U. Sauer, "Calendar and cycle life study of Li(NiMnCo)O2-based 18650 lithium-ion batteries," *Journal of Power Sources*, vol. 248, pp. 839–851, 2014.

[95] M. Petzl, M. Kasper, and M. A. Danzer, "Lithium plating in a commercial lithium-ion battery – A low-temperature aging study," *Journal of Power Sources*, vol. 275, pp. 799–807, 2015.

[96] M. Rogge, D. Müller, and D. U. Sauer, "Lithium-Titanate Cells for Fast Charging Battery Buses - Results of a Performance and Aging Analysis," in *Proceedings of Advanced Battery Power Conference Aachen*, 2015.

[97] MATLAB, "The MathWorks," *Inc, Natick, Massachusetts, United States*, vol. 488, 2013.

[98] Verband Deutscher Verkehrsunternehmen (VDV), *VDV Schrift 451: ÖPNV-Datenmodell 5.0*. Köln, 1999.

[99] Verband Deutscher Verkehrsunternehmen, *VDV Schrift 452: VDV-Standardschnittstelle Liniennetz/Fahrplan*. Köln, 2013.

[100] Verband Deutscher Verkehrsunternehmen (VDV), *VDV Schrift 455: VDV-Standardschnittstelle Dienstplan*. Köln, 2005.

[101] R. W. Floyd, "Algorithm 97: Shortest path," *Commun. ACM*, vol. 5, no. 6, p. 345–345, 1962.

[102] S. Warshall, “A Theorem on Boolean Matrices,” *J. ACM*, vol. 9, no. 1, pp. 11–12, 1962.

[103] A. Jarvis, H. I. Reuter, A. Nelson, and E. Guevara, “Hole-filled SRTM for the globe Version 4,” *available from the CGIAR-CSI SRTM 90m Database (http://srtm. csi. cgiar. org)*, vol. 15, 2008.

[104] UITP - International Association of Public Transport, *UITP Project ‘SORT’: Standardised On-Road Test Cycles*. Brussles, 2014.

[105] V. A. W. Hillier, *Hillier's fundamentals of motor vehicle technology*: Oxford University Press, 2014.

[106] M. Ehsani, Y. Gao, S. Gay, and A. Emadi, *Modern Electric, Hybrid Electric, and Fuel Cell Vehicles*: Cengage Learning, 2004.

[107] D. Jefferies, T.-A. Ly, A. Kunith, and D. Göhlich, “Energiebedarfverschiede-nerKlimatisierungssysteme für Elektro-Linienbusse,” in *Proceedings of Deutsche Kälte und Klimatagung 2015*

[108] R. Basile, “Challenges for HVAC Solutions in the Electric Bus – Status Quo,” in *Proceedings of 5th VDV Conference Electric Buses 2014*, 2014.

[109] A. Alahmer, A. Mayyas, A. Mayyas, M. A. Omar, and S. Dongri, “Vehicular thermal comfort models; a comprehensive review,” *Applied Thermal Engineering*, vol. 31, no. 6-7, pp. 995–1002, 2011.

[110] M. Sonnekalb and W. Laber, “Heizung und Klimatisierung im E-Bus – Aktuell verfügbare Technologien und weitere Effizienzpotentiale,” in *Proceedings of 2. Energietechnologieforum Hessen*, 2015.

[111] R. Basile, H. Scheid, D. Tanke, M. Moeseler, and R. Häring, “Thermal Bus Systems: Beheizungsstrategien für Elektrobusse,” Bremen, Dec. 2017.

[112] O. Klawikowski, *Aufbau eines Werkzeugs zur einsatzspezifischen Auslegung von Elektrobussen: Master Thesis*. Aachen: Institut for Power Electronics and Electrical Drives (ISEA), RWTH Aachen University, 2014.

[113] C. Müller, *Aufbau eines Simulationstools zur Auslegung von Energiespeichern für Hybridbusse: Master Thesis*. Aachen: Institut for Power Electronics and Electrical Drives (ISEA), RWTH Aachen University, 2013.

[114] M. Sistig, *Weiterentwicklung eines Auslegungswerkzeuges für das Energiespeichersystem eines Hybridbusses: Bachelor Thesis*. Aachen: Institut for Power Electronics and Electrical Drives (ISEA), RWTH Aachen University, 2013.

[115] M. Ecker, J. B. Gerschler, J. Vogel, S. Käbitz, F. Hust, P. Dechent, and D. U. Sauer, “Development of a lifetime prediction model for lithium-ion batteries based on extended accelerated aging test data,” *Journal of Power Sources*, vol. 215, pp. 248–257, 2012.

[116] M. Musallam and C. M. Johnson, “An Efficient Implementation of the Rainflow Counting Algorithm for Life Consumption Estimation,” *IEEE Transactions on Reliability*, vol. 61, no. 4, pp. 978–986, 2012.

[117] L. Gopi Reddy, L. Tolbert, and B. Ozpineci, “Power Cycle Testing of Power Switches: A Literature Survey,” *IEEE Transactions on Power Electronics*, p. 1–1, 2014.

[118] I. Shancita, H. H. Masjuki, M. A. Kalam, I. M. Rizwanul Fattah, M. M. Rashed, and H. K. Rashedul, “A review on idling reduction strategies to improve fuel economy and reduce exhaust emissions of transport vehicles,” *Energy Conversion and Management*, vol. 88, pp. 794–807, 2014.

[119] F. Stodolsky, L. Gaines, and A. Vyas, *Analysis of Technology Options to Reduce the Fuel Consumption of Idling Trucks*: Argonne National Laboratory, 2000.

[120] H. Lim, “Study of Exhaust Emissions from Idling Heavy Duty Diesel Trucks and Commercially Available Idle Reducing Devices,” *SAE Technical Paper*, no. 2003-01-0288, 2003.

[121] L. L. Gaines, C.-J. B. Hartman, and M. Solomon, “Energy Use and Emissions of Idling-Reduction Options for Heavy-Duty Diesel Trucks,” *Transportation Research Record*, vol. 2123, no. 1, pp. 8–16, 2009.

[122] J. M. E. Storey, J. F. Thomas, S. A. Lewis, T. Dam, K. D. Edwards, G. Devault, and D. Retrossa, “Particulate Matter and Aldehyde Emissions from Idling Heavy-Duty Diesel Trucks,” in *Proceedings of SAE World Congress & Exhibition*, 2003.

[123] M. Sistig, *Erschließung von Kostensenkungspotentialen bei der Auslegung von Batteriebusflotten durch eine vorgelagerte Modifikation der Betriebsplanung: Master Thesis*. Aachen: TIME, RWTH Aachen University, 2016.

[124] M. Rogge, E. van der Hurk, A. Larsen, and D. U. Sauer, “Electric bus fleet size and mix problem with optimization of charging infrastructure,” *Applied Energy*, vol. 211, pp. 282–295, 2018.

[125] E. Falkenauer, *Genetic algorithms and grouping problems*. New York: John Wiley & Sons, 1998.

[126] G. Pankratz, “A Grouping Genetic Algorithm for the Pickup and Delivery Problem with Time Windows,” *OR Spectrum*, vol. 27, no. 1, pp. 21–41, 2005.

[127] I. I.M. CPLEX, “V12. 1: User’s Manual for CPLEX,” *International Business Machines Corporation*, vol. 46, no. 53, p. 157–157, 2009.

[128] S. Jones, *Heuliez GX337 Linium Elec – Bus Euro Test 2018.* Available: https://www.busandcoachbuyer.com/heuliez-gx337-linium-elec-bus-euro-test-2018/ (2019, Jun. 01).

[129] A. Matthey and B. Bünger, *Methodological Convention 3.0 for the Assessment of Environmental Costs: Cost Rates*. Berlin: Umweltbundesamt, 2019.

A Appendix

A.1 Abbreviations and Glossary

Term	Definition
BEB	Battery electric bus
Block	Sequence of trips (service and deadhead) operated by one vehicle starting from and ending at the depot
Bus Run	Combination of blocks at a certain day
Bus Stop	Place where a bus stops for passenger access
Charging Station	Infrastructure at a certain location to charge the battery of BEB
CO_2	Carbon Dioxide
Commercial Speed	Average speed in service trip operation
COP	Coefficient of performance describing heat pump efficiency
Deadhead Trip	Trip without passengers
Deadheading	Deadhead trip operation
Depot	Location where buses are parked and maintained
Depot Charging	BEB charging concept with exclusive charging in the depot
DOD	Battery depth of discharge
Drivetrain	Combination of inverter, motor and (where necessary) gear-box
Dwell Time	Duration of scheduled presence at a bus stop
GGA	Grouping genetic algorithm
Grid Connection	Connection to the electricity grid
LCC	Life cycle costs
NO_X	Nitrous oxides
Operating Scheme	Set of bus runs describing the entire fleet operation
Opportunity Charging	BEB charging concept with charging at the depot and at locations on the route
PM	Particular matter
PTA	Public Transport Authority
PTO	Public Transport Operator
Pull-In Trip	Deadhead trip to the bus depot

Term	Definition
Pull-Out Trip	Deadhead trip from the bus depot
Route	A defined set of ways connecting bus stops
Service Trip	Trip in regular passenger service
SOC	Battery state of charge
Terminal Stop	Bus stop at the beginning or the end of a route
Track	Path described by geo locations
Trip	One-way bus trip from one location to another potentially passing by several bus stops
Trip Sequence	Series of subsequently operated trips between charging events
Vehicle Scheduling	Process of assigning trips to blocks and blocks to vehicles
Worst-Case	Worst scenario that could be expected under given circumstances

Own Publications

Scientific journal publications and conference contributions have been prepared by the author in framework of this thesis. Content of these publications is used in this work and marked by a reference to the publication in accordance to the “Promotionsordnung der Fakultät für Elektrotechnik und Informationstechnik der RWTH Aachen” and in agreement with the supervising professor Dirk Uwe Sauer.

- M. Rogge, E. van der Hurk, A. Larsen, and D. U. Sauer, “Electric bus fleet size and mix problem with optimization of charging infrastructure,” Applied Energy, vol. 211, pp. 282–295, 2018.
- S. Rothgang, M. Rogge, J. Becker, and D. U. Sauer, “Battery Design for Successful Electri-fication in Public Transport,” Energies, vol. 8, no. 7, pp. 6715–6737, 2015.
- M. Rogge, S. Wollny, and D. U. Sauer, “Fast Charging Battery Buses for the Electrification of Urban Public Transport—A Feasibility Study Focusing on Charging Infrastructure and Energy Storage Requirements,” Energies, vol. 8, no. 5, pp. 4587–4606, 2015.
- M. Rogge, P. Sinhuber, and D. U. Sauer, “Development of Cost-Efficient Electrification Strategies for Public Transport Bus Networks,” at ICEEV 2015: Visions, Trends and Solutions for Energy Efficient Vehicle Systems, 2015.
- M. Rogge, D. U. Sauer, “Analysis of lithium-ion cell degradation based on realistic power profiles representing the fast charging battery bus application” at 17th International Energy & Power Supply Conference, Nice 2015.
- M. Rogge, D. Müller, and D. U. Sauer, “Lithium-Titanate Cells for Fast Charging Bat-tery Buses - Results of a Performance and Aging Analysis,” at Advanced Battery Power Conference Aachen, 2015.
- M. Rogge, D. U. Sauer, “Potentiale und technologische Optionen für vollelektrische Busse im ÖPNV,“ at Batterietag NRW 2014 Münster, 2014.
- M. Rogge, W. Rohlfs, and D. U. Sauer, “Fast charging of battery buses and its impact on the aging of various lithium-ion cell types,” at 10th Braunschweig Symposium Hybrid and Electric Vehicles, Braunschweig, 2013.

- M. Rogge, S. Rothgang, and D. U. Sauer, “Operating Strategies for a Range Extender Used in Battery Electric Vehicles,” at IEEE Vehicle Power and Propulsion Conference (VPPC), 2013.

Supervised Theses

Bachelor, master and diploma theses were conducted in the framework of this thesis. The definition of scope and topic as well as the scientific supervision was substantially done by the author. Corresponding content is not explicitly referenced.

- M. Sistig, “Erschließung von Kostensenkungspotentialen bei der Auslegung von Batteriebusflotten durch eine vorgelagerte Modifikation der Betriebsplanung,“: Master Thesis. Aachen: TIME, RWTH Aachen University, 2016.
- H. Pigerl, “Development of a Methodology for Cost Optimized Operation Planning for Electric Bus Fleets,“: Master Thesis. Aachen: ISEA, RWTH Aachen University, 2016.
- F. Langen, “Verifizierung und Optimierung einer Energieverbrauchssimulation für Elektrobusse“, Master Thesis. Aachen: ISEA, RWTH Aachen University, 2015.
- D. Mueller, “Analyse von Lithium-Titanat-Zellen für den Einsatz in schnellladefähigen Batteriebussen,“: Bachelor Thesis. Aachen: ISEA, RWTH Aachen University, 2014.
- O. Klawikowski, “Aufbau eines Werkzeugs zur einsatzspezifischen Auslegung von Elektrobussen“, Master Thesis. Aachen: ISEA, RWTH Aachen University, 2014.
- S. Wollny, “ Analyse des Leistungs- und Energiebedarfs elektrifizierter Busflotten in Großstädten“, Master Thesis. Aachen: ISEA, RWTH Aachen University, 2014.
- V. Falter, “Ökologischer Fußabdruck von Energiespeichern in verschiedenen Anwendungen“, Master Thesis. Aachen: ISEA, RWTH Aachen University, 2013.
- K. Pasch, “Analyse von Kühlkonzepten für die DC-Schnellladung von Batteriebussen“, Master Thesis. Aachen: ISEA, RWTH Aachen University, 2013.
- H. Hasni, “Entwicklung eines Energiemanagements für schnellladefähige Elektrobusse mit verteilten Batteriesystemen“, Diploma Thesis. Aachen: ISEA, RWTH Aachen University, 2013.

ABISEA Band 1
Eßer, Albert
Berührungslose, kombinierte Energie- und Informationsübertragung für bewegliche Systeme
1. Aufl. 1992, 129 S.
ISBN 3-86073-046-0

ABISEA Band 2
Vogel, Ulrich
Entwurf und Beurteilung von Verfahren zur Hochausnutzung des Rad-Schiene-Kraftschlusses durch Triebfahrzeuge
1. Aufl. 1992, 131 S.
ISBN 3-86073-060-6

ABISEA Band 3
Reckhorn, Thomas
Stromeinprägendes Antriebssystem mit fremderregter Synchronmaschine
1. Aufl. 1992, 128 S.
ISBN 3-86073-061-4

ABISEA Band 4
Ackva, Ansgar
Spannungseinprägendes Antriebssystem mit Synchronmaschine und direkter Stromregelung
1. Aufl. 1992, 137 S.
ISBN 3-86073-062-2

ABISEA Band 5
Mertens, Axel
Analyse des Oberschwingungsverhaltens von taktsynchronen Delta - Modulationsverfahren zur Steuerung von Pulsstromrichtern bei hoher Taktzahl
1. Aufl. 1992, 178 S.
ISBN 3-86073-069-X

ABISEA Band 6
Geuer, Wolfgang
Untersuchungen über das Alterungsverhalten von Blei-Akkumulatoren
1. Aufl. 1993, 97 S.
ISBN 3-86073-097-5

ABISEA Band 7
Langheim, Jochen
Einzelradantrieb für Elektrostraßenfahrzeuge
1. Aufl. 1993, 213 S.
ISBN 3-86073-123-8
(vergriffen)

ABISEA Band 8
Fetz, Joachim
Fehlertolerante Regelung eines Asynchron-Doppelantriebes für ein Elektrospeicherfahrzeug
1. Aufl. 1993, 136 S.
ISBN 3-86073-124-6
(vergriffen)

ABISEA Band 9
Schülting, Ludger
Optimierte Auslegung induktiver Bauelemente für den Mittelfrequenzbereich
1. Aufl. 1993, 126 S.
ISBN 3-86073-174-2
(vergriffen)

ABISEA Band 10
Skudelny, H.-Ch.
Stromrichtertechnik
4. Aufl. 1997, 259 S.
ISBN 3-86073-189-0

ABISEA Band 11
Skudelny, H.-Ch.
Elektrische Antriebe
3. Aufl. 1997, 124 S.
ISBN 3-86073-231-5

ABISEA Band 12
Schöpe, Friedhelm
Batterie-Management für Nickel-Cadmium Akkumulatoren
1. Aufl. 1994, 148 S.
ISBN 3-86073-232-3
(vergriffen)

ABISEA Band 13
v. d. Weem, Jürgen
Schmalbandige aktive Filter für Schienentriebfahrzeuge am Gleichspannungsfahrdraht
1. Aufl. 1995, 126 S.
ISBN 3-86073-233-1

ABISEA Band 14
Backhaus, Klaus
Spannungseinprägendes Direktantriebssystem mit schnelllaufender geschalteter Reluktanzmaschine
1. Aufl. 1995, 146 S.
ISBN 3-86073-234-X
(vergriffen)

ABISEA Band 15
Reinold, Harry
Optimierung dreiphasiger Pulsdauermodulationsverfahren
1. Aufl. 1996, 107 S.
ISBN 3-86073-235-8

ABISEA Band 16
Köpken, Hans-Georg
Regelverfahren für Parallelschwingkreisumrichter
1. Aufl. 1996, 125 S.
ISBN 3-86073-236-6

ABISEA Band 17
Mauracher, Peter
Modellbildung und Verbundoptimierung bei Elektrostraßenfahrzeugen
1. Aufl. 1996, 192 S.
ISBN 3-86073-237-4

ABISEA Band 18
Protiwa, Franz-Ferdinand
Vergleich dreiphasiger Resonanz-Wechselrichter in Simulation und Messung
1. Aufl. 1997, 178 S.
ISBN 3-86073-238-2

ABISEA Band 19
Brockmeyer, Ansgar
Dimensionierungswerkzeug für magnetische Bauelemente in Stromrichteranwendungen
1. Aufl. 1997, 175 S.
ISBN 3-86073-239-0

ABISEA Band 20
Apeldoorn, Oscar
Simulationsgestützte Bewertung von Steuerverfahren für netzgeführte Stromrichter mit verringerter Netzrückwirkung
1. Aufl. 1997, 134 S.
ISBN 3-86073-680-9

ABISEA Band 21
Lohner, Andreas
Batteriemanagement für verschlossene Blei-Batterien am Beispiel von Unterbrechungsfreien Stromversorgungen
1. Aufl. 1998, 126 S.
ISBN 3-86073-681-7

ABISEA Band 22
Reinert, Jürgen
Optimierung der Betriebseigenschaften von Antrieben mit geschalteter Reluktanzmaschine
1. Aufl. 1998, 153 S.
ISBN 3-86073-682-5

ABISEA Band 23
Nagel, Andreas
Leitungsgebundene Störungen in der Leistungselektronik: Entstehung, Ausbreitung und Filterung
1. Aufl. 1999, 140 S.
ISBN 3-86073-683-3

ABISEA Band 24
Menne, Marcus
Drehschwingungen im Antriebsstrang von Elektrostraßenfahrzeugen - Analyse und aktive Dämpfung
1. Aufl. 2001, 169 S.
ISBN 3-86073-684-1

ABISEA Band 25
von Bloh, Jochen
Multilevel-Umrichter zum Einsatz in Mittelspannungs-Gleichspannungs-Übertragungen
1. Aufl. 2001, 137 S.
ISBN 3-86073-685-X

ABISEA Band 26
Karden, Eckhard
Using low-frequency impedance spectroscopy for characterization, monitoring, and modeling of industrial batteries
1. Aufl. 2002, 137 S.
ISBN 3-8265-9766-4

ABISEA Band 27
Karipidis, Claus-Ulrich
A Versatile DSP/ FPGA Structure optimized for Rapid Prototyping and Digital Real-Time Simulation of Power Electronic and Electrical Drive Systems
1. Aufl. 2001, 164 S.
ISBN 3-8265-9738-9

ABISEA Band 28
Kahlen, Klemens
Regelungsstrategien für permanentmagnetische Direktantriebe mit mehreren Freiheitsgraden
1. Aufl. 2002, 154 S.
ISBN 3-8322-1222-1

ABISEA Band 29
Inderka, Robert B.
Direkte Drehmomentregelung Geschalteter Reluktanzantriebe
1. Aufl. 2003, 182 S.
ISBN 3-8322-1175-6

ABISEA Band 30
Schröder, Stefan
Circuit-Simulation Models of High-Power Devices Based on Semiconductor Physics
1. Aufl. 2003, 123 S.
ISBN 3-8322-1250-7

ABISEA Band 31
Buller, Stephan
Impedance-Based Simulation Models for Energy Storage Devices in Advanced Automotive Power Systems
1. Aufl. 2003, 138 S.
ISBN 3-8322-1225-6

ABISEA Band 32
Schönknecht, Andreas
Topologien und Regelungsstrategien für das induktive Erwärmen mit hohen Frequenz-Leistungsprodukten
1. Aufl. 2004, 157 S.
ISBN 3-8322-2408-4

ABISEA Band 33
Tolle, Tobias
Konvertertopologien für ein aufwandsarmes, zweistufiges Schaltnetzteil zum Laden von Batterien aus dem Netz
1. Aufl. 2004, 148 S.
ISBN 3-8322-2676-1

ABISEA Band 34
Götting, Gunther
Dynamische Antriebsregelung von Elektrostraßenfahrzeugen unter Berücksichtigung eines schwingungsfähigen Antriebsstrangs
1. Aufl. 2004, 157 S.
ISBN 3-8322-2804-7

ABISEA Band 35
Dieckerhoff, Sibylle
Transformatorlose Stromrichterschaltungen für Bahnfahrzeuge am 16 2/3Hz Netz
1. Aufl. 2004, 147 S.
ISBN 3-8322-3094-7

ABISEA Band 36
Hu, Jing
Bewertung von DC-DC-Topologien und Optimierung eines DC-DC-Leistungsmoduls für das 42-V-Kfz-Bordnetz
1. Aufl. 2004, 148 S.
ISBN 3-8322-3201-X

ABISEA Band 37
Detjen, Dirk-Oliver
Characterization and Modeling of Si-Si Bonded Hydrophobie Interfaces for Novel High-Power BIMOS Devices
1. Aufl. 2004, 135 S.
ISBN 3-8322-2963-9

ABISEA Band 38
Walter, Jörg
Simulationsbasierte Zuverlässigkeitsanalyse in der modernen Leistungselektronik
1. Aufl. 2004, 121 S.
ISBN 3-8322-3481-0

ABISEA Band 39
Schwarzer, Ulrich
IGBT versus GCT in der Mittelspannungsanwendung - ein experimenteller und simulativer Vergleich
1. Aufl. 2005, 170 S.
ISBN 3-8322-4489-1

ABISEA Band 40
Bartram, Markus
IGBT-Umrichtersysteme für Windkraftanlagen: Analyse der Zyklenbelastung, Modellbildung, Optimierung und Lebensdauervorhersage
1. Aufl. 2006, 185 S.
ISBN 3-8322-5039-5

ABISEA Band 41
Ponnaluri, Srinivas
Generalized Design, Analysis and Control of Grid side converters with integrated UPS or Islanding functionality
1. Aufl. 2006, 163 S.
ISBN 3-8322-5281-9

ABISEA Band 42
Jacobs, Joseph
Multi-Phase Series Resonant DC-to-DC Converters
1. Aufl. 2006, 185 S.
ISBN 3-8322-5532-X

ABISEA Band 43
Linzen, Dirk
Impedance-Based Loss Calculation and Thermal Modeling of Electrochemical Energy Storage Devices for Design Considerations of Automotive Power Systems
1. Aufl. 2006, 185 S.
ISBN 3-8322-5706-3

ABISEA Band 44
Fiedler, Jens
Design of Low-Noise Switched Reluctance Drives
1. Aufl. 2007, 176 S.
ISBN 978-3-8322-5864-1

ABISEA Band 45
Fuengwarodsakul, Nisai
Predictive PWM-based Direct Instantaneous Torque Control for Switched Reluctance Machines
1. Aufl. 2007, 141 S.
ISBN 978-3-8322-6210-5

ABISEA Band 46
Meyer, Christoph
Key Components for Future Offshore DC Grids
1. Aufl. 2007, 187 S.
ISBN 978-3-8322-6571-7

ABISEA Band 47
Fujii, Kansuke
Characterization and Optimization of Soft-Switched Multi-Level Converters for STATCOMs
1. Aufl. 2008, 199 S.
ISBN 978-3-8322-6981-4

ABISEA Band 48
Carstensen, Christian
Eddy Currents in Windings of Switched Reluctance Machines
1. Aufl. 2008, 179 S.
ISBN 978-3-8322-7118-3

ABISEA Band 49
Bohlen, Oliver
Impedance-based battery monitoring
1. Aufl. 2008, 190 S.
ISBN 978-3-8322-7606-5

ABISEA Band 50
Thele, Marc
A contribution to the modelling of the charge acceptance of lead-acid batteries - using frequency and time domain based concepts
1. Aufl. 2008, 165 S.
ISBN 978-3-8322-7659-1

ABISEA Band 51
König, Andreas
High Temperature DC-to-DC Converters for Downhole Applications
1. Aufl. 2009, 154 S.
ISBN 978-3-8322-8489-3

ABISEA Band 52
Dick, Christian Peter
Multi-Resonant Converters as Photovoltaic Module-Integrated Maximum Power Point Tracker
1. Aufl. 2010, 182 S.
ISBN 978-3-8322-9199-0

ABISEA Band 53
Kowal, Julia
Spatially resolved impedance of nonlinear inhomogeneous devices: using the example of lead-acid batteries
1. Aufl. 2010, 203 S.
ISBN 978-3-8322-9483-0

ABISEA Band 54
Roscher, Michael Andreas
Zustandserkennung von LiFeP04-Batterien für Hybrid- und Elektrofahrzeuge
1. Aufl. 2011, 186 S.
ISBN 978-3-8322-9738-1

ABISEA Band 55
Hirschmann, Dirk
Highly Dynamic Piezoelectric Positioning
1. Aufl. 2011, 146 S.
ISBN 978-3-8322-9746-6

ABISEA Band 56
Rigbers, Klaus
Highly Efficient Inverter Architectures for Three-Phase Grid Connection of Photovoltaic Generators
1. Aufl. 2011, 244 S.
ISBN 978-3-8322-9816-9

ABISEA Band 57
Kasper, Knut
Analysis and Control of the Acoustic Behavior of Switched Reluctance Drives
1. Aufl. 2011, 205 S.
ISBN 978-3-8322-9869-2

ABISEA Band 58
Köllensperger, Peter
The Internally Commutated Thyristor - Concept, Design and Application
1. Aufl. 2011, 214 S.
ISBN 978-3-8322-9909-5

ABISEA Band 59
Schoenen, Timo
Einsatz eines DC/DC-Wandlers zur Spannungsanpassung zwischen Antrieb und Energiespeicher in Elektro-und Hybridfahrzeugen
1. Aufl. 2011, 128 S.
ISBN 978-3-8440-0622-3

ABISEA Band 60
Hennen, Martin
Switched Reluctance Direct Drive with Integrated Distributed Inverter
1. Aufl. 2012, 141 S.
ISBN 978-3-8440-0731-2

ABISEA Band 61
van Treek, Daniel
Position Sensorless Torque Control of Switched Reluctance Machines
1. Aufl. 2012, 144 S.
ISBN 978-3-8440-1014-5

ABISEA Band 62
Bragard, Michael
The Integrated Emitter Turn-Off Thyristor. An Innovative MOS-Gated High-Power Device
1. Aufl. 2012, 164 S.
ISBN 978-3-8440-1152-4

ABISEA Band 63
Gerschler, Jochen B.
Ortsaufgelöste Modellbildung von Lithium-Ionen-Systemen unter spezieller Berücksichtigung der Batteriealterung
1. Aufl. 2012, 334 S.
ISBN 978-3-8440-1307-8

ABISEA Band 64
Neuhaus, Christoph R.
Schaltstrategien für Geschaltete Reluktanzantriebe mit kleinem Zwischenkreis
1. Aufl. 2012, 133 S.
ISBN 978-3-8440-1487-7

ABISEA Band 65
Butschen, Thomas
Dual-ICT- A Clever Way to Unite Conduction and Switching Optimized Properties in a Single Wafer
1. Aufl. 2012, 168 S.
ISBN 978-3-8440-1771-7

ABISEA Band 66
Plum, Thomas
Design and Realization of High-Power MOS Turn-Off Thyristors
1. Aufl. 2013, 113 S.
ISBN 978-3-8440-1884-4

ABISEA Band 67
Kiel, Martin
Impedanzspektroskopie an Batterien unter besonderer Berücksichtigung von Batteriesensoren für den Feldeinsatz
1. Aufl. 2013, 226 S.
ISBN 978-3-8440-1973-5

ABISEA Band 68
Brauer, Helge
Schnelldrehender Geschalteter Reluktanzantrieb mit extremem Längendurchmesserverhältnis
1. Aufl. 2013, 192 S.
ISBN 978-3-8440-2345-9

ABISEA Band 69
Thomas, Stephan
A Medium-Voltage Multi-Level DC/DC Converter with High Voltage Transformation Ratio
1. Aufl. 2014, 226 S.
ISBN 978-3-8440-2605-4

ABISEA Band 70
Richter, Sebastian
Digitale Regelung von PWM Wechselrichtern mit niedrigen Trägerfrequenzen
1. Aufl. 2014, 126 S.
ISBN 978-3-8440-2641-2

ABISEA Band 71
Bösing, Matthias
Acoustic Modeling of Electrical Drives - Noise and Vibration Synthesis based on Force Response Superposition
1. Aufl. 2014, 188 S.
ISBN 978-3-8440-2752-5

ABISEA Band 72
Waag, Wladislaw
Adaptive algorithms for monitoring of lithium-ion batteries in electric vehicles
1. Aufl. 2014, 232 S.
ISBN 978-3-8440-2976-5

ABISEA Band 73
Sanders, Tilman
Spatially Resolved Electrical In-Situ Measurement Techniques for Fuel Cells
1. Aufl. 2014, 126 S.
ISBN 978-3-8440-3121-8

ABISEA Band 74
Baumhöfer, Thorsten
Statistische Betrachtung experimenteller Alterungsuntersuchungen an Lithium-Ionen Batterien
1. Aufl. 2015, 157 S.
ISBN 978-3-8440-3423-3

ABISEA Band 75
Andre, Dave
Systematic Characterization of Ageing Factors for High-Energy Lithium-Ion Cells and Approaches for Lifetime Modelling Regarding an Optimized Operating Strategy in Automotive Applications
1. Aufl. 2015, 196 S.
ISBN 978-3-8440-3587-2

ABISEA Band 76
Merei, Ghada
Optimization of off-grid hybrid PV-wind-diesel power supplies with multi-technology battery systems taking into account battery aging
1. Aufl. 2015, 184 S.
ISBN 978-3-8440-4148-4

ABISEA Band 77
Schulte, Dominik
Modellierung und experimentelle Validierung der Alterung von Blei-Säure Batterien durch inhomogene Stromverteilung und Säureschichtung
1. Aufl. 2016, 165 S.
ISBN 978-3-8440-4216-0

ABISEA Band 78
Schenk, Mareike
Simulative Untersuchung der Wicklungsverluste in Geschalteten Reluktanzmaschinen
1. Aufl. 2016, 126 S.
ISBN 978-3-8440-4282-5

ABISEA Band 79
Wang, Yu
Development of Dynamic Models with Spatial Resolution for Electrochemical Energy Converters as Basis for Control and Management Strategies
1. Aufl. 2016, 188 S.
ISBN 978-3-8440-4303-7

ABISEA Band 80
Ecker, Madeleine
Lithium Plating in Lithium-Ion Batteries:
An Experimental and Simulation Approach
1. Aufl. 2016, 154 S.
ISBN 978-3-8440-4525-3

ABISEA Band 81
Zhou, Wei
Modellbasierte Auslegungsmethode von Temperierungssystemen für Hochvolt-Batterien in Personenkraftfahrzeugen
1. Aufl. 2016, 175 S.
ISBN 978-3-8440-4589-5

ABISEA Band 82
Lunz, Benedikt
Deutschlands Stromversorgung im Jahr 2050
Ein szenariobasiertes Verfahren zur vergleichenden Bewertung von Systemvarianten und Flexibilitätsoptionen
1. Aufl. 2016, 187 S.
ISBN 978-3-8440-4627-4

ABISEA Band 83
Hofmann, Andreas G.
Direct Instantaneous Force Control: Key to Low-Noise Switched Reluctance Traction Drives
1. Aufl. 2016, 228 S.
ISBN 978-3-8440-4715-8

ABISEA Band 84
Budde-Meiwes, Heide
Dynamic Charge Acceptance of Lead-Acid Batteries for Micro-Hybrid Automotive Applications
1. Aufl. 2016, 157 S.
ISBN 978-3-8440-4733-2

ABISEA Band 85
Engel, Stefan P.
Thyristor-Based High-Power On-Load Tap Changers Control under Harsh Load Conditions
1. Aufl. 2016, 156 S.
ISBN 978-3-8440-4986-2

ABISEA Band 86
Van Hoek, Hauke
Design and Operation Considerations of Three-Phase Dual Active Bridge Converters for Low-Power Applications with Wide Voltage Ranges
1. Aufl. 2017, 231 S.
ISBN 978-3-8440-5011-0

ABISEA Band 87
Diekhans, Tobias
Wireless Charging of Electric Vehicles - a Pareto-Based Comparison of Power Electronic Topologies
1. Aufl. 2017, 151 S.
ISBN 978-3-8440-5048-6

ABISEA Band 88
Lehner, Susanne
Reliability Assessment of Lithium-Ion Battery Systems with Special Emphasis on Cell Performance Distribution
1. Aufl. 2017, 184 S.
ISBN 978-3-8440-5090-5

ABISEA Band 89
Käbitz, Stefan
Untersuchung der Alterung von Lithium-Ionen-Batterien mittels Elektroanalytik und elektrochemischer Impedanzspektroskopie
1. Aufl. 2016, 258 S.
DOI: 10.18154/RWTH-2016-12094

ABISEA Band 90
Witzenhausen, Heiko
Elektrische Batteriespeichermodelle: Modellbildung, Parameteridentifikation und Modellreduktion
1. Aufl. 2017, 266 S.
DOI: 10.18154/RWTH-2017-03437

ABISEA Band 91
Münnix, Jens
Einfluss von Stromstärke und Zyklentiefe auf graphitische Anoden
1. Aufl. 2017, 171 S.
DOI: 10.18154/RWTH-2017-01915

ABISEA Band 92
Pilatowicz, Grzegorz
Failure Detection and Battery Management Systems of Lead-Acid Batteries for Micro-Hybrid Vehicles
1. Aufl. 2017, 212 S.
DOI: 10.18154/RWTH-2017-09156

ABISEA Band 93
Drillkens, Julia
Aging in Electrochemical Double Layer Capacitors:
An Experimental and Modeling Approach
1. Aufl. 2017, 179 S.
DOI: 10.18154/RWTH-2018-223434

ABISEA Band 94
Magnor, Dirk
Globale Optimierung netzgekoppelter PV-Batteriesysteme unter besonderer Berücksichtigung der Batteriealterung
1. Aufl. 2017, 210 S.
DOI: 10.18154/RWTH-2017-06592

ABISEA Band 95
Iliksu, Merve
Elucidation and Comparison of the Effects of Lithium Salts on Discharge Chemistry of Nonaqueous $Li-O_2$ Batteries
1. Aufl. 2018, 160 S.
DOI: 10.18154/RWTH-2018-223782

ABISEA Band 96
Schmalstieg, Johannes
Physikalisch-elektrochemische Simulation von Lithium-Ionen-Batterien: Implementierung, Parametrierung und Anwendung
1. Aufl. 2017, 168 S.
DOI: 10.18154/RWTH-2017-04693

ABISEA Band 97
Soltau, Nils
High-Power Medium-Voltage DC-DC Converters: Design, Control and Demonstration
1. Aufl. 2017, 176 S.
DOI: 10.18154/RWTH-2017-04084

ABISEA Band 98
Stieneker, Marco
Analysis of Medium-Voltage Direct-Current Collector Grids in Offshore Wind Parks
1. Aufl. 2017, 144 S.
DOI: 10.18154/RWTH-2017-04667

ABISEA Band 99
Masomtob, Manop
A New Conceptual Design of Battery Cell with an Internal Cooling Channel
1. Aufl. 2017, 167 S.
DOI: 10.18154/RWTH-2018-223281

ABISEA Band 100
Marongiu, Andrea
Performance and Aging Diagnostic on Lithium Iron Phosphate Batteries for Electric Vehicles and Vehicle-to-Grid Strategies
1. Aufl. 2017, 222 S.
DOI: 10.18154/RWTH-2017-09944

ABISEA Band 101
Gitis, Alexander
Flaw detection in the coating process of lithium-ion battery electrodes with acoustic guided waves
1. Aufl. 2017, 109 S.
DOI: 10.18154/RWTH-2017-099519

ABISEA Band 102
Neeb, Christoph
Packaging Technologies for Power Electronics in Automotive Applications
1. Aufl. 2017, 132 S.
DOI: 10.18154/RWTH-2018-224569

ABISEA Band 103
Adler, Felix
A Digital Hardware Platform for Distributed Real-Time Simulation of Power Electronic Systems
1. Aufl. 2017, 156 S.
DOI: 10.18154/RWTH-2017-10761

ABISEA Band 104
Becker, Jan
Flexible Dimensionierung und Optimierung hybrider Lithium-Ionenbatteriespeichersysteme mit verschiedenen Auslegungszielen
1. Aufl., 2017, 157 S.
DOI: 10.18154/RWTH-2017-09278

ABISEA Band 105
Warnecke, Alexander J.
Degradation Mechanisms in NMC Based Lithium-Ion Batteries
1. Aufl. 2017, 158 S.
DOI: 10.18154/RWTH-2017-09646

ABISEA Band 106
Taraborrelli, Silvano
Bidirectional Dual Active Bridge Converter using a Tap Changer for Extended Voltage Ranges
1. Aufl. 2017, 94 S.
DOI: 10.18154/RWTH-2018-228242

ABISEA Band 107
Sarriegi, Garikoitz
SiC and GaN Semiconductors: The Future Enablers of Compact and Efficient Converters for Electromobility
1. Aufl. 2017, 106 S.
DOI: 10.18154/RWTH-2018-227548

ABISEA Band 108
Senol, Murat
Drivetrain Integrated Dc-Dc Converters utilizing Zero Sequence Currents
1. Aufl. 2017, 134 S.
DOI: 10.18154/RWTH-2018-226170

ABISEA Band 109
Kojima, Tetsuya
Efficiency Optimized Control of Switched Reluctance Machines
1. Aufl. 2017, 142 S.
DOI: 10.18154/RWTH-2018-226697

ABISEA Band 110
Lewerenz, Meinert
Dissection and Quantitative Description of Aging of Lithium-Ion Batteries Using Non-Destructive Methods Validated by Post-Mortem-Analyses
1. Aufl. 2018, 139 S.
DOI: 10.18154/RWTH-2018-228663

ABISEA Band 111
Büngeler, Johannes
Optimierung der Verfügbarkeit und der Lebensdauer von Traktionsbatterien für den Einsatz in Flurförderfahrzeugen
1. Aufl. 2018, 171 S.
DOI: 10.18154/RWTH-2018-226569

ABISEA Band 112
Wegmann, Raphael
Betriebsstrategien und Potentialbewertung hybrider Batteriespeichersysteme in Elektrofahrzeugen
1. Auflage 2018, 184 S.
DOI: 10.18154/RWTH-2018-228833

ABISEA Band 113
Nordmann, Hannes
Batteriemanagementsysteme unter besonderer Berücksichtigung von Fehlererkennung und Peripherieanalyse
1. Aufl. 2018, 222 S.
DOI: 10.18154/RWTH-2018-228763

ABISEA Band 114
Engelmann, Georges
Reducing Device Stress and Switching Losses Using Active Gate Drivers and Improved Switching Cell Design
1. Aufl. 2018, 195 S.
DOI: 10.18154/RWTH-2018-228973

ABISEA Band 115
Klein-Heßling, Annegret
Active DC-Power Filters for Switched Reluctance Drives during Single-Pulse Operation
1. Aufl. 2018, 166 S.
DOI: 10.18154/RWTH-2018-231030

ABISEA Band 116
Burkhart, Bernhard
Switched Reluctance Generator for Range Extender Applications - Design, Control and Evaluation
1. Aufl. 2018, 194 S.
DOI: 10.18154/RWTH-2019-00025

ABISEA Band 117
Biskoping, Matthias
Discrete Modeling and Control of a versatile Power Electronic Test Bench with Special Focus on Central Photovoltaic Inverter Testing
1. Aufl. 2018, 236 S.
DOI: 10.18154/RWTH-2019-03346

ABISEA Band 118
Schubert, Michael
High-Precision Torque Control of Inverter-Fed Induction Machines with Instantaneous Phase Voltage Sensing
1. Aufl. 2019, 221 S.
DOI: 10.18154/RWTH-2018-231364

ABISEA Band 119
Van der Broeck, Christoph
Methodology for Thermal Modeling, Monitoring and Control of Power Electronic Modules
1. Aufl. 2019, 290 S.
DOI: 10.18154/RWTH-2019-01370

ABISEA Band 120
Hust, Friedrich Emanuel
Physico-chemically motivated parameterization and modelling of real-time capable lithium-ion battery models – a case study on the Tesla Model S battery
1. Aufl. 2019, 203 S.
DOI: 10.18154/RWTH-2019-00249

ABISEA Band 121
Ralev, Iliya
Accurate Torque Control of Position Sensorless Switched Reluctance Drives
1. Aufl. 2019, 154 S.
DOI: 10.18154/RWTH-2019-03071

ABISEA Band 122
Ayeng'o, Sarah Paul
Optimization of number of PV cells connected in series for a direct-coupled PV system with lead-acid and lithium-ion batteries
1. Aufl. 2019, 114 S.
DOI: 10.18154/RWTH-2019-01843

ABISEA Band 123
Koschik, Stefan Andreas
Permanenterregte Synchronmaschinen mit verteilter Einzelzahnsteuerung - Regelkonzepte und Betriebsstrategien für hochintegrierte Antriebssysteme
1. Aufl. 2019, 158 S.
DOI: 10.18154/RWTH-2019-03446

ABISEA Band 124
Farmann, Alexander
A comparative study of reduced-order equivalent circuit models for state-of-available-power prediction of lithium-ion batteries in electric vehicles
1. Aufl. 2019, 214 S.
DOI: 10.18154/RWTH-2019-04700

ABISEA Band 125
Mareev, Ivan
Analyse und Bewertung von batteriegetriebenen, oberleitungsversorgten und brennstoffzellengetriebenen Lastkraftwagen für den Einsatz im Güterfernverkehr in Deutschland
1. Aufl. 2019, 158 S.
DOI: 10.18154/RWTH-2019-04698

ABISEA Band 126
Qi, Fang
Online Model-predictive Thermal Management of Inverter-fed Electrical Machines
1. Aufl. 2019, 154 S.
DOI: 10.18154/RWTH-2019-08304

ABISEA Band 127
Kairies, Kai-Philipp
Auswirkungen dezentraler Solarstromspeicher auf Netzbetreiber und Energieversorger
1. Aufl. 2019, 140 S.
DOI: 10.18154/RWTH-2019-06706

ABISEA Band 128
Fleischer, Michael
Traction control for Railway Vehicles
1. Aufl. 2019, 162 S.
DOI: 10.18154/RWTH-2019-10570

ABISEA Band 129
Teuber, Moritz
Lifetime Assessment and Degradation Mechanisms in Electric Double-Layer Capacitors
1. Aufl. 2019, 150 S.
DOI: 10.18154/RWTH-2019-10071

ABISEA Band 130
Bußar, Christian
Investigation of Optimal Transformation Pathways towards 2050 for the Successful Implementation of a Sustainable Reduction of Carbon Emissions from Power Generation
1. Aufl. 2019, 204 S.
DOI: 10.18154/RWTH-2019-09975

ABISEA Band 131
Wienhausen, Arne Hendrik
High Integration of Power Electronic Converters enabled by 3D Printing
1. Aufl. 2019, 146 S.
DOI: 10.18154/RWTH-2019-08746

ABISEA Band 132
Kwiecien, Monika
Electrochemical Impedance Spectroscopy on Lead-Acid Cells during Aging
1. Aufl. 2019, 138 S.
DOI: 10.18154/RWTH-2019-09480

ABISEA Band 133
Titiz, Furkan Kaan
A Three-phase Low-voltage Grid-connected Current Source Inverter
1. Aufl. 2019, 128 S.
DOI: 10.18154/RWTH-2020-00458

ABISEA Band 134
Wünsch, Martin
Separation der Kathodenalterung in Lithium-Ionen-Batteriezellen mittels elektrochemischer Impedanzspektroskopie
1. Aufl. 2019, 177 S.
DOI: 10.18154/RWTH-2019-11017

ABISEA Band 135
Badeda, Julia
Modeling and Steering of Multi-Use Operation with Uninterruptible Power Supply Systems - utilizing the example of lead-acid batteries
1. Aufl. 2020, 282 S.
DOI: 10.18154/RWTH-2020-05456

ABISEA Band 136
Kleinsteinberg, Björn
Energy Efficiency Increase of a Vanadium Redox Flow Battery with a Power-Based Model
1. Aufl. 2020, 163 S.
DOI: 10.18154/RWTH-2020-06092

ABISEA Band 137
Cai, Zhuang
Optimization of dimension and operation strategy for a wind-battery energy system in German electricity market under consideration of battery ageing process
1. Aufl. 2020, 144 S.
DOI: 10.18154/RWTH-2020-06525

ABISEA Band 138
Sabet, Pouyan Shafiei
Analysis of Predominant Processes in Electrochemical Impedance Spectra and Investigation of Aging Processes of Lithium-Ion Batteries with Layered Oxide Cathodes and Graphitic Anodes
1. Aufl. 2020, 136 S.
DOI: 10.18154/RWTH-2020-07683

ABISEA Band 139
Angenendt, Georg
Operation, Optimization and Additional Market Participation of Households with PV Battery Storage System and Power-to-Heat Application
1. Aufl. 2020, 221 S.
DOI: 10.18154/RWTH-2020-05200

ABISEA Band 140
Oberdieck, Karl Friedrich
Measurement and Mitigation of Electromagnetic Emissions of Propulsion Inverters for Electric Vehicles
1. Aufl. 2020, 181 S.
DOI: 10.18154/RWTH-2020-09215

ABISEA Band 141
Bubert, Andreas Martin
Optimierung des elektrischen Antriebsstrangs von Elektrofahrzeugen mit Betrachtung parasitärer Ströme innerhalb der elektrischen Maschine
1. Aufl. 2020, 215 S.
DOI: 10.18154/RWTH-2020-09556

ABISEA Band 142
Fleischer, Christian Georg
Model-Driven Software Development and Verification Solutions for Safety Critical Battery Management Systems
1. Aufl. 2020, S.
DOI: 10.18154/RWTH-2020-

ABISEA Band 143
Arzberger, Arno
Thermografische Methoden zur zerstörungsfreien Messung der anisotropen Wärmeleitfähigkeit von Lithium-Ionen Zellen
1. Aufl. 2020, S.
DOI: 10.18154/RWTH-2020-

ABISEA Band 144
Lange, Tobias
Oberwellenbasierte Modellierung, Regelung und Auslegung von Permanentmagnet- und Reluktanz-Synchronmaschinen
1. Aufl. 2020, S.
DOI: 10.18154/RWTH-2020-

ABISEA Band 145
Weiss, Claude
Fault Tolerant Switched Reluctance Machines with Distributed Inverters – Modeling and Control
1. Aufl. 2020, S.
DOI: 10.18154/RWTH-2020-

ABISEA Band 146
Huck, Moritz
Modelling the Transient Behaviour of Lead-Acid Batteries: Electrochemical Impedance of Adsorbed Species
1. Aufl. 2020, 151 S.
DOI: 10.18154/RWTH-2020-08362

ABISEA Band 147
Willenberg, Lisa
Volumenausdehnung und ihre Auswirkungen auf die Alterung einer zylindrischen Lithium-Ionen-Batterie
1. Aufl. 2020, S.
DOI: 10.18154/RWTH-2020-

Electric buses are entering public transport bus fleets and introduce a new level of complexity in the strategic planning of public transport operators. Although numerous research activities focus on the field of electrification planning, there is thus far an absence of a comprehensive planning approach for the public transport domain covering all thematic areas, from technical design over operational planning to the assessment of lifecycle costs. The present thesis closes this gap by providing a software-based planning approach whose applicability has been proven through various case studies.

The novelty of this approach regards the high level of detail for all planning phases, which is enabled by the developed software toolchain utilizing state-of-the-art simulation and optimization methods as well as interfaces with existing planning software and third-party data. Efficient calculation methods facilitate analysis of large scenarios and a wide range of technical alternatives. The consequences of electrification with battery electric buses are elucidated for all stakeholders involved in the electrification process, such as operational planning and infrastructure departments. Furthermore, aggregated and normalized figures are provided to allow a neutral comparison of technical alternatives.

ISSN 1437-675X